UNIFORMLY CONVERGENT NUMERICAL SCHEMES FOR SINGULARLY PERTURBED PARABOLIC PARTIAL DIFFERENTIAL EQUATIONS ON ADAPTIVE GRID

by

S. Gowrisankar

DEPARTMENT OF MATHEMATICS
INDIAN INSTITUTE OF TECHNOLOGY GUWAHATI
GUWAHATI-781039, INDIA

October, 2013

UNIFORMLY CONVERGENT NUMERICAL SCHEMES FOR SINGULARLY PERTURBED PARABOLIC PARTIAL DIFFERENTIAL EQUATIONS ON ADAPTIVE GRID

A thesis submitted
in partial fulfillment of the requirements
for the degree of

DOCTOR OF PHILOSOPHY

by

S. Gowrisankar
(Roll Number: 09612316)

to the

DEPARTMENT OF MATHEMATICS
INDIAN INSTITUTE OF TECHNOLOGY GUWAHATI
October, 2013

DECLARATION

It is certified that the work contained in this thesis entitled **"Uniformly Convergent Numerical Schemes for Singularly Perturbed Parabolic Partial Differential Equations on Adaptive Grid"** has done by me, under the supervision of **Dr. Natesan Srinivasan**, Professor, Department of Mathematics, Indian Institute of Technology Guwahati for the award of the degree of Doctor of Philosophy and this work has not been submitted elsewhere for a degree.

October, 2013

S. Gowrisankar
Roll No. 09612316
Department of Mathematics
Indian Institute of Technology Guwahati

CERTIFICATE

It is certified that the work contained in this thesis entitled **"Uniformly Convergent Numerical Schemes for Singularly Perturbed Parabolic Partial Differential Equations on Adaptive Grid"** by **S. Gowrisankar,** a student of Department of Mathematics, Indian Institute of Technology Guwahati, for the award of the degree of Doctor of Philosophy has been carried out under my supervision and this work has not been submitted elsewhere for a degree.

October, 2013

Dr. Natesan Srinivasan
Professor
Department of Mathematics
Indian Institute of Technology Guwahati

Dedicated

to

my Mother

Mrs. S. Nallammal

Acknowledgement

It gives me great pleasure in expressing my gratitude to all those people who have supported me and had their contributions in making this thesis possible. Foremost, I would like to express my sincere gratitude to my thesis advisor, Prof. Natesan Srinivasan, who always supported me in all the best ways and encouraging my studies. Also, I want to show my deepest appreciation to him for valuable advice, extreme support and friendship. His tireless working ability, patience, motivation and enthusiasm have strongly motivated me. Without his guidance and persistent help this dissertation would not have been possible.

I am grateful to Indian Institute of Technology Guwahati and the Department of Mathematics, IIT Guwahati, which allowed for a fruitful and inspiring stay. Also, for providing me financial assistance and facilities for the completion of my thesis work.

Besides my advisor, I would like to thank the doctoral committee members: Prof. D. C. Dalal, Prof. R. K. Sinha and Prof. S. N. Bora for their encouragement, invaluable advice and insightful comments. Also, I would like to take the opportunity to thank all my teachers.

I thank our technical superintendent Mr. Shantanu Majumdar and Mr. Pranpratim Borgohain for their technical support in various issues. Also, I would like to thank the staff members Mr. Sridhar Samal, Mr. Phatik Kumar and Mr. Udai Sankar of the Department of Mathematics, IIT Guwahati for their assistance in several official related matters.

In my daily work I have been blessed with a friendly and cheerful group of fellow students. I thank my fellow students and for all the fun we have had in these years. I would particularly like to thank Somesh, Murali, Barun and Dinesh for their friendly and wonderful company in throughout my research life. They are always there for me, when I need help and when I need moral support. I take this opportunity to thank Dr. Venkat, Dr. Ravi, Dr. Shubh, Dr. Biswajit, Manideepa, Raj Bhawan, Jitender, Kaushik, Santu, Arnab, Kalyan, Bidyut, Himadri, Hassan, Punit, Kalyan, Swarup, Debopam, Shibsankar and Chiranjit for their encouragement and support. I am also thankful to my seniors Dr. Kaushik Mukherjee, Dr. Jugal Mahapatra and Dr. Pratibhamoy Das; and my juniors Mr. Anirban Majumdar and Mr. Abhishek Das.

Finally, I am indebted to my father, Mr. M. Subramaniam, my mother, Mrs. S. Nallammal and my younger brother, Mr. S. Sasikumar for supporting me throughout all my studies at IIT Guwahati and encouraging me with their best wishes. I also convey my gratitude to my uncle, Mr. R. Periannan, for his support throughout my studies. Specially, I would like to acknowledge my mother for her endless love and support. My love and gratitude for her can hardly be expressed in words. I dedicate this thesis to her.

October, 2013

S. Gowrisankar

Abstract

This thesis provides some efficient numerical techniques for solving singularly perturbed parabolic initial-boundary-value problems of convection-diffusion and reaction-diffusion types with boundary layers. These types of problems are identified by partial differential equations in which the highest spatial derivative is multiplied by an arbitrarily small parameter ε. The perturbation is 'singular' in the sense that, as $\varepsilon \to 0$, the problem becomes ill-posed since the order of the differential equation is reduced, but the number of boundary conditions remain the same. It is a well-known fact that the solution of singularly perturbed boundary-value problem exhibits a multiscale character. That is, there is a thin layer where the solution varies rapidly, while away from the layer the solution behaves regularly and varies slowly. The study of singular perturbation problems (SPPs) is exceptionally useful because they describe the physics of many event of academic and practical interest. This class of problems has recently gained importance in the literature because of its application nature. These problems have been treated numerically by means of exponential-fitting, adaptive meshes, and ideas based on the method of matched asymptotic expansions. Due to this layer phenomena, it is a very difficult and challenging task to provide ε-uniform numerical methods for solving SPPs. The term "ε-uniform" is meant to identify those numerical methods in which the approximate solution converges in some norm (preferably the supremum norm) independently with respect to the parameter ε to the corresponding exact solution of SPP.

It is well-known that uniform meshes with classical schemes fail to converge uniformly with respect to the singular perturbation parameter. It is desired to develop methods which converge uniformly. In this thesis we develop and analyze the ε-uniform numerical methods for solving singularly perturbed parabolic PDEs of convection-diffusion and reaction-diffusion initial-boundary-value problems (IBVPs) on a nonuniform mesh, which is obtained by equidistribution of a positive monitor function.

We begin the thesis with an introduction followed by a section describing the motivation. Then, we introduce the equidistribution principle, the terminology used throughout the thesis. The monitor functions are introduced, further, the numerical algorithm for generating adaptive nonuniform grids are given. Then, ε-uniform numerical schemes are developed for reaction-diffusion and convection-diffusion parabolic IBVPs exhibiting parabolic and regular boundary layers. Numerical experiments are carried out to validate theoretical error estimates. Convergence rates are calculated for the numerical solutions and the flux for linear and semilinear parabolic PDEs. We, then extended the method to wider class of problems of singularly perturbed parabolic convection-diffusion and reaction-diffusion nature. Subsequently the numerical experiment results are presented to verify the theoretical results. Then, the analysis for singularly perturbed delay parabolic reaction-diffusion and convection-diffusion are given using equidistribution and the piecewise-uniform Shishkin mesh, respectively. We also compared the results produced in this thesis with the corresponding layer adapted nonuniform meshes like the piecewise-uniform Shishkin mesh and the Bakhvalov mesh. Finally, we summarizes the results obtained in this thesis. It also provides a few possible extensions of the adaptive grid idea with the equidistribution techniques.

Contents

NOMENCLATURE

BVP	boundary-value problem
IBVP	initial-boundary-value problem
PDE	partial differential equation
SPP	singular perturbation problem
$\mathbb{R}$	set of real numbers
ε	singular perturbation parameter
τ	delay parameter
C	generic positive constant independent of ε
$O(\cdot)$	landau order symbol
N	number of mesh-intervals in spatial direction
M	number of mesh-intervals in time direction
T	maximum time limit
x, x_i, x_i^n	continuous and discrete spatial variables
t, t_n	continuous and discrete temporal variables
h, h_i, h_i^n	mesh-sizes in spatial direction
Δt	mesh-size in time direction
D	bounded open subset in $\mathbb{R} \times [0, T]$
$\overline{D}$	closure of D
$\|\cdot\|_{\infty,D}$ or $\|\cdot\|_{\infty}$	standard supremum norm on D
Ω	open interval $(0, 1)$
Λ	time interval $(0, T]$
G	domain $\Omega \times \Lambda$
$\overline{G}^{N,\Delta t}$	discretization of domain $\overline{G}$
$\mathfrak{C}^k(D), \mathfrak{C}^k(\overline{D}), \mathfrak{C}^{k+\lambda}(D),\ L^1$	function spaces
$L, \mathscr{L}, \mathfrak{L}, \mathfrak{L}, \mathcal{L}, \mathbb{L}$	differential operators
$L^N, \mathscr{L}^N, \mathfrak{L}^N, \mathfrak{L}^N, \mathcal{L}^N, \mathbb{L}^N$	difference operators
$\delta_x^+, \delta_x^-, \delta_x^0, \delta_x^2, \delta_t^-, \delta_t^*$	finite difference operators
$e_\varepsilon^{N,\Delta t}, e^{N,\Delta t}, E_\varepsilon^{N,\Delta t}, E^{N,\Delta t}, \tilde{e}_\varepsilon^{N,\Delta t}$	maximum point-wise errors
$p_\varepsilon^{N,\Delta t}, p^{N,\Delta t}, P_\varepsilon^{N,\Delta t}, P^{N,\Delta t}, \tilde{p}_\varepsilon^{N,\Delta t}$	rate of convergence
$r_\varepsilon^{N,\Delta t}, R_\varepsilon^{N,\Delta t}, \tilde{r}_\varepsilon^{N,\Delta t}$	maximum point-wise errors of normalized flux
$q_\varepsilon^{N,\Delta t}, Q_\varepsilon^{N,\Delta t}, \tilde{q}_\varepsilon^{N,\Delta t}$	rate of convergence of normalized flux

List of Figures

List of Tables

CHAPTER 1

Introduction

1.1 Brief Background

Singular perturbation problems (SPPs) arise in many branches of mathematics like computational fluid dynamics, financial modeling, heat transfer, hydrodynamics, chemical-reactor theory, mathematical biology and its modeling, electrical engineering, semiconductor device modeling and the convective heat transport problems with large Péclet number. These types of problems are identified by partial differential equations in which the highest order spatial derivative is multiplied by an arbitrarily small parameter ε. The perturbation is 'singular' in the sense that, as $\varepsilon \to 0$, the problem becomes ill-posed since the order of the differential equation is reduced, but the number of boundary conditions remains the same. It is a well-known fact that the solution of SPP exhibits a multiscale character. That is, there is a thin layer where the solution varies rapidly, while away from the layer the solution behaves regularly and varies slowly. The study of singular perturbation problems is exceptionally useful because they describe the physics of many event of academic and practical interest. This class of problems has recently gained importance in the literature because of its application nature. These problems have been treated numerically by means of exponential-fitting, adaptive grids (meshes) and ideas based on the method of matched asymptotic expansions. They occur frequently in many areas of science and engineering, for example, the Navier-Stokes equation with a large *Reynolds number* is one of the most striking examples of SPPs. For instance, consider the unsteady incompressible viscous fluid flow problems governed by the Navier-Stokes

equations:

$$\begin{cases} \dfrac{\partial \mathbf{u}}{\partial t} + \mathbf{u} \cdot \nabla \mathbf{u} + \nabla p \;=\; \dfrac{1}{Re} \nabla^2 \mathbf{u}, \\ \nabla \cdot \mathbf{u} \;=\; 0, \end{cases} \tag{1.1.1}$$

where p is the pressure and $\mathbf{u} = (u_1, u_2)$ is the velocity field with the respective velocity components u_1, u_2 along x and y directions. The parameter $Re = |\mathbf{u}|L/\nu$ is the *Reynolds number* with L being the length scale and ν the kinematic viscosity of the fluid. For sufficiently large Re ($\gg 1$), the equations given in (1.1.1) will be considered as to singularly perturbed PDE. Generally the solution exhibits layers at the boundaries and they can be seen in experiments with flows. Especially for high Reynolds numbers, the treatment of such phenomena is important, but complicated. Moreover, experiments can hardly be conducted for high Reynolds numbers. Consequently, understanding the numerical handling of boundary layers is important. The drift-diffusion equation describing the flow of electrons through semi-conductor devices in electrical engineering is another significant example to be noted. More applications of SPPs can be found in the book of Morton [62].

The Navier-Stokes equations arise frequently in the modeling of physical processes. These differential equations typically have a small parameter multiplying the highest-order derivative, and their solutions have layers that is, they vary rapidly in some region of small measure. The numerical solution of such problems is difficult; standard methods that were originally devised for diffusion-dominated processes suffer reduced rates of convergence when applied in a singularly perturbed situation. SPPs came into the picture at the Third International Congress of Mathematicians in Heidelberg in 1904 through Prandtl's seven-page report published in the proceedings [72]. He pioneered the subject of boundary layer theory in his explanation of how a quantity as small as the viscosity of common fluids such as water and air could nevertheless play a crucial role in determining their flow. The term "singular perturbation" was first introduced by Friedrichs and Wasow in their paper [25]. In general, the solutions of SPPs possess boundary (or interior) layers which are basically thin regions in the neighborhood of the boundary (or interior) of the domain, where the gradients of the solutions steepen as the perturbation parameter ε tends to zero. This characterizes the multi-scale nature of the solution as they vary rapidly within the layer regions and behave regularly away from the layer regions. Away from any corner of the domain a boundary layer of either regular or parabolic type may occur. A boundary layer is said to be of parabolic type if the characteristics of the reduced equation, corresponding to $\varepsilon = 0$ are parallel to the boundary, and of regular type if these characteristics are not parallel to the boundary.

Whereas, a boundary layer near a corner is said to be of corner type. The discussion along with the diagram is given in the book of Farrell *et al.* [21].

Singular perturbation theory, the study of differential equations which are modified by the addition of small coefficients multiplying the higher order derivative, is of importance in many fields. It is strange that until the late 1930's this type of problem was almost completely ignored by mathematicians, although the phenomena met in the boundary layer theory of fluid dynamics were known to be mathematically described by such differential equations. Since then, the theory of singular perturbations has grown into a substantial field of study, which has attracted numerous mathematicians. It has been recognized that questions of this sort often have surprising and fascinating mathematical answers and that singular perturbation phenomena explain more physical phenomena than anybody would have foreseen forty years ago. In the past few decades, various ε–uniform numerical schemes are proposed in the literature for SPPs, for more details, one can refer the books of Farrell *et al.* [21], Miller *et al.* [54] and Roos *et al.* [78]. The numerical methods for SPPs are widely classified into two categories, namely, the fitted operator methods (FOMs) and the fitted mesh methods (FMMs). In FOMs, exponential fitting factors (artificial viscosity) will be used to control rapid growth or decay of the numerical solution in the boundary layers. The extensions of FOMs to higher-dimensional problems are too difficult and in some cases it may not be even possible. Whereas, FMMs use nonuniform grids, which will be fine (dense) in the boundary layer regions and coarse outside the layer regions. The well-known layer resolving fitted meshes are the Bakhvalov meshes [4], which will be obtained from some nonlinear mesh generating function, the Shishkin meshes [54], which are piecewise-uniform and easy to obtain. These two meshes will require *apriori* information about the location and width of the boundary layers. The most general nonuniform meshes will be obtained from the equidistribution of some monitor function, which involves the first or/and the second derivatives of the solution of the SPPs and its linear combinations.

Over the last few decades, many ε-uniform numerical methods including finite difference, finite element, finite volume, spline collocations methods etc. have been developed by many researchers for singularly perturbed stationary and non-stationary problems. The subject is now commonly a part of graduate curriculum in applied mathematics and in many fields of engineering. Numerous good textbooks have appeared in this area which either dealt with the asymptotic approach or with the numerical ones. Some of the books dealt with both of these. The list is quite long but we mention a few of them. One may refer to the books of Miller [57], Nayfeh [69], Lagerstrom [46], Doolan *et al.* [19], Eckhaus [20], Morton [62], O'Malley and Robert [70, 71], Kevorkian and Cole [39], Bush [11], Farrell *et al.* [21], Miller *et al.* [54], Ladyženskaja [45], and Roos *et al.* [78].

For SPPs the aim is to cluster automatically the grid points within the boundary layer and an obvious choice of adaptivity criterion is therefore the solution gradient, for one-dimensional stationary problems, one can refer the articles of Mackenzie [52], and Qiu *et. al.* [74]. Beckett and Mackenzie applied the adaptive meshes obtained via equidistribution of a monitor function to one-dimensional linear reaction-diffusion in [7] and convection-diffusion problems in [6]. For time-dependent problems, Adjerid and Flaherty proposed a moving finite element method in [1]. Huang *et. al.* [32] obtained nonuniform grids through mesh equidistribution principle for parabolic PDEs, here they derived various moving mesh PDEs from the mesh equidistribution relation. Recently, in [8], Beckett *et. al.* obtained the numerical solution of one-dimensional parabolic PDEs on adaptive grids via grid equidistribution principle.

Kopteva and Stynes [44] considered semilinear reaction-diffusion two-point boundary-value problem with a small parameter ε. The authors analyzed the numerical computation of solutions with interior transition layer and proposed an artificial-diffusion stabilization. Kopteva in [41] analyzed a singularly perturbed semilinear two-point boundary-value problem and the problem is discretized on arbitrary nonuniform grids. The author presents second-order maximum norm *aposteriori* error estimates that hold true uniformly with respect to the small parameter ε. Moreover, the monitor function equidistribution and *aposteriori* gird refinement are also discussed. The numerical solution of a linear singularly perturbed reaction-diffusion two-point boundary-value problem is considered in [42]. The method used the adaptive movement of a fixed number of grid points by monitor-function equidistribution. A partly heuristic argument based on truncation error analysis leads to several suitable monitor functions, but also shows that the standard arc-length monitor function is unsuitable for this problem. An upwind finite difference scheme is applied for a quasilinear conservative convection-diffusion two-point boundary-value problem in [43]. The grid used has a fixed number $(N+1)$ of nodes and is initially uniform, but its nodes are moved adaptively using a simple algorithm of de Boor based on equidistribution of the arc-length of the currently computed piecewise-linear solution.

Linß *et al.* [51] developed a collocation method for singularly perturbed reaction-diffusion BVP that uses quadratic C^1-splines on a Shishkin-type grid. Although the discrete operator is not inverse-monotone, it is nevertheless shown to be stable in the discrete maximum norm. It is then proved that the discrete solution is almost second-order convergent in $L_\infty[0,1]$, uniformly with respect to the singular perturbation parameter ε. An *aposteriori* bound for the method on arbitrary grids are also derived, and this motivates an adaptive algorithm for the solution of the boundary-value problem. Franz and Linß [23] analyzed the superconvergence property of the Galerkin finite element method

(FEM) for elliptic convection-diffusion problems with characteristic layers. This method on the Shishkin grid is known to be almost first-order accurate (up to a logarithmic factor) in the energy norm induced by the bilinear form of the weak formulation, uniformly in the perturbation parameter.

In [49], Linß considered the issue of efficiently computing solutions to a class of one-dimension singularly perturbed reaction diffusion type. Convergence and stability for a numerical scheme that is first-order in time and second-order in space is analyzed. Linß and Madden [50] analyzed the error of numerical approximations for a time-dependent singularly perturbed reaction-diffusion equation. The underlying discretizations are central difference in space and backward difference in time. By a discrete Green's function technique it is possible to analyze the approximation on the Shishkin and the Bakhvalov grids within the same framework. Linß [48] studied convergence properties of a finite element method with lumping for the solution of a linear one-dimensional reaction-diffusion problem on arbitrary grids. This type of problem possesses a solution which typically has boundary layers of width $O(\varepsilon \ln 1/\varepsilon)$ at each end of the underlying interval. The author gave a new derivation of the decomposition of the solution in the regular and the singular components. Then he derived sufficient conditions for convergence of the method in the L_∞-norm, uniformly in the diffusion parameter. His analysis mainly depends on bounds for the discrete Green function associated with the discretization.

Layered meshes may be used to improve the convergence of finite elements applied to convection-diffusion equations when boundary layers are present. Roos and Schopf [77] assessed the convergence properties of the Bakhvalov mesh layering technique. They proved that the adaption techniques based on such meshes provide an almost optimal convergence in a suitable scaled norm. In [76], Roos and Reibiger used two piecewise-uniform Shishkin meshes for linear finite elements to generate approximations to the coupled system of one-dimensional singularly perturbed differential equations. Parameter-uniform energy norm estimates are established and numerical results are presented to support the theoretical error bounds. Franz *et al.* [24] proposed and analyzed a special instance of the two-scale finite element method, called the "combination" method, for the numerical approximation of a singularly perturbed convection-diffusion problem on the unit square. The main feature of such a problem is that the exact solution contains a regular part, and exponential and corner boundary layers whose width depends on the diffusion coefficient ε (singular perturbation parameter). The main idea of the two-scale finite element method is to use a coarse grid to approximate the low frequencies and to use a suitable combination of univariate fine and coarse grids to approximate the high frequencies. Using *apriori* knowledge of the layer behavior of the solution, the authors constructed the piecewise-uniform Shishkin meshes that allow them to re-

solve the layer phenomena and yield uniform convergence of the scheme with respect to ε. Clavero *et al.* [18] presented a numerical method to solve a one-dimensional time-dependent convection-diffusion problem with dominating convection term using the classical implicit-Euler method for the time discretization and the simple upwind scheme on the piecewise-uniform Shishkin mesh for the spatial discretization. It is also shown that the resulting method is uniformly convergent with respect to the diffusion parameter. In [16], Clavero *et al.* considered a two-dimensional linear scalar parabolic initial-boundary-value problem in the unit square with the small parameter ε multiplying the second-order derivative. They designed and analyzed a finite difference scheme which is uniformly convergent with respect to the perturbation parameter.

Stynes and Roos [84] introduced a modified upwind scheme for a class of singularly perturbed two-point boundary-value problems whose solution has a single boundary layer. The scheme is analyzed on an arbitrary mesh as well as on the Shishkin mesh. The method converges uniformly with respect to the singular perturbation parameter ε. The articles of Clavero *et al.* [14, 15] deals with the numerical approximation of the solution of 1D parabolic singularly perturbed problems of reaction-diffusion and convection-diffusion types, respectively. The numerical method combines the standard implicit-Euler and the Crank-Nicolson method to discretize the time derivative and a HODIE finite difference scheme, defined on a piecewise-uniform Shishkin mesh, to discretize the spatial variable. In both the cases the authors proved that the numerical method is uniformly convergent with respect to the singular perturbation parameter ε. Singularly perturbed parabolic convection-diffusion problem with a moving interior layer is analyzed in [29, 30] where the coefficients are smooth, but the solution contains an interior layer, generated from the fact that the initial condition contains is discontinuous. Gracia and Clavero [28] constructed a set of positive type compact finite difference schemes for a class of 2D reaction-diffusion singularly perturbed elliptic problems. The set of schemes is proved to be able to provide better approximations than the classical schemes when constructed on a piecewise-uniform mesh of Shishkin type. The set of schemes is further proved to be third-order accurate in the maximum norm when the singular perturbation parameter is sufficiently small.

Ansari and Hegarty [3] analyzed a one-dimensional steady-state convection dominated convection-diffusion problem with Robin boundary conditions using an upwind finite difference scheme on the Shishkin meshes and are uniformly convergent with respect to the diffusion coefficient. Zhang [94] considers a singularly perturbed two-point boundary-value problem of convection-diffusion type, and solved it approximately by means of an *hp* finite element method. The mesh used is uniform and resembles a Shishkin mesh except that the width of its fine-layer region is $O(\varepsilon p)$, where ε is the dif-

fusion coefficient. In [95] he analyzed the superconvergence of a bilinear finite element scheme for a convection-dominated convection-diffusion problem in two-dimension. The standard Galerkin approach is combined the Shishkin mesh. The author showed that this superconvergence is uniformly valid with respect to the singular perturbation parameter for the combined mesh considered in the model problem. The author also showed under certain regularity assumptions the superconvergence in a discrete ε-weighted energy norm. And in [93] superconvergent approximations of singularly perturbed two-point boundary-value problems of reaction-diffusion type and convection-diffusion type are studied. By applying the standard finite element method of any fixed order p on a modified Shishkin mesh. Superconvergence of DG method for one-dimensional singularly perturbed problems are studied in [90, 91]. Zhu *et al.* [96] applied the so-called Local Discontinuous Galerkin (LDG) method for solving one-dimensional singularly perturbed two-point boundary-value problems of convection-diffusion-reaction type. In order to numerically solve the problem and to avoid non-physical oscillations in those regions where layers occur, a numerical scheme on a layer adapted mesh of Shishkin type is proposed. Specific choices for the Shishkin-type meshes are, respectively, selected for convection-diffusion and reaction-diffusion problems by taking advantage of the regularity of the exact solution. For these two cases, L^2-error bounds are obtained and they are uniformly valid regarding the singular perturbation parameter ε.

Before concluding this section, let us cite some of the articles which dealt with the ε–uniform numerical methods for singularly perturbed parabolic PDEs: Stynes and O'Riordan studied the IBVP by applying exponentially fitted difference scheme in [83], Clavero *et. al.* proposed a uniformly convergent numerical scheme on Shishkin meshes in [18]. Recently, Mukherjee and Natesan [63] developed higher-order numerical scheme for the IBVP of parabolic type by using a hybrid scheme on the piecewise-uniform Shishkin meshes; and in [66], they obtained higher-order convergence *via* Richardson extrapolation technique. For parabolic convection-diffusion PDEs with discontinuous coefficients, Mukherjee and Natesan proposed an ε-uniform hybrid scheme in [64], and obtained optimal error estimates for Shishkin type meshes in [65].

Before proceeding to the next section, a concise literature survey of numerical methods concerning general PDEs are presented here. As the model problems considered in the thesis are mainly parabolic PDEs, many applied mathematicians and engineers showed their interest to devise various numerical techniques for solving these parabolic PDEs; the information regrading these numerical methods can be obtained from the standard text books [61, 81, 36]. One may refer to the books of Thomée [85], Šolín [82], Brenner and Scott [9], Ciarlet and Lions [13] and Quarteroni *et al.* [75] and the papers of Wade [40, 86, 88, 87] to gain further theoretical knowledge of finite difference and

finite element methods associated with PDEs of parabolic and elliptic nature.

1.2 Objective and Motivation

The main objective of the thesis is to develop, analyze and optimize ε-uniform numerical methods based on nonuniform meshes for singularly perturbed convection-diffusion and reaction-diffusion parabolic PDEs. The nonuniform meshes are obtained by equidistributing a predefined positive monitor function. A brief survey of the literature illustrating motivation behind the present work, carried out in the thesis, is presented below:

Many areas of science and engineering produce difficult mathematical problems, *i.e.* problems that cannot be solved in any conventional sense. In many cases, against all the apparent odds, it is possible to construct systematic approximations that lead to useful solutions. The most powerful of these approximation techniques is singular perturbation theory. It is well-known that the classical finite difference schemes on uniform meshes fail to converge uniformly with respect to the singular perturbation parameter. It is desirable to develop methods which converges uniformly. In this thesis we develop and analyze the ε-uniform numerical methods for solving singularly perturbed parabolic convection-diffusion and reaction-diffusion initial-boundary-value problems (IBVPs) on nonuniform meshes, which are obtained by equidistribution of a positive monitor function.

The piecewise-uniform Shishkin mesh is a union of finite number of uniform meshes in which the mesh-sizes are different inside and outside the layer regions. These piecewise-uniform fitted meshes were first introduced by Shishkin in the year 1989 [80, 53]. Practically, the *fitted mesh methods* are recommended whenever possible, because of their simpler implementation than the *fitted operator methods*. Moreover, the *fitted mesh methods* have the extra advantage that they can be easily extended to higher dimensional problems and to nonlinear problems. The above two approaches are based on the *apriori* knowledge of the solution before solving the original problem which is not always available. For solving SPPs, the aim is to cluster automatically the grid points within the boundary layer. A commonly used technique for determining the grid points that they equidistribute a positive function of the solution over the domain. The positive function is known as *monitor function* and has to be approximated from the numerical solution of the original problem. The adaptive grid approach has the advantage that it can be applied using little or no *apriori* information about the width and the location of the boundary layer. The monitor function automatically detects the presence of the boundary layers together with their location and width and distributes mesh points accordingly if layers are of different thickness. The purpose of the monitor function is

to generate a grid which is adapted to the features of the solution. There are many influences on the choice of the monitor functions, including, the type of the problem to be solved, the choice of norm for error management and numerical discretization to be used. In this thesis we primarily use monitor function which is a linear combination of second-order derivative of the singular component of the solution and its total measure. This equidistributed grid is exponentially stretched within the boundary layers and therefore, responsible for an improved rate of convergence compared to the related piecewise-uniform Shishkin mesh. Hence, for solving singular perturbation problems, an obvious choice of adaptive criterion is therefore the solution gradient. Now-a-days, these *adaptive grid* methods are established as a valuable computational technique in approximating effectively the solutions of problems with boundary (or interior) layers.

Here, we cite some of the articles which dealt with the ε-uniform numerical methods for singularly perturbed problems using equidistribution adaptive meshes. White [89] in 1979 developed a general theory for calculating equidistributing meshes for difference methods for boundary-value problems of a standard form. It is shown that the original problem and the equidistribution constraints on the mesh can be replaced by a transformed boundary-value problem on a uniform mesh. Existence, uniqueness, and convergence of Newton's method for the discrete solution and the equidistributing mesh are proved. Equidistribution of arc-length is given for boundary layer problems. A commonly used algorithm for generating adaptive meshes for a given adaptation function in one-dimension is due to de Boor [92]. In its original form the algorithm produces a sequence of meshes upon using piecewise-constant interpolation for the adaptation function on the current mesh and generating a new mesh that exactly equidistributes the interpolant.

Qiu *et al.* [74] considered the singularly perturbed two-point boundary-value problem. The discrete solutions are generated by an upwind finite difference scheme and the grid is formed by equidistributing a monitor function based on the arc-length. The objective of this work is to analyze the convergence of the adaptive finite difference solution of the problem. An error analysis shows that the discrete solutions are uniformly convergent in ε. The numerical solution obtained by using an upwind difference scheme with an uneven grid generated by equidistributing the arc-length monitor function. The analysis deals with only semi-discretization of the adaptive method, *i.e.* the exact solution is used to generate the mesh. Qiu and Solan [73] used adaptive mesh for SPP, the mesh is designed to equidistribute some monitoring function. For the actual analysis the monitor function is computed from an explicit solution, but it is argued that a fully discrete implementation computing the mesh along with the solution will give similar results. Here, instead of the arc-length monitor function the monitor function

$M(u(x), x) = |u'(x)|^{1/m}$ for some integer m is used, and ε-uniform convergence of orders one and two is proved in the maximum norm for an upwind scheme and for a fitted symmetric scheme, respectively.

Chen [12] improved the above error bound to the optimal order which is independent of the perturbation parameter. The main ingredient used to obtain the improved result is the theory of the discrete Green's function. In [47], Linß studied the application of a simple upwind finite difference scheme to singularly perturbed quasilinear two-point boundary-value problems. Moreover, adaptive meshes obtained by requiring grid equidistribution of suitable monitor functions are used with the difference scheme. Sufficient conditions on the monitor function are derived that are independent of the perturbation parameter and guarantee uniform convergence in the discrete maximum norm. Recently, in [92], a proof for the existence of a limit mesh and convergence of de Boors algorithm are given. Numerical results are given to illustrate the theoretical findings, and stopping criteria necessary for the implementation of the algorithm are examined. In [52], Mackenzie analyzed an upwind finite-difference approximation for a convection-diffusion boundary-value problem using adaptive grid. The adaptive grid is constructed by equidistribution of the power of the gradient of the solution of a constant coefficient problem. The use of equidistribution principle appears in many grid adaption schemes and the analysis indicates the convergence behavior of such grids. Mohapatra and Natesan [59, 60] used grid equidistribution algorithm, based on discretizing the arc-length monitor function for solving singularly perturbed boundary-value problems. The performance of upwinding on this grid is compared with the performance of upwinding on a standard piecewise-uniform Shishkin mesh.

For SPPs the aim is to cluster automatically the grid points within the boundary layer and an obvious choice of adaptivity criterion is therefore the solution gradient, for one-dimensional stationary problems one can refer the articles of Mackenzie [52], and Qiu *et al.* [74]. Beckett and Mackenzie applied the adaptive mesh obtained via equidistribution of a monitor function to one-dimensional linear reaction-diffusion problem in [7] and convection-diffusion problem in [6]. For time-dependent SPPs, Adjerid and Flaherty proposed a moving finite element method in [1]. Huang *et al.* [32] obtained nonuniform grids through mesh equidistribution principle for parabolic PDEs, here they derived various moving mesh PDEs from the mesh equidistribution relation. Recently, in [8], Beckett *et al.* obtained the numerical solution of one-dimensional parabolic PDEs on adaptive grids via mesh equidistribution principle. One can get more information on adaptive mesh and equidistribution of a monitor function in the thesis of Beckett [5].

An alternative dynamic methods often called moving mesh methods, for these type of problems a mesh equation that involves node speeds is employed to move a mesh

having a fixed number of nodes in such a way that the nodes remain concentrated in regions of rapid variation of the solution. The key to the success of moving mesh methods lies in a suitable choice of a monitor function. the monitor function controls mesh concentration through the equidistribution principle and measures the difficulty in the spatial numerical approximation of the underlying problem. Several moving mesh partial differential equations (MMPDES) based on the equidistribution principle are derived and studied both theoretically and numerically. Some of these MMPDES are developed in the work of Huang and Russell [35, 34], Huang *et al.* [33, 32] and Mulholland *et al.* [67]. Adaptivity with moving mesh and moving finite element methods (MFEM) can be found [10] and [56], respectively.

We begin the thesis by introducing the equidistribution principle, the terminology used throughout the thesis. The monitor functions are introduced further and numerical algorithms for generating adaptive nonuniform grids are given. Then, ε-uniform numerical schemes are developed for reaction-diffusion and convection-diffusion parabolic IBVP exhibiting a regular boundary layer. Numerical experiments are carried out to validate the theoretical results. Convergence rates are calculated for the numerical solutions and the flux for linear and semilinear parabolic PDEs. We, then extended the method to a wider class of problems of singularly perturbed parabolic convection-diffusion and reaction-diffusion nature. Subsequently the numerical experiment results are presented to verify the theoretical findings. Then, the analysis for singularly perturbed delay parabolic reaction-diffusion and convection-diffusion are given using the equidistribution mesh and the piecewise-uniform Shishkin mesh, respectively. We also compared results produced in this thesis with the corresponding layer adapted nonuniform meshes like the piecewise-uniform Shishkin mesh and the Bakhvalov mesh. Finally, we summarize the results obtained in this thesis. It also provides a few possible extensions of the adaptive grid idea with the equidistribution techniques.

1.3 Some Notations and Terminology

In this section, we introduce notations and terminology which will be used throughout the thesis. For small values of the parameter ε boundary layer may appear that give rise to difficulties when classical discretization methods are applied on uniform mesh. Moreover, the error in the approximate solution depends on the variable ε. An adapted placement of the nodes is needed to ensure that the error is independent of the parameter value and depends only on the number of nodes in the mesh. The discretization with this properties is called *ε-uniform numerical method.* It can be defined formally as follows

Definition 1.3.1. ε-Uniform Numerical Method *Consider (P_ε) be a family of singularly perturbed parabolic PDEs parameterized by a singular parameter ε, where ε satisfies $0 < \varepsilon \ll 1$. Assume that each problem in (P_ε) has a unique solution denoted by u_ε, and that each u_ε is approximated by sequence of numerical solutions $\{(U_\varepsilon, \overline{G}^{N,\Delta t})\}$ obtained by using a monotone numerical method $(P_\varepsilon^{N,\Delta t})$, where U_ε is defined on the mesh $\overline{G}^{N,\Delta t}$ and; N and Δt are discretization parameters. Let $\overline{U}_\varepsilon$ denote the piecewise-linear interpolation over $\overline{G}^{N,\Delta t}$ of the discrete solution U_ε. Then $\overline{U}_\varepsilon$ is said to converge ε-uniformly to the exact solution u_ε, if there exists positive integers N_0, M_0 and positive numbers C, p and q, such that for all $N \geq N_0$ and $M \geq M_0$, where $M = T/\Delta t$, we have*

$$\sup_{0<\varepsilon\ll 1} \left\| \overline{U}_\varepsilon - u_\varepsilon \right\|_\infty \leq C\left(\Delta t^p + N^{-q}\right),$$

where N_0, M_0, C, p and q are all independent of ε.

Here p and q are called the ε-uniform order of convergence of the temporal and the spatial variables, respectively, and C is called the ε-uniform error constant.

Definition 1.3.2. *Let D be a bounded open subset in $\mathbb{R} \times [0, T]$. For any non-negative integer k, we denote by $\mathcal{C}^k(D)$ the space of all functions whose derivatives up-to order k are continuous on D. Suppose that $\lambda \in (0, 1)$. Then a function $g(x, t)$ defined on D is said to be Hölder continuous in D with exponent λ, if and only if*

$$\sup_{(x,t),(x',t')\in D} \frac{\left|g(x,t) - g(x',t')\right|}{\left((x-x')^2 + |t-t'|\right)^{\lambda/2}} \;<\; \infty.$$

An equivalent definition is used by Ladyzenskaja *et al.* [45]. We denote the set of Hölder continuous functions in D with exponent λ by $\mathcal{C}^\lambda(D)$. For each integer $k \geq 1$, we define the parabolic Hölder space $\mathcal{C}^{k+\lambda}(D)$ as

$$\mathcal{C}^{k+\lambda}(D) = \left\{ g : \frac{\partial^{i+j} g}{\partial x^i \partial t^j} \in \mathcal{C}^\lambda(D) \text{ for all non-negative integers } i, j \text{ with } 0 \leq i + 2j \leq k \right\}.$$

Note that for each integer $k \geq 0$, any function $g \in \mathcal{C}^{k+\lambda}(D)$ is uniformly continuous in D and admits a unique continuous extension on $\overline{D}$. This allows us to speak about values on $\partial D = \overline{D} \backslash D$ of a function $g \in \mathcal{C}^{k+\lambda}(D)$ and without ambiguity one can write $\mathcal{C}^{k+\lambda}(D) = \mathcal{C}^{k+\lambda}(\overline{D})$.

In the analysis, we use the standard supremum norm $\| \cdot \|_{\infty,D}$, which is defined by

$$\left\| g \right\|_{\infty,D} = \sup_{(x,t)\in D} \left| g(x,t) \right|.$$

It is a convention that when the domain is obvious, or of no particular significance, D is omitted.

Throughout the thesis, C denotes a generic positive constant that is independent of the perturbation parameter ε, N and M (number of mesh-intervals in the spatial and the temporal directions, respectively) and the mesh sizes. Note that the constant C may take different values in different places.

In the analysis, it is frequently assumed that $\varepsilon \leq N^{-1}$, which is the case of actual interest from the practical point of view. If $\varepsilon \geq N^{-1}$, then in practice the model problems considered in the thesis are not difficult to solve computationally. So the assumption is not restrictive. It can also be replaced by the hypothesis that $\varepsilon \leq C_0 N^{-1}$ for some fixed constant C_0 without altering the results obtained in the thesis.

We now define the following standard finite difference operators which will be used for describing the difference schemes (particularly, for the discretization of the one-dimensional parabolic IBVPs) in the subsequent chapters.

On the time domain [0,T], we introduce the equidistant meshes with uniform time step Δt such that

$$\overline{\Lambda}_t^M = \{t_n = n\Delta t,\ n = 0, \ldots, M,\ \Delta t = T/M\},$$

where M denotes the number of mesh intervals in the t-direction.

We consider the finite difference approximation on a nonuniform spatial discretization

$$\overline{\Omega}_x^N = \{0 = x_0 < x_1 < \cdots < x_N = 1\},$$

and denote the spatial step sizes by

$$h_i = x_i - x_{i-1}, \quad i = 1, \ldots, N.$$

For a given mesh function $v(x_i, t_n) = v_i^n$, define the forward and backward differences δ_x^+, δ_x^- in space by

$$\delta_x^+ v_i^n = \frac{v_{i+1}^n - v_i^n}{h_{i+1}}, \quad \delta_x^- v_i^n = \frac{v_i^n - v_{i-1}^n}{h_i},$$

respectively, the second-order finite difference operator δ_x^2 as

$$\delta_x^2 v_i^n = \frac{2(\delta_x^+ v_i^n - \delta_x^- v_i^n)}{h_i + h_{i+1}},$$

and define the backward difference operator δ_t in time by

$$\delta_t v_i^n = \frac{v_i^n - v_i^{n-1}}{\Delta t}.$$

Definition 1.3.3. *A matrix* $\mathbf{A} = (a_{i,j}) \in \mathbb{R}^{k\times k}$ *is an* M*-matrix if* $\mathbf{A}$ *is nonsingular,* $\mathbf{A}^{-1} \geq 0$ *and* $a_{i,j} \leq 0$*, for all* $i \neq j,\ 1 \leq i, j \leq k$.

Finally, this section is concluded by introducing ***Landau's order symbol*** O (big-oh) to be used throughout the thesis. Let $f(\varepsilon)$ and $g(\varepsilon)$ be two real-valued functions, where $0 < \varepsilon \leq \varepsilon_0 \ll 1$.

Definition 1.3.4. *The expression* $f(\varepsilon) = O(g(\varepsilon))$ *as* $\varepsilon \to 0$ *means that there exist some constants* $C > 0$, ε_0 *such that in* $(0, \varepsilon_0]$,

$$\big|f(\varepsilon)\big| \leq C\big|g(\varepsilon)\big| \quad \text{as } \varepsilon \to 0.$$

1.3.1 Ideas of mesh-construction

Let us consider the linear convection-diffusion two-point boundary value ordinary differential equation

$$-\varepsilon u''(x) - b(x)u'(x) + c(x)u(x) = f(x), \quad x \in \Omega := (0,1), \tag{1.3.1}$$

with the boundary conditions

$$u(0) = 0 = u(1).$$

We assume that the functions $b(x)$, $c(x)$ and $f(x)$ are continuous. The parameter ε satisfies $0 < \varepsilon \ll 1$ and $b(x) \geq \beta > 0$. The boundary value problem (1.3.1) has a unique solution that typically has an exponential boundary later at $x = 0$ which behaves like $\exp(-\beta x/\varepsilon)$. Using (1.3.1) as a model problem we now review some standard mesh-construction ideas.

1.3.2 The Shishkin mesh

Here, we report the piecewise-uniform Shishkin mesh, a frequently-studied simple mesh, for the spatial discretization of the domain $\overline{\Omega}$ for the problem (1.3.1). Let $N \geq 4$ be an even positive integer. To define the piecewise-uniform Shishkin mesh, the domain $\overline{\Omega}$ is divided into two subintervals $[0, \tau]$ and $[\tau, 1]$ and on each subinterval a uniform mesh with $N/2$ mesh-intervals is placed such that $\overline{\Omega}_x^N = \{0 = x_0, x_1, \ldots, x_{N/2} = \tau, \ldots, x_N = 1\}$. Here, the transition point τ, which separates the coarse and fine portions of the mesh, is obtained by taking

$$\tau = \min\left\{\frac{1}{2}, \tau_0 \varepsilon \ln N\right\}, \tag{1.3.2}$$

where τ_0 is a positive constant. Typically the parameter τ_0 will be chosen sufficiently large to accommodate the error analysis.

Let the mesh widths in space be denoted by

$$h_i = x_i - x_{i-1}, \ i = 1, \ldots, N, \quad \widehat{h}_i = h_i + h_{i+1}, \ i = 1, \ldots, N-1.$$

Further, let $h = 2\tau/N$ and $H = 2(1-\tau)/N$ be the mesh widths in $[0,\tau]$ and $[\tau,1]$ respectively. Then, it is easy to see that

$$h = 2\tau_0 \varepsilon N^{-1} \ln N, \quad N^{-1} \leq H \leq 2N^{-1}.$$

The above outlines can be modified appropriates to apply for various problems, in particular problems with layer(s) on the right-hand side and both sides. From these considerations a typical convergence result for simple upwinding of the problem (1.3.1) on the Shishkin mesh is

$$\|u - U\|_{\infty,\Omega} \leq CN^{-1} \ln N,$$

where u and U are the exact and the computational solution of the problem (1.3.1), respectively.

1.3.3 The Bakhvalov mesh

This section describes the Bakhvalov mesh for the spatial discretization of the domain $\overline{\Omega}$. Before presenting the Bakhvalov mesh ideas we recall a basic concept for describing layer-adapted meshes, mesh generating function.

Definition 1.3.5. (**Mesh generating function**) *A strictly monotone function* $\phi : [0,1] \to [0,1]$ *that maps a uniform mesh in* ξ *onto a layer-adapted mesh in* x *by* $x = \phi(\xi)$ *is called a mesh generating function.*

The mesh generation function for the Bakhvalov mesh is

$$\phi(\xi) = \begin{cases} \psi(\xi) := -A\varepsilon \ln(1 - \xi/q) & \text{for } \xi \in [0,\tau], \\ \pi(\xi) := \psi(\tau) + \psi'(\tau)(\xi - \tau) & \text{for } \xi \in [\tau,1], \end{cases}$$

for the problem (1.3.1). Here A and q are user-chosen positive parameters and the point τ satisfies

$$\psi(\tau) + \psi'(\tau)(1-\tau) = 1. \tag{1.3.3}$$

Geometrically this means that $(\tau, \psi(\tau))$ is the contact point of the tangent π to ψ that passes through the point $(1,1)$. The nonlinear equation (1.3.3) has to be solved approximately to define the Bakhvalov mesh. If the boundary layer is at $x = 1$, we redefine ϕ by means of $\phi(\xi) := 1 - \phi(1-\xi)$.

The Bakhvalov meshes give numerical results that are superior to those obtained by the Shishkin meshes:

$$\|u - U\|_{\infty,\Omega} \leq CN^{-1},$$

for the problem (1.3.1) with simple upwind scheme and; u and U are the exact and the computational solution of the problem (1.3.1), respectively.

1.3.4 Adaptive spatial meshes via equidistribution

Since the solution of the problem (1.3.1) exhibits a boundary layer, one has to use a layer-adapted nonuniform spatial meshes, which are dense inside the boundary layer region and coarse in the outer region. To obtain such a mesh, the idea of equidistribution of a positive monitor function given in (1.3.5) are used. A mesh $\overline{\Omega}_x^N = x_0 < x_1 < \cdots < x_N$ is said to be equidistributing $u(x)$, if

$$\int_{x_{i-1}}^{x_i} M(u(s), s)ds = \int_{x_i}^{x_{i+1}} M(u(s), s)ds, \quad \text{for } i = 1, \ldots, N-1, \tag{1.3.4}$$

where $M(u(x), x)$ is a strictly positive, L_1–integrable function. Here, we consider the monitor function

$$M(u(x), x) = \alpha_c + |w''(x)|^{1/m}, \quad m \geq 2, \tag{1.3.5}$$

where α_c is a positive constant that is independent of N and $w(x)$ is the singular component of $u(x)$. We take

$$\alpha_c = \int_0^1 |w''(s)|^{1/m} ds. \tag{1.3.6}$$

The selection of this α_c will help to equally distribute the number mesh points inside and outside the boundary layer region. The effect of increasing m is to smoothen the monitor function, which in turn leads to a smoother distribution of the mesh points. From [6], we clearly notice the influence of the parameter m. For the following convergence result we assume that the mesh satisfies equidistribution principle given in (1.3.4).

From these considerations a convergence result for simple upwinding on equidistribution mesh is

$$\|u - U\|_{\infty,\Omega} \leq CN^{-1},$$

where u and U are the exact and the computational solution of the problem (1.3.1), respectively.

1.4 Model Problems

The following types of model problems are considered in the thesis and their concise descriptions are given below

1.4.1 Singularly perturbed parabolic reaction-diffusion problem

Consider the singularly perturbed parabolic initial-boundary-value problem (IBVP)

$$\begin{cases} u_t(x,t) + L_\varepsilon u(x,t) = f(x,t), \quad (x,t) \in G = (0,1)\times(0,T], \\ u(x,0) = s(x), \quad \text{on } S_x = \{(x,0) : 0 \le x \le 1\}, \\ u(0,t) = a_0(t), \quad \text{on } S_0 = \{(0,t) : 0 \le t \le T\}, \\ u(1,t) = a_1(t), \quad \text{on } S_1 = \{(1,t) : 0 \le t \le T\}, \end{cases} \tag{1.4.1}$$

where $L_\varepsilon u \equiv -\varepsilon u_{xx} + b(x)u$, $0 < \varepsilon \ll 1$ is a small parameter, and b, f are sufficiently smooth functions with $b(x) \ge \beta > 0$ for $x \in [0,1]$.

1.4.2 Singularly perturbed parabolic convection-diffusion problem

Here, we consider the following singularly perturbed parabolic initial-boundary-value problem (IBVP):

$$\begin{cases} u_t(x,t) + \mathscr{L}_\varepsilon u(x,t) = f(x,t), \quad (x,t) \in G = \Omega\times(0,T] \equiv (0,1)\times(0,T], \\ u(x,0) = u_0(x), \quad x \in \overline{\Omega}, \\ u(0,t) = u(1,t) = 0, \quad t \in (0,T], \end{cases} \tag{1.4.2}$$

where $\mathscr{L}_\varepsilon u \equiv -\varepsilon u_{xx} + a(x)u_x + b(x)u$, $0 < \varepsilon \ll 1$ is a small parameter and the coefficients a, b are sufficiently smooth functions such that $a(x) \ge \alpha > 0$, $b(x) \ge \beta \ge 0$ on $\overline{\Omega} = [0,1]$.

1.4.3 Semilinear singular perturbation parabolic problem

Here, we consider the following semilinear singular perturbation parabolic PDE of the form

$$\begin{cases} u_t - \varepsilon u_{xx} + a(x)u_x = b(x,t,u), \quad (x,t) \in G = \Omega\times(0,T] \equiv (0,1)\times(0,T], \\ u(x,0) = u_0(x), \quad x \in \overline{\Omega}, \\ u(0,t) = u(1,t) = 0, \quad t \in (0,T], \end{cases} \tag{1.4.3}$$

where ε is the small positive parameter. Under sufficient smoothness and compatibility conditions imposed on the functions $a(x)$, $b(x,t,u)$ and $u_0(x)$ the parabolic problem (1.4.3) in general admits a unique solution $u(x,t)$ which exhibits a boundary layer.

To solve (1.4.3), we use the Newton linearization process and obtain the sequence $\{u^m\}$, for the initial guess u^0 satisfying the initial and boundary conditions of the problem.

1.4.4 Singularly perturbed delay parabolic reaction-diffusion problem

Let $\Omega = (0,1)$, $G = (0,1) \times (0,T]$, and $\Gamma = \Gamma_l \cup \Gamma_b \cup \Gamma_r$, where Γ_l and Γ_r are the left and right sides of the rectangular G corresponding to $x = 0$ and 1, respectively, and $\Gamma_b = [0,1] \times [-\tau, 0]$.

$$\begin{cases} \left(\dfrac{\partial}{\partial t} + \mathcal{L}_\varepsilon\right) u(x,t) = -b(x,t)u(x,t-\tau) + f(x,t), \quad (x,t) \in G, \\ u(x,t) = \phi_b(x,t), \quad (x,t) = \Gamma_b, \\ u(0,t) = \phi_l(t), \quad \text{on } \Gamma_l = \{(0,t) : 0 \le t \le T\}, \\ u(1,t) = \phi_r(t), \quad \text{on } \Gamma_r = \{(0,t) : 0 \le t \le T\}, \end{cases} \tag{1.4.4}$$

where $\mathcal{L}_\varepsilon u(x,t) = -\varepsilon u_{xx}(x,t) + a(x)u(x,t)$, $0 < \varepsilon \ll 1$ and $\tau > 0$ are given constants, $a(x)$, $b(x,t)$, $f(x,t)$, $(x,t) \in \overline{G}$, and $\phi_l(t)$, $\phi_r(t)$, $\phi_b(x,t)$, $(x,t) \in \Gamma$, are sufficiently smooth and bounded functions that satisfy $a(x) \ge 0$, $b(x,t) \ge \beta > 0$, $(x,t) \in \overline{G}$. The terminal time T is assumed to satisfy the condition $T = k\tau$ for some positive integer k.

1.4.5 Singularly perturbed delay parabolic convection-diffusion problem

Let $\Omega = (0,1)$, $G = (0,1) \times (0,T]$, and $\Gamma = \Gamma_l \cup \Gamma_b \cup \Gamma_r$, where Γ_l and Γ_r are the left and right sides of the rectangular G corresponding to $x = 0$ and 1, respectively, and $\Gamma_b = [0,1] \times [-\tau, 0]$:

$$\begin{cases} \left(\dfrac{\partial}{\partial t} + \mathbb{L}_\varepsilon\right) u(x,t) = -b(x,t)u(x,t-\tau) + f(x,t), \quad (x,t) \in G, \\ u(x,t) = \phi_b(x,t), \quad (x,t) = \Gamma_b, \\ u(0,t) = \phi_l(t), \quad \text{on } \Gamma_l = \{(0,t) : 0 \le t \le T\}, \\ u(1,t) = \phi_r(t), \quad \text{on } \Gamma_r = \{(1,t) : 0 \le t \le T\}, \end{cases} \tag{1.4.5}$$

where $\mathbb{L}_\varepsilon u(x,t) = -\varepsilon u_{xx}(x,t) + c(x)u_x(x,t) + a(x,t)u(x,t)$, $0 < \varepsilon \ll 1$ and $\tau > 0$ are given constants, $a(x,t)$, $b(x,t)$, $f(x,t)$, $c(x)$, $(x,t) \in \overline{G}$, and $\phi_l(t)$, $\phi_r(t)$, $\phi_b(x,t)$, $(x,t) \in \Gamma$, are sufficiently smooth and bounded functions, satisfies $a(x,t) \ge 0$, $b(x,t) \ge \beta >$

$0, \quad c(x) \geq \alpha > 0 \quad (x,t) \in \overline{G}$. The terminal time T is assumed to satisfy the condition $T = k\tau$ for some positive integer k.

1.5 General Outline of the Thesis

In this thesis, we develop ε-uniform numerical methods for various singularly perturbed parabolic partial differential equations using adaptive meshes. First, we consider the singularly perturbed reaction-diffusion problems. Here, we use the backward-Euler scheme for the time derivative on uniform mesh and central difference scheme for the spatial derivative on adaptive spatial mesh to solve the problem. The adaptive spatial meshes are generated by using the equidistribution principle. We also derive second-order convergence in the maximum norm in the space and first-order in the time. Numerical experiments are conducted. The numerically results are coincides with the theoretical bound.

Then, convection-diffusion parabolic problems are analyzed. It is well-known that the classical second-order schemes introduce non-physical oscillation in the calculated solution when applied on uniform meshes. The same is true for finite element method with continuous piecewise-linear basis functions on uniform mesh. To overcome such difficulties we need to restrict to lower-order upwind schemes. Although the upwind schemes are of first-order, they are stable schemes. Then, we develop adaptive mesh for the problem using equidistribution principle by the help of a monitor function. The monitor is a linear combination of second-order partial derivative of the singular component of the solution and its total measure. The monitor functions have been analyzed for singular perturbed ordinary differential equation by Beckett and Mackenzie [6, 7]. As the solution of the IBVP (2.1.1) exhibits an exponential layer only in the spatial variable, for that reason we used nonuniform meshes only in the spatial direction. The adaptive meshes are obtained as like in the stationary one-dimensional problem. Uniform meshes are used for the temporal direction. More precisely, at a fixed time level, we obtain the nonuniform adaptive mesh by solving the mesh equidistribution relation, and we use this mesh for all time levels. Therefore, obtaining the adaptive mesh by the present method is very economy. ε–uniform error estimates of order $O(N^{-1} + \Delta\, t)$ are derived in the maximum norm for the numerical solution, where N is number of intervals in the space and Δt is the discretization parameter in the time. Numerical experiments reveal the fact of ε–uniform first-order convergence of the scheme. Also, we apply the moving mesh method for the convection-diffusion and reaction-diffusion problems. It is computationally costlier than the above method but it gives the flexibility of applying to a wide range of problems. Particularly, the moving mesh method works well for the

problem with moving layers than its counterpart of parabolic boundary layers.

Next, we consider the singularly perturbed delay parabolic problems. In these problems, in addition to the source term there will be a delay term. We permit delay only in the time because it is a physically relevant to consider. These problems are solved using adaptive grids and ε-uniform numerical methods. Numerical experiments are carried out to show the convergence rate. The thesis consists of seven chapters and is organized as follows:

In **Chapter 2**, a parameter uniform numerical method are developed for singularly perturbed parabolic reaction-diffusion PDEs of the form (1.4.1) using the equidistribution principle. The method converges second-order in the space and first-order in the time irrespective of the singular perturbation parameter. Numerical experiments are carried to validate the theoretical error estimates.

Chapter 3 presents the analysis for singularly perturbed parabolic convection-diffusion PDEs of the type (1.4.2) using equidistribution principle. The methods converges first-order ε-uniformly in the space as well as in the time. The numerical results reveal the theoretical finding. We also carried out numerical experiment for semilinear convection-diffusion singularly perturbed parabolic PDEs.

Chapter 4 is concerned with the construction of ε-uniform numerical method for singularly perturbed parabolic reaction-diffusion PDEs of the type (1.4.1). Here, the equidistribution grids are obtained on every time level using the equidistribution principle. The method converges second-order in the space and first-order in the time irrespective of the singular perturbation parameter. Numerical experiments are carried to validate the theoretical error estimates.

Chapter 5 is devoted for singularly perturbed parabolic convection-diffusion PDEs of the form (1.4.2). Here, the equidistribution grids are obtained on every time level using the equidistribution principle. The methods converges first-order ε-uniformly in the space as well as in the time. The numerical results carried out to validate theoretical error estimates. We also carried out numerical experiment for semilinear convection-diffusion singularly perturbed parabolic PDEs.

Parameter uniform method for singularly perturbed delay parabolic reaction-diffusion problems of the form (1.4.4) are derived in **Chapter 6**. Here, we used adaptive grids which are obtained using the equidistribution principle. The method converges uniformly second-order in the space and first-order in the time irrespective of the singular perturbation parameter and the delay term. Numerical experiments are carried to validate the theoretical results.

Chapter 7 addresses the derivation of uniform numerical methods for singularly perturbed delay parabolic PDEs of the type (1.4.5). The piecewise-uniform Shishkin

meshes are used for resolving the boundary layer. The above method converges uniformly first-order in the time and first-order up-to logarithmic in the space. Numerical results are given to validate the theoretical error estimates.

In **Chapter 8**, we provided the summary of the results highlighting the contribution made by this thesis and future scope in this direction.

Extensive numerical experiments are conducted to support the theoretical results and also to demonstrate the accuracy of the numerical methods. The corresponding numerical results are presented at the end of each chapter of the thesis. For clarity of the presentation, we have repeatedly described the model problems with suitable information on the given data at the beginning of the subsequent chapters.

CHAPTER 2

Robust Numerical Scheme for Singularly Perturbed Parabolic Reaction-Diffusion Problems on Equidistributed Grid

In this chapter, we propose a parameter-uniform computational technique to solve singularly perturbed parabolic initial-boundary-value problems exhibiting parabolic layers. The domain is discretized with a uniform mesh on the time direction and a nonuniform mesh obtained via equidistribution of a monitor function for the spatial variable. The numerical scheme consists of the implicit-Euler scheme for the time derivative and the classical central difference scheme for the spatial derivative. Truncation error and stability analysis are carried out. Error estimates are derived, and numerical examples are presented.

2.1 Introduction

Consider the singularly perturbed parabolic initial-boundary-value problem (IBVP) in the domain $G = (0,1) \times (0,T]$:

$$\begin{cases} u_t(x,t) + L_\varepsilon u(x,t) = f(x,t), \quad (x,t) \in G, \\ u(x,0) = s(x), \quad \text{on } S_x = \{(x,0) : 0 \le x \le 1\}, \\ u(0,t) = a_0(t), \quad \text{on } S_0 = \{(0,t) : 0 \le t \le T\}, \\ u(1,t) = a_1(t), \quad \text{on } S_1 = \{(1,t) : 0 \le t \le T\}, \end{cases} \tag{2.1.1}$$

where

$$L_\varepsilon u(x,t) \equiv -\varepsilon u_{xx}(x,t) + b(x)u(x,t),$$

$0 < \varepsilon \ll 1$ is a small parameter, and b, f are sufficiently smooth functions with $b(x) \ge \beta > 0$ on $0 \le x \le 1$. Then the required compatibility conditions at the two corners of

the domain G are

$$s(0) = a_0(0), \quad s(1) = a_1(0) \tag{2.1.2}$$

and

$$\begin{aligned} -\varepsilon \frac{d^2 s(0)}{dx^2} + b(0)s(0) + b(0)\frac{da_0(0)}{dt} &= f(0,0), \\ -\varepsilon \frac{d^2 s(1)}{dx^2} + b(1)s(1) + b(1)\frac{da_1(0)}{dt} &= f(1,0). \end{aligned} \tag{2.1.3}$$

The functions s, a_0 and a_1 are sufficiently smooth for the equations (2.1.2) and (2.1.3) to make sense, namely $s \in \mathcal{C}^2(S_x)$, $a_0 \in \mathcal{C}^1(S_0)$ and $a_1 \in \mathcal{C}^1(S_1)$. Under the mentioned continuity and compatibility conditions on the data, the IBVP (2.1.1) has a unique solution $u(x,t)$. Boundary layers occur in the solution when $\varepsilon \to 0$. These boundary layers are neighbors of the boundaries of the domain, where the solution varies rapidly, while away from the layers the solution changes slowly, and smoothly.

Here, the main goal is to provide an ε-uniform method for the IBVP (2.1.1) with an adaptive mesh. We obtain the adaptive mesh through the idea of equidistribution of the singular component $w(x,t)$ at some fixed time T_0, $0 < T_0 \leq T$, because the problem (2.1.1) exhibits boundary layers along the boundary $x = 0$ and $x = 1$ which do not have any effect on time. In this method, the time derivative is replaced by the backward-Euler scheme, and the spatial derivative is replaced by the central difference scheme. The proposed scheme is parameter-uniform convergent of order $O(\Delta t + N^{-2})$. Truncation errors are derived, stability analysis is carried out; and ε-uniform error estimates are obtained.

We organize the rest of the chapter as follows: In Section 2.2, we provide *apriori* bounds on the derivatives of the analytical solution via decomposition. Section 2.3 introduces the finite difference scheme and also adaptive spatial mesh via equidistribution principle. Moreover, we present the detailed numerical algorithm in Section 2.3.3. Afterwards, we carry out the error analysis for the difference scheme in Section 2.4 and prove the main theoretical error estimates, *i.e.,* the ε-uniform optimal error bounds of the difference scheme on the adaptive mesh. Section 2.5 describes application of the present method for semilinear singularly perturbed parabolic PDEs. In Section 2.6, we present the numerical results for two linear parabolic PDEs and a semilinear problem to validate the theoretical results. Finally in Section 2.7, we summarize the main conclusions.

2.2 Analytical Behavior of the Solution

In this section, we present some bounds for the analytical solution $u(x,t)$ of (2.1.1) and its derivatives. The proof of the theorems can be found in the article [55].

Theorem 2.2.1. *Assume that the coefficients of the parabolic PDE, and the initial and boundary conditions given in (2.1.1) are sufficiently smooth, and satisfy the necessary compatibility conditions stated in (2.1.2) and (2.1.3). Then, the IBVP (2.1.1) has a unique solution* $u(x,t) \in \mathcal{C}^{4+\lambda}(\overline{G})$. *Furthermore, the derivatives of the solution* u *satisfy, for all non-negative integers* i, j, *such that* $0 \leq i + 2j \leq 4$,

$$\left\| \frac{\partial^{i+j} u}{\partial x^i \partial t^j} \right\|_\infty \leq C\varepsilon^{-i/2}. \tag{2.2.1}$$

Proof. Refer [55] for the detailed proof. ∎

We shall decompose the solution u as $u = v + w$, where v, w are respectively the regular and the singular components. The regular part is further decomposed into $v = v_0 + \varepsilon v_1$, where

$$\begin{cases} (v_0)_t(x,t) + b(x)v_0(x,t) = f(x,t), & (x,t) \in G, \\ v_0(x,0) = s(x), & \text{on } S_x, \end{cases}$$

and

$$\begin{cases} (v_1)_t(x,t) + L_\varepsilon v_1(x,t) = \dfrac{\partial^2 v_0}{\partial x^2}, & (x,t) \in G, \\ v_1(x,0) = 0, & \text{on } S_x, \\ v_1(0,t) = 0, \quad v_1(1,t) = 0, & \text{on } S_0, S_1. \end{cases}$$

Thus, v satisfies the following IBVP

$$\begin{cases} v_t(x,t) + L_\varepsilon v(x,t) = f(x,t), & (x,t) \in G, \\ v(x,0) = s(x), & \text{on } S_x, \\ v(0,t) = v_0(0,t), \quad v(1,t) = v_0(1,t), & \text{on } S_0, S_1. \end{cases}$$

The singular component w is the solution of the IBVP

$$\begin{cases} w_t(x,t) + L_\varepsilon w(x,t) = 0, & (x,t) \in G, \\ w(x,0) = 0, & \text{on } S_x, \\ w(0,t) = a_0(t) - v_0(0,t), \quad w(1,t) = a_1(t) - v_0(1,t), & \text{on } S_0, S_1. \end{cases}$$

Further, we decompose the singular component w into the left and the right components as $w = w_\ell + w_r$, where w_ℓ and w_r respectively, satisfy the following problems:

$$\begin{cases} (w_\ell)_t(x,t) + L_\varepsilon w_\ell(x,t) = 0, & (x,t) \in G, \\ w_\ell(x,0) = 0, & \text{on } S_x, \\ w_\ell(0,t) = a_0(t) - v_0(0,t), \quad w_\ell(1,t) = 0, & \text{on } S_0, S_1, \end{cases}$$

and

$$\begin{cases} (w_r)_t(x,t) + L_\varepsilon w_r(x,t) = 0, \quad (x,t) \in G, \\ w_r(x,0) = 0, \quad \text{on } S_x, \\ w_r(0,t) = 0, \quad w_r(1,t) = a_1(t) - v_0(1,t), \quad \text{on } S_0, S_1. \end{cases}$$

The regular and the singular components v, and w satisfy the following bounds.

Theorem 2.2.2. *Let $u(x,t)$ be the solution of the IBVP (2.1.1). And assume that the coefficients of the parabolic PDE, and the initial and boundary conditions given in (2.1.1) are sufficiently regular, and satisfy the necessary compatibility conditions. Then, for all non-negative integers i, j, such that $0 \le i + 2j \le 4$, we have*

$$\begin{aligned} &\left\| \frac{\partial^{i+j} v}{\partial x^i \partial t^j} \right\|_\infty \le C(1 + \varepsilon^{1-i/2}), \quad \forall (x,t) \in G, \\ &\left| \frac{\partial^{i+j} w_\ell}{\partial x^i \partial t^j} \right| \le C\varepsilon^{-i/2} \exp\left(-x/\sqrt{\varepsilon}\right), \quad \text{and} \quad \left| \frac{\partial^{i+j} w_r}{\partial x^i \partial t^j} \right| \le C\varepsilon^{-i/2} \exp\left(-(1-x)/\sqrt{\varepsilon}\right). \end{aligned} \tag{2.2.2}$$

Proof. The proof can be found in [55]. ∎

2.3 The Numerical Solution

In this section, we discretize the parabolic IBVP (2.1.1), the time derivative is replaced by the implicit-Euler scheme, and the spatial derivative is replaced by the central difference scheme. Later, we introduce the equidistribution mesh, and derive the finite difference scheme (2.3.2). Finally, we provide the numerical algorithm to obtain the equidistributed mesh.

2.3.1 Finite difference scheme

On the time domain [0,T], we introduce the equidistant meshes with uniform time step Δt such that

$$\overline{\Lambda}_t^M = \{t_n = n\Delta t,\ n = 0, \ldots, M,\ \Delta t = T/M\},$$

where M denotes the number of mesh divisions in the t-direction.

We consider the finite difference approximation of (2.1.1) on a nonuniform spatial discretization

$$\overline{\Omega}_x^N = \{0 = x_0 < x_1 < \cdots < x_N = 1\},$$

and denote the spatial step sizes by

$$h_i = x_i - x_{i-1}, \quad i = 1, \ldots, N.$$

We discretize the PDE (2.1.1) by means of the backward-Euler scheme for the time derivative and the central difference scheme for the spatial derivative. Hence the discretization of (2.1.1) takes the following form, for $n = 0, 1, \ldots, M-1$,

$$\begin{cases} \dfrac{U_i^{n+1} - U_i^n}{\Delta t} + L_\varepsilon^N U_i^{n+1} = f(x_i, t_{n+1}), \quad \text{for } i = 1, \ldots, N-1, \\ U_0^{n+1} = a_0(t_{n+1}), \quad U_N^{n+1} = a_1(t_{n+1}), \\ U_i^0 = s(x_i), \quad \text{for } i = 1, \ldots, N-1, \end{cases} \tag{2.3.1}$$

where L_ε^N is the discretization of the differential operator L_ε using the central difference for the spatial derivative,

$$L_\varepsilon^N U_i^{n+1} = -\varepsilon \delta_x^2 U_i^{n+1} + b_i U_i^{n+1}.$$

After rearranging the terms in (2.3.1), we obtain the following form of the difference scheme, for $n = 0, 1, \ldots, M-1$,

$$\begin{cases} r_i^- U_{i-1}^{n+1} + r_i^c U_i^{n+1} + r_i^+ U_{i+1}^{n+1} = g_i^n, \quad \text{for } i = 1, \ldots, N-1, \\ U_0^{n+1} = a_0(t_{n+1}), \quad U_N^{n+1} = a_1(t_{n+1}), \\ U_i^0 = s(x_i), \quad \text{for } i = 1, \ldots, N-1, \end{cases} \tag{2.3.2}$$

where

$$r_i^- = \frac{-2\varepsilon\Delta t}{h_i(h_i + h_{i+1})}, \qquad r_i^+ = \frac{-2\varepsilon\Delta t}{h_{i+1}(h_i + h_{i+1})}, \qquad r_i^c = 1 + \Delta t b_i - r_i^- - r_i^+,$$
$$b_i = b(x_i), \qquad g_i^n = U_i^n + \Delta t f(x_i, t_{n+1}).$$

To determine the value of the monitor function (2.3.5), we have to know the approximate value of the singular component $w(x,t)$. To calculate the numerical value W_i^n of $w(x_i, t_n)$, we use the numerical approximate value V_i^n of $v(x_i, t_n)$ from the following recurrence relation, for $n = 0, 1, \ldots, M-1$,

$$\begin{cases} (1 + \Delta t b(x_i)) V_i^{n+1} = V_i^n + \Delta t f(x_i, t_{n+1}), \quad \text{for } i = 1, \ldots, N, \\ V_i^0 = s(x_i). \end{cases} \tag{2.3.3}$$

Then, the value of W_i^n will be calculated from $W_i^n = U_i^n - V_i^n$.

2.3.2 Adaptive spatial mesh via equidistribution

Since the solution $u(x,t)$ of the IBVP(2.1.1) exhibits boundary layers (only for the spatial variable), one has to use layer-adapted nonuniform spatial mesh, which are fine

inside the boundary layer region, and coarse in the outer region. To obtain such a mesh, we use the idea of equidistribution of a positive monitor function given in (2.3.5). Here we consider equidistribution of $u(x,t)$ at some fixed time T_0, $0 < T_0 \leq T$, because the problem (2.1.1) exhibits regular layer along the boundaries, which will not have any impact on the temporal component. Moreover, we assume that $u(x,T_0)$ exhibit the layer phenomena. A mesh is said to be equidistributing $u(x,T_0)$, if

$$\int_{x_{i-1}}^{x_i} M(u(s,T_0),s)ds = \int_{x_i}^{x_{i+1}} M(u(s,T_0),s)ds, \quad i = 1,\ldots,N-1, \tag{2.3.4}$$

where $M(u(x,T_0),x)$ is a strictly positive, L_1–integrable function.

Here, we consider the following monitor function

$$M(u(x,T_0),x) = \alpha + |w_{xx}(x,T_0)|^{1/m}, \quad m \geq 2, \tag{2.3.5}$$

where α is a positive constant that is independent of N and $w(x,t)$ is the singular component of the solution $u(x,t)$. One-dimensional version of the monitor function (2.3.5) given by [6] impressed us to take

$$\alpha = \int_0^1 |w_{xx}(s,T_0)|^{1/m} ds. \tag{2.3.6}$$

The selection of this α will help to equally distribute the number of mesh points inside and outside the boundary layer region. The effect of increasing m is to smoothen the monitor function, which in turn leads to a smoother distribution of the mesh points. From [6], one can clearly see the influence of the parameter m. In all of our numerical experiments, we have taken $m = 2$.

In order to compute the approximation of the monitor function at the ith interior node of the spatial mesh, M_i, we assume for some integer S$(0 < S \leq M)$ that $w(x_i,T_0) = W_i^S$, where $S\Delta t = T_0$,

$$M_i = \alpha_{dis} + |\delta_x^2 W_i^S|^{1/m}, \quad \text{for } i = 1,\ldots,N-1, \tag{2.3.7}$$

where $W_i^S = U_i^S - V_i^S$ and α_{dis} is the discrete form of (2.3.6), which can be written as

$$\alpha_{dis} = h_1 \,|\delta_x^2 W_1^S|^{1/m} + \sum_{i=2}^{N-1} h_i \left\{ \frac{|\delta_x^2 W_{i-1}^S|^{1/m} + |\delta_x^2 W_i^S|^{1/m}}{2} \right\} + h_N \,|\delta_x^2 W_{N-1}^S|^{1/m}.$$

For a truly adaptive algorithm, the monitor function has to be approximated from the numerical solution. For example, a simple discretization of (2.3.4) results in the set of equations

$$M_{i-1/2}(x_i - x_{i-1}) = M_{i+1/2}(x_{i+1} - x_i), \quad \text{for } i = 1,\ldots,N-1,$$

where $M_{i\pm1/2}$ is an approximation to $M(u(x_{i\pm1/2},T_0),x_{i\pm1/2})$.

The detailed numerical algorithm to obtain the equidistribution mesh is given in Section 2.3.3.

2.3.3 Numerical algorithm

To get the equidistribution gird and the corresponding numerical solution, we use the following algorithm:

Step 1. Take $k = 0$. Take the uniform spatial mesh $\{x_i^{(0)}\}$ as the initial value for the iteration. Choose a constant $C > 1$ that determines when the algorithm has to be terminated.

Step 2. Compute the discrete solutions $\{U_i^{n,(k)}\}$ and $\{V_i^{n,(k)}\}$ satisfying (2.3.2) and (2.3.3), respectively with the help of the spatial mesh $\{x_i^{(k)}\}$.

Step 3. Find the singular component of the discrete solution by $W_i^{n,(k)} = U_i^{n,(k)} - V_i^{n,(k)}$.

Step 4. For a given mesh $\{x_i^{(k)}\}$ and the singular component of the discrete solution $\{W_i^{n,(k)}\}$, set

$$H_i^{(k)} = \left(\frac{M_{i-1}^{(k)} + M_i^{(k)}}{2}\right)(x_i^{(k)} - x_{i-1}^{(k)}), \quad \text{for } i = 1, \ldots, N,$$

where $M_i^{(k)}$ is calculated from (2.3.7), and set $M_0^{(k)} = M_1^{(k)}$ and $M_N^{(k)} = M_{N-1}^{(k)}$.

Step 5. Set $L_0 = 0$ and $L_i = \sum_{j=1}^{i} H_i^{(k)}$ for $i = 1, \ldots, N$. Define

$$C^{(k)} := \frac{N}{L_N} \max_{i=0,1,\ldots,N} H_i^{(k)}.$$

Step 6. If $C^{(k)} \leq C$, then go to Step 9.

Step 7. Set $Y_i = iL_N/N$ for $i = 0, 1, \ldots, N$. Interpolate the points (L_i, x_i). Generate the new mesh $\{x_i^{(k+1)}\}$ by evaluating this interpolant at Y_i for $i = 0, 1, \ldots, N$.

Step 8. Set $k = k + 1$, return to Step 2.

Step 9. Take $\{x_i^{(k)}\}$ as the final mesh and compute $U_i^{n,(k)}$ then stop.

2.4 Error Analysis

Here, we derive the truncation error for the numerical scheme, and carry out the stability analysis. Finally, we obtain the ε-uniform error estimate.

The following lemma provides the stability result for a general numerical scheme for the IBVP (2.1.1).

Lemma 2.4.1. *Consider the IBVP (2.1.1) and the difference scheme (2.3.1), the difference scheme (excluding the initial and boundary conditions) can be written as*

$$\delta_t U^{n+1} + L_\varepsilon^N U^{n+1} := AU^{n+1} - DU^n = F^n, \quad \text{for } n = 0, \cdots, M-1, \tag{2.4.1}$$

where $U^n = (U_1^n, \cdots, U_{N-1}^n)^T$, F^n *is a vector independent of the computed solution, and* A *and* D *are matrices and also that* A *is an* M*-matrix, and* $D \geq 0$.

Let y *and* z *be two mesh functions, such that* $y^n = (y_0^n, \cdots, y_N^n)^T$, *and* $z^n = (z_0^n, \cdots, z_N^n)^T$ *for each* n. *Assume that* $\left|\delta_t y^{n+1} + L_\varepsilon^N y^{n+1}\right| \leq \delta_t z^{n+1} + L_\varepsilon^N z^{n+1}$, *for* $n = 0, \cdots, M-1$, *and* $|y| \leq z$ *on the boundary* $S_x \cup S_0 \cup S_1$. *Then,* $|y| \leq z$ *on* $\overline{\Omega}_x^N \times \overline{\Lambda}_t^M$.

Proof. The difference scheme (2.3.2) can be written in the form of (2.4.1) with $A = (a_{ij})$ and $D = (d_{ij})$ as

$$a_{i,i-1} = \frac{r_i^-}{\Delta t}, \quad a_{i,i} = \frac{r_i^c}{\Delta t}, \quad a_{i,i+1} = \frac{r_i^+}{\Delta t},$$
$$d_{i,i} = \frac{1}{\Delta t}.$$

Simple calculation shows that the matrix A is an M-matrix and the matrix $D \geq 0$. Therefore, the difference scheme satisfies the hypotheses of the Lemma and immediately the result follows. ∎

Corollary 2.4.2. *The difference scheme given in (2.3.2) satisfies the discrete maximum principle.*

Theorem 2.4.3. *Let* u *and* U *be respectively the continuous and the numerical solutions of the IBVPs (2.1.1), and (2.3.2). Then, we have the following bound, for* $n = 1, 2, \ldots, M$, $i = 0, \ldots, N$,

$$\max_{i,n} |u(x_i, t_n) - U_i^n| \leq C[\Delta t + N^{-2}]. \tag{2.4.2}$$

Proof. Let $\eta_i^n = u_i^n - U_i^n$ be the error in the computed solution at each mesh point (x_i, t_n). Write the scheme (2.3.1) as

$$\delta_t U_i^n + L_\varepsilon^N U_i^n = f_i^n, \quad i = 1, \ldots, N-1, \quad n = 1, \ldots, M.$$

Then at each point $(x_i, t_n) \in \overline{\Omega}_x^N \times \overline{\Lambda}_t^M$, the truncation error of the scheme is given by

$$\delta_t \eta_i^n + L_\varepsilon^N \eta_i^n = \chi_{1,i}^n + \chi_{2,i}^n,$$

where

$$\chi_{1,i}^n := L_\varepsilon^N u_i^n - (L_\varepsilon u)_i^n \quad \text{and} \quad \chi_{2,i}^n := \delta_t u_i^n - (u_t)_i^n,$$

are the truncation errors for the spatial and the temporal discretizations, respectively.

Decompose η as $\eta = \phi + \psi$. Here the function ϕ_i^n is, for each fixed $n = 1, 2, \ldots, M$, the solution of the discrete two-point boundary-value problem

$$\begin{cases} L_\varepsilon^N \phi_i^n = \chi_{1,i}^n \quad \text{for } i = 1, \ldots, N-1, \\ \phi_0^n = \phi_N^n = 0, \end{cases} \tag{2.4.3}$$

while ψ_i^n, the solution of the discrete parabolic problem, defined by, for $n = 1, 2, \ldots, M$,

$$\begin{cases} \delta_t \psi_i^n + L_\varepsilon^N \psi_i^n = \chi_{2,i}^n - \delta_t \phi_i^n \quad \text{for } i = 1, \ldots, N-1, \\ \psi_0^n = \psi_N^n = 0 \quad \text{for } n = 1, \ldots, M, \\ \psi_i^0 = -\phi_i^0 \quad \text{for } i = 0, \ldots, N. \end{cases} \tag{2.4.4}$$

Equation (2.4.3) is precisely the same identity as one gets when analyzing the error ϕ in a two-point boundary-value problem that has been discretized using L_ε^N, with $\chi_{1,i}^n$ playing the role of truncation error and can be bounded using technique from [7] and the inequality (2.2.1) with $j = 0$. The problem (2.1.1) exhibits regular boundary layers and the same is true for the equation (2.4.3) consequently the error bound derived in [7] can be invoked for all temporal levels:

$$|\phi_i^n| \leq CN^{-2}, \quad \text{for all } i, n, \tag{2.4.5}$$

with the assumption that $N^{-1} \gg \sqrt{\varepsilon}$ and the fact that our problem exhibits regular boundary layers.

Next, consider the other error component ψ. Lemma 2.4.1 implies that the problem (2.4.4) satisfies a discrete maximum principle just as (2.3.1) does, so

$$\begin{aligned} \|\psi\|_\infty &= C \left(\max_i |\phi_i^0| + \|\chi_2 - \delta_t \phi\|_\infty \right) \\ &= C \left[N^{-2} + \Delta t + \|\delta_t \phi\|_\infty \right], \end{aligned} \tag{2.4.6}$$

where we used (2.4.5) with $n = 0$ and also

$$|\chi_{2,i}^n| \leq C\Delta t \quad \text{for } i = 1, \ldots, N-1 \text{ and } n = 1, \ldots, M,$$

which is easily verified by using the Taylor's expansion and (2.2.1). It remains to deal only with $\delta_t \phi$ in (2.4.6). Using the assumption that $b = b(x)$ is independent of t, simple calculation shows that for each fixed n, the definition (2.4.3) implies that $\delta_t \phi$ satisfies, for $n = 1, \ldots, M$,

$$\begin{cases} L_\varepsilon^N (\delta_t \phi)_i^n = \delta_t \chi_{1,i}^n \quad \text{for } i = 1, \ldots, N-1, \\ (\delta_t \phi)_0^n = (\delta_t \phi)_N^n = 0. \end{cases} \tag{2.4.7}$$

To analyze the discrete two-point boundary-value problem (2.4.7), observe that

$$\begin{aligned}\delta_t\chi_{1,i}^n &= \frac{1}{\Delta t}\left(\chi_{1,i}^n - \chi_{1,i}^{n-1}\right)\\ &= \frac{1}{\Delta t}\left((L_\varepsilon^N u_i^n - (L_\varepsilon u)_i^n) - (L_\varepsilon^N u_i^{n-1} - (L_\varepsilon u)_i^{n-1})\right)\\ &= \frac{1}{\Delta t}\left((L_\varepsilon^N u_i^n - L_\varepsilon^N u_i^{n-1}) - ((L_\varepsilon u)_i^n - (L_\varepsilon u)_i^{n-1})\right).\end{aligned}$$

Let $\hat{L}_\varepsilon u = -\varepsilon u_{xx}$ and $\hat{L}_\varepsilon^N u_i^n = -\varepsilon\delta_x^2 u_i^n$. That is, $\hat{L}_\varepsilon^N u$ is the discretization of $\hat{L}_\varepsilon u$. Then one can write the above formula as

$$\delta_t\chi_{1,i}^n = \frac{1}{\Delta t}\int_{t_{n-1}}^{t_n}[\hat{L}_\varepsilon^N u_t(x_i,t) - \hat{L}_\varepsilon u_t(x_i,t)].$$

Hence, using the Peano kernel theorem as in [38], one can obtain the same estimate on $\delta_t\chi_{1,i}^n$ as the corresponding truncation error bounds arising in [7] for a standard two-point reaction-diffusion boundary-value problem, since the bounds of (2.2.1) are unaffected by the presence of an extra $t-$derivative.

This observation implies that (2.4.7) can be analyzed in the same way as (2.4.3), except that one uses the bound (2.2.1) with $j = 1$. We therefore obtain

$$|\delta_t\phi_i^n| \le CN^{-2} \quad \text{for all } i, n. \tag{2.4.8}$$

Combining (2.4.5), (2.4.6) and (2.4.8), we get (2.4.2). ∎

2.5 Semilinear Parabolic Problem

In this section, we consider the following semilinear singularly perturbed parabolic PDE of the form

$$\begin{cases} u_t - \varepsilon u_{xx} = b(x,t,u), & (x,t)\in G,\\ u(x,0) = u_0(x), & x\in\Omega,\\ u(0,t) = u(1,t) = 0, & t\in[0,T], \end{cases} \tag{2.5.1}$$

where $0 < \varepsilon \ll 1$ is a parameter. We assume that b is continuous in $\overline{\Omega}\times[0,T]\times\mathbb{R}$, is differentiable in the third argument, for some non-negative constants γ and $\bar{\gamma}$, satisfies

$$0 < \gamma \le b_s(x,t,s) \le \bar{\gamma} \quad \text{for } (x,t,s)\in\overline{\Omega}\times[0,T]\times\mathbb{R}.$$

We also assume the functions u_0 is sufficiently smooth. Under sufficient compatibility conditions imposed on the functions $b(x,t,u)$ and $u_0(x)$, the parabolic problem (2.5.1), in general, admits a unique solution $u(x,t)$ which exhibits boundary layers. For more information on the existence and the uniqueness of the IBVP (2.5.1) one can refer [45].

To solve (2.5.1), we use the Newton linearization process and obtain the sequence $\{u^m\}$ for the initial guess u^0 satisfying the initial and boundary conditions of the problem. Thus we define u^{m+1} for each fixed m, to be the solution of the following linear parabolic IBVP:

$$\begin{cases} u_t^{m+1} - \varepsilon u_{xx}^{m+1} - b^m(x,t)u^{m+1} = f^m(x,t), \quad (x,t) \in G \\ u^{m+1}(x,0) = u_0(x), \quad 0 < x < 1, \\ u^{m+1}(0,t) = 0, \quad u^{m+1}(1,t) = 0, \quad 0 \le t \le T, \end{cases} \tag{2.5.2}$$

where $m \geq 0$ and $b^m(x,t)$ and $f^m(x,t)$ are given by

$$\begin{cases} b^m(x,t) = b_u(x,t,u^m), \\ f^m(x,t) = b(x,t,u^m) - b^m(x,t)u^m. \end{cases} \tag{2.5.3}$$

Hence for a fixed m, we solve (2.5.2) using the computational method discussed earlier. Moreover, we assume that the problem admits regular boundary layers. Numerical results of (2.5.1) are presented in the following section.

2.6 Numerical Results

In this section, we shall present the numerical results obtained by the discrete scheme (2.3.2) for two linear problems and a semilinear test problem on the rectangular mesh $\overline{G}^{N,\Delta t} = \overline{\Omega}_x^N \times \overline{\Lambda}_t^M$, where $\overline{\Omega}_x^N$ is the equidistribution mesh obtained from the numerical algorithm. In all the numerical experiments we will fix $m = 2$ and $T_0 = 1$, which is necessary to define the monitor function (2.3.5). Moreover, in all the tables we begin with $N = 32$ and the time step $\Delta t = 0.1$ and we multiply N by two and divide Δt by four. The reason for dividing Δt by four is to highlight the spatial order of convergence properly.

Example 2.6.1. *Consider the following parabolic initial-boundary-value problem:*

$$u_t(x,t) - \varepsilon u_{xx}(x,t) + u(x,t) = f(x,t), \quad (x,t) \in (0,1) \times (0,1]. \tag{2.6.1}$$

The right-hand side source term, initial and boundary conditions are calculated from the exact solution

$$u(x,t) = \left(t + \frac{x^2}{2\varepsilon}\right) \operatorname{erfc}\left(\frac{x}{2\sqrt{\varepsilon t}}\right) - \sqrt{\frac{t}{\pi\varepsilon}}\, x \exp\left(\frac{-x^2}{4\varepsilon t}\right),$$

where erfc is the complementary error function. As the exact solution of the problem (2.6.1) is known, for each ε, we calculate the maximum point-wise error by

$$e_\varepsilon^{N,\Delta t} = \max_{(x_i,t_n) \in \overline{G}^{N,\Delta t}} |u(x_i,t_n) - U^{N,\Delta t}(x_i,t_n)|,$$

where $u(x_i, t_n)$ and $U^{N,\Delta t}(x_i, t_n)$ respectively, denote the exact and the numerical solution obtained on the mesh with N mesh intervals in the spatial direction and M mesh intervals in the $t-$direction such that $\Delta t = T/M$ is the uniform time step. In addition, we determine the corresponding rate of convergence by

$$p_\varepsilon^{N,\Delta t} = \log_2 \left(\frac{e_\varepsilon^{N,\Delta t}}{e_\varepsilon^{2N,\Delta t/4}} \right).$$

The calculated maximum point-wise errors $e_\varepsilon^{N,\Delta t}$ and the corresponding rate of convergence $p_\varepsilon^{N,\Delta t}$ for Example 2.6.1 are given in Table 2.1 and Table 2.2, respectively. From these results one can observe that the ε-uniform first-order convergence of the numerical solution.

Further, we have calculated the normalized flux

$$F_\varepsilon u(x,t) = \sqrt{\varepsilon} \frac{\partial u(x,t)}{\partial x},$$

and its numerical approximation

$$F_\varepsilon^N U^{N,\Delta t}(x_i, t_n) = \sqrt{\varepsilon} \delta_x^+ U_i^n.$$

The errors in the normalized flux is calculated as

$$r_\varepsilon^{N,\Delta t} = \max_{1 \le n \le M} |F_\varepsilon u(x_0, t_n) - F_\varepsilon^N U^{N,\Delta t}(x_0, t_n)|,$$

and the rate of convergence is determined from

$$q_\varepsilon^{N,\Delta t} = \log_2 \left(\frac{r_\varepsilon^{N,\Delta t}}{r_\varepsilon^{2N,\Delta t/4}} \right).$$

The calculated maximum point-wise errors in the normalized flux $r_\varepsilon^{N,\Delta t}$ and the corresponding rate of convergence $q_\varepsilon^{N,\Delta t}$ for Example 2.6.1 are given in Table 2.3 and Table 2.4, respectively. Again, one can see the ε–uniform convergence in Table 2.3, and the first-order convergence rate from Table 2.4. In Figures 2.1 (a) and (b), the maximum point-wise errors in the solution and the normalized flux are plotted respectively, which reflect the fact of first-order convergence independent of ε.

Example 2.6.2. *Consider the following parabolic initial-boundary-value problem:*

$$\begin{cases} u_t - \varepsilon u_{xx} + \left(\sqrt{x+1}\right) u = 1, \quad (x,t) \in (0,1) \times (0,1], \\ u(x,0) = 0, \quad 0 < x < 1, \\ u(0,t) = 0, \quad u(1,t) = 0, \quad 0 \le t \le 1. \end{cases} \tag{2.6.2}$$

Table 2.1: *Maximum point-wise error of the solution* $e_\varepsilon^{N,\Delta t}$ *for Example* 2.6.1 *using equidistribution mesh.*

	Number of Intervals N/Time Step Size Δt					
ε	$32/\frac{1}{10}$	$64/\frac{1}{40}$	$128/\frac{1}{160}$	$256/\frac{1}{640}$	$512/\frac{1}{2560}$	$1024/\frac{1}{10240}$
10^{0}	8.3624e-03	2.6269e-03	7.1243e-04	1.8369e-04	4.6626e-05	1.1745e-05
10^{-2}	9.5404e-03	2.7104e-03	7.2159e-04	1.8606e-04	4.7251e-05	1.1905e-05
10^{-4}	9.5334e-03	2.7205e-03	7.3760e-04	1.8837e-04	4.7627e-05	1.1983e-05
10^{-6}	9.6177e-03	2.7165e-03	7.2577e-04	1.8717e-04	4.7525e-05	1.2266e-05
10^{-8}	9.6062e-03	2.7314e-03	7.2639e-04	1.8723e-04	4.7546e-05	1.1978e-05
10^{-10}	9.5997e-03	2.7503e-03	7.2762e-04	1.8755e-04	4.7532e-05	1.1980e-05

Table 2.2: *Rate of convergence of the solution* $p_\varepsilon^{N,\Delta t}$ *for Example* 2.6.1 *using equidistribution mesh.*

	Number of Intervals N/Time Step Size Δt				
ε	$32/\frac{1}{10}$	$64/\frac{1}{40}$	$128/\frac{1}{160}$	$256/\frac{1}{640}$	$512/\frac{1}{2560}$
10^{0}	1.6705	1.8826	1.9554	1.9781	1.9891
10^{-2}	1.8155	1.9093	1.9554	1.9773	1.9887
10^{-4}	1.8091	1.8829	1.9693	1.9837	1.9907
10^{-6}	1.8239	1.9042	1.9551	1.9776	1.9541
10^{-8}	1.8143	1.9108	1.9560	1.9774	1.9889
10^{-10}	1.8034	1.9183	1.9559	1.9803	1.9883

Table 2.3: *Maximum point-wise error of the normalized flux* $r_\varepsilon^{N,\Delta t}$ *for Example* 2.6.1 *using equidistribution mesh.*

	Number of Intervals N/Time Step Size Δt					
ε	$32/\frac{1}{10}$	$64/\frac{1}{40}$	$128/\frac{1}{160}$	$256/\frac{1}{640}$	$512/\frac{1}{2560}$	$1024/\frac{1}{10240}$
10^{0}	5.3355e-02	2.7699e-02	1.3932e-02	6.9761e-03	3.4893e-03	1.7448e-03
10^{-2}	8.7792e-02	4.3418e-02	2.1557e-02	1.0736e-02	5.3570e-03	2.6756e-03
10^{-4}	9.6645e-02	4.6782e-02	2.3437e-02	1.2285e-02	5.9339e-03	2.9212e-03
10^{-6}	1.0178e-01	4.8033e-02	2.3727e-02	1.1715e-02	5.8266e-03	2.9129e-03
10^{-8}	9.9448e-02	5.0228e-02	2.4087e-02	1.1768e-02	5.8576e-03	2.9163e-03
10^{-10}	1.0395e-01	5.3663e-02	2.4445e-02	1.2024e-02	5.8370e-03	2.9196e-03

Table 2.4: *Rate of convergence of the normalized flux* $q_\varepsilon^{N,\Delta t}$ *for Example* 2.6.1 *using equidistribution mesh.*

	Number of Intervals N/Time Step Size Δt				
ε	$32/\frac{1}{10}$	$64/\frac{1}{40}$	$128/\frac{1}{160}$	$256/\frac{1}{640}$	$512/\frac{1}{2560}$
10^{0}	0.9458	0.9914	0.9979	0.9995	0.9999
10^{-2}	1.0158	1.0101	1.0057	1.0030	1.0016
10^{-4}	1.0467	0.9972	0.9319	1.0498	1.0224
10^{-6}	1.0834	1.0175	1.0182	1.0076	1.0002
10^{-8}	0.9855	1.0602	1.0334	1.0065	1.0062
10^{-10}	0.9539	1.1344	1.0236	1.0426	0.9995

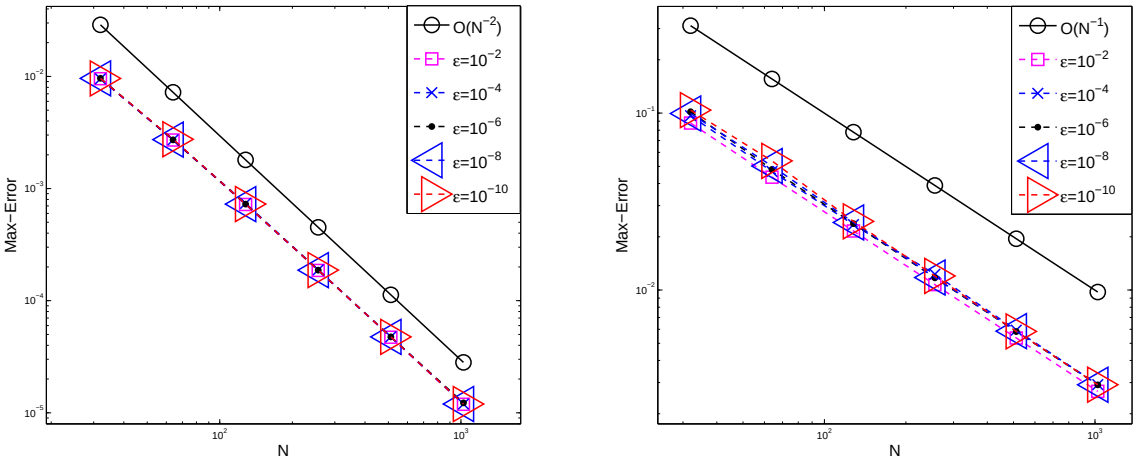

(a) *Maximum point-wise error of the solution* $e_\varepsilon^{N,\Delta t}$.

(b) *Maximum point-wise error of the normalized flux* $r_\varepsilon^{N,\Delta t}$.

Figure 2.1: *Loglog plot for Example 2.6.1.*

As the exact solution of the problem (2.6.2) is not known, to obtain the accuracy of the numerical solution and also to demonstrate the $\varepsilon-$uniform convergence of the proposed scheme, we use the double mesh principle which is given in the following. The numerical solution of IBVP (2.6.2) is plotted in Figures 2.2 (a) and (b) for $\varepsilon = 1e-1$ and $\varepsilon = 1e-4$, respectively. These figures show the existence of the boundary layer near $x = 1$.

Let $\widetilde{U}^{2N,\Delta t/4}(x_i, t_n)$ be the numerical solution obtained on the fine mesh $\widetilde{G}^{2N,\Delta t/4} = \overline{\Omega}_x^{2N} \times \overline{\Lambda}_t^{4M}$ with $2N$ mesh intervals in the spatial direction and $4M$ mesh intervals in the $t-$direction. Then for each ε, we calculate the maximum point-wise error by

$$E_\varepsilon^{N,\Delta t} = \max_{(x_i,t_n)\in\overline{G}^{N,\Delta t}} \left| U^{N,\Delta t}(x_i, t_n) - \widetilde{U}^{2N,\Delta t/4}(x_i, t_n) \right|,$$

and the corresponding rate of convergence by

$$P_\varepsilon^{N,\Delta t} = \log_2 \left(\frac{E_\varepsilon^{N,\Delta t}}{E_\varepsilon^{2N,\Delta t/4}} \right).$$

The calculated maximum point-wise errors $E_\varepsilon^{N,\Delta t}$ and the corresponding rate of convergence $P_\varepsilon^{N,\Delta t}$ for Example 2.6.2 are given in Table 2.5 and Table 2.6, respectively. The numerical results given in these tables reveal the first-order convergence independent of the diffusion parameter ε.

Further, the errors in the normalized flux have been calculated as

$$R_\varepsilon^{N,\Delta t} = \max_{1\le n\le M} |F_\varepsilon^N U^{N,\Delta t}(x_N, t_n) - F_\varepsilon^N \widetilde{U}^{2N,\Delta t/4}(x_N, t_n)|,$$

and the rate of convergence is determined from

$$Q_\varepsilon^{N,\Delta t} = \log_2 \left(\frac{R_\varepsilon^{N,\Delta t}}{R_\varepsilon^{2N,\Delta t/4}} \right).$$

The calculated maximum point-wise errors in the normalized flux $R_\varepsilon^{N,\Delta t}$ and the corresponding rate of convergence $Q_\varepsilon^{N,\Delta t}$ for Example 2.6.2 are given in Table 2.7 and Table 2.8, respectively. The maximum point-wise errors are plotted in log-log scale in Figures 2.3 (a) and (b), for the solution and the normalized flux, respectively. From these figures, one can easily observe the first-order ε–uniform convergence.

Example 2.6.3. *Consider the following semilinear parabolic initial-boundary-value problem:*

$$u_t(x,t) - \varepsilon u_{xx}(x,t) + \exp(u(x,t)) = f(x,t), \quad (x,t) \in (0,1)\times(0,1]. \tag{2.6.3}$$

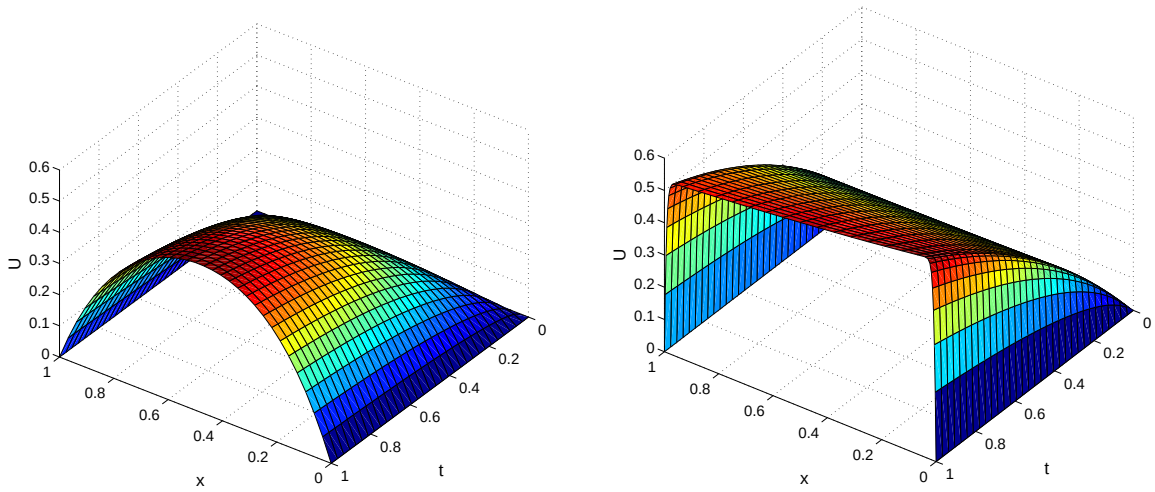

(a) $\varepsilon = 10^{-1}$. (b) $\varepsilon = 10^{-4}$.

Figure 2.2: *Numerical solution of Example 2.6.2 for* $N = 32$ *and* $\Delta t = 1/32$.

Table 2.5: *Maximum point-wise error of the solution* $E_\varepsilon^{N,\Delta t}$ *for Example* 2.6.2 *using equidistribution mesh.*

	Number of Intervals N/Time Step Size Δt				
ε	$64/\frac{1}{10}$	$128/\frac{1}{40}$	$256/\frac{1}{160}$	$512/\frac{1}{640}$	$1024/\frac{1}{2560}$
10^{0}	1.0917e-02	3.8150e-03	1.0572e-03	2.7173e-04	6.8413e-05
10^{-2}	1.4096e-02	3.7384e-03	9.5054e-04	2.3869e-04	5.9756e-05
10^{-4}	1.3535e-02	3.6162e-03	9.4849e-04	2.3289e-04	5.8590e-05
10^{-6}	1.3226e-02	3.5997e-03	8.9781e-04	2.3232e-04	5.8252e-05
10^{-8}	1.3310e-02	3.5222e-03	9.0320e-04	2.3240e-04	5.8142e-05
10^{-10}	1.4050e-02	3.6114e-03	9.2446e-04	2.2594e-04	5.6480e-05

Table 2.6: *Rate of convergence of the solution* $P_\varepsilon^{N,\Delta t}$ *for Example* 2.6.2 *using equidistribution mesh.*

	Number of Intervals N/Time Step Size Δt			
ε	$64/\frac{1}{10}$	$128/\frac{1}{40}$	$256/\frac{1}{160}$	$512/\frac{1}{640}$
10^{0}	1.5169	1.8515	1.9600	1.9898
10^{-2}	1.9148	1.9756	1.9936	1.9980
10^{-4}	1.9041	1.9308	2.0260	1.9909
10^{-6}	1.8775	2.0034	1.9503	1.9957
10^{-8}	1.9179	1.9634	1.9584	1.9989
10^{-10}	1.9599	1.9659	2.0327	2.0002

Table 2.7: *Maximum point-wise error of the normalized flux* $R_\varepsilon^{N,\Delta t}$ *for Example* 2.6.2 *using equidistribution mesh.*

	Number of Intervals N/Time Step Size Δt				
ε	$64/\frac{1}{10}$	$128/\frac{1}{40}$	$256/\frac{1}{160}$	$512/\frac{1}{640}$	$1024/\frac{1}{2560}$
10^{0}	4.0516e-02	1.5649e-02	7.4488e-03	3.7028e-03	1.8486e-03
10^{-2}	2.8779e-02	1.3846e-02	6.8861e-03	3.4549e-03	1.7334e-03
10^{-4}	2.4718e-02	1.1629e-02	5.3376e-03	2.9149e-03	1.5512e-03
10^{-6}	2.3159e-02	1.2046e-02	6.2308e-03	3.2183e-03	1.6336e-03
10^{-8}	2.2182e-02	1.1756e-02	6.1431e-03	3.2159e-03	1.6105e-03
10^{-10}	2.1247e-02	1.0875e-02	5.9366e-03	3.2089e-03	1.6278e-03

Table 2.8: *Rate of convergence of the normalized flux* $Q_\varepsilon^{N,\Delta t}$ *for Example* 2.6.2 *using equidistribution mesh.*

	Number of Intervals N/Time Step Size Δt			
ε	$64/\frac{1}{10}$	$128/\frac{1}{40}$	$256/\frac{1}{160}$	$512/\frac{1}{640}$
10^{0}	1.3724	1.0710	1.0084	1.0022
10^{-2}	1.0556	1.0077	0.9950	0.9950
10^{-4}	1.0879	1.1234	0.8727	0.9101
10^{-6}	0.9430	0.9511	0.9531	0.9782
10^{-8}	0.9160	0.9364	0.9337	0.9977
10^{-10}	0.9663	0.8733	0.8876	0.9791

The right-hand side source term, initial and boundary conditions are calculated from the exact solution

$$u(x,t) = \left(t + \frac{x^2}{2\varepsilon}\right) \operatorname{erfc}\left(\frac{x}{2\sqrt{\varepsilon t}}\right) - \sqrt{\frac{t}{\pi\varepsilon}}\, x \exp\left(\frac{-x^2}{4\varepsilon t}\right),$$

where erfc is the complementary error function.

If we use the Newton linearization process given in (2.5.2), we obtain the following system of linear singularly perturbed parabolic PDEs:

$$\begin{cases} u_t^{m+1} - \varepsilon u_{xx}^{m+1} + \exp(u^m)u^{m+1} = f(x,t) - \exp(u^m)(1-u^m), \quad (x,t) \in (0,1)\times(0,1], \\ u^{m+1}(x,0) = u(x,0), \quad 0 < x < 1, \\ u^{m+1}(0,t) = u(0,t), \quad u^{m+1}(1,t) = u(1,t), \quad 0 \le t \le 1. \end{cases} \tag{2.6.4}$$

Hence for each fixed m, we solve (2.6.4) using the computational methods discussed earlier. Once we get the prescribed tolerance error bound we terminate the computation and take that as the solution to the problem.

As the exact solution of the problem (2.6.3) is known, for each ε, we calculate the maximum point-wise error by

$$\tilde{e}_\varepsilon^{N,\Delta t} = \max_{(x_i,t_n)\in\overline{G}^{N,\Delta t}} |u(x_i,t_n) - U^{N,\Delta t}(x_i,t_n)|,$$

where $u(x_i,t_n)$ and $U^{N,\Delta t}(x_i,t_n)$ respectively, denote the exact and the numerical solution obtained on the mesh with N mesh intervals in the spatial direction and M mesh intervals in the $t-$direction such that $\Delta t = T/M$ is the uniform time step. In addition, we determine the corresponding rate of convergence by

$$\tilde{p}_\varepsilon^{N,\Delta t} = \log_2\left(\frac{\tilde{e}_\varepsilon^{N,\Delta t}}{\tilde{e}_\varepsilon^{2N,\Delta t/4}}\right).$$

The calculated maximum point-wise errors $\tilde{e}_\varepsilon^{N,\Delta t}$ and the corresponding rate of convergence $\tilde{p}_\varepsilon^{N,\Delta t}$ for Example 2.6.3 are given in Table 2.9 and Table 2.10, respectively. From these results one can observe the ε–uniform first-order convergence of the numerical solution.

The errors in the normalized flux have been calculated as

$$\tilde{r}_\varepsilon^{N,\Delta t} = \max_{1\le n\le M} |F_\varepsilon u(x_0,t_n) - F_\varepsilon^N U^{N,\Delta t}(x_0,t_n)|,$$

and the rate of convergence is determined from

$$\tilde{q}_\varepsilon^{N,\Delta t} = \log_2\left(\frac{\tilde{r}_\varepsilon^{N,\Delta t}}{\tilde{r}_\varepsilon^{2N,\Delta t/4}}\right).$$

Table 2.9: *Maximum point-wise error of the solution* $\tilde{e}_{\varepsilon}^{N,\Delta t}$ *for Example* 2.6.3 *using equidistribution mesh.*

	Number of Intervals N/Time Step Size Δt					
ε	$32/\frac{1}{10}$	$64/\frac{1}{40}$	$128/\frac{1}{160}$	$256/\frac{1}{640}$	$512/\frac{1}{2560}$	$1024/\frac{1}{10240}$
10^{0}	8.3530e-03	2.6259e-03	7.1230e-04	1.8369e-04	4.6626e-05	1.1745e-05
10^{-2}	9.5058e-03	2.7076e-03	7.2145e-04	1.8605e-04	4.7250e-05	1.1905e-05
10^{-4}	9.4968e-03	2.7178e-03	7.3745e-04	1.8835e-04	4.7626e-05	1.1983e-05
10^{-6}	9.5866e-03	2.7136e-03	7.2560e-04	1.8717e-04	4.7525e-05	1.2264e-05
10^{-8}	9.5733e-03	2.7296e-03	7.2625e-04	1.8722e-04	4.7546e-05	1.1978e-05
10^{-10}	9.5725e-03	2.7475e-03	7.2749e-04	1.8754e-04	4.7531e-05	1.1979e-05

Table 2.10: *Rate of convergence of the solution* $\tilde{p}_{\varepsilon}^{N,\Delta t}$ *for Example* 2.6.3 *using equidistribution mesh.*

	Number of Intervals N/Time Step Size Δt				
ε	$32/\frac{1}{10}$	$64/\frac{1}{40}$	$128/\frac{1}{160}$	$256/\frac{1}{640}$	$512/\frac{1}{2560}$
10^{0}	1.6695	1.8822	1.9553	1.9780	1.9891
10^{-2}	1.8118	1.9080	1.9552	1.9773	1.9887
10^{-4}	1.8050	1.8818	1.9691	1.9836	1.9907
10^{-6}	1.8208	1.9030	1.9549	1.9776	1.9542
10^{-8}	1.8103	1.9101	1.9558	1.9773	1.9889
10^{-10}	1.8007	1.9172	1.9557	1.9802	1.9883

The calculated maximum point-wise errors in the normalized flux $\tilde{r}_{\varepsilon}^{N,\Delta t}$ and the corresponding rate of convergence $\tilde{q}_{\varepsilon}^{N,\Delta t}$ for Example 2.6.3 are given in Table 2.11 and Table 2.12. Again, one can see the ε–uniform convergence in Table 2.11, and the first-order convergence rate from Table 2.12.

2.7 Conclusions

In this chapter, we solved the singularly perturbed time-dependent reaction-diffusion problems (2.1.1) numerically by finite difference scheme on layer-adapted nonuniform grids obtained equidistributing the monitor function given in (2.3.5). The truncation error and stability analysis are obtained. The proposed numerical scheme is of first-order convergent in the temporal variable and second-order convergent in the spatial variable, *i.e.*, $O(\Delta t + N^{-2})$. Error estimates are derived for the numerical scheme, which are

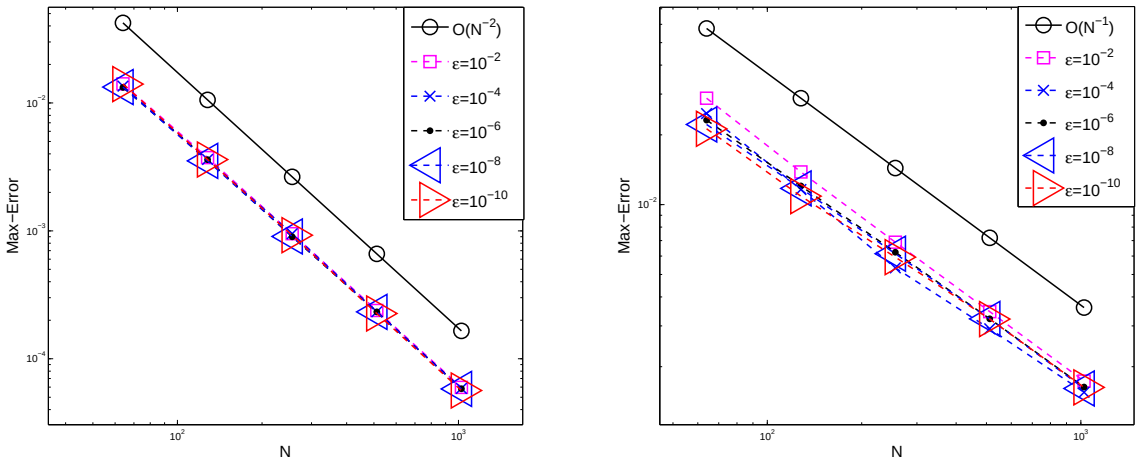

(a) *Maximum point-wise error of the solution* $E_\varepsilon^{N,\Delta t}$.

(b) *Maximum point-wise error of the normalized flux* $R_\varepsilon^{N,\Delta t}$.

Figure 2.3: *Loglog plot for Example 2.6.2.*

Table 2.11: *Maximum point-wise error of the normalized flux* $\tilde{r}_\varepsilon^{N,\Delta t}$ *for Example* 2.6.3 *using equidistribution mesh.*

	Number of Intervals N/Time Step Size Δt					
ε	$32/\frac{1}{10}$	$64/\frac{1}{40}$	$128/\frac{1}{160}$	$256/\frac{1}{640}$	$512/\frac{1}{2560}$	$1024/\frac{1}{10240}$
10^{0}	2.2918e-02	1.2507e-02	6.3366e-03	3.1787e-03	1.5906e-03	7.9548e-04
10^{-2}	4.3572e-02	2.2997e-02	1.1821e-02	5.9944e-03	3.0187e-03	1.5148e-03
10^{-4}	5.3688e-02	2.6997e-02	1.7934e-02	7.8518e-03	3.7102e-03	1.8090e-03
10^{-6}	6.0318e-02	2.8525e-02	1.4424e-02	7.1679e-03	3.5816e-03	2.5805e-03
10^{-8}	5.7455e-02	3.1194e-02	1.4862e-02	7.2315e-03	3.6193e-03	1.8034e-03
10^{-10}	6.2618e-02	3.5452e-02	1.5299e-02	7.5450e-03	3.5942e-03	1.8074e-03

Table 2.12: *Rate of convergence of the normalized flux* $\tilde{q}_\varepsilon^{N,\Delta t}$ *for Example* 2.6.3 *using equidistribution mesh.*

	Number of Intervals N/Time Step Size Δt				
ε	$32/\frac{1}{10}$	$64/\frac{1}{40}$	$128/\frac{1}{160}$	$256/\frac{1}{640}$	$512/\frac{1}{2560}$
10^{0}	0.8737	0.9810	0.9953	0.9988	0.9997
10^{-2}	0.9219	0.9602	0.9796	0.9897	0.9948
10^{-4}	0.9918	0.5901	1.1916	1.0815	1.0363
10^{-6}	1.0804	0.9837	1.0089	1.0010	0.4729
10^{-8}	0.8812	1.0696	1.0393	0.9986	1.0050
10^{-10}	0.8207	1.2124	1.0199	1.0698	0.9918

independent of the diffusion parameter ε. Numerical results reveal the theoretical error estimate.

CHAPTER 3

ε-Uniform Numerical Scheme for Singularly Perturbed Convection-Diffusion Parabolic Initial-Boundary-Value Problems on Equidistributed Grids

In this chapter, we study the numerical solution of singularly perturbed parabolic convection-diffusion problems exhibiting regular boundary layers. To solve these problems, we use the classical backward-Euler difference scheme for the time variable on uniform mesh and upwind finite difference scheme for the spatial variable on layer-adapted nonuniform meshes. The nonuniform meshes are obtained by equidistribution of a positive monitor function, which depends on the second-order spatial derivative of the singular component of the solution. Truncation errors are obtained and the stability analysis is carried out. The parameter-uniform error estimates are derived for the numerical solution. Semilinear and quasilinear IBVPs are also solved. To support the theoretical results, numerical experiments are carried out.

3.1 Introduction

Here, we consider the following singularly perturbed parabolic initial-boundary-value problem (IBVP):

$$\begin{cases} u_t(x,t) + \mathscr{L}_\varepsilon u(x,t) = f(x,t), \quad (x,t) \in G = \Omega \times (0,T] \equiv (0,1) \times (0,T], \\ u(x,0) = u_0(x), \quad x \in \Omega, \\ u(0,t) = u(1,t) = 0, \quad t \in [0,T], \end{cases} \tag{3.1.1}$$

where

$$\mathscr{L}_\varepsilon u \equiv -\varepsilon u_{xx} + a(x)u_x + b(x)u,$$

$0 < \varepsilon \ll 1$ is a small parameter and the coefficients a, b are sufficiently smooth functions such that

$$a(x) \geq \alpha > 0, \quad b(x) \geq \beta \geq 0 \quad \text{on} \quad \overline{\Omega} = [0, 1]. \tag{3.1.2}$$

Let $u_0(x) \in \mathcal{C}^2[0, 1]$ with $u_0(0) = 0$ and $u_0(1) = 0$. Assume also that

$$-\varepsilon \frac{d^2 u_0(0)}{dx^2} + a(0)\frac{du_0(0)}{dx} + b(0)u_0(0) = f(0, 0),$$
$$-\varepsilon \frac{d^2 u_0(1)}{dx^2} + a(1)\frac{du_0(1)}{dx} + b(1)u_0(1) = f(1, 0).$$

Under the above smoothness and compatibility conditions imposed on the functions u_0 and f, the IBVP (3.1.1), in general admits a unique solution $u(x, t)$ [78] which exhibits a regular boundary layer of width $\mathrm{O}(\varepsilon)$ at $x = 1$. The boundary of the domain G is defined as $\partial G := \overline{G} \setminus G$, where $\overline{G}$ is the closure of the domain G.

Singularly perturbed parabolic convection-diffusion problems of the form (3.1.1) arise in various branches of science and engineering. The well-known examples are the Navier-Stokes equation with large Reynolds number in fluid dynamics, the convective heat transport problems with large Péclet number, etc. Numerical treatment of the IBVP (3.1.1) is difficult because of the presence of the boundary layer in its solution. In particular, classical finite difference methods on uniform meshes fail to yield satisfactory numerical results and to obtain stability one has to reduce the spatial step-size with respect to ε.

Here, our main objective is to provide an ε–uniform convergent numerical scheme for singularly perturbed parabolic PDEs (3.1.1), via layer-adapted nonuniform grids obtained through equidistribution of a monitor function (which contains only the second-order spatial derivative of the singular component of the solution). In all the existing articles in the literature, the nonuniform grids were obtained by solving two PDEs, one the original equation, and the other one corresponding to the mesh distribution (for both the spatial and temporal grids). But, here, in this chapter, as a first time, we are using the idea of equidistributing the spatial grids for a fixed time level. This will help to reduce the computational cost as well as the round-off error. Here, we solve the parabolic IBVP (3.1.1) numerically by the finite difference scheme on an adaptive mesh obtained through equidistribution of a positive monitor function, which is a linear combination of a constant and the second-order spatial derivative of the singular component of the solution. As the solution of the IBVP (3.1.1) exhibits an exponential layer only in the spatial variable, we will use nonuniform meshes only in the spatial direction obtained as like in the stationary one-dimensional problem, and uniform meshes for the temporal direction. More precisely, at a fixed time level, we obtain the nonuniform adaptive mesh by solving the mesh equidistribution relation and we use this mesh for all time levels.

Therefore, obtaining the adaptive mesh by the present method is very economy. The time derivative in the PDE (3.1.1) is approximated by the backward-Euler scheme, and an upwind finite difference is used to discretize the spatial derivatives. ε–uniform error estimates of order $O(N^{-1} + \Delta t)$ are derived for the numerical solution, where N is number of intervals in space and Δt is the discretization parameter in time. Numerical experiments reveal the fact of ε–uniform first-order convergence of the scheme.

This chapter is organized in the following manner: Section 3.2 studies the bound on the analytic solution of the IBVP (3.1.1), and the bounds on the regular and the singular components of the solution. Section 3.3 presents the idea behind the adaptive meshes through equidistribution, the numerical scheme and the numerical algorithm to obtain the adaptive meshes. The ε–uniform error estimates are obtained in Section 3.4. Numerical results are presented in Section 3.6, and this chapter ends with the conclusions.

3.2 The Analytic Solution

In the study of the numerical aspects of SPPs, their analytical aspects play an important role. In this section, we are concerned with the analytical aspects that will be required to prove the convergence.

Lemma 3.2.1. (**Maximum principle**) *Let $\psi(x,t) \geq 0$ for all $(x,t) \in \partial G$ and $\psi_t(x,t) + \mathscr{L}_\varepsilon \psi(x,t) \geq 0$ for all $(x,t) \in G$, then $\psi(x,t) \geq 0$ for all $(x,t) \in \overline{G}$.*

Proof. The proof of this theorem can be found in [78]. ∎

We decompose the exact solution $u(x,t)$ of the IBVP (3.1.1) into the regular and the singular components as

$$u(x,t) = v(x,t) + w(x,t), \quad (x,t) \in \overline{G}.$$

We take further decomposition of the regular component v for any prescribed order k by

$$v(x,t) = \sum_{j=0}^{k+1} \varepsilon^j v_j(x,t), \quad (x,t) \in \overline{G},$$

where the functions v_j, $j = 0, 1, \ldots, k$, are the solutions of the following first-order problems

$$\begin{cases} (v_0)_t + a(x)(v_0)_x + b(x)v_0 = f(x,t), & (x,t) \in (0,1] \times (0,T], \\ v_0(x,0) = u(x,0), & 0 \leq x \leq 1, \\ v_0(0,t) = u(0,t), & 0 \leq t \leq T, \end{cases} \tag{3.2.1}$$

and

$$\begin{cases} (v_j)_t + a(x)(v_j)_x + b(x)v_j = (v_{j-1})_{xx}(x,t), \quad j = 1,2,\ldots,k, \quad (x,t) \in (0,1] \times (0,T], \\ v_j(x,0) = 0, \quad 0 \le x \le 1, \\ v_j(0,t) = 0, \quad 0 \le t \le T, \end{cases} \tag{3.2.2}$$

and lastly, the function v_{k+1} satisfies

$$\begin{cases} (v_{k+1})_t(x,t) + \mathscr{L}_\varepsilon v_{k+1}(x,t) = (v_k)_{xx}(x,t), \quad (x,t) \in G, \\ v_{k+1}(x,0) = 0, \quad 0 \le x \le 1, \\ v_{k+1}(0,t) = 0 = v_{k+1}(1,t), \quad 0 \le t \le T. \end{cases} \tag{3.2.3}$$

Hence, the regular component $v(x,t)$ satisfies the following IBVP:

$$\begin{cases} v_t(x,t) + \mathscr{L}_\varepsilon v(x,t) = f(x,t), \quad (x,t) \in G, \\ v(x,0) = u(x,0), \quad 0 \le x \le 1, \\ v(0,t) = u(0,t), \quad 0 \le t \le T, \\ v(1,t) = \displaystyle\sum_{j=0}^{k+1} \varepsilon^j v_j(1,t), \quad 0 \le t \le T, \end{cases} \tag{3.2.4}$$

and therefore, the singular component $w(x,t)$ must satisfies the homogeneous problem

$$\begin{cases} w_t(x,t) + \mathscr{L}_\varepsilon w(x,t) = 0, \quad (x,t) \in G, \\ w(x,0) = 0, \quad 0 \le x \le 1, \\ w(0,t) = 0, \quad 0 \le t \le T, \\ w(1,t) = u(1,t) - v(1,t), \quad 0 \le t \le T. \end{cases} \tag{3.2.5}$$

Theorem 3.2.2. *Let $u(x,t)$ be the solution of (3.1.1). The derivatives of $u(x,t)$ satisfy the following bound*

$$\left| \frac{\partial^k u(x,t)}{\partial x^k} \right| \le C \left(1 + \varepsilon^{-k} \exp(-\alpha(1-x)/\varepsilon)\right), \quad (x,t) \in \overline{G}, \ k = 0,1,$$

for any $t \in [0,T]$.

Proof. The proof of this theorem can be found in [18]. ∎

Theorem 3.2.3. *Let $w(x,t)$ be the solution of (3.2.5). The bound of $w(x,t)$ is given by*

$$|w(x,t)| \le C \exp(-\alpha(1-x)/\varepsilon), \qquad \forall (x,t) \in \overline{G}.$$

Proof. Consider the barrier functions

$$\psi^{\pm}(x,t) = C\exp(-\alpha(1-x)/\varepsilon)\exp(t) \pm w(x,t), \quad (x,t) \in \overline{G}.$$

The values of $\psi^{\pm}(x,t)$ at the boundaries are

$$\begin{aligned}
\psi^{\pm}(0,t) &= C\exp(-\alpha/\varepsilon)\exp(t) \pm w(0,t), \quad 0 \le t \le T \\
&= C\exp(-\alpha/\varepsilon)\exp(t), \quad \text{using (3.2.5)} \\
&\ge 0, \quad 0 \le t \le T
\end{aligned}$$

$$\begin{aligned}
\psi^{\pm}(1,t) &= C\exp(t) \pm w(1,t), \quad 0 \le t \le T \\
&\ge 0, \quad \text{by choosing } C \text{ sufficiently large, } 0 \le t \le T
\end{aligned}$$

$$\begin{aligned}
\psi^{\pm}(x,0) &= C\exp(-\alpha(1-x)/\varepsilon) \pm w(x,0), \quad 0 \le x \le 1 \\
&= C\exp(-\alpha(1-x)/\varepsilon), \quad \text{using (3.2.5)} \\
&\ge 0, \quad 0 \le x \le 1
\end{aligned}$$

Thus from the above estimates, we have

$$\psi^{\pm}(x,t) \ge 0, \quad \forall (x,t) \in \partial G.$$

Now, from the differential equation, we obtain that

$$\begin{aligned}
\psi_t^{\pm}(x,t) + \mathscr{L}_{\varepsilon}\psi^{\pm}(x,t) &= (\psi_t^{\pm} - \varepsilon\psi_{xx}^{\pm} + a(x)\psi_x^{\pm} + b(x)\psi^{\pm})(x,t) \\
&\ge C\exp(-\alpha(1-x)/\varepsilon)\exp(t)\left[1 - \frac{\alpha^2}{\varepsilon} + \frac{a(x)\alpha}{\varepsilon} + b(x)\right] \\
&\ge C\exp(-\alpha(1-x)/\varepsilon)\exp(t)[1+\beta], \quad \text{using (3.1.2).}
\end{aligned}$$

Now by using the maximum principle given in Lemma 3.2.1, we obtain

$$\psi^{\pm}(x,t) \ge 0, \quad \forall (x,t) \in \overline{G}.$$

That is, for all $(x,t) \in \overline{G}$, we have

$$\begin{aligned}
|w(x,t)| &\le C\exp(-\alpha(1-x)/\varepsilon)\exp(t) \\
&\le C\exp(-\alpha(1-x)/\varepsilon)\exp(T) \\
&\le C\exp(-\alpha(1-x)/\varepsilon).
\end{aligned}$$

■

Theorem 3.2.4. *For all non-negative integers p, q satisfying $0 \le p+q \le k+2$, and with sufficient compatibility condition at the corners, the regular component $v(x,t)$ and the singular component $w(x,t)$, defined in (3.2.4) and (3.2.5), respectively, satisfy the following bounds*

$$\left\| \frac{\partial^{p+q} v}{\partial x^p \partial t^q}(x,t) \right\|_\infty \le C\big(1+\varepsilon^{k+1-p}\big), \quad (x,t) \in G$$

and

$$\left| \frac{\partial^{p+q} w}{\partial x^p \partial t^q}(x,t) \right| \le C\varepsilon^{-p} \exp\big(-\alpha(1-x)/\varepsilon\big), \quad (x,t) \in G.$$

Proof. Refer [66] for the detailed proof for $k=3$. The arguments presented in [66] can be extended for any arbitrary k. ∎

3.3 The Numerical Approximation

In this section, we study the semidiscretization of the parabolic IBVP (3.1.1) which is essential for the proof of convergence analysis of the fully discrete scheme, then we obtain the condition for stability and the error estimate. Later, we introduce the equidistribution mesh, and derive the finite difference scheme (3.3.12). Finally, we provide the numerical algorithm to obtain the equidistributed meshes.

3.3.1 Semidiscretization

On the time domain [0,T], we introduce the equidistant meshes with uniform time step Δt such that $\overline{\Lambda}_t^M = \{t_n = n\Delta t,\ n = 0,\dots,M,\ \Delta t = T/M\}$, where M denotes the number of mesh intervals in the t-direction.

Discretizing the IBVP (3.1.1) with respect to the time by the backward-Euler scheme, we obtain the following semidiscrete problem.

$$\begin{cases} u^0(x) = u(x,0) = u_0(x), \quad x \in \Omega, \\ (I + \Delta t \mathscr{L}_\varepsilon) u^{n+1}(x) = u^n(x) + \Delta t f(x, t_{n+1}), \quad x \in \Omega, \quad n = 0,1,\dots,M-1, \\ u^{n+1}(0) = u^{n+1}(1) = 0, \quad n = 0,1,\dots,M-1, \end{cases} \tag{3.3.1}$$

where $u^n(x)$ is the semidiscrete approximation to the exact solution $u(x,t)$ of the continuous problem (3.1.1) at time level $t_n = n\Delta t$.

In order to analyze the uniform convergence of the solution $u^n(x)$ of (3.3.1) to the exact solution $u(x,t_n)$, we will do the stability analysis and also derive the consistency result for the scheme (3.3.1). It is clear that the operator $(I + \Delta t \mathscr{L}_\varepsilon)$ satisfies the

following maximum principle result

$$\|(I + \Delta t \mathscr{L}_\varepsilon)^{-1}\|_\infty \leq \frac{1}{1 + \beta \Delta t}, \tag{3.3.2}$$

which ensures the stability of the scheme (3.3.1). We define the local error e_{n+1} of the time semidiscretization scheme (3.3.1)

$$e_{n+1} = u(x, t_{n+1}) - \widehat{u}^{n+1}(x),$$

where $\widehat{u}^{n+1}(x)$ is the solution obtained after one step of the semidiscrete scheme (3.3.1) by taking the exact value $u(x, t_n)$, instead of $u^n(x)$ as the starting data. Consequently, we have the following system, for $n = 0, 1, \ldots, M-1$

$$\begin{cases} (I + \Delta t \mathscr{L}_\varepsilon)\widehat{u}^{n+1}(x) = u(x, t_n) + \Delta t f(x, t_{n+1}), \quad x \in \Omega, \\ \widehat{u}^{n+1}(0) = \widehat{u}^{n+1}(1) = 0. \end{cases} \tag{3.3.3}$$

Now, from [18] one can obtain the following consistency result.

Lemma 3.3.1. *Assume that*

$$\left| \frac{\partial^i}{\partial t^i} u(x, t) \right| \leq C, \quad (x, t) \in \overline{G}, \quad 0 \leq i \leq 2.$$

Then, the local error corresponding to the scheme (3.3.1) satisfies

$$\| e_{n+1} \|_\infty \leq C(\Delta t)^2. \tag{3.3.4}$$

Finally, combining the consistency result (3.3.4) with the stability result (3.3.2) of the scheme (3.3.1), we deduce the following convergence result.

Theorem 3.3.2. *Under the hypothesis of Lemma 3.3.1, we have*

$$\sup_{n \leq T/\Delta t} \| u(t_n) - u^n \|_\infty \leq C \Delta t. \tag{3.3.5}$$

Therefore, the time semidiscretization process is uniformly convergent of first-order in time.

3.3.2 Adaptive spatial meshes via equidistribution

Since the solution $u(x, t)$ of the IBVP (3.1.1) exhibits a boundary layer only at $x = 1$, one has to use layer-adapted nonuniform spatial meshes, which are fine inside the boundary layer region, and coarse in the outer region. To obtain such a mesh, we use the idea of equidistribution of a positive monitor function given in (3.3.7). Here we consider equidistribution of $u(x, t)$ at some fixed time T_0, $0 < T_0 \leq T$, because the problem

(3.1.1) exhibits a regular layer only along the boundary $x = 1$, which will not have any impact on the temporal component. Moreover, we assume that $u(x, T_0)$ exhibit the layer phenomena. A mesh is said to be equidistributing $u(x, T_0)$, if

$$\int_{x_{i-1}}^{x_i} M(u(s, T_0), s)ds = \int_{x_i}^{x_{i+1}} M(u(s, T_0), s)ds, \quad i = 1, \ldots, N-1, \tag{3.3.6}$$

where $M(u(x, T_0), x)$ is a strictly positive, L_1–integrable function.

Here, we consider the following monitor function

$$M(u(x, T_0), x) = \alpha_c + |w_{xx}(x, T_0)|^{1/m}, \quad m \geq 2, \tag{3.3.7}$$

where α_c is a positive constant that is independent of N and $w(x, t)$ is the singular component of the solution $u(x, t)$. One-dimensional version of the monitor function (3.3.7) given by Beckett and Mackenzie [6] suggests that to distribute grid points evenly we have to take

$$\alpha_c = \int_0^1 |w_{xx}(s, T_0)|^{1/m} ds. \tag{3.3.8}$$

The selection of this α_c will help to equally distribute the number mesh points inside and outside the boundary layer region. The effect of increasing m is to smoothen the monitor function, which in turn leads to a smoother distribution of the mesh points. From [6], we clearly notice the influence of the parameter m. In all of our numerical experiments, we have $m = 2$.

In order to compute the value of the monitor function $M(u(x, T_0), x)$ at the ith interior node of the spatial mesh, M_i, we assume without loss of generality that $w(x_i, T_0) = W_i^S$, where $S\Delta t = T_0$,

$$M_i = \alpha_{dis} + |\delta_x^2 W_i^S|^{1/m}, \quad \text{for } i = 1, \ldots, N-1, \tag{3.3.9}$$

where α_{dis} is the discrete form of (3.3.8), which can be written as

$$\alpha_{dis} = h_1 \, |\delta_x^2 W_1^S|^{1/m} + \sum_{i=2}^{N-1} h_i \left\{ \frac{|\delta_x^2 W_{i-1}^S|^{1/m} + |\delta_x^2 W_i^S|^{1/m}}{2} \right\} + h_N \, |\delta_x^2 W_{N-1}^S|^{1/m}.$$

For a truly adaptive algorithm, the monitor function has to be approximated from the numerical solution. For example, a simple discretization of (3.3.6) results in the set of equations

$$M_{i-1/2}(x_i - x_{i-1}) = M_{i+1/2}(x_{i+1} - x_i), \quad \text{for } i = 1, \ldots, N-1, \tag{3.3.10}$$

where $M_{i+1/2}$ is an approximation to $M(u(x_{i+1/2}, T_0), x_{i+1/2})$. This is equivalent to the approximation of the monitor function by the piecewise-constant function.

The detailed numerical algorithm to obtain the equidistribution meshes is given in Section 3.3.4.

3.3.3 Finite difference scheme

We consider the finite difference approximation of (3.3.1) on a nonuniform spatial discretization given by

$$\overline{\Omega}_x^N = \{0 = x_0 < x_1 < \cdots < x_N = 1\}$$

and the spatial step sizes are denoted by

$$h_i = x_i - x_{i-1}, \quad i = 1, \ldots, N.$$

The simple upwind finite difference spatial discretization of (3.3.1) takes the form, for $n = 0, 1, \ldots, M-1$,

$$\begin{cases} (I + \Delta t \mathscr{L}_\varepsilon^N) U_i^{n+1} = U_i^n + \Delta t f(x, t_{n+1}), & \text{for } i = 1, \ldots, N-1, \\ U_0^{n+1} = U_N^{n+1} = 0, \end{cases} \tag{3.3.11}$$

where $\mathscr{L}_\varepsilon^N$ is the discretization of the differential operator $\mathscr{L}_\varepsilon$ using the upwind finite difference scheme for the spatial derivatives, which takes the following form

$$\mathscr{L}_\varepsilon^N U_i^{n+1} = -\varepsilon \delta_x^2 U_i^{n+1} + a_i \delta_x^- U_i^{n+1} + b_i U_i^{n+1}.$$

After rearranging the terms in (3.3.11), we obtain the following form of the difference scheme: for $n = 0, 1, \ldots, M-1$,

$$\begin{cases} r_i^- U_{i-1}^{n+1} + r_i^c U_i^{n+1} + r_i^+ U_{i+1}^{n+1} = g_i^n, & \text{for } i = 1, \ldots, N-1, \\ U_0^{n+1} = U_N^{n+1} = 0, \end{cases} \tag{3.3.12}$$

where

$$r_i^- = \frac{-2\varepsilon \Delta t}{h_i(h_i + h_{i+1})} - \frac{a_i \Delta t}{h_i}, \qquad r_i^+ = \frac{-2\varepsilon \Delta t}{h_{i+1}(h_i + h_{i+1})}, \qquad r_i^c = 1 + \Delta t b_i - r_i^- - r_i^+,$$

$$a_i = a(x_i), \qquad b_i = b(x_i), \qquad g_i^n = U_i^n + \Delta t f(x_i, t_{n+1}).$$

To determine the value of the monitor function (3.3.7), we have to know the approximate value of the singular component $w(x,t)$. To calculate the numerical value W_i^n of $w(x_i, t_n)$, we use the numerical approximate value V_i^n of $v(x_i, t_n)$ from the following recurrence relation: for $n = 0, 1, \ldots, M-1$,

$$\begin{cases} (I + \Delta t \mathscr{L}_0^N) V_i^{n+1} \equiv \tilde{r}_i^- V_{i-1}^{n+1} + \tilde{r}_i^c V_i^{n+1} = \tilde{g}_i^n, & \text{for } i = 1, \ldots, N, \\ V_0^{n+1} = 0, \end{cases} \tag{3.3.13}$$

where

$$\tilde{r}_i^- = -\frac{a_i \Delta t}{h_i}, \qquad \tilde{r}_i^c = 1 + \Delta t b_i - \tilde{r}_i^-,$$

$$a_i = a(x_i), \qquad b_i = b(x_i), \qquad \tilde{g}_i^n = V_i^n + \Delta t f(x_i, t_{n+1}).$$

Then, the value of W_i^n will be calculated from $W_i^n = U_i^n - V_i^n$.

3.3.4 Numerical algorithm

To obtain the equidistribution gird and the corresponding numerical solution, we use the following algorithm:

Step 1. Let $k = 0$. Take the uniform spatial mesh $\{x_i^{(0)}\}$ as the initial value for the iteration. Choose a constant $C_0 > 1$ that determines when the algorithm has to be terminated.

Step 2. Compute the discrete solutions $\{U_i^{n,(k)}\}$ and $\{V_i^{n,(k)}\}$ satisfying (3.3.12) and (3.3.13), respectively with the help of the spatial mesh $\{x_i^{(k)}\}$.

Step 3. Find the singular component of the discrete solution by $W_i^{n,(k)} = U_i^{n,(k)} - V_i^{n,(k)}$.

Step 4. For a given mesh $\{x_i^{(k)}\}$ and the singular component of the discrete solution $\{W_i^{n,(k)}\}$, set

$$H_i^{(k)} = \left(\frac{M_{i-1}^{(k)} + M_i^{(k)}}{2}\right)(x_i^{(k)} - x_{i-1}^{(k)}), \quad \text{for } i = 1, \ldots, N,$$

where $M_i^{(k)}$ is calculated from (3.3.9), and set $M_0^{(k)} = M_1^{(k)}$ and $M_N^{(k)} = M_{N-1}^{(k)}$.

Step 5. Set $L_0 = 0$ and $L_i = \sum_{j=1}^{i} H_j^{(k)}$ for $i = 1, \ldots, N$. Define

$$C^{(k)} := \frac{N}{L_N} \max_{i=0,1,\ldots,N} H_i^{(k)}.$$

Step 6. If $C^{(k)} \leq C_0$, then go to Step 9.

Step 7. Set $Y_i = iL_N/N$ for $i = 0, 1, \ldots, N$. Interpolate the points (L_i, x_i). Generate the new mesh $\{x_i^{(k+1)}\}$ by evaluating this interpolant at Y_i for $i = 0, 1, \ldots, N$.

Step 8. Set $k = k + 1$, return to Step 2.

Step 9. Take $\{x_i^{(k)}\}$ as the final mesh and compute $U_i^{n,(k)}$ then stop.

For the convergence of the algorithm one can refer [43], where the authors analyzed the predetermined number of iterations for ε-uniform convergence, the results are proved for the well-known arc-length monitor function, different from the one given in (3.3.7).

3.4 Error Analysis

Here, we study the consistency and the stability of the proposed numerical scheme (3.3.12). Finally, we analyze the ε-uniform convergence of the numerical solution on the adaptive mesh obtained through the monitor function (3.3.7).

Instead of analyzing the fully discrete scheme (3.3.12), we will analysis the following discrete scheme of (3.3.3) and we will generalize that result to the fully discretize scheme (3.3.12). Applying the upwind finite difference to the problem (3.3.3), we obtain for $n = 0, 1, \ldots, M-1$,

$$\begin{cases} (I + \Delta t \mathscr{L}_\varepsilon^N)\widehat{U}_i^{n+1} \equiv r_i^- \widehat{U}_{i-1}^{n+1} + r_i^c \widehat{U}_i^{n+1} + r_i^+ \widehat{U}_{i+1}^{n+1} = \widehat{g}_i^n, \quad \text{for } i = 1, \ldots, N-1, \\ U_0^{n+1} = U_N^{n+1} = 0, \end{cases} \tag{3.4.1}$$

where

$$r_i^- = \frac{-2\varepsilon\Delta t}{h_i(h_i + h_{i+1})} - \frac{a_i \Delta t}{h_i}, \qquad r_i^+ = \frac{-2\varepsilon\Delta t}{h_{i+1}(h_i + h_{i+1})}, \qquad r_i^c = 1 + \Delta t b_i - r_i^- - r_i^+,$$
$$a_i = a(x_i), \qquad b_i = b(x_i), \qquad \widehat{g}_i^n = u(x_i, t_n) + \Delta t f(x_i, t_{n+1}).$$

3.4.1 Decomposition of numerical solution

As like in the continuous solution, we decompose the numerical solution into the regular and the singular components. That is, we decompose $\widehat{U}_i^n$ as

$$\widehat{U}_i^n = \widehat{V}_i^n + \widehat{W}_i^n, \quad 1 \le i \le N,\ 1 \le n \le M, \tag{3.4.2}$$

where

$$\begin{aligned} (I + \Delta t \mathscr{L}_\varepsilon^N)\widehat{V}_i^{n+1} &= v(x_i, t_n) + \Delta t f(x_i, t_{n+1}), \\ \widehat{V}_0^{n+1} = v(x_0, t_{n+1}),\ \widehat{V}_N^{n+1} &= v(x_N, t_{n+1}), \end{aligned} \tag{3.4.3}$$

and

$$(I + \Delta t \mathscr{L}_\varepsilon^N)\widehat{W}_i^{n+1} = w(x_i, t_n), \quad \widehat{W}_0^{n+1} = w(x_0, t_{n+1}),\ \widehat{W}_N^{n+1} = w(x_N, t_{n+1}), \tag{3.4.4}$$

and $n = 0, 1, \ldots, M-1$. Now, the error at the mesh points in the numerical solution can also be decomposed as

$$|\widehat{u}^{n+1}(x_i) - \widehat{U}_i^{n+1}| \le |\widehat{v}^{n+1}(x_i) - \widehat{V}_i^{n+1}| + |\widehat{w}^{n+1}(x_i) - \widehat{W}_i^{n+1}|, \tag{3.4.5}$$

where $\widehat{v}$ and $\widehat{w}$ are the regular and the singular components of the solution $\widehat{u}$, respectively.

Lemma 3.4.1. (**Discrete comparison principle**) *The system* $(I + \Delta t\mathscr{L}_\varepsilon^N)u_i^{n+1} = g_i^n$, *with* u_0^{n+1} *and* u_N^{n+1} *specified, has a unique solution. If* $(I + \Delta t\mathscr{L}_\varepsilon^N)u_i^{n+1} \leq (I + \Delta t\mathscr{L}_\varepsilon^N)v_i^{n+1}$, $1 \leq i \leq N-1$, *and if* $u_0^{n+1} \leq v_0^{n+1}$, $u_N^{n+1} \leq v_N^{n+1}$, *then* $u_i^{n+1} \leq v_i^{n+1}$, $1 \leq i \leq N-1$.

Proof. The matrix associated with $(I + \Delta t\mathscr{L}_\varepsilon^N)$ is an irreducible M-matrix and so has a positive inverse. Hence, the result follows. ∎

Lemma 3.4.2. *The error of the regular component satisfies* $|\widehat{v}^{n+1}(x_i) - \widehat{V}_i^{n+1}| \leq CN^{-1}$, *for* $n = 0, 1, \ldots, M-1$.

Proof. The local truncation error of the regular component at the node (x_i, t_{n+1}) will be given by

$$\begin{aligned}
\tau_{i,n+1}^{\widehat{V}} &= \left(I + \Delta t\mathscr{L}_\varepsilon^N\right)\left(\widehat{v}^{n+1}(x_i) - \widehat{V}_i^{n+1}\right) \\
&= r_i^-\widehat{v}^{n+1}(x_{i-1}) + r_i^c\widehat{v}^{n+1}(x_i) + r_i^+\widehat{v}^{n+1}(x_{i+1}) - (v(x_i, t_n) + \Delta t f(x_i, t_{n+1})) \\
&= r_i^-\widehat{v}^{n+1}(x_{i-1}) + r_i^c\widehat{v}^{n+1}(x_i) + r_i^+\widehat{v}^{n+1}(x_{i+1}) - (I + \Delta t\mathscr{L}_\varepsilon)\,\widehat{v}^{n+1}(x_i).
\end{aligned}$$

Using the Peano's kernel theorem for every value of n, the truncation error of the the regular component reduces to

$$\begin{aligned}
\tau_{i,n+1}^{\widehat{V}} = &-\frac{\Delta t\varepsilon}{(h_i + h_{i+1})}\left\{\frac{1}{h_{i+1}}\int_{x_i}^{x_{i+1}}(s - x_{i+1})^2(\widehat{v}^{n+1})'''(s)ds\right. \\
&\left.-\frac{1}{h_i}\int_{x_{i-1}}^{x_i}(s - x_{i-1})^2(\widehat{v}^{n+1})'''(s)ds\right\} - \frac{\Delta t a(x(i))}{h_{i-1}}\int_{x_{i-1}}^{x_i}(s - x_{i-1})(\widehat{v}^{n+1})''(s)ds.
\end{aligned}$$

We obtain the bound

$$|\tau_{i,n+1}^{\widehat{V}}| \leq \Delta t\varepsilon\int_{x_{i-1}}^{x_{i+1}}|(\widehat{v}^{n+1})'''(s)|ds + \Delta t\tilde{\alpha}\int_{x_{i-1}}^{x_i}|(\widehat{v}^{n+1})''(s)|ds,$$

where $\tilde{\alpha}$ is the upper bound of $a(x)$ for $x \in [0, 1]$. If we use the bounds of the regular part $\widehat{v}$ this may be simplified to

$$|\tau_{i,n+1}^{\widehat{V}}| \leq C\int_{x_{i-1}}^{x_{i+1}}\left(|(\widehat{v}^{n+1})''(s)| + |(\widehat{v}^{n+1})'(s)| + |(\widehat{v}^{n+1})(s)| + 1\right)ds.$$

From the bound of the regular part $\widehat{v}$ and the spatial discretization satisfying the equidistribution principle (3.3.6) with the monitor function given in (3.3.9), the local truncation error of the regular component reduces to

$$|\tau_{i,n+1}^{\widehat{V}}| \leq CN^{-1}, \quad \text{for } i = 1, 2, \ldots, N-1,\ n = 0, 1, \ldots, M-1.$$

That is,

$$\left|\left(I+\Delta t\mathscr{L}_\varepsilon^N\right)\left(\widehat{v}^{n+1}(x_i)-\widehat{V}_i^{n+1}\right)\right| \le CN^{-1}, \text{ for } i=1,2,\ldots,N-1,\ n=0,1,\ldots,M-1.$$

Now using the fact that the operator $\left(I+\Delta t\mathscr{L}_\varepsilon^N\right)$ satisfies the discrete maximum principle (Lemma 3.4.1) and the inverse operator is uniformly bounded, we can conclude that

$$|\widehat{v}^{n+1}(x_i)-\widehat{V}_i^{n+1}| \le CN^{-1}, \quad \text{for } i=1,2,\ldots,N-1,\ n=0,1,\ldots,M-1.$$

This completes the proof. ∎

Lemma 3.4.3. *Numerical solution of the singular component satisfies*

$$|\widehat{W}_i^{n+1}| \le C\prod_{k=i+1}^{N}\left(1+\frac{\alpha h_k}{m\varepsilon}\right)^{-1}, \quad \textit{for } i=0,1,\ldots,N-1,\ n=0,1,\ldots,M-1$$

and

$$|\widehat{W}_N^{n+1}| \le C, \quad \textit{for } n=0,1,\ldots,M-1.$$

Proof. Define

$$S_i := \prod_{k=i+1}^{N}\left(1+\frac{\alpha h_k}{m\varepsilon}\right)^{-1}, \quad \text{for } i=0,1,\ldots,N-1,$$
$$S_N := 1.$$

We know from (3.4.4) that

$$\widehat{W}_N^{n+1} \le C = CS_N.$$

Similarly, we have

$$\begin{aligned}\widehat{W}_0^{n+1} &\le C\exp\left(-\frac{\alpha}{\varepsilon}\right) \le C\exp\left(-\frac{\alpha}{m\varepsilon}\right)\\ &\le C\prod_{k=1}^{N}\exp\left(-\frac{\alpha h_k}{m\varepsilon}\right)\\ &< C\prod_{k=1}^{N}\left(1+\frac{\alpha h_k}{m\varepsilon}\right)^{-1}\end{aligned}$$

and

$$\begin{aligned}\left(I+\Delta t\mathscr{L}_\varepsilon^N\right)\widehat{W}_i^{n+1} &= w(x_i,t_n) \le C\exp\left(-\frac{\alpha(1-x_i)}{m\varepsilon}\right)\\ &\le \exp\left(-\frac{\alpha(1-x_i)}{m\varepsilon}\right)\\ &\le CS_i,\end{aligned}$$

by an easy calculation it can be shown that S_i is bounded by $C\left(I+\Delta t\mathscr{L}_\varepsilon^N\right)S_i$ and using the linearity of the operator it reduces to

$$\left(I+\Delta t\mathscr{L}_\varepsilon^N\right)\widehat{W}_i^{n+1} \;\leq\; \left(I+\Delta t\mathscr{L}_\varepsilon^N\right)\Upsilon_i^{n+1},$$

where $\Upsilon_i^{n+1}=CS_i$, for all n. By using the discrete maximum principle (Lemma 3.4.1), we obtain

$$\widehat{W}_i^{n+1}\leq CS_i, \qquad \text{for } n=0,1,\ldots,M-1.$$

With the same argument we can bound $-\widehat{W}_i^{n+1}$ as follows

$$-\widehat{W}_i^{n+1}\leq CS_i, \qquad \text{for } n=0,1,\ldots,M-1.$$

Hence, we have

$$\left|\widehat{W}_i^{n+1}\right|\leq CS_i, \qquad \text{for } n=0,1,\ldots,M-1,$$

which is the required bound. ∎

Lemma 3.4.4. *The error of the singular component satisfies*

$$\left|\widehat{w}^{n+1}(x_i)-\widehat{W}_i^{n+1}\right|\leq CN^{-1}, \qquad \text{for } i=0,1,\ldots,N-1,\ n=0,1,\ldots,M-1.$$

Proof. We prove this lemma by separating the region into the regular and the layer regions, that is, for $i=0,1,\ldots,N/2-1$, and $i=N/2-1,N/2,\ldots,N$, respectively. For $i=0,1,\ldots,N/2-1$, we have

$$\begin{aligned}\left|\widehat{w}^{n+1}(x_i)-\widehat{W}_i^{n+1}\right| &\leq \left|\widehat{w}^{n+1}(x_i)\right|+\left|\widehat{W}_i^{n+1}\right|\\ &\leq CN^{-1}+CS_i,\end{aligned}$$

where we used Lemma 3.4.3 and bounds of the singular component $\widehat{w}$. The above inequality further simplified by using the monotonicity of S_i,

$$\left|\widehat{w}^{n+1}(x_i)-\widehat{W}_i^{n+1}\right| \;\leq\; CN^{-1}+S_{\frac{N}{2}-1}, \quad \text{for } 0\leq i\leq \frac{N}{2}-1. \tag{3.4.6}$$

The following identity will be used in proving the above result

$$\log\left(\prod_{k=\frac{N}{2}}^{N}\left(1+\frac{\alpha h_k}{m\varepsilon}\right)\right) \;=\; \sum_{k=\frac{N}{2}}^{N}\log\left(1+\frac{\alpha h_k}{m\varepsilon}\right).$$

For $\xi>0$ implies $\log(1+\xi)\geq\xi-\xi^2/2$ using this result in the above identity, we obtain that

$$\log\left(\prod_{k=\frac{N}{2}}^{N}\left(1+\frac{\alpha h_k}{m\varepsilon}\right)\right) \;\geq\; \sum_{k=\frac{N}{2}}^{N}\left(\frac{\alpha h_k}{m\varepsilon}-\frac{1}{2}\left(\frac{\alpha h_k}{m\varepsilon}\right)^2\right),$$

multiplying both the sides by (-1) and taking exponential, we get

$$\begin{aligned}\left(\prod_{k=\frac{N}{2}}^{N}\left(1+\frac{\alpha h_k}{m\varepsilon}\right)\right)^{-1} &\leq \exp\left(\sum_{k=\frac{N}{2}}^{N}\left(-\frac{\alpha h_k}{m\varepsilon}+\frac{1}{2}\left(\frac{\alpha h_k}{m\varepsilon}\right)^2\right)\right)\\ &\leq \exp\left(\sum_{k=\frac{N}{2}}^{N}\left(-\frac{\alpha h_k}{m\varepsilon}\right)\right)\exp\left(\frac{1}{2}\sum_{k=\frac{N}{2}}^{N}\left(\frac{\alpha h_k}{m\varepsilon}\right)^2\right)\\ &\leq \exp\left(-\frac{\alpha x_{\frac{N}{2}-1}}{m\varepsilon}\right)\exp\left(\frac{1}{2}\sum_{k=\frac{N}{2}}^{N}\left(\frac{\alpha h_k}{m\varepsilon}\right)^2\right)\\ &\leq CN^{-1}\exp\left(\frac{1}{2}\sum_{k=\frac{N}{2}}^{N}\left(\frac{\alpha h_k}{m\varepsilon}\right)^2\right)\end{aligned}$$

and finally, we have

$$\left(\prod_{k=\frac{N}{2}}^{N}\left(1+\frac{\alpha h_k}{m\varepsilon}\right)\right)^{-1} \leq CN^{-1}.$$

Substituting in (3.4.6), we obtain

$$\left|\widehat{w}^{n+1}(x_i)-\widehat{W}_i^{n+1}\right| \leq CN^{-1}, \quad \text{for } 0\leq i\leq \frac{N}{2}-1. \tag{3.4.7}$$

The local truncation error of the singular component at the node (x_i, t_{n+1}), is given by

$$\begin{aligned}\tau_{i,n+1}^{\widehat{W}} &= \left(I+\Delta t\mathscr{L}_\varepsilon^N\right)\left(\widehat{w}^{n+1}(x_i)-\widehat{W}_i^{n+1}\right)\\ &= r_i^-\widehat{w}^{n+1}(x_{i-1})+r_i^c\widehat{w}^{n+1}(x_i)+r_i^+\widehat{w}^{n+1}(x_{i+1})-(w(x_i,t_n)+\Delta t f(x_i,t_{n+1}))\\ &= r_i^-\widehat{w}^{n+1}(x_{i-1})+r_i^c\widehat{w}^{n+1}(x_i)+r_i^+\widehat{w}^{n+1}(x_{i+1})-\left(I+\Delta t\mathscr{L}_\varepsilon\right)\widehat{w}^{n+1}(x_i).\end{aligned}$$

As like before, the truncation error in singular component can be bounded as follows,

$$\begin{aligned}|\tau_{i,n+1}^{\widehat{W}}| &\leq C\int_{x_{i-1}}^{x_{i+1}}|(\widehat{w}^{n+1})''(s)|ds, \quad \text{for } \frac{N}{2}-1\leq i\leq N\\ &\leq \frac{C}{\varepsilon^2}\int_{x_{i-1}}^{x_{i+1}}\exp\left(-\alpha(1-s)/\varepsilon\right)ds\\ &\leq \frac{C}{\varepsilon^2}\frac{\varepsilon\exp(-\alpha(1-x_i)/m\varepsilon)}{N}\\ &\leq \frac{C}{\varepsilon N}\exp\left(\sum_{k=i+1}^{N}-\frac{\alpha h_k}{m\varepsilon}\right)\leq\frac{C}{\varepsilon N}\prod_{k=i+1}^{N}\exp\left(-\frac{\alpha h_k}{m\varepsilon}\right)\\ &\leq \frac{C}{\varepsilon N}\prod_{k=i+1}^{N}\left(1+\frac{\alpha h_k}{m\varepsilon}\right)^{-1}\leq\frac{C}{\varepsilon N}S_i, \quad \text{for } \frac{N}{2}-1\leq i\leq N.\end{aligned}$$

Now using $\Upsilon_j^{n+1} = \frac{C}{N}(1+S_i)$, as the barrier function and the discrete maximum principle (Lemma 3.4.1), we obtain

$$\left(\widehat{w}^{n+1}(x_i) - \widehat{W}_i^{n+1}\right) \leq CN^{-1}, \quad \text{for } \frac{N}{2} - 1 \leq i \leq N. \tag{3.4.8}$$

Similarly, repeating the same argument for $-(\widehat{w}^{n+1}(x_i) - \widehat{W}_i^{n+1})$,

$$-\left(\widehat{w}^{n+1}(x_i) - \widehat{W}_i^{n+1}\right) \leq CN^{-1}, \quad \text{for } \frac{N}{2} - 1 \leq i \leq N. \tag{3.4.9}$$

Combining (3.4.7), (3.4.8) and (3.4.9) we have

$$\left|\widehat{w}^{n+1}(x_i) - \widehat{W}_i^{n+1}\right| \leq CN^{-1}, \quad \text{for } i = 0, 1, \cdots, N,\ n = 0, 1, \ldots, M-1. \tag{3.4.10}$$

This completes the proof. ∎

Theorem 3.4.5. *Let $\widehat{u}^{n+1}$ and $\{\widehat{U}^{n+1}\}$ are the solutions corresponds to the semidiscrete discretization (3.3.3) and the discrete solution (3.4.1), respectively. Then, we have the following bound*

$$|\widehat{u}_i^{n+1} - \widehat{U}_i^{n+1}| \leq CN^{-1}, \quad \textit{for } 1 \leq i \leq N-1. \tag{3.4.11}$$

Proof. By using the error bounds of the regular and the singular components from Lemmas 3.4.2 and 3.4.4 in the inequality (3.4.5), we obtain the required estimate. ∎

Corollary 3.4.6. *If we take $N^{-q} \leq C\Delta t$ with $0 < q < 1$, then from (3.4.11), we obtain*

$$|\widehat{u}_i^{n+1} - \widehat{U}_i^{n+1}| \leq C\Delta t N^{-1+q}, \quad \textit{for } 1 \leq i \leq N-1. \tag{3.4.12}$$

This bound is required to prove the uniform convergence of the fully discrete scheme.

3.4.2 Uniform convergence of the fully discrete scheme

Here, we provide the important theorem for the ε–uniform convergence of the fully discrete scheme (3.3.12) on the adaptive gird obtained through the monitor function given in (3.3.7).

Theorem 3.4.7. *Let $u(x, t_n)$ be the exact solution of (3.1.1) and $\{U^n\}$ be the discrete solution of the fully discrete scheme (3.3.12), at time level $t_n = n\Delta t$. Assume that $N^{-q} \leq C\Delta t$ with $0 < q < 1$. Then the error associated to the fully discrete scheme (3.3.12) at the time level t_n satisfies*

$$\|\{u(x_i, t_n)\}_i - \{U_i^n\}_i\|_\infty \leq C(\Delta t + N^{-1+q}), \quad \textit{for } x_i \in \overline{\Omega}_x^N. \tag{3.4.13}$$

Proof. Let us denote the global error at time level t_n by $E^n_{x_i} = u(x_i, t_n) - U^n_i$, for $0 \le i \le N$. Now, splitting the global error $\{E^n_{x_i}\}_i$, we have

$$\|\{E^n_{x_i}\}_i\|_\infty \le \|\{u(x_i,t_n)\}_i - \{\widehat{u}^n_i\}_i\|_\infty + \|\{\widehat{u}^n_i\}_i - \{\widehat{U}^n_i\}_i\|_\infty + \|\{\widehat{U}^n_i\}_i - \{U^n_i\}_i\|_\infty. \quad (3.4.14)$$

Now, using the estimates given in (3.3.4) and (3.4.12), we deduce that

$$\|\{E^n_{x_i}\}_i\|_\infty \le C\Delta t(\Delta t + N^{-1+q}) + \|\{\widehat{U}^n_i\}_i - \{U^n_i\}_i\|_\infty, \quad \text{for } \overline{\Omega}^N_x. \quad (3.4.15)$$

Then, applying the stability of the fully discrete scheme, it can be shown that

$$\|\{\widehat{U}^n_i\}_i - \{U^n_i\}_i\|_\infty \le \|\{u(x_i,t_{n-1})\}_i - \{U^{n-1}_i\}_i\|_\infty. \quad (3.4.16)$$

Finally, from (3.4.15) and (3.4.16) we obtain the following error bound

$$\|\{E^n_{x_i}\}_i\|_\infty \le C\Delta t(\Delta t + N^{-1+q}) + \|\{E^{n-1}_{x_i}\}_i\|_\infty, \quad \text{for } \overline{\Omega}^N_x,$$

and hence, the result (3.4.13) follows from it. ∎

3.5 Semilinear Parabolic Problem

In this section, we consider the following semilinear singularly perturbed parabolic PDE of the form

$$\begin{cases} u_t - \varepsilon u_{xx} + a(x)u_x = r(x,t,u), & (x,t) \in G, \\ u(x,0) = u_0(x), & x \in \Omega, \\ u(0,t) = u(1,t) = 0, & t \in (0,T], \end{cases} \quad (3.5.1)$$

where $\varepsilon > 0$ is parameter. The functions $a(x)$ and $u_0(x)$ are sufficiently smooth. We assume that r is continuous in $\overline{\Omega} \times [0,T] \times \mathbb{R}$, is differentiable in the third argument, for some non-negative constants γ and $\bar{\gamma}$, satisfies

$$0 \le \gamma \le r_s(x,t,s) \le \bar{\gamma} \quad \text{for } (x,t,s) \in \overline{\Omega} \times [0,T] \times \mathbb{R}.$$

Under suitable continuity and compatibility conditions on the data, a unique solution $u(x,t)$ of the parabolic problem (3.5.1) exists (see [45] for details). For $0 < \varepsilon \ll 1$, problem (3.5.1) is of singularly perturbed in nature and has boundary layers near $\partial\Omega \times [0,T]$.

To solve (3.5.1), we use the Newton linearization process and obtain the sequence $\{u^m\}$ for the initial guess u^0 satisfying the initial and boundary conditions of the problem. Thus we define u^{m+1} for each fixed m, to be the solution of the following linear parabolic IBVP,

$$\begin{cases} u^{m+1}_t - \varepsilon u^{m+1}_{xx} + a(x)u^{m+1}_x - b^m(x,t)u^{m+1} = g^m(x,t), & (x,t) \in G, \\ u^{m+1}(x,0) = u_0(x), & 0 < x < 1, \\ u^{m+1}(0,t) = 0, \quad u^{m+1}(1,t) = 0, & 0 \le t \le T, \end{cases} \quad (3.5.2)$$

where $m \geq 0$ and $b^m(x,t)$ and $g^m(x,t)$ are given by

$$\begin{cases} b^m(x,t) = r_u(x,t,u^m), \\ g^m(x,t) = r(x,t,u^m) - b^m(x,t)u^m. \end{cases} \tag{3.5.3}$$

Hence for a fixed m, we solve (3.5.2) by using the computational method discussed earlier. Moreover, we assume that the problem admits regular boundary layers. Numerical results of semilinear IBVPs of the form (3.5.1) are presented in the following section.

3.6 Numerical Results

In this section, we shall present the numerical results obtained by the fully discrete scheme (3.3.12) for four (two linear, one semilinear and one quasilinear) test problems on the rectangular mesh $\overline{G}^{N,\Delta t} = \overline{\Omega}_x^N \times \overline{\Lambda}_t^M$, where $\overline{\Omega}_x^N$ is the equidistribution mesh obtained from the numerical algorithm. The constant C_0 in the numerical algorithm gives an intimation of how close we are from the equidistribution of the monitor function. In case of $C_0 = 1$, the equidistribution principle is satisfied exactly which is too difficult to achieve by numerical methods. We have taken $C_0 = 1.2$ in all our numerical results presented in this section and also $m = 2$, which is necessary to define the monitor function (3.3.7). Moreover, in all the tables we begin with $N = 32$ and the time step $\Delta t = 0.1$ and we multiply N by two and divide Δt by two.

Example 3.6.1. *Consider the following parabolic initial-boundary-value problem:*

$$\begin{cases} u_t - \varepsilon u_{xx} + (1 + x(1-x))u_x = f(x,t), \quad (x,t) \in (0,1) \times (0,1], \\ u(x,0) = u_0(x), \quad 0 < x < 1, \\ u(0,t) = 0, \quad u(1,t) = 0, \quad 0 \leq t \leq 1. \end{cases} \tag{3.6.1}$$

We choose the initial data $u_0(x)$ and the source function $f(x,t)$ to fit with the exact solution

$$u(x,t) = \exp(-t)(C_1 + C_2 x - \exp(-(1-x)\varepsilon)),$$

where $C_1 = \exp(-1/\varepsilon)$, and $C_2 = 1 - \exp(-1/\varepsilon)$. As the exact solution of the problem (3.6.1) is known, for each ε, we calculate the maximum point-wise error by

$$e_\varepsilon^{N,\Delta t} = \max_{(x_i,t_n) \in \overline{G}^{N,\Delta t}} |u(x_i,t_n) - U^{N,\Delta t}(x_i,t_n)|,$$

where $u(x_i,t_n)$ and $U^{N,\Delta t}(x_i,t_n)$ respectively, denote the exact and the numerical solution obtained on the mesh with N mesh intervals in the spatial direction and M mesh

intervals in the $t-$direction such that $\Delta t = T/M$ is the uniform time step. In addition, we determine the corresponding rate of convergence by

$$p_{\varepsilon}^{N,\Delta t} = \log_2 \left(\frac{e_{\varepsilon}^{N,\Delta t}}{e_{\varepsilon}^{2N,\Delta t/2}} \right).$$

The calculated maximum point-wise errors $e_{\varepsilon}^{N,\Delta t}$ and the corresponding rate of convergence $p_{\varepsilon}^{N,\Delta t}$ for Example 3.6.1 are given in Table 3.1 and Table 3.2, respectively. From these results one can observe the ε–uniform first-order convergence of the numerical solution. To compare our results, we also produced the maximum point-wise errors and the corresponding rate of convergence for the well-known layer adapted meshes, particulary, the Shishkin mesh and the Bakhvalov mesh in Tables 3.5, 3.6, 3.7 and 3.8. More information about the Shishkin mesh and the Bakhvalov mesh and its generating function can be found in [78].

Further, we have calculated the normalized flux

$$F_{\varepsilon} u(x,t) = \varepsilon \frac{\partial u(x,t)}{\partial x},$$

and its numerical approximation

$$F_{\varepsilon}^{N} U^{N,\Delta t}(x_i, t_n) = \varepsilon D_x^{-} U_i^n.$$

The errors in the normalized flux have been calculated as

$$r_{\varepsilon}^{N,\Delta t} = \max_{1 \le n \le M} |F_{\varepsilon} u(x_N, t_n) - F_{\varepsilon}^{N} U^{N,\Delta t}(x_N, t_n)|,$$

and the rate of convergence is determined from

$$q_{\varepsilon}^{N,\Delta t} = \log_2 \left(\frac{r_{\varepsilon}^{N,\Delta t}}{r_{\varepsilon}^{2N,\Delta t/2}} \right).$$

The calculated maximum point-wise errors in the normalized flux $r_{\varepsilon}^{N,\Delta t}$ and the corresponding rate of convergence $q_{\varepsilon}^{N,\Delta t}$ for Example 3.6.1 are given in Table 3.3 and Table 3.4. Again, one can see the ε–uniform convergence in Table 3.3, and the first-order convergence rate from Table 3.4. In Figures 3.1 (a) and (b), the maximum point-wise errors in the solution and the normalized flux are plotted respectively, which reflect the fact of first-order convergence independent of ε.

Example 3.6.2. *Consider the following parabolic initial-boundary-value problem with variable coefficients*

$$\begin{cases} u_t - \varepsilon u_{xx} + (2 - x^2) u_x + xu = 10t^2 \exp(-t) x(1-x), & (x,t) \in (0,1) \times (0,1] \\ u(x,0) = 0, \quad 0 < x < 1, \\ u(0,t) = 0, \quad u(1,t) = 0, \quad 0 \le t \le 1. \end{cases} \tag{3.6.2}$$

Table 3.1: *Maximum point-wise error of the solution* $e_\varepsilon^{N,\Delta t}$ *for Example* 3.6.1 *using equidistribution mesh.*

	Number of Intervals N/Time Step Size Δt					
ε	$32/\frac{1}{10}$	$64/\frac{1}{20}$	$128/\frac{1}{40}$	$256/\frac{1}{80}$	$512/\frac{1}{160}$	$1024/\frac{1}{320}$
10^0	7.5333e-04	4.1685e-04	2.1748e-04	1.0922e-04	5.4081e-05	2.6669e-05
10^{-2}	5.2036e-02	2.8915e-02	1.5784e-02	8.4430e-03	4.5493e-03	2.5235e-03
10^{-4}	8.1473e-02	4.2740e-02	2.1362e-02	1.0776e-02	5.4258e-03	2.7360e-03
10^{-6}	8.7828e-02	4.3819e-02	2.2051e-02	1.1062e-02	5.5220e-03	2.7590e-03
10^{-8}	9.2101e-02	4.5172e-02	2.3305e-02	1.1137e-02	5.5484e-03	2.7720e-03

Table 3.2: *Rate of convergence of the solution* $p_\varepsilon^{N,\Delta t}$ *for Example* 3.6.1 *using equidistribution mesh.*

	Number of Intervals N/Time Step Size Δt				
ε	$32/\frac{1}{10}$	$64/\frac{1}{20}$	$128/\frac{1}{40}$	$256/\frac{1}{80}$	$512/\frac{1}{160}$
10^0	0.8537	0.9386	0.9936	1.0140	1.0200
10^{-2}	0.8476	0.8733	0.9026	0.8921	0.8502
10^{-4}	0.9307	1.0005	0.9872	0.9899	0.9877
10^{-6}	1.0031	0.9907	0.9952	1.0023	1.0010
10^{-8}	1.0278	0.9547	1.0653	1.0052	1.0011

Table 3.3: *Maximum point-wise error of the normalized flux* $r_\varepsilon^{N,\Delta t}$ *for Example* 3.6.1 *using equidistribution mesh.*

	Number of Intervals N/Time Step Size Δt					
ε	$32/\frac{1}{10}$	$64/\frac{1}{20}$	$128/\frac{1}{40}$	$256/\frac{1}{80}$	$512/\frac{1}{160}$	$1024/\frac{1}{320}$
10^0	1.7715e-02	9.2953e-03	4.7435e-03	2.3785e-03	1.1847e-03	5.8868e-04
10^{-2}	1.9081e-01	1.0528e-01	5.4741e-02	2.8976e-02	1.5603e-02	8.0615e-03
10^{-4}	2.4928e-01	1.3044e-01	6.4797e-02	3.2659e-02	1.6359e-02	8.2432e-03
10^{-6}	2.7126e-01	1.3258e-01	6.6422e-02	3.3243e-02	1.6586e-02	8.2846e-03
10^{-8}	2.8243e-01	1.3546e-01	7.0427e-02	3.3473e-02	1.6660e-02	8.3193e-03

Table 3.4: *Rate of convergence of the normalized flux* $q_\varepsilon^{N,\Delta t}$ *for Example* 3.6.1 *using equidistribution mesh.*

	Number of Intervals N/Time Step Size Δt				
ε	$32/\frac{1}{10}$	$64/\frac{1}{20}$	$128/\frac{1}{40}$	$256/\frac{1}{80}$	$512/\frac{1}{160}$
10^{0}	0.9304	0.9706	0.9959	1.0055	1.0090
10^{-2}	0.8579	0.9435	0.9178	0.8930	0.9527
10^{-4}	0.9344	1.0094	0.9885	0.9974	0.9888
10^{-6}	1.0328	0.9971	0.9986	1.0031	1.0015
10^{-8}	1.0600	0.9437	1.0731	1.0066	1.0019

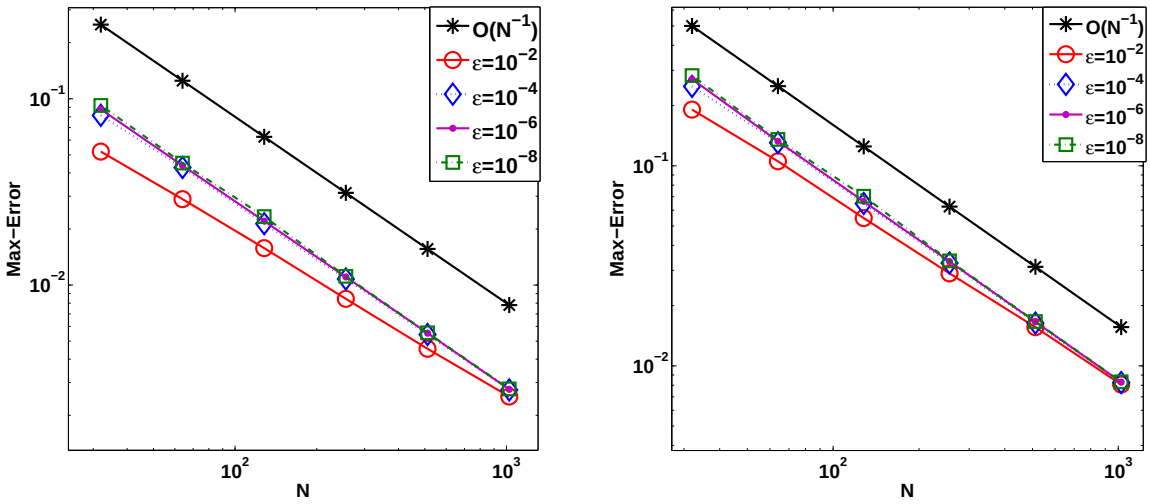

(a) *Maximum point-wise error of the solution* $e_\varepsilon^{N,\Delta t}$.

(b) *Maximum point-wise error of the normalized flux* $r_\varepsilon^{N,\Delta t}$.

Figure 3.1: *Loglog plot for Example 3.6.1.*

Table 3.5: *Maximum point-wise error of the solution for Example* 3.6.1 *using the Shishkin mesh.*

	Number of Intervals N/Time Step Size Δt					
ε	$32/\frac{1}{10}$	$64/\frac{1}{20}$	$128/\frac{1}{40}$	$256/\frac{1}{80}$	$512/\frac{1}{160}$	$1024/\frac{1}{320}$
10^{0}	6.8921e-04	3.7085e-04	1.9290e-04	9.8440e-05	4.9739e-05	2.5002e-05
10^{-2}	5.5988e-02	3.8931e-02	2.4826e-02	1.4919e-02	8.6489e-03	4.8876e-03
10^{-4}	6.4187e-02	4.3984e-02	2.7665e-02	1.6409e-02	9.4977e-03	5.3572e-03
10^{-6}	6.4292e-02	4.4129e-02	2.7833e-02	1.6608e-02	9.5732e-03	5.3890e-03
10^{-8}	6.4293e-02	4.4130e-02	2.7834e-02	1.6610e-02	9.5755e-03	5.3916e-03

Table 3.6: *Rate of convergence of the solution for Example* 3.6.1 *using the Shishkin mesh.*

	Number of Intervals N/Time Step Size Δt				
ε	$32/\frac{1}{10}$	$64/\frac{1}{20}$	$128/\frac{1}{40}$	$256/\frac{1}{80}$	$512/\frac{1}{160}$
10^{0}	0.8941	0.9430	0.9705	0.9849	0.9923
10^{-2}	0.5242	0.6491	0.7346	0.7866	0.8234
10^{-4}	0.5453	0.6689	0.7536	0.7889	0.8261
10^{-6}	0.5429	0.6649	0.7449	0.7948	0.8290
10^{-8}	0.5429	0.6649	0.7448	0.7947	0.8286

Table 3.7: *Maximum point-wise error of the solution for Example* 3.6.1 *using the Bakhvalov mesh.*

	Number of Intervals N/Time Step Size Δt					
ε	$32/\frac{1}{10}$	$64/\frac{1}{20}$	$128/\frac{1}{40}$	$256/\frac{1}{80}$	$512/\frac{1}{160}$	$1024/\frac{1}{320}$
10^{0}	6.8921e-04	3.7085e-04	1.9290e-04	9.8440e-05	4.9739e-05	2.5002e-05
10^{-2}	3.6778e-02	2.2324e-02	1.2953e-02	7.2482e-03	3.9080e-03	2.0439e-03
10^{-4}	6.6889e-02	3.7859e-02	2.0136e-02	1.0334e-02	5.2851e-03	2.6686e-03
10^{-6}	7.3993e-02	4.2358e-02	2.2715e-02	1.1750e-02	5.9784e-03	3.0145e-03
10^{-8}	7.6146e-02	4.3468e-02	2.3305e-02	1.2073e-02	6.1429e-03	3.0988e-03

Table 3.8: *Rate of convergence of the solution for Example* 3.6.1 *using the Bakhvalov mesh.*

	Number of Intervals N/Time Step Size Δt				
ε	$32/\frac{1}{10}$	$64/\frac{1}{20}$	$128/\frac{1}{40}$	$256/\frac{1}{80}$	$512/\frac{1}{160}$
10^{0}	0.8941	0.9430	0.9705	0.9849	0.9923
10^{-2}	0.7203	0.7853	0.8376	0.8912	0.9351
10^{-4}	0.8211	0.9108	0.9624	0.9674	0.9858
10^{-6}	0.8048	0.8990	0.9509	0.9749	0.9879
10^{-8}	0.8088	0.8993	0.9489	0.9748	0.9872

As the exact solution of the problem (3.6.2) is not known, to obtain the accuracy of the numerical solution and also to demonstrate the $\varepsilon-$uniform convergence of the proposed scheme, we use the double mesh principle which is given in the following.

Let $\tilde{U}^{2N,\Delta t/2}(x_i,t_n)$ be the numerical solution obtained on the fine mesh $\overline{G}^{2N,\Delta/2} = \overline{\Omega}_x^{2N} \times \overline{\Lambda}_t^{2M}$ with $2N$ mesh intervals in the spatial direction and $2M$ mesh intervals in the $t-$direction. Then for each ε, we calculate the maximum point-wise error by

$$E_\varepsilon^{N,\Delta t} = \max_{(x_i,t_n)\in\overline{G}^{N,\Delta t}} \left| U^{N,\Delta t}(x_i,t_n) - \tilde{U}^{2N,\Delta t/2}(x_i,t_n) \right|,$$

and the corresponding rate of convergence by

$$P_\varepsilon^{N,\Delta t} = \log_2 \left(\frac{E_\varepsilon^{N,\Delta t}}{E_\varepsilon^{2N,\Delta t/2}} \right).$$

The calculated maximum point-wise errors $E_\varepsilon^{N,\Delta t}$ and the corresponding rate of convergence $P_\varepsilon^{N,\Delta t}$ for Example 3.6.2 are given in Table 3.9 and Table 3.10 respectively. The numerical results given in these tables reveal the first-order convergence independent of the diffusion parameter ε. Further, the errors in the normalized flux have been calculated as

$$R_\varepsilon^{N,\Delta t} = \max_{1\le n\le M} |F_\varepsilon^N U^{N,\Delta t}(x_N,t_n) - F_\varepsilon^N \tilde{U}^{2N,\Delta t/2}(x_N,t_n)|,$$

and the rate of convergence is determined from

$$Q_\varepsilon^{N,\Delta t} = \log_2 \left(\frac{R_\varepsilon^{N,\Delta t}}{R_\varepsilon^{2N,\Delta t/2}} \right).$$

The calculated maximum point-wise errors in the normalized flux $R_\varepsilon^{N,\Delta t}$ and the corresponding rate of convergence $Q_\varepsilon^{N,\Delta t}$ for Example 3.6.2 are given in Table 3.11 and Table 3.12 respectively.

The numerical solution is plotted in Figures 3.2 (a) and (b) for $\varepsilon = 1e-1$ and $\varepsilon = 1e-4$, respectively. These figures show the existence of the boundary layer near $x = 1$. The maximum point-wise errors are plotted in log-log scale in Figures 3.3 (a) and (b), for the solution and the normalized flux, respectively. From these figures, one can easily observe the first-order ε–uniform convergence.

Example 3.6.3. *Consider the following semilinear parabolic initial-boundary-value problem:*

$$\begin{cases} u_t - \varepsilon u_{xx} + (1 + x(1-x))u_x + \exp(u) = f(x,t), \quad (x,t) \in (0,1)\times(0,1], \\ u(x,0) = u_0(x), \quad 0 < x < 1, \\ u(0,t) = 0, \quad u(1,t) = 0, \quad 0 \le t \le 1. \end{cases} \tag{3.6.3}$$

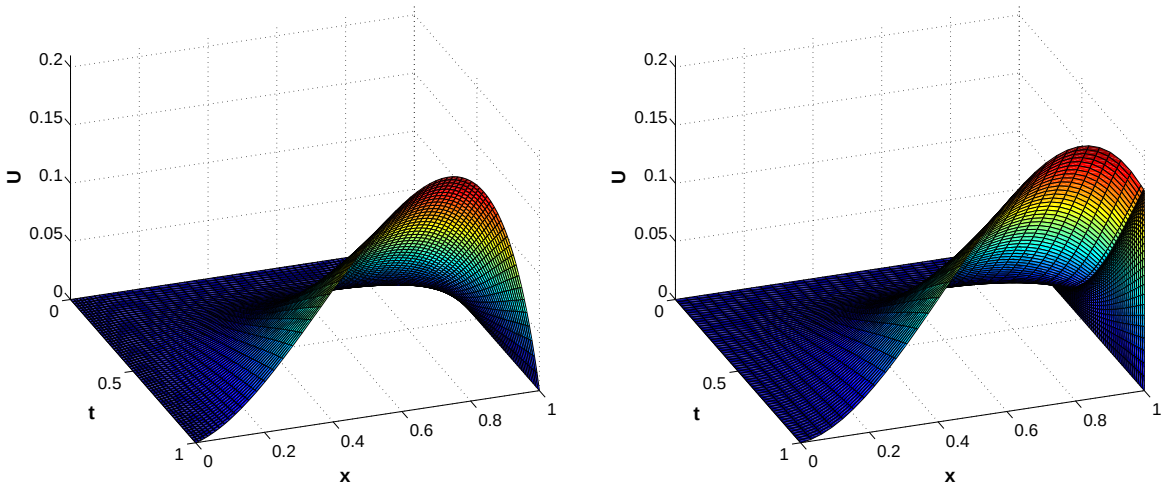

(a) $\varepsilon = 10^{-1}$. (b) $\varepsilon = 10^{-4}$.

Figure 3.2: *Numerical solution of Example 3.6.2 for* $N = 64$ *and* $\Delta t = 1/64$.

Table 3.9: *Maximum point-wise error of the solution* $E_{\varepsilon}^{N,\Delta t}$ *for Example* 3.6.2 *using equidistribution mesh.*

	Number of Intervals N/Time Step Size Δt					
ε	$32/\frac{1}{10}$	$64/\frac{1}{20}$	$128/\frac{1}{40}$	$256/\frac{1}{80}$	$512/\frac{1}{160}$	$1024/\frac{1}{320}$
10^{0}	9.2151e-04	4.6408e-04	2.3891e-04	1.2182e-04	6.2135e-05	3.1334e-05
10^{-2}	7.2044e-03	4.3255e-03	2.4862e-03	1.1676e-03	6.0758e-04	3.1001e-04
10^{-4}	1.1342e-02	6.2851e-03	3.2988e-03	1.7175e-03	8.6996e-04	4.3954e-04
10^{-6}	1.3838e-02	6.6509e-03	3.4377e-03	1.7677e-03	8.9286e-04	4.4781e-04
10^{-8}	1.4524e-02	6.7667e-03	3.6247e-03	1.7939e-03	8.9428e-04	4.4947e-04

Table 3.10: *Rate of convergence of the solution* $P_{\varepsilon}^{N,\Delta t}$ *for Example* 3.6.2 *using equidistribution mesh.*

	Number of Intervals N/Time Step Size Δt				
ε	$32/\frac{1}{10}$	$64/\frac{1}{20}$	$128/\frac{1}{40}$	$256/\frac{1}{80}$	$512/\frac{1}{160}$
10^{0}	0.9896	0.9579	0.9717	0.9712	0.9876
10^{-2}	0.7360	0.7989	1.0904	0.9424	0.9707
10^{-4}	0.8517	0.9299	0.9416	0.9812	0.9849
10^{-6}	1.0570	0.9521	0.9595	0.9853	0.9955
10^{-8}	1.1019	0.9005	1.0148	1.0043	0.9925

Table 3.11: *Maximum point-wise error of the normalized flux* $R_\varepsilon^{N,\Delta t}$ *for Example* 3.6.2 *using equidistribution mesh.*

	Number of Intervals N/Time Step Size Δt					
ε	$32/\frac{1}{10}$	$64/\frac{1}{20}$	$128/\frac{1}{40}$	$256/\frac{1}{80}$	$512/\frac{1}{160}$	$1024/\frac{1}{320}$
10^{0}	6.6944e-03	3.6205e-03	1.9628e-03	1.0418e-03	5.4044e-04	2.7485e-04
10^{-2}	3.5063e-02	1.8508e-02	9.5745e-03	4.7036e-03	2.2391e-03	1.0918e-03
10^{-4}	3.7795e-02	2.0402e-02	1.0968e-02	5.3067e-03	2.6980e-03	1.3512e-03
10^{-6}	3.9989e-02	2.2236e-02	1.0708e-02	5.4603e-03	2.7607e-03	1.3710e-03
10^{-8}	4.2794e-02	2.3378e-02	1.2040e-02	5.6309e-03	2.7344e-03	1.3739e-03

Table 3.12: *Rate of convergence of the normalized flux* $Q_\varepsilon^{N,\Delta t}$ *for Example* 3.6.2 *using equidistribution mesh.*

	Number of Intervals N/Time Step Size Δt				
ε	$32/\frac{1}{10}$	$64/\frac{1}{20}$	$128/\frac{1}{40}$	$256/\frac{1}{80}$	$512/\frac{1}{160}$
10^{0}	0.8868	0.8833	0.9138	0.9469	0.9755
10^{-2}	0.9218	0.9509	1.0254	1.0708	1.0362
10^{-4}	0.8895	0.8954	1.0474	0.9759	0.9977
10^{-6}	0.8467	1.0542	0.9716	0.9840	1.0098
10^{-8}	0.8723	0.9573	1.0964	1.0421	0.9930

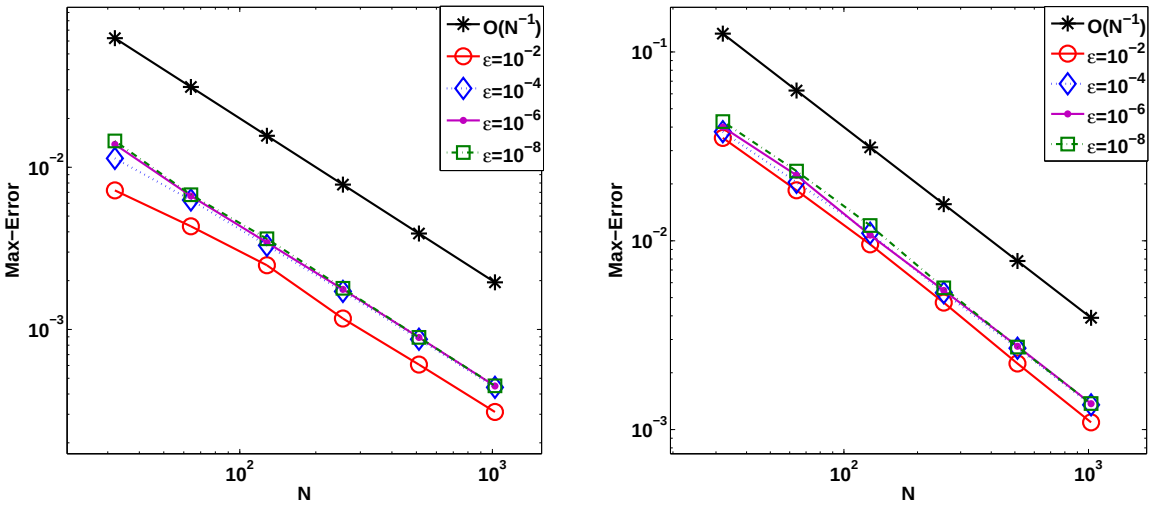

(a) *Maximum point-wise error of the solution* $E_\varepsilon^{N,\Delta t}$.

(b) *Maximum point-wise error of the normalized flux* $R_\varepsilon^{N,\Delta t}$.

Figure 3.3: *Loglog plot for Example 3.6.2.*

We choose the initial data $u_0(x)$ and the source function $f(x,t)$ to fit with the exact solution

$$u(x,t) = \exp(-t)(C_1 + C_2 x - \exp(-(1-x)\varepsilon)),$$

where $C_1 = \exp(-1/\varepsilon)$, and $C_2 = 1 - \exp(-1/\varepsilon)$.

If we use the Newton linearization process given in (3.5.2), we obtain the following system of linear singular perturbation parabolic PDEs:

$$\begin{cases} u_t^{m+1} - \varepsilon u_{xx}^{m+1} + (1 + x(1-x))u_x^{m+1} + \exp(u^m)u^{m+1} = f(x,t) - \exp(u^m)(1-u^m), \\ u^{m+1}(x,0) = u_0(x), \quad 0 < x < 1, \\ u^{m+1}(0,t) = 0, \quad u^{m+1}(1,t) = 0, \quad 0 \le t \le 1. \end{cases} \tag{3.6.4}$$

Hence for a fixed m, we solve (3.6.4) using computational method discussed earlier. For the above Newton linearization process, the following convergence criterion for the numerical solution is used:

$$\max_{(x_i,t_n)\in\overline{G}^{N,\Delta t}} \left| U^{m+1}(x_i,t_n) - U^m(x_i,t_n) \right| \le \delta, \quad m \ge 0,$$

where $U^m(x_i,t_n)$ is the mth iteration numerical solution at mesh point (x_i,t_n) and δ is prescribed error constant. We used $\delta = 10^{-10}$ for the Table 3.13-3.16.

As the exact solution of the problem (3.6.3) is known, for each ε, we calculate the maximum point-wise error by

$$\tilde{e}_\varepsilon^{N,\Delta t} = \max_{(x_i,t_n)\in\overline{G}^{N,\Delta t}} |u(x_i,t_n) - U^{N,\Delta t}(x_i,t_n)|,$$

where $u(x_i,t_n)$ and $U^{N,\Delta t}(x_i,t_n)$ respectively, denote the exact and the numerical solution obtained on the mesh with N mesh intervals in the spatial direction and M mesh intervals in the $t-$direction such that $\Delta t = T/M$ is the uniform time step. In addition, we determine the corresponding rate of convergence by

$$\tilde{p}_\varepsilon^{N,\Delta t} = \log_2 \left(\frac{\tilde{e}_\varepsilon^{N,\Delta t}}{\tilde{e}_\varepsilon^{2N,\Delta t/2}} \right).$$

The calculated maximum point-wise errors $\tilde{e}_\varepsilon^{N,\Delta t}$ and the corresponding rate of convergence $\tilde{p}_\varepsilon^{N,\Delta t}$ for Example 3.6.3 are given in Table 3.13 and Table 3.14, respectively. From these results one can observe the ε–uniform first-order convergence of the numerical solution. The errors in the normalized flux have been calculated as

$$\tilde{r}_\varepsilon^{N,\Delta t} = \max_{1\le n\le M} |F_\varepsilon u(x_N,t_n) - F_\varepsilon^N U^{N,\Delta t}(x_N,t_n)|,$$

and the rate of convergence is determined from

$$\tilde{q}_\varepsilon^{N,\Delta t} = \log_2 \left(\frac{\tilde{r}_\varepsilon^{N,\Delta t}}{\tilde{r}_\varepsilon^{2N,\Delta t/2}} \right).$$

Table 3.13: *Maximum point-wise error of the solution* $\tilde{e}_{\varepsilon}^{N,\Delta t}$ *for Example* 3.6.3 *using equidistribution mesh.*

	Number of Intervals N/Time Step Size Δt					
ε	$32/\frac{1}{10}$	$64/\frac{1}{20}$	$128/\frac{1}{40}$	$256/\frac{1}{80}$	$512/\frac{1}{160}$	$1024/\frac{1}{320}$
10^{0}	6.2917e-04	3.3732e-04	1.7567e-04	8.9685e-05	4.5320e-05	2.2782e-05
10^{-2}	3.8609e-02	2.0426e-02	1.0867e-02	5.5871e-03	2.8348e-03	1.4198e-03
10^{-4}	6.0421e-02	3.0601e-02	1.5362e-02	7.6465e-03	3.8456e-03	1.9328e-03
10^{-6}	6.3921e-02	3.2940e-02	1.5797e-02	7.9255e-03	3.9204e-03	1.9592e-03
10^{-8}	6.5823e-02	3.3413e-02	1.6458e-02	7.9930e-03	3.9513e-03	1.9628e-03

Table 3.14: *Rate of convergence of the solution* $\tilde{p}_{\varepsilon}^{N,\Delta t}$ *for Example* 3.6.3 *using equidistribution mesh.*

	Number of Intervals N/Time Step Size Δt				
ε	$32/\frac{1}{10}$	$64/\frac{1}{20}$	$128/\frac{1}{40}$	$256/\frac{1}{80}$	$512/\frac{1}{160}$
10^{0}	0.8993	0.9413	0.9699	0.9847	0.9923
10^{-2}	0.9185	0.9105	0.9597	0.9788	0.9975
10^{-4}	0.9815	0.9942	1.0065	0.9916	0.9925
10^{-6}	0.9564	1.0602	0.9950	1.0155	1.0007
10^{-8}	0.9782	1.0216	1.0420	1.0164	1.0094

The calculated maximum point-wise errors in the normalized flux $\tilde{r}_{\varepsilon}^{N,\Delta t}$ and the corresponding rate of convergence $\tilde{q}_{\varepsilon}^{N,\Delta t}$ for Example 3.6.3 are given in Table 3.15 and Table 3.16. Again, one can see the ε–uniform convergence in Table 3.15, and the first-order convergence rate from Table 3.16.

Example 3.6.4. *Consider the following quasilinear parabolic initial-boundary-value problem:*

$$\begin{cases} u_t - \varepsilon u_{xx} + (1 + x(1-x))uu_x + \exp(u) = f(x,t), \quad (x,t) \in (0,1) \times (0,1], \\ u(x,0) = u_0(x), \quad 0 < x < 1, \\ u(0,t) = 0, \quad u(1,t) = 0, \quad 0 \le t \le 1. \end{cases} \tag{3.6.5}$$

We choose the initial data $u_0(x)$ and the source function $f(x,t)$ to fit with the exact solution

$$u(x,t) = \exp(-t)(C_1 + C_2 x - \exp(-(1-x)\varepsilon)),$$

where $C_1 = \exp(-1/\varepsilon)$, and $C_2 = 1 - \exp(-1/\varepsilon)$.

Table 3.15: *Maximum point-wise error of the normalized flux* $\tilde{r}_{\varepsilon}^{N,\Delta t}$ *for Example* 3.6.3 *using equidistribution mesh.*

	Number of Intervals N/Time Step Size Δt					
ε	$32/\frac{1}{10}$	$64/\frac{1}{20}$	$128/\frac{1}{40}$	$256/\frac{1}{80}$	$512/\frac{1}{160}$	$1024/\frac{1}{320}$
10^{0}	1.5348e-02	7.8679e-03	3.9899e-03	2.0113e-03	1.0098e-03	5.0595e-04
10^{-2}	1.4129e-01	7.4090e-02	3.7692e-02	1.9134e-02	9.6534e-03	5.0352e-03
10^{-4}	1.8879e-01	9.3858e-02	4.6700e-02	2.3249e-02	1.1606e-02	5.8293e-03
10^{-6}	1.9787e-01	1.0008e-01	4.7661e-02	2.3881e-02	1.1784e-02	5.8849e-03
10^{-8}	2.3302e-01	1.0190e-01	4.9689e-02	2.4052e-02	1.1870e-02	5.8929e-03

Table 3.16: *Rate of convergence of the normalized flux* $\tilde{q}_{\varepsilon}^{N,\Delta t}$ *for Example* 3.6.3 *using equidistribution mesh.*

	Number of Intervals N/Time Step Size Δt				
ε	$32/\frac{1}{10}$	$64/\frac{1}{20}$	$128/\frac{1}{40}$	$256/\frac{1}{80}$	$512/\frac{1}{160}$
10^{0}	0.9640	0.9796	0.9882	0.9941	0.9969
10^{-2}	0.9313	0.9750	0.9781	0.9870	0.9390
10^{-4}	1.0082	1.0070	1.0063	1.0022	0.9935
10^{-6}	0.9834	1.0703	0.9970	1.0191	1.0017
10^{-8}	1.1933	1.0361	1.0468	1.0188	1.0103

Table 3.17: *Maximum point-wise error of the solution* $\tilde{e}_{\varepsilon}^{N,\Delta t}$ *for Example* 3.6.4 *using equidistribution mesh.*

	Number of Intervals N/Time Step Size Δt				
ε	$32/\frac{1}{10}$	$64/\frac{1}{20}$	$128/\frac{1}{40}$	$256/\frac{1}{80}$	$512/\frac{1}{160}$
10^{0}	2.1224e-04	1.1016e-04	5.6114e-05	2.8358e-05	1.4255e-05
10^{-2}	3.1235e-02	1.8433e-02	1.0046e-02	5.2075e-03	2.7049e-03
10^{-4}	6.2231e-02	3.3148e-02	1.6691e-02	8.2822e-03	4.1686e-03
10^{-6}	6.8282e-02	3.5852e-02	1.7505e-02	8.8524e-03	4.2776e-03
10^{-8}	7.2542e-02	3.7821e-02	1.7690e-02	8.6522e-03	4.3006e-03

If we use the Newton linearization process, we obtain the following system of linear singularly perturbed parabolic PDEs:

$$\begin{cases} u_t^{m+1} - \varepsilon u_{xx}^{m+1} + (1+x(1-x))u^m u_x^{m+1} + (\exp(u^m) + (1+x(1-x)))u^{m+1} \\ \qquad = f(x,t) + (1+x(1-x))u^m - \exp(u^m)(1-u^m), \quad (x,t) \in (0,1)\times(0,1], \\ u^{m+1}(x,0) = u_0(x), \quad 0 < x < 1, \\ u^{m+1}(0,t) = 0, \quad u^{m+1}(1,t) = 0, \quad 0 \le t \le 1. \end{cases} \tag{3.6.6}$$

Hence for a fixed m, we solve (3.6.4) using the computational method discussed earlier. For the above Newton linearization process, the following convergence criterion for the numerical solution is used:

$$\max_{(x_i,t_n)\in\overline{G}^{N,\Delta t}} \left|U^{m+1}(x_i,t_n) - U^m(x_i,t_n)\right| \le \delta, \quad m \ge 0,$$

where $U^m(x_i,t_n)$ is the mth iteration numerical solution at mesh point (x_i,t_n) and δ is prescribed error constant. We used $\delta = 10^{-10}$ for the Table 3.17-3.18.

We have calculated the maximum point-wise error and corresponding rate of convergence as given for Example 3.6.3 and presented in Table 3.17 and Table 3.18, respectively. The numerical results given in these tables reveal the first-order convergence independent of the diffusion parameter ε.

3.7 Conclusions

In this chapter, we have solved the singularly perturbed time-dependent convection-diffusion problems (3.1.1) numerically by the upwind finite difference scheme on layer-adapted nonuniform meshes obtained through a positive monitor function given in (3.3.7). The truncation error is obtained and the stability is analyzed. The proposed

Table 3.18: *Rate of convergence of the solution* $\tilde{p}_{\varepsilon}^{N,\Delta t}$ *for Example* 3.6.4 *using equidistribution mesh.*

	Number of Intervals N/Time Step Size Δt			
ε	$32/\frac{1}{10}$	$64/\frac{1}{20}$	$128/\frac{1}{40}$	$256/\frac{1}{80}$
10^{0}	0.9460	0.9732	0.9846	0.9923
10^{-2}	0.7609	0.8757	0.9479	0.9450
10^{-4}	0.9087	0.9898	1.0110	0.9904
10^{-6}	0.9294	1.0343	0.9836	1.0493
10^{-8}	0.9396	1.0963	1.0318	1.0085

numerical scheme is of first-order convergence in both the spatial and temporal variables, *i.e.*, $O(\Delta t + N^{-1})$. Error estimates are derived for the numerical scheme, which are independent of the diffusion parameter ε. Semilinear and quasilinear IBVPs are also solved by the present method. Numerical results reveal the theoretical error estimate.

CHAPTER 4

The Parameter-Uniform Numerical Method for Parabolic Reaction-Diffusion Problems on Equidistributed Grids

This chapter presents the study of singularly perturbed parabolic reaction-diffusion problems with boundary layers. To solve these problems, we use a modified backward-Euler scheme for the time derivative with uniform mesh and central difference scheme for the spatial derivative on layer-adapted nonuniform meshes at each time level. The nonuniform meshes are obtained by equidistribution of a positive monitor function, which involves the second-order spatial derivative of the singular component of the solution. Equidistributing monitor function at each time level allows us to use this technique to a general class of parabolic problems where the layer may vary with respect to the time. Truncation error and the stability analysis are obtained. Parameter-uniform error estimates are derived for the numerical solution. To support the theoretical results, numerical experiments are carried out.

4.1 Introduction

Consider the singularly perturbed parabolic initial-boundary-value problem (IBVP)

$$\begin{cases} u_t(x,t) + \mathcal{L}_\varepsilon u(x,t) = f(x,t), \quad (x,t) \in G = (0,1)\times(0,T], \\ u(x,0) = s(x), \quad \text{on } S_x = \{(x,0) : 0 \le x \le 1\}, \\ u(0,t) = a_0(t), \quad \text{on } S_0 = \{(0,t) : 0 \le t \le T\}, \\ u(1,t) = a_1(t), \quad \text{on } S_1 = \{(1,t) : 0 \le t \le T\}, \end{cases} \tag{4.1.1}$$

where $\mathcal{L}_\varepsilon u \equiv -\varepsilon u_{xx} + b(x)u$, $0 < \varepsilon \ll 1$ is a small parameter, and b, f are sufficiently smooth functions with $b(x) \ge \beta > 0$ for $x \in [0,1]$. Under the continuity and the

compatibility conditions on the data as given in (2.1.2) and (2.1.3), the IBVP (4.1.1) has a unique solution $u(x,t)$. Boundary layers occur in the solution when $\varepsilon \to 0$.

In recent studies much interest have been given to solve singulary perturbed problem using equidistribution principle because it does not require any information about the location and the width of the layers. Although it is computationally costly it can be applied successfully to semilinear and nonlinear singular perturbation problems. Domain decomposition and moving mesh method based on equidistribution principle for the space-time evolution problem can be found in [26]. Moreover, parabolic reaction-diffusion and convection-diffusion evolution problems are analyzed in [68, 27] respectively.

Here, in this chapter, the main goal is to provide an ε-uniform numerical method for the IBVP (4.1.1). To solve this problem, we use a modified backward-Euler scheme for the time derivative on uniform mesh and the central difference scheme for the spatial derivative on layer-adapted nonuniform meshes at each time level. The nonuniform meshes are obtained by equidistribution of a positive monitor function, which involves the second-order spatial derivative of the singular component of the solution. In this chapter, we analyze the linear parabolic reaction-diffusion problems. To match the mesh points on successive time levels we use linear interpolation that gives the modified-Euler scheme which is given in Section 4.2. The proposed scheme is ε-uniform convergent of order $O(\Delta t + N^{-2})$. Truncation errors are derived, stability analysis is carried out and ε-uniform error estimates are obtained.

4.2 The Numerical Solution

In this section, we discretize the parabolic IBVP (4.1.1), the time derivative is replaced by a modified backward-Euler scheme, and the spatial derivative is replaced by the central difference scheme. Later, we introduce the equidistribution grid, and derive the finite difference scheme. Finally, we provide the numerical algorithm to obtain the equidistributed grids on each time levels.

4.2.1 Finite difference scheme

On the time domain [0,T], we introduce the equidistant meshes with uniform time step Δt such that $\{t_n = n\Delta t,\ n = 0, \ldots, M,\ \Delta t = T/M\}$, where M denotes the number of mesh intervals in the t-direction. We consider the finite difference approximation of (4.1.1) on a non-uniform spatial discretization on n^{th} time level by $\{0 = x_0^n < x_1^n < \cdots < x_N^n = 1\}$, and denote the spatial step sizes by $h_i^n = x_i^n - x_{i-1}^n$, $i = 1, \ldots, N$. Therefore, the computational mesh is defined as $\overline{G}^{N,\Delta t} := \{(x_i^n, t_n) : i = 0, \ldots, N \text{ and } n = 0, \ldots M\}$.

Before describing the scheme, for a given mesh function $v(x_i^n, t_n) = v_i^n$, define the forward and backward differences δ_x^+, δ_x^- in spatial by $\delta_x^+ v_i^n = (v_{i+1}^n - v_i^n)/h_{i+1}^n$, $\delta_x^- v_i^n = (v_i^n - v_{i-1}^n)/h_i^n$, respectively, the second-order finite difference operator δ_x^2 as $\delta_x^2 v_i^n = (2(\delta_x^+ v_i^n - \delta_x^- v_i^n))/(h_i^n + h_{i+1}^n)$, and define a variation of backward difference operator δ_t^* in time by $\delta_t^* v_i^n = (v_i^n - \widehat{v}^{n-1}(x_i^n))/\Delta t$, where $\widehat{v}^n(x)$ is the linear interpolant of v_i^n at time level t_n. We discretize equation (4.1.1) by means of the modified backward difference for the time derivative, and the central difference for the space derivative. Hence the discretization of (4.1.1) takes the form, for $n = 0, 1, \ldots, M-1$,

$$\begin{cases} \dfrac{U_i^{n+1} - \widehat{U}^n(x_i^{n+1})}{\Delta t} + \mathcal{L}_\varepsilon^N U_i^{n+1} = f(x_i^{n+1}, t_{n+1}), \quad \text{for } i = 1, \ldots, N-1, \\ U_0^{n+1} = a_0(t_{n+1}), \quad U_N^{n+1} = a_1(t_{n+1}), \\ \widehat{U}^0(x_i) = s(x_i), \quad \text{for } i = 1, \ldots, N-1, \end{cases} \tag{4.2.1}$$

where $\mathcal{L}_\varepsilon^N U_i^{n+1} = -\varepsilon \delta_x^2 U_i^{n+1} + b_i U_i^{n+1}$. After rearranging the terms in (4.2.1), we obtain the following form of the difference scheme: for $n = 0, 1, \ldots, M-1$,

$$\begin{cases} r_{i,n+1}^- U_{i-1}^{n+1} + r_{i,n+1}^c U_i^{n+1} + r_i^+ U_{i+1}^{n+1} = g_i^n, \quad \text{for } i = 1, \ldots, N-1, \\ U_0^{n+1} = a_0(t_{n+1}), \quad U_N^{n+1} = a_1(t_{n+1}), \\ \widehat{U}^0(x_i) = s(x_i), \quad \text{for } i = 1, \ldots, N-1, \end{cases} \tag{4.2.2}$$

where

$$r_{i,n+1}^- = \frac{-2\varepsilon\Delta t}{h_i^{n+1}(h_i^{n+1} + h_{i+1}^{n+1})}, \quad r_{i,n+1}^+ = \frac{-2\varepsilon\Delta t}{h_{i+1}^{n+1}(h_i^{n+1} + h_{i+1}^{n+1})},$$
$$r_{i,n+1}^c = 1 + \Delta t b_{i,n+1} - r_{i,n+1}^- - r_{i,n+1}^+,$$
$$b_{i,n+1} = b(x_i^{n+1}), \qquad g_i^n = \widehat{U}^n(x_i^{n+1}) + \Delta t f(x_i^{n+1}, t_{n+1}),$$

and $\widehat{U}^n(x)$ is the linear interpolant of U_i^n at time level t_n for $n > 1$.

To determine the value of the monitor function (4.2.5), we have to know the approximate value of the singular component $w(x,t)$. To calculate the numerical value W_i^n of $w(x_i^n, t_n)$, we use the numerical approximate value V_i^n of $v(x_i^n, t_n)$ from the following recurrence relation:

$$\begin{cases} \tilde{r}_{i,n+1}^c V_i^{n+1} = \tilde{g}_i^n, \quad \text{for } i = 0, \ldots, N, \quad n = 0, 1, \ldots, M-1, \\ \widehat{V}^0(x_i) = s_0(x_i), \quad \text{for } i = 0, \ldots, N, \end{cases} \tag{4.2.3}$$

where $\tilde{r}_{i,n+1}^c = 1 + \Delta t b(x_i^{n+1})$, $\tilde{g}_i^n = \widehat{V}^n(x_i^{n+1}) + \Delta t f_0(x_i^{n+1}, t_{n+1})$, $\widehat{V}^n(x)$ is the linear interpolant of V_i^n at time level t_n for $n > 1$ and s_0, f_0 are the regular components corresponding to s, f respectively.

4.2.2 Adaptive spatial grids via equidistribution

Since the solution $u(x,t)$ of the IBVP(4.1.1) exhibits boundary layers, one has to use layer-adapted nonuniform spatial grids, which are fine inside the boundary layer region, and coarse in the outer region. To obtain such a grid, we use the idea of equidistribution of a positive monitor function given in (4.2.5). Here we consider equidistribution of $u(x,t)$ on every temporal level, because the problem (4.1.1) exhibits layer, which will not have any impact on the temporal component. A grid is said to be equidistributing $u(x,t)$, if

$$\int_{x_{i-1}^n}^{x_i^n} M(u(s,t),s)ds = \int_{x_i^n}^{x_{i+1}^n} M(u(s,t),s)ds, \quad i = 1,\ldots,N-1, \tag{4.2.4}$$

where $M(u(x,t),x)$ is a strictly positive, L_1–integrable function.

Here, we consider the following monitor function

$$M(u(x,t),x) = \alpha_c + |w_{xx}(x,t)|^{1/m}, \quad m \geq 2, \tag{4.2.5}$$

where $\alpha_c = \int_0^1 |w_{xx}(s,t)|^{1/m} ds$ is a positive constant that is independent of N, and $w(x,t)$ is the singular component of $u(x,t)$. The selection of this α_c will help to distribute the number of mesh points inside and outside the boundary layer region equally. The effect of increasing m is to smoothen the monitor function, which in turn leads to a smoother distribution of the grid points. In all of our numerical experiments, we will take $m = 2$.

In order to compute the value of the monitor function at the ith interior node of the spatial mesh, M_i^n,

$$M_i^n = \alpha + |\delta_x^2 W_i^n|^{1/m}, \quad \text{for } i = 1,\ldots,N-1, \tag{4.2.6}$$

where α is a discrete form of α_c, which can be written as

$$\alpha = h_1^n \, |\delta_x^2 W_1^n|^{1/m} + \sum_{i=2}^{N-1} h_i^n \left\{ \frac{|\delta_x^2 W_{i-1}^n|^{1/m} + |\delta_x^2 W_i^n|^{1/m}}{2} \right\} + h_N^n \, |\delta_x^2 W_{N-1}^n|^{1/m}.$$

For a truly adaptive algorithm, the monitor function has to be approximated from the numerical solution. For example, a simple discretization of (4.2.4) results in the set of equations $M_{i-1/2}^n (x_i^n - x_{i-1}^n) = M_{i+1/2}^n (x_{i+1}^n - x_i^n)$, where $M_{i+1/2}^n$ is an approximation to $M(u(x_{i+1/2}^n, t_n), x_{i+1/2}^n)$.

The detailed numerical algorithm to obtain the equidistribution grids is given in the following section.

4.2.3 Numerical algorithm

To get the equidistribution grid and the corresponding numerical solution, we use the following algorithm:

Step 1. Take $n = 1$ and choose a constant $C > 1$ that controls when the iteration has to be terminated.

Step 2. Take $k = 0$. Take the uniform spatial mesh $\{x_i^{n,(0)}\}$ as the initial value for $n = 1$ otherwise $\{x_i^{n-1}\}$ for the iteration.

Step 3. Compute the discrete solutions $\{U_i^{n,(k)}\}$ and $\{V_i^{n,(k)}\}$ satisfying (4.2.2) and (4.2.3), respectively with the help of the spatial mesh $\{x_i^{n,(k)}\}$.

Step 4. Find the singular component of the discrete solution by $W_i^{n,(k)} = U_i^{n,(k)} - V_i^{n,(k)}$.

Step 5. For a given mesh $\{x_i^{n,(k)}\}$ and the singular component of the discrete solution $\{W_i^{n,(k)}\}$, set $H_i^{(k)} = \left(\frac{M_{i-1}^{n,(k)} + M_i^{n,(k)}}{2}\right)(x_i^{n,(k)} - x_{i-1}^{n,(k)})$, for $i = 1, \ldots, N$, where $M_i^{n,(k)}$ is calculated from (4.2.6), and set $M_0^{n,(k)} = M_1^{n,(k)}$ and $M_N^{n,(k)} = M_{N-1}^{n,(k)}$.

Step 6. Set $L_0 = 0$ and $L_i = \sum_{j=1}^{i} H_j^{(k)}$ for $i = 1, \ldots, N$. Define $C^{(k)} := \frac{N}{L_N} \max_{i=0,1,\ldots,N} H_i^{(k)}$.

Step 7. If $C^{(k)} \leq C$, then go to Step 10.

Step 8. Set $Y_i = iL_N/N$ for $i = 0, 1, \ldots, N$. Interpolate the points (L_i, x_i). Generate the new mesh $\{x_i^{n,(k+1)}\}$ by evaluating this interpolant at Y_i for $i = 0, 1, \ldots, N$.

Step 9. Set $k = k + 1$, return to Step 3.

Step 10. Take $\{x_i^{n,(k-1)}\}$ as the final mesh $\{x_i^n\}$ and set $U_i^{n,(k-1)} = U_i^n$ and $V_i^{n,(k-1)} = V_i^n$.

Step 11. If $n = M$, then goto Step 13.

Step 12. Set $n = n + 1$, return to Step 2.

Step 13. Stop. U_i^n is the required numerical solution and $\{x_i^n\}$ is the required equidistribution mesh at time level t_n.

4.3 Error Analysis

Here, we derive the truncation error for the numerical scheme, and carry out the stability analysis. Finally, we obtain the ε-uniform error estimate.

The following lemma states the discrete maximum principle, which follows from Lemma 2.4.1.

Lemma 4.3.1. *Consider the IBVP (4.1.1), and the numerical scheme given in (4.2.2). Assume that the statement given in Lemma 2.4.1 holds true for the difference scheme (4.2.2). Then, the difference operator defined in (4.2.2) satisfies the discrete maximum principle.*

Theorem 4.3.2. *Let u and U be respectively the continuous and the numerical solutions of the IBVPs (4.1.1), and (4.2.2). Then, we have the following bound, for $j = 1, 2, \ldots, M$, $i = 0, 1, \ldots, N$,*

$$\max_{i,j} \left| u(x_i^j, t_j) - U_i^j \right| \leq C[\Delta t + N^{-2}]. \tag{4.3.1}$$

Proof. Let $\eta_i^j = u_i^j - U_i^j$ be the truncation error in the computed solution at each mesh point (x_i^j, t_j). We write the scheme (4.2.1) as $[\delta_t^* U]_i^j + [\mathfrak{L}_\varepsilon^N U]_i^j = f_i^j$. Therefore, the truncation error of the above scheme can be written in the following way as given in [49] and [17], $[\delta_t^* \eta]_i^j + [\mathfrak{L}_\varepsilon^N \eta]_i^j = \chi_{1,i}^j + \chi_{2,i}^j$, where $\chi_{1,i}^j$ and $\chi_{2,i}^j$ are as follows, $\chi_{1,i}^j := [\mathfrak{L}_\varepsilon^N u]_i^j - (\mathfrak{L}_\varepsilon^N u)_i^j$ and $\chi_{2,i}^j := \delta_t^* u_i^j - (u_t)_i^j$. With this splitting of the truncation error we can decompose the error η as $\eta = \phi + \psi$. Here the function ϕ_i^j is, for each fixed $j = 1, \ldots, M$, the solution of the discrete two-point boundary-value problem

$$\begin{cases} [\mathfrak{L}_\varepsilon^N \phi]_i^j = \chi_{1,i}^j \quad \text{for } i = 1, \ldots, N-1, \\ \phi_0^j = \phi_N^j = 0, \end{cases} \tag{4.3.2}$$

while ψ_i^j, the solution of the discrete parabolic problem is defined by

$$\begin{cases} [\delta_t^* \psi + \mathfrak{L}_\varepsilon^N \psi]_i^j = \chi_{2,i}^j - \delta_t^* \phi_i^j \quad \text{for } i = 1, \ldots, N-1, \\ \psi_0^j = \psi_N^j = 0, \quad \text{for } j = 1, \ldots, M, \\ \psi_i^0 = -\phi_i^0, \quad \text{for } i = 0, \ldots, N. \end{cases} \tag{4.3.3}$$

Equation (4.3.2) is a sequence of two-point boundary-value problems that has been discretized using $\mathfrak{L}_\varepsilon^N$, with $\chi_{1,i}^j$ playing the role of truncation error and can be bounded using the technique from [7]. The problem (4.1.1) exhibits regular boundary layers and the same is true for the equation (4.3.2) using the bounds in (2.2.2), the error bound derived in [7] can be invoked for all the temporal levels:

$$|\phi_i^j| \leq CN^{-2} \quad \text{for all } i, j, \tag{4.3.4}$$

with the assumption that $N^{-1} \gg \sqrt{\varepsilon}$ and the fact that our problem exhibits regular boundary layers. All it remains is to bound the other error component ψ. By Lemma 2.4.1 and the discrete maximum principle we get the following bound for the error component ψ,

$$|\psi_i^j| \;=\; C\left(\max_i |\phi_i^0| + \max_{i,j} |\chi_{2,i}^j - \delta_t^* \phi_i^j|\right) \quad \text{for all } i, j.$$

Using the bounds of $\chi_{2,i}^j$ and (4.3.4) we obtain

$$|\psi_i^j| \;=\; C\left[N^{-2} + \Delta t + \max_{i,j} |\delta_t^* \phi_i^j|\right] \quad \text{for all } i, j. \tag{4.3.5}$$

It remains to bound the term $\delta_t^* \phi$ in (4.3.5). Using the assumption that $b(x)$ is independent of t, the definition (4.3.2) implies that $\delta_t^* \phi$ satisfies

$$\begin{cases} \mathfrak{L}_\varepsilon^N (\delta_t^* \phi)_i^j = \delta_t^* \chi_{1,i}^j \quad \text{for } i = 1, \ldots, N-1, \\ (\delta_t^* \phi)_0^j = (\delta_t^* \phi)_N^j = 0. \end{cases} \tag{4.3.6}$$

To analyze the above sequence of two-point boundary-value problems (4.3.6), observe that the right-hand side of the above equation can be written as

$$\begin{aligned} \delta_t^* \chi_{1,i}^j \;&=\; \frac{1}{\Delta t}\left(\chi_{1,i}^j - \widehat{\chi}_1^{j-1}(x_i^{j-1})\right) \\ &=\; \frac{1}{\Delta t}\left(\mathfrak{L}_\varepsilon^N u_i^j - (\mathfrak{L}_\varepsilon u)_i^j\right) \\ &\quad -\frac{1}{\Delta t}\left((\mathfrak{L}_\varepsilon^N u_{k-1}^{j-1} - (\mathfrak{L}_\varepsilon u)_{k-1}^{j-1})\phi_{k-1}(x_i^j) + (\mathfrak{L}_\varepsilon^N u_k^{j-1} - (\mathfrak{L}_\varepsilon u)_k^{j-1})\phi_k(x_i^j)\right), \end{aligned}$$

where $\phi_{k-1}(x) = \frac{x_k^{j-1} - x}{x_k^{j-1} - x_{k-1}^{j-1}}$, $\phi_k(x) = \frac{x - x_{k-1}^{j-1}}{x_k^{j-1} - x_{k-1}^{j-1}}$ and $x_{k-1}^{j-1} \le x_i^j < x_{k-1}^j$, for some k. The above step is precisely applying the linear interpolation, one can also use higher-order interpolation such as cubic spline for higher-order convergence rate. Let $\hat{\mathfrak{L}}_\varepsilon u = -\varepsilon u_{xx}$ and $\hat{\mathfrak{L}}_\varepsilon^N u_i^j = -\varepsilon \delta_x^2 u_i^j$. By using the fact that the interpolation error is of order $O(N^{-2})$, one can obtain the following inequality

$$\left|\delta_t^* \chi_{1,i}^j\right| \le \left|\frac{1}{\Delta t}\int_{t_{j-1}}^{t_j} \left[\hat{\mathfrak{L}}_\varepsilon^N \frac{\partial}{\partial t} u(x_i^j, t) - \hat{\mathfrak{L}}_\varepsilon \frac{\partial}{\partial t} u(x_i^j, t)\right] dt\right| + CN^{-2}.$$

By using the Peano kernel theorem as in [38], and following the argument given in [17], we obtain the same estimate on $\delta_t^* \chi_{1,i}^j$ as the corresponding truncation error bounds arising in [7] for a standard two-point reaction-diffusion boundary-value problem. Now analyzing the problem in the same way as (4.3.2) with the bounds (2.2.2), we obtain the following bound for $\delta_t^* \phi_i^j$

$$|\delta_t^* \phi_i^j| \le CN^{-2} \quad \text{for all } i, j. \tag{4.3.7}$$

Now, using (4.3.4), (4.3.5) and (4.3.7), we get the required bound. ∎

4.4 Numerical Results

In this section, we shall present the numerical results obtained by the discrete scheme (4.2.2) for a test problem on the rectangular mesh $\overline{G}^{N,\Delta t}$. In the numerical experiment we will fix $m = 2$, which is necessary to define the monitor function (4.2.5). Moreover, in all the tables we begin with $N = 16$ and the time step $\Delta t = 0.2$ and we multiply N by two and divide Δt by four. The reason of dividing Δt by four is to justify the spatial order of convergence properly.

Example 4.4.1. *Consider the following parabolic initial-boundary-value problem:*

$$u_t(x,t) - \varepsilon u_{xx}(x,t) + u(x,t) = f(x,t), \quad (x,t) \in (0,1) \times (0,1]. \tag{4.4.1}$$

The right-hand side source term, initial and boundary conditions are calculated from the exact solution

$$u(x,t) = \left(t + \frac{x^2}{2\varepsilon}\right) \operatorname{erfc}\left(\frac{x}{2\sqrt{\varepsilon t}}\right) - \sqrt{\frac{t}{\pi\varepsilon}}\, x \exp\left(\frac{-x^2}{4\varepsilon t}\right).$$

As the exact solution of the problem (4.4.1) is known, for each ε, we calculate the maximum point-wise error by

$$e_\varepsilon^{N,\Delta t} = \max_{(x_i^j,t_j)\in\overline{G}^{N,\Delta t}} \left|u(x_i^j,t_j) - U^{N,\Delta t}(x_i^j,t_j)\right|,$$

where $u(x_i^j,t_j)$ and $U^{N,\Delta t}(x_i^j,t_j)$ respectively, denote the exact and the numerical solution obtained on the mesh with N mesh intervals in the spatial direction and M mesh intervals in the $t-$direction such that $\Delta t = T/M$ is the uniform time step. In addition, we determine the corresponding rate of convergence by $p_\varepsilon^{N,\Delta t} = \log_2\left(\frac{e_\varepsilon^{N,\Delta t}}{e_\varepsilon^{2N,\Delta t/4}}\right)$. The calculated maximum point-wise errors $e_\varepsilon^{N,\Delta t}$ and the corresponding rate of convergence $p_\varepsilon^{N,\Delta t}$ for Example 4.4.1 are given in Tables 4.1 and 4.2 respectively. From these results one can observe the ε–uniform second-order convergence in the space and first-order in the time. Figure 4.1 (a) shows the solution plot at time $t = 1$ for various values of ε and the log-log plot (b) shows the slope of maximum point-wise error of the proposed numerical method is of second-order in space.

4.5 Conclusions

In this chapter, we provided an ε-uniform numerical method for the IBVP (4.1.1). The spatial grid is obtained via equidistribution of a positive monitor function, which involves second-order spatial derivative of the singular component of the solution u. The time derivative is replaced by the modified backward-Euler scheme in order to accommodate

Table 4.1: *Maximum point-wise error of the solution* $e_\varepsilon^{N,\Delta t}$ *for Example* 4.4.1 *using equidistribution mesh.*

	Number of Intervals N/Time Step Size Δt				
ε	$16/\frac{1}{5}$	$32/\frac{1}{20}$	$64/\frac{1}{80}$	$128/\frac{1}{320}$	$256/\frac{1}{1280}$
10^0	1.3208e-02	4.8368e-03	1.3771e-03	3.6046e-04	9.2406e-05
10^{-2}	1.6934e-02	5.0200e-03	1.3741e-03	3.6053e-04	9.2542e-05
10^{-4}	1.7916e-02	4.9202e-03	1.3730e-03	3.6186e-04	9.2662e-05
10^{-6}	1.6650e-02	5.0290e-03	1.3953e-03	3.6384e-04	9.2886e-05
10^{-8}	1.7696e-02	4.9719e-03	1.4662e-03	3.6911e-04	9.3160e-05

Table 4.2: *Rate of convergence of the solution* $p_\varepsilon^{N,\Delta t}$ *for Example* 4.4.1 *using equidistribution mesh.*

	Number of Intervals N/Time Step Size Δt			
ε	$16/\frac{1}{5}$	$32/\frac{1}{20}$	$64/\frac{1}{80}$	$128/\frac{1}{320}$
10^0	1.4493	1.8124	1.9337	1.9638
10^{-2}	1.7542	1.8693	1.9302	1.9619
10^{-4}	1.8645	1.8414	1.9238	1.9654
10^{-6}	1.7272	1.8497	1.9392	1.9698
10^{-8}	1.8316	1.7617	1.9900	1.9863

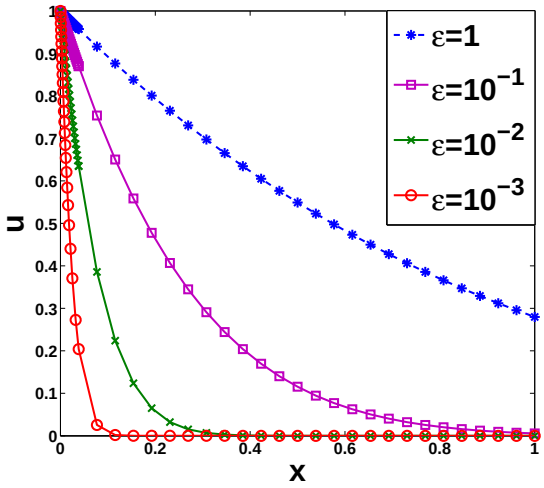

(a) *Exact solution at time* $t = 1$ *for different values of* ε.

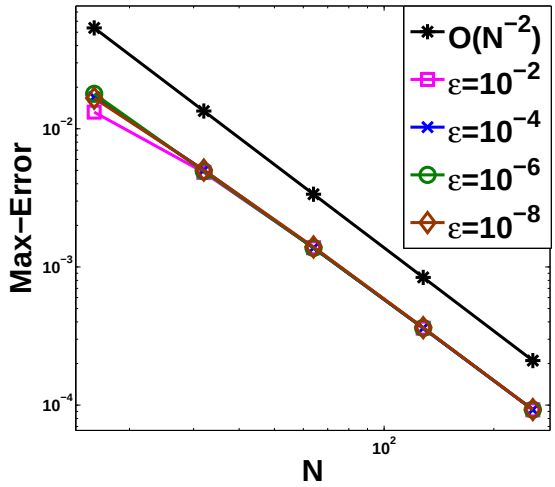

(b) *Log-log plot of maximum point-wise error of the solution* $e_\varepsilon^{N,\Delta t}$.

Figure 4.1: *Solution and error plots for Example 4.4.1.*

the grids properly, and the spatial derivative is replaced by the central difference scheme. The proposed scheme is parameter-uniform convergent of order $O(\Delta t+N^{-2})$. Truncation errors are derived, stability analysis is carried out and ε-uniform error estimates are obtained.

CHAPTER 5

Uniformly Convergent Numerical Method for Singularly Perturbed Parabolic Initial-Boundary-Value Problems on Equidistributed Grids

In this chapter, we study the numerical solution of singularly perturbed parabolic convection-diffusion problems exhibiting regular boundary layers. To solve these problems, we use the classical upwind finite difference scheme on layer-adapted nonuniform grids. The nonuniform grids are obtained by equidistribution of a positive monitor function, which is a linear combination of a constant and the second-order spatial derivative of the singular component of the solution on every temporal level. Truncation error and the stability analysis are obtained. Parameter-uniform error estimates are derived for the numerical solution. To support the theoretical results, numerical experiments are carried out.

5.1 Introduction

Here, we consider the following singularly perturbed parabolic initial-boundary-value problem (IBVP):

$$\begin{cases} u_t(x,t) + \mathfrak{L}_\varepsilon u(x,t) = f(x,t), \quad (x,t) \in G = \Omega \times (0,T] \equiv (0,1) \times (0,T], \\ u(x,0) = u_0(x), \quad x \in \Omega, \\ u(0,t) = u(1,t) = 0, \quad t \in [0,T], \end{cases} \tag{5.1.1}$$

where

$$\mathfrak{L}_\varepsilon u \equiv -\varepsilon u_{xx} + a(x)u_x + b(x)u,$$

$0 < \varepsilon \ll 1$ is a small parameter and the coefficients a, b are sufficiently smooth functions such that

$$a(x) \geq \alpha > 0, \quad b(x) \geq \beta \geq 0 \quad \text{on} \quad \overline{\Omega} = [0, 1]. \tag{5.1.2}$$

Under sufficient smoothness and compatibility conditions imposed on the functions u_0 and f, the parabolic problem (5.1.1)-(5.1.2), in general admits a unique solution $u(x, t)$ which exhibits a regular boundary layer of width $\mathrm{O}(\varepsilon)$ at $x = 1$.

Our main goal is to solve the parabolic IBVP (5.1.1)-(5.1.2) numerically by finite difference scheme on an adaptive grid obtained through equidistribution of a positive monitor function, which is a linear combination of a constant and the second-order spatial derivative of the singular component of the solution. As the solution of the IBVP (5.1.1)-(5.1.2) exhibits an exponential layer only in the spatial variable, we will use nonuniform grids only in the spatial direction obtained as like in the stationary one-dimensional problem, and uniform grids for the temporal direction. More precisely, at each time level, we obtain the nonuniform adaptive grid by solving the mesh equidistribution relation. Therefore, obtaining the adaptive grid by the present method is very economy. The time derivative in the PDE (5.1.1) is approximated by the backward-Euler scheme, and an upwind finite difference is used to discretize the spatial derivatives. ε–uniform error estimates of order $O(N^{-1} + \Delta t)$ are derived for the numerical solution, where N and Δt are the discretization parameters in space and time respectively. Numerical experiments reveal the fact of ε–uniform first-order convergent results.

We organize the rest of the chapter as follows: In Section 5.2 we introduce the implicit-Euler scheme for the time derivative and upwind finite difference scheme for the spatial derivatives and also adaptive spatial mesh via equidistribution principle. Afterwards, we carry out the error analysis for the scheme in Section 5.3 and prove the main theoretical error estimates, *i.e.,* the ε-uniform optimal error bounds of the scheme on the adaptive mesh. Section 5.4 describes application of the present method for semilinear singularly perturbed parabolic PDEs. In Section 5.5, we present the numerical results for two linear problems and a semilinear test problem to validate the theoretical error estimate. Moreover, numerical results for the Burger's equation are also presented. Finally in Section 5.6, we summarize the main conclusions.

5.2 The Numerical Solution

In this section, we introduce the equidistribution gird, and derive the finite difference scheme for the parabolic IBVP (5.1.1) also to the corresponding regular problem. The fully discrete scheme (5.2.2) is obtain by applying simple upwind difference scheme to corresponding semidiscrete problem (3.3.1).

5.2.1 Finite difference scheme

We consider the finite difference approximation of (5.1.1) on a nonuniform spatial discretization at each temporal level by

$$\overline{\Omega}_x^n = \{0 = x_0^n < x_1^n < \cdots < x_N^n = 1\},$$

where n denotes the time level, and denote the spatial step sizes by

$$h_i^n = x_i^n - x_{i-1}^n, \quad i = 1, \ldots, N.$$

The simple upwind finite difference spatial discretization of (3.3.1) takes the form, for $n = 0, 1, \ldots, M-1$,

$$\begin{cases} (I + \Delta t \mathfrak{L}_\varepsilon^N) U_i^{n+1} = U_i^n + \Delta t f(x_i^{n+1}, t_{n+1}), & \text{for } i = 1, \ldots, N-1, \\ U_0^{n+1} = U_N^{n+1} = 0, \end{cases} \tag{5.2.1}$$

where $\mathfrak{L}_\varepsilon^N$ is the discretization of the differential operator $\mathfrak{L}_\varepsilon$ using the simple upwind finite difference scheme for the spatial derivatives, which takes the following form

$$\mathfrak{L}_\varepsilon^N U_i^{n+1} = -\varepsilon \delta_x^2 U_i^{n+1} + a_i^{n+1} D_x^- U_i^{n+1} + b_i^{n+1} U_i^{n+1}.$$

After rearranging the terms in (5.2.1), we obtain the following form of the difference scheme: for $n = 0, 1, \ldots, M-1$,

$$\begin{cases} r_{i,n+1}^- U_{i-1}^{n+1} + r_{i,n+1}^c U_i^{n+1} + r_{i,n+1}^+ U_{i+1}^{n+1} = g_i^n, & \text{for } i = 1, \ldots, N-1, \\ U_0^{n+1} = U_N^{n+1} = 0, \end{cases} \tag{5.2.2}$$

where

$$r_{i,n+1}^- = \frac{-2\varepsilon\Delta t}{h_i^{n+1}(h_i^{n+1} + h_{i+1}^{n+1})} - \frac{a_i^{n+1}\Delta t}{h_i^{n+1}}, \qquad r_{i,n+1}^+ = \frac{-2\varepsilon\Delta t}{h_{i+1}^{n+1}(h_i^{n+1} + h_{i+1}^{n+1})},$$

$$r_{i,n+1}^c = 1 + \Delta t b_i^{n+1} - r_{i,n+1}^- - r_{i,n+1}^+,$$

$$a_i^{n+1} = a(x_i^{n+1}), \qquad b_i^{n+1} = b(x_i^{n+1}), \qquad g_i^n = \tilde{U}(x_i^{n+1}, t_n) + \Delta t f(x_i^{n+1}, t_{n+1}),$$

and $\tilde{U}$ is the linear interpolant of U.

To determine the value of the monitor function (5.2.6), we have to know the approximate value of the singular component $w(x,t)$. To calculate the numerical value W_i^n of $w(x_i, t_n)$, we use the numerical approximate value V_i^n of $v(x_i^n, t_n)$ from the following recurrence relation: for $n = 0, 1, \ldots, M-1$,

$$\begin{cases} (I + \Delta t \mathfrak{L}_0^N) V_i^{n+1} \equiv \tilde{r}_{i,n+1}^- V_{i-1}^{n+1} + \tilde{r}_{i,n+1}^c V_i^{n+1} = \tilde{g}_i^n, & \text{for } i = 1, \ldots, N, \\ V_0^{n+1} = 0, \end{cases} \tag{5.2.3}$$

where

$$\tilde{r}^{-}_{i,n+1} = -\frac{a_i^{n+1}\Delta t}{h_i^{n+1}}, \qquad \tilde{r}^{c}_{i,n+1} = 1 + \Delta t b_i^{n+1} - \tilde{r}^{-}_{i,n+1},$$

$$a_i^{n+1} = a(x_i^{n+1}), \qquad b_i^{n+1} = b(x_i^{n+1}), \qquad \tilde{g}_i^n = \tilde{V}(x_i^{n+1}, t_n) + \Delta t f(x_i^{n+1}, t_{n+1}).$$

and $\tilde{V}$ is the linear interpolant of V.

5.2.2 Adaptive spatial grids via equidistribution

Since the solution $u(x,t)$ of the IBVP (5.1.1) exhibits boundary layers, one has to use layer-adapted nonuniform spatial grids, which are fine inside the boundary layer region, and coarse in the outer region. To obtain such a grid, we use the idea of equidistribution of a positive monitor function given in (5.2.6). Here we consider equidistribution of $u(x,t)$ on every temporal level. A grid is said to be equidistributing $u(x,t)$ on time level t_n, if

$$\int_{x_{i-1}^n}^{x_i^n} M(u(s,t_n),s)ds = \int_{x_i^n}^{x_{i+1}^n} M(u(s,t_n),s)ds, \quad i = 1,\ldots,N-1, \tag{5.2.4}$$

where $M(u(x,t_n),x)$ is a strictly positive, L_1–integrable function. Equation (5.2.4) can also be written in the following form:

$$\int_{x_{i-1}^n}^{x_i^n} M(u(s,t_n),s)ds = \frac{1}{N}\int_0^1 M(u(s,t_n),s)ds, \quad i = 1,\ldots,N. \tag{5.2.5}$$

Here, we consider the following monitor function

$$M(u(x,t_n),x) = \alpha_c + |w_{xx}(x,t_n)|^{1/m}, \quad m \geq 2, \tag{5.2.6}$$

here α_c is a positive constant that is independent of N and $w(x,t)$ is the singular component of $u(x,t)$. Precisely, α_c is given by

$$\alpha_c = \int_0^1 |w_{xx}(s,t_n)|^{1/m} ds. \tag{5.2.7}$$

The selection of this α_c will help to distribute the number of mesh points inside and outside the boundary layer region equally. The effect of increasing m is to smoothen the monitor function, which in turn leads to a smooth distribution of the grid points. From [6], we clearly see the influence of the parameter m. For all of the numerical experiments, we will take $m = 2$.

In order to compute the value of the monitor function at the ith interior node of the spatial mesh, M_i^n,

$$M_i^n = \alpha + |\delta_x^2 W_i^n|^{1/m}, \quad \text{for } i = 1,\ldots,N-1, \tag{5.2.8}$$

where α is the discrete form of (5.2.7), which can be written as

$$\alpha = h_1^{n+1} \left|\delta_x^2 W_1^n\right|^{1/m} + \sum_{i=2}^{N-1} h_i^{n+1} \left\{ \frac{\left|\delta_x^2 W_{i-1}^n\right|^{1/m} + \left|\delta_x^2 W_i^n\right|^{1/m}}{2} \right\} + h_N^{n+1} \left|\delta_x^2 W_{N-1}^n\right|^{1/m}.$$

For a truly adaptive algorithm, the monitor function has to be approximated from the numerical solution. For example, a simple discretization of (5.2.4) results in the set of equations

$$M_{i-1/2}^n (x_i^n - x_{i-1}^n) = M_{i+1/2}^n (x_{i+1}^n - x_i^n), \quad \text{for } i = 1, \ldots, N-1,$$

where $M_{i+1/2}^n$ is an approximation to $M(u(x_{i+1/2}^n, t_n), x_{i+1/2}^n)$.

In the numerical algorithm given in Section 4.2.3, we use the discrete form of the monitor function given in (5.2.8). For the convergence of the algorithm one can refer [43], where the authors analyzed the predetermined number of iterations for ε-uniform convergence, the results are proved for the well-known arc-length monitor function, which is different from the one as given in (5.2.6).

5.3 Error Analysis

Here, we study the consistency and stability of the proposed numerical scheme (5.2.2). Finally, we analyze the ε-uniform convergence of the numerical solution on the adaptive grid obtain through the monitor function (5.2.6).

Instead of analyzing the fully discrete scheme (5.2.2) directly, first we analyze the following variant discrete scheme of (5.2.2) then we generalize the result to prove the ε-uniform convergence of the fully discrete scheme, for $n = 0, 1, \ldots, M-1$, $i = 1 \ldots N-1$,

$$\begin{cases} (I + \Delta t \mathfrak{L}_\varepsilon^N)\widehat{U}_i^{n+1} \equiv r_{i,n+1}^- \widehat{U}_{i-1}^{n+1} + r_{i,n+1}^c \widehat{U}_i^{n+1} + r_{i,n+1}^+ \widehat{U}_{i+1}^{n+1} = \widehat{g}_i^n, \\ U_0^{n+1} = U_N^{n+1} = 0, \end{cases} \tag{5.3.1}$$

where

$$\begin{aligned} r_{i,n+1}^- &= \frac{-2\varepsilon\Delta t}{h_i(h_i + h_{i+1})} - \frac{a_i \Delta t}{h_i}, \qquad r_{i,n+1}^+ = \frac{-2\varepsilon\Delta t}{h_{i+1}(h_i + h_{i+1})}, \\ r_{i,n+1}^c &= 1 + \Delta t b_i - r_{i,n+1}^- - r_{i,n+1}^+, \\ a_i &= a(x_i^{n+1}), \qquad b_i = b(x_i^{n+1}), \qquad \widehat{g}_i^n = u(x_i^{n+1}, t_n) + \Delta t f(x_i^{n+1}, t_{n+1}). \end{aligned}$$

5.3.1 Decomposition of the numerical solution

As like in the continuous solution, we will decompose the numerical solution into the regular and the singular components. That is, we decompose $\widehat{U}_i^n$ as

$$\widehat{U}_i^n = \widehat{V}_i^n + \widehat{W}_i^n, \quad 1 \le i \le N,\, 1 \le n \le M, \tag{5.3.2}$$

where

$$\begin{cases} (I + \Delta t \mathfrak{L}_\varepsilon^N)\widehat{V}_i^{n+1} = v(x_i^{n+1}, t_n) + \Delta t f(x_i^{n+1}, t_{n+1}), \\ \widehat{V}_0^{n+1} = v(x_0^{n+1}, t_{n+1}),\ \widehat{V}_N^{n+1} = v(x_N^{n+1}, t_{n+1}), \end{cases} \tag{5.3.3}$$

and

$$\begin{cases} (I + \Delta t \mathfrak{L}_\varepsilon^N)\widehat{W}_i^{n+1} = w(x_i^{n+1}, t_n), \\ \widehat{W}_0^{n+1} = w(x_0^{n+1}, t_{n+1}),\ \widehat{W}_N^{n+1} = w(x_N^{n+1}, t_{n+1}). \end{cases} \tag{5.3.4}$$

Now, the nodal error in the numerical solution can also be decomposed as

$$|\widehat{u}^{n+1}(x_i^{n+1}) - \widehat{U}_i^{n+1}| \le |\widehat{v}^{n+1}(x_i^{n+1}) - \widehat{V}_i^{n+1}| + |\widehat{w}^{n+1}(x_i^{n+1}) - \widehat{W}_i^{n+1}|, \tag{5.3.5}$$

where $\widehat{v}$ and $\widehat{w}$ are the time semidiscretization of the regular and the singular components of $\widehat{u}$, respectively.

Lemma 5.3.1. (**Discrete comparison principle**) *The system* $(I + \Delta t \mathfrak{L}_\varepsilon^N)u_i^{n+1} = g_i^n$, *with* u_0^{n+1} *and* u_N^{n+1} *specified, has a unique solution. If* $(I+\Delta t \mathfrak{L}_\varepsilon^N)u_i^{n+1} \le (I+\Delta t \mathfrak{L}_\varepsilon^N)z_i^{n+1}$, $1 \le i \le N-1$, *and if* $u_0^{n+1} \le z_0^{n+1}$, $u_N^{n+1} \le z_N^{n+1}$, *then* $u_i^{n+1} \le z_i^{n+1}$, $1 \le i \le N-1$.

Proof. The matrix associated with $(I + \Delta t \mathfrak{L}_\varepsilon^N)$ is an irreducible M-matrix and so has a positive inverse. Hence, the result follows. ∎

Lemma 5.3.2. *The error of the regular component satisfies* $|\widehat{v}^{n+1}(x_i^{n+1}) - \widehat{V}_i^{n+1}| \le CN^{-1}$, *for* $n = 0, 1, \ldots, M-1$.

Proof. The local truncation error of the regular component at the node (x_i^{n+1}, t_{n+1}),

$$\begin{aligned} \tau_{i,n+1}^{\widehat{V}} &= \left(I + \Delta t \mathfrak{L}_\varepsilon^N\right)\left(\widehat{v}^{n+1}(x_i^{n+1}) - \widehat{V}_i^{n+1}\right) \\ &= r_{i,n+1}^{-}\widehat{v}^{n+1}(x_{i-1}^{n+1}) + r_{i,n+1}^{c}\widehat{v}^{n+1}(x_i^{n+1}) + r_{i,n+1}^{+}\widehat{v}^{n+1}(x_{i+1}^{n+1}) \\ &\qquad - \left(v(x_i^{n+1}, t_n) + \Delta t f(x_i^{n+1}, t_{n+1})\right) \\ &= r_{i,n+1}^{-}\widehat{v}^{n+1}(x_{i-1}^{n+1}) + r_{i,n+1}^{c}\widehat{v}^{n+1}(x_i^{n+1}) + r_{i,n+1}^{+}\widehat{v}^{n+1}(x_{i+1}^{n+1}) \\ &\qquad - \left(I + \Delta t \mathfrak{L}_\varepsilon\right)\widehat{v}^{n+1}(x_i^{n+1}). \end{aligned}$$

Using the Peano's kernel theorem for every value of n, the truncation error of the regular component reduces to,

$$\begin{aligned}\tau_{i,n+1}^{\widehat{V}} = \quad & -\frac{\Delta t\varepsilon}{(h_i^{n+1}+h_{i+1}^{n+1})}\left\{\frac{1}{h_{i+1}^{n+1}}\int_{x_i^{n+1}}^{x_{i+1}^{n+1}}(s-x_{i+1}^{n+1})^2(\widehat{v}^{n+1})'''(s)ds\right.\\ & \left.-\frac{1}{h_i^{n+1}}\int_{x_{i-1}^{n+1}}^{x_i^{n+1}}(s-x_{i-1}^{n+1})^2(\widehat{v}^{n+1})'''(s)ds\right\}\\ & -\frac{\Delta t a(x_i^{n+1})}{h_{i-1}^{n+1}}\int_{x_{i-1}^{n+1}}^{x_i^{n+1}}(s-x_{i-1}^{n+1})(\widehat{v}^{n+1})''(s)ds.\end{aligned}$$

And, we obtain the bound

$$|\tau_{i,n+1}^{\widehat{V}}| \leq \quad \Delta t\varepsilon\int_{x_{i-1}^{n+1}}^{x_{i+1}^{n+1}}|(\widehat{v}^{n+1})'''(s)|ds+\Delta t\tilde{\alpha}\int_{x_{i-1}^{n+1}}^{x_i^{n+1}}|(\widehat{v}^{n+1})''(s)|ds,$$

where $\tilde{\alpha}$ is the upper bound of $a(x)$ on $[0,1]$. If we use the bounds of the regular part $\widehat{v}$ this may be simplified to

$$|\tau_{i,n+1}^{\widehat{V}}| \leq \quad C\int_{x_{i-1}^{n+1}}^{x_{i+1}^{n+1}}\left(|(\widehat{v}^{n+1})''(s)|+|(\widehat{v}^{n+1})'(s)|+|(\widehat{v}^{n+1})(s)|+1\right)ds.$$

From the bound of the regular part $\widehat{v}$ and the spatial discretization satisfying the equidistribution principle (5.2.5) with the monitor function given in (5.2.8), the local truncation error of the regular component reduced to

$$|\tau_{i,n+1}^{\widehat{V}}| \leq CN^{-1}, \text{ for } i=1,2,\ldots,N-1,\ n=0,1,\ldots,M-1.$$

That is,

$$\left|\left(I+\Delta t\mathfrak{L}_\varepsilon^N\right)\left(\widehat{v}^{n+1}(x_i^{n+1})-\widehat{V}_i^{n+1}\right)\right| \leq CN^{-1}.$$

Now using the fact that the operator $\left(I+\Delta t\mathfrak{L}_\varepsilon^N\right)$ satisfies the discrete comparison principle (Lemma 5.3.1) and the inverse operator is uniformly bounded we can conclude that,

$$|\widehat{v}^{n+1}(x_i^{n+1})-\widehat{V}_i^{n+1}| \leq CN^{-1}, \text{ for } i=1,2,\ldots,N-1,\ n=0,1,\ldots,M-1.$$

This completes the proof. ∎

Lemma 5.3.3. *Numerical solution of the singular component satisfies*

$$|\widehat{W}_i^{n+1}| \leq C\prod_{k=i+1}^{N}\left(1+\frac{\alpha h_k^{n+1}}{m\varepsilon}\right)^{-1}, \text{ for } i=0,1,\ldots,N-1,\ n=0,1,\ldots,M-1,$$

and

$$|\widehat{W}_N^{n+1}| \leq C, \quad \text{for } n=0,1,\ldots,M-1.$$

Proof. Define

$$S_i^{n+1} := \prod_{k=i+1}^{N} \left(1 + \frac{\alpha h_k^{n+1}}{m\varepsilon}\right)^{-1}, \quad \text{for } i = 0, 1, \ldots, N-1,$$
$$S_N^{n+1} := 1.$$

We know from (5.3.4) that

$$\widehat{W}_N^{n+1} \leq C = CS_N^{n+1},$$

and

$$\begin{aligned} \widehat{W}_0^{n+1} &\leq C \exp\left(-\frac{\alpha}{\varepsilon}\right) \leq C \exp\left(-\frac{\alpha}{m\varepsilon}\right) \\ &\leq C \prod_{k=1}^{N} \exp\left(-\frac{\alpha h_k^{n+1}}{m\varepsilon}\right) \\ &< C \prod_{k=1}^{N} \left(1 + \frac{\alpha h_k^{n+1}}{m\varepsilon}\right)^{-1}. \end{aligned}$$

For $i = 1 \ldots, N-1$, we have

$$\begin{aligned} \left(I + \Delta t \mathfrak{L}_\varepsilon^N\right) \widehat{W}_i^{n+1} &= w(x_i^{n+1}, t_n) \leq C \exp\left(-\frac{\alpha(1 - x_i^{n+1})}{m\varepsilon}\right) \\ &\leq \exp\left(-\frac{\alpha(1 - x_i^{n+1})}{m\varepsilon}\right) \\ &\leq CS_i^{n+1}, \end{aligned}$$

by simple calculation it can be shown that S_i^{n+1} is bounded by $C\left(I + \Delta t \mathfrak{L}_\varepsilon^N\right) S_i^{n+1}$ and using the linearity of the operator it reduces to

$$\left(I + \Delta t \mathfrak{L}_\varepsilon^N\right) \widehat{W}_i^{n+1} \leq \left(I + \Delta t \mathfrak{L}_\varepsilon^N\right) \Upsilon_i^{n+1},$$

where $\Upsilon_i^{n+1} = CS_i^{n+1}$, for all n. By using the discrete comparison principle (Lemma 5.3.1) we obtain

$$\widehat{W}_i^{n+1} \leq CS_i^{n+1}, \quad \text{for } n = 0, 1, \ldots, M-1.$$

With the same argument we can bound $-\widehat{W}_i^{n+1}$ as follows

$$-\widehat{W}_i^{n+1} \leq CS_i^{n+1}, \quad \text{for } n = 0, 1, \ldots, M-1.$$

Hence, we have

$$\left|\widehat{W}_i^{n+1}\right| \leq CS_i^{n+1}, \quad \text{for } n = 0, 1, \ldots, M-1,$$

which is the required bound. ∎

Lemma 5.3.4. *The error of the singular component satisfies*

$$\left|\widehat{w}^{n+1}(x_i^{n+1}) - \widehat{W}_i^{n+1}\right| \leq CN^{-1}, \quad \text{for } i = 0, 1, \ldots, N-1,\ n = 0, 1, \ldots, M-1.$$

Proof. We prove this lemma by separating the region in to the regular and the layer region, *i.e.,* $i = 0, 1, \ldots, N/2-1$, and $i = N/2-1, N/2, \ldots, N$, respectively.
For $i = 0, 1, \ldots, N/2-1$,

$$\begin{aligned}\left|\widehat{w}^{n+1}(x_i^{n+1}) - \widehat{W}_i^{n+1}\right| &\leq \left|\widehat{w}^{n+1}(x_i^{n+1})\right| + \left|\widehat{W}_i^{n+1}\right| \\ &\leq CN^{-1} + CS_i^{n+1},\end{aligned}$$

where we used Lemma 5.3.3 and bounds of the singular component $\widehat{w}$. The above inequality further simplified by using the monotonicity of S_i^{n+1},

$$\left|\widehat{w}^{n+1}(x_i^{n+1}) - \widehat{W}_i^{n+1}\right| \leq CN^{-1} + S_{\frac{N}{2}-1}^{n+1}, \text{ for } 0 \leq i \leq \frac{N}{2} - 1. \tag{5.3.6}$$

We use the following identity to prove this theorem:

$$\log\left(\prod_{k=\frac{N}{2}}^{N}\left(1 + \frac{\alpha h_k^{n+1}}{m\varepsilon}\right)\right) = \sum_{k=\frac{N}{2}}^{N}\log\left(1 + \frac{\alpha h_k^{n+1}}{m\varepsilon}\right).$$

For $\xi > 0$ implies $\log(1+\xi) \geq \xi - \xi^2/2$ gives

$$\log\left(\prod_{k=\frac{N}{2}}^{N}\left(1 + \frac{\alpha h_k^{n+1}}{m\varepsilon}\right)\right) \geq \sum_{k=\frac{N}{2}}^{N}\left(\frac{\alpha h_k^{n+1}}{m\varepsilon} - \frac{1}{2}\left(\frac{\alpha h_k^{n+1}}{m\varepsilon}\right)^2\right),$$

multiplying both the sides by (-1) and taking the exponential we get

$$\begin{aligned}\left(\prod_{k=\frac{N}{2}}^{N}\left(1 + \frac{\alpha h_k^{n+1}}{m\varepsilon}\right)\right)^{-1} &\leq \exp\left(\sum_{k=\frac{N}{2}}^{N}\left(-\frac{\alpha h_k^{n+1}}{m\varepsilon} + \frac{1}{2}\left(\frac{\alpha h_k^{n+1}}{m\varepsilon}\right)^2\right)\right) \\ &\leq \exp\left(\sum_{k=\frac{N}{2}}^{N}\left(-\frac{\alpha h_k^{n+1}}{m\varepsilon}\right)\right)\exp\left(\frac{1}{2}\sum_{k=\frac{N}{2}}^{N}\left(\frac{\alpha h_k^{n+1}}{m\varepsilon}\right)^2\right) \\ &\leq \exp\left(-\frac{\alpha x_{\frac{N}{2}-1}^{n+1}}{m\varepsilon}\right)\exp\left(\frac{1}{2}\sum_{k=\frac{N}{2}}^{N}\left(\frac{\alpha h_k^{n+1}}{m\varepsilon}\right)^2\right) \\ &\leq CN^{-1}\exp\left(\frac{1}{2}\sum_{k=\frac{N}{2}}^{N}\left(\frac{\alpha h_k^{n+1}}{m\varepsilon}\right)^2\right) \leq CN^{-1}.\end{aligned}$$

Substituting the above inequity in (5.3.6), we obtain

$$\left|\widehat{w}^{n+1}(x_i^{n+1}) - \widehat{W}_i^{n+1}\right| \leq CN^{-1}, \text{ for } 0 \leq i \leq \frac{N}{2} - 1. \tag{5.3.7}$$

The local truncation error of the singular component at the node (x_i^{n+1}, t_{n+1}) becomes

$$\begin{aligned}
\tau_{i,n+1}^{\widehat{W}} &= \left(I + \Delta t \mathfrak{L}_\varepsilon^N\right)\left(\widehat{w}^{n+1}(x_i^{n+1}) - \widehat{W}_i^{n+1}\right) \\
&= r_{i,n+1}^{-}\widehat{w}^{n+1}(x_{i-1}^{n+1}) + r_{i,n+1}^{c}\widehat{w}^{n+1}(x_i^{n+1}) + r_{i,n+1}^{+}\widehat{w}^{n+1}(x_{i+1}^{n+1}) \\
&\quad - \left(w(x_i^{n+1}, t_n) + \Delta t f(x_i^{n+1}, t_{n+1})\right) \\
&= r_{i,n+1}^{-}\widehat{w}^{n+1}(x_{i-1}^{n+1}) + r_{i,n+1}^{c}\widehat{w}^{n+1}(x_i^{n+1}) + r_{i,n+1}^{+}\widehat{w}^{n+1}(x_{i+1}^{n+1}) \\
&\quad - \left(I + \Delta t \mathfrak{L}_\varepsilon\right)\widehat{w}^{n+1}(x_i^{n+1}).
\end{aligned}$$

As like before, the truncation error of the singular component can be bounded as follows. For $N/2 - 1 \le i \le N$,

$$\begin{aligned}
|\tau_{i,n+1}^{\widehat{W}}| &\le C\int_{x_{i-1}^{n+1}}^{x_{i+1}^{n+1}} |(\widehat{w}^{n+1})''(s)|ds \\
&\le \frac{C}{\varepsilon^2}\int_{x_{i-1}^{n+1}}^{x_{i+1}^{n+1}} \exp\left(-\alpha(1-s)/\varepsilon\right) ds \\
&\le \frac{C}{\varepsilon^2}\frac{\varepsilon \exp(-\alpha(1-x_i^{n+1})/m\varepsilon)}{N} \\
&\le \frac{C}{\varepsilon N}\exp\left(\sum_{k=i+1}^{N} -\frac{\alpha h_k^{n+1}}{m\varepsilon}\right) \le \frac{C}{\varepsilon N}\prod_{k=i+1}^{N}\exp\left(-\frac{\alpha h_k^{n+1}}{m\varepsilon}\right) \\
&\le \frac{C}{\varepsilon N}\prod_{k=i+1}^{N}\left(1 + \frac{\alpha h_k^{n+1}}{m\varepsilon}\right)^{-1} \le \frac{C}{\varepsilon N} S_i^{n+1}, \text{ for } \frac{N}{2} - 1 \le i \le N.
\end{aligned}$$

Now using $\Upsilon_j^{n+1} = \frac{C}{N}(1 + S_i^{n+1})$, as the barrier function and the discrete maximum principle (Lemma 5.3.1) we obtain

$$\left(\widehat{w}^{n+1}(x_i^{n+1}) - \widehat{W}_i^{n+1}\right) \le CN^{-1}, \text{ for } \frac{N}{2} - 1 \le i \le N. \tag{5.3.8}$$

Similarly, repeating the same argument for $-(\widehat{w}^{n+1}(x_i) - \widehat{W}_i^{n+1})$

$$-\left(\widehat{w}^{n+1}(x_i^{n+1}) - \widehat{W}_i^{n+1}\right) \le CN^{-1}, \text{ for } \frac{N}{2} - 1 \le i \le N. \tag{5.3.9}$$

Combining (5.3.6), (5.3.8) and (5.3.9) we have

$$\left|\widehat{w}^{n+1}(x_i^{n+1}) - \widehat{W}_i^{n+1}\right| \le CN^{-1}, \quad \text{for } i = 0, 1, \cdots, N, \ n = 0, 1, \ldots, M-1. \tag{5.3.10}$$

Hence the result follows. ∎

Theorem 5.3.5. *Let $\widehat{u}^{n+1}$ and $\{\widehat{U}^{n+1}\}$ are the solutions corresponds to the semidiscrete discretization (3.3.3) and the discrete solution (5.3.1), respectively. Then, we have the following bound*

$$|\widehat{u}_i^{n+1} - \widehat{U}_i^{n+1}| \le CN^{-1}, \quad \text{for } 1 \le i \le N-1. \tag{5.3.11}$$

Proof. By using the error bounds of the regular and the singular components from Lemmas 5.3.2 and 5.3.4 in the inequality (5.3.5), we obtain the required estimate. ∎

Corollary 5.3.6. *If we take $N^{-q} \leq C\Delta t$ with $0 < q < 1$, then from (5.3.11) we obtain*

$$|\widehat{u}_i^{n+1} - \widehat{U}_i^{n+1}| \leq C\Delta t N^{-1+q}, \quad \text{for } 1 \leq i \leq N-1. \tag{5.3.12}$$

This bound is required to prove the uniform convergence of the fully discrete scheme.

5.3.2 Uniform convergence of the fully discrete scheme

Here, we provide the important theorem for the ε–uniform convergence of the fully discrete scheme (5.2.2) on the adaptive gird obtained through the monitor function given in (5.2.6).

Theorem 5.3.7. *Let $u(x, t_n)$ be the exact solution of (5.1.1) and $\{U^n\}$ be the discrete solution of the fully discrete scheme (5.2.2), at time level $t_n = n\Delta t$. Assume that $N^{-q} \leq C\Delta t$ with $0 < q < 1$. Then, the error associated to the fully discrete scheme (5.2.2) at time level t_n satisfies*

$$\|\{u(x_i^n, t_n)\}_i - \{U_i^n\}_i\|_\infty \leq C(\Delta t + N^{-1+q}), \quad \text{for } x_i^n \in \overline{\Omega}_x^n. \tag{5.3.13}$$

Proof. Let us denote the global error at time level t_n by $E_{x_i^n}^n = u(x_i^n, t_n) - U_i^n$, for $0 \leq i \leq N$. Now, splitting the global error $\{E_{x_i}^n\}_i$, we have

$$\|\{E_{x_i^n}^n\}_i\|_\infty \leq \|\{u(x_i^n, t_n)\}_i - \{\widehat{u}_i^n\}_i\|_\infty + \|\{\widehat{u}_i^n\}_i - \{\widehat{U}_i^n\}_i\|_\infty + \|\{\widehat{U}_i^n\}_i - \{U_i^n\}_i\|_\infty. \tag{5.3.14}$$

Now, using the estimates given in (3.3.4) and (5.3.12), we deduce that

$$\|\{E_{x_i^n}^n\}_i\|_\infty \leq C\Delta t(\Delta t + N^{-1+q}) + \|\{\widehat{U}_i^n\}_i - \{U_i^n\}_i\|_\infty, \quad \text{for } \overline{\Omega}_x^n. \tag{5.3.15}$$

Then, applying the stability result of the fully discrete scheme, it can be shown that

$$\|\{\widehat{U}_i^n\}_i - \{U_i^n\}_i\|_\infty \leq \|\{u(x_i^n, t_{n-1})\}_i - \{\tilde{U}(x_i^n, t_{n-1})\}_i\|_\infty. \tag{5.3.16}$$

And,

$$\begin{aligned}
\|(u - \tilde{U})(x_i^n, t_{n-1})\|_\infty &= \|u(x_i^n, t_{n-1}) - (U(x_{j-1}^{n-1}, t_{n-1})\phi_{j-1}(x_i^n) + U(x_j^{n-1}, t_{n-1})\phi_j(x_i^n))\|_\infty \\
&\leq \|u(x_i^n, t_{n-1}) - (u(x_{j-1}^{n-1}, t_{n-1})\phi_{j-1}(x_i^n) + u(x_j^{n-1}, t_{n-1})\phi_j(x_i^n))\|_\infty \\
&\quad + \|(u - U)(x_{j-1}^{n-1}, t_{n-1})\phi_{j-1}(x_i^n) + (u - U)(x_j^{n-1}, t_{n-1})\phi_j(x_i^n))\|_\infty \\
&\leq \|u(x_i^n, t_{n-1}) - (u(x_{j-1}^{n-1}, t_{n-1})\phi_{j-1}(x_i^n) + u(x_j^{n-1}, t_{n-1})\phi_j(x_i^n))\|_\infty \\
&\quad + \|\{E_{x_i^{n-1}}^{n-1}\}_i\|_\infty
\end{aligned} \tag{5.3.17}$$

where $\phi_{j-1}(x) = \frac{x_j^{n-1}-x}{x_j^{n-1}-x_{j-1}^{n-1}}$, $\phi_j(x) = \frac{x-x_{j-1}^{n-1}}{x_j^{n-1}-x_{j-1}^{n-1}}$ and $x_{j-1}^{n-1} \le x_i^n \le x_{j-1}^n$ for some j.

All that remains is to bound the interpolation error in (5.3.17). As given in [6] the interpolation error can be bounded as follows,

$$\|u(x_i^n, t_{n-1}) - (u(x_{j-1}^{n-1}, t_{n-1})\phi_{j-1}(x_i^n) + u(x_j^{n-1}, t_{n-1})\phi_j(x_i^n))\|_\infty \le CN^{-1}.$$

By using the assumption that $N^{-q} \le C\Delta t$, we can get

$$\|u(x_i^n, t_{n-1}) - (u(x_{j-1}^{n-1}, t_{n-1})\phi_{j-1}(x_i^n) + u(x_j^{n-1}, t_{n-1})\phi_j(x_i^n))\|_\infty \le C\Delta t N^{-1+q}. \quad (5.3.18)$$

Finally, from (5.3.15), (5.3.16), (5.3.17) and (5.3.18), we obtain the following error bound

$$\|\{E_{x_i^n}^n\}_i\|_\infty \le C\Delta t(\Delta t + N^{-1+q}) + \|\{E_{x_i^{n-1}}^{n-1}\}_i\|_\infty, \quad \text{for } \overline{\Omega}_x^n,$$

and hence, the result (5.3.13) follows from it. ∎

5.4 Semilinear Parabolic Problem

In this section, we consider the following semilinear singularly perturbed parabolic PDE of the form

$$\begin{cases} u_t - \varepsilon u_{xx} + a(x)u_x = b(x,t,u), \quad (x,t) \in G = \Omega \times (0,T] \equiv (0,1) \times (0,T], \\ u(x,0) = u_0(x), \quad x \in \Omega, \\ u(0,t) = u(1,t) = 0, \quad t \in (0,T], \end{cases} \quad (5.4.1)$$

where ε is small positive parameter. We assume that b is continuous in $\overline{\Omega} \times [0,T] \times \mathbb{R}$, is differentiable in the third argument, for some non-negative constants γ and $\bar{\gamma}$, satisfies

$$0 \le \gamma \le b_s(x,t,s) \le \bar{\gamma} \quad \text{for } (x,t,s) \in \overline{\Omega} \times [0,T] \times \mathbb{R}.$$

Under sufficient smoothness and compatibility conditions imposed on the functions $a(x)$ and $u_0(x)$ the parabolic problem (5.4.1) in general, admits a unique solution $u(x,t)$ which exhibits a boundary layer. For more information on the existence and uniqueness of the semilinear PDE (5.4.1) one can refer [45].

To solve (5.4.1), we use the Newton linearization process and obtain the sequence $\{u^m\}$ for the initial guess u^0 satisfying the initial and boundary conditions of the problem. Thus, we define u^{m+1} for each fixed m, to be the solution of the following linear parabolic IBVP

$$\begin{cases} u_t^{m+1} - \varepsilon u_{xx}^{m+1} + a(x)u_x^{m+1} - b^m(x,t)u^{m+1} = f^m(x,t), \quad (x,t) \in G \\ u^{m+1}(x,0) = u_0(x), \quad 0 < x < 1, \\ u^{m+1}(0,t) = 0, \quad u^{m+1}(1,t) = 0, \quad 0 \le t \le T, \end{cases} \quad (5.4.2)$$

where $m \geq 0$ and $b^m(x,t)$ and $f^m(x,t)$ are given by

$$\begin{cases} b^m(x,t) = b_u(x,t,u^m), \\ f^m(x,t) = b(x,t,u^m) - b^m(x,t)u^m. \end{cases} \tag{5.4.3}$$

Hence for a fixed m, we solve (5.4.2) using the computational method discussed as earlier. Moreover, we assume that the problem admits regular boundary layers. Numerical results for semilinear SPPs are presented in the following section.

5.5 Numerical Results

In this section, we shall present the numerical results obtained by the difference scheme (5.2.2) for two linear, one semilinear and one quasilinear problems on the rectangular mesh $\overline{G}^{N,\Delta t} := \{(x_i^n, t_n) : i = 0, \ldots, N \text{ and } n = 0, \ldots M\}$. In all the numerical experiments we will fix $m = 2$, which is necessary to define the monitor function (5.2.6). Moreover, in all the tables we begin with $N = 32$ and the time step $\Delta t = 0.1$ and we multiply N by two and divide Δt by two.

Example 5.5.1. *Consider the following parabolic initial-boundary-value problem:*

$$\begin{cases} u_t - \varepsilon u_{xx} + (1 + x(1-x))u_x = f(x,t), \quad (x,t) \in (0,1) \times (0,1], \\ u(x,0) = u_0(x), \quad 0 < x < 1, \\ u(0,t) = 0, \quad u(1,t) = 0, \quad 0 \leq t \leq 1. \end{cases} \tag{5.5.1}$$

We choose the initial data $u_0(x)$ and the source function $f(x,t)$ to fit with the exact solution

$$u(x,t) = \exp(-t)(C_1 + C_2 x - \exp(-(1-x)\varepsilon)),$$

where $C_1 = \exp(-1/\varepsilon)$, and $C_2 = 1 - \exp(-1/\varepsilon)$. As the exact solution of the problem (5.5.1) is known, for each ε, we calculate the maximum point-wise error by

$$e_\varepsilon^{N,\Delta t} = \max_{(x_i,t_n) \in \overline{G}^{N,\Delta t}} |u(x_i^n, t_n) - U^{N,\Delta t}(x_i^n, t_n)|,$$

where $u(x_i^n, t_n)$ and $U^{N,\Delta t}(x_i^n, t_n)$ respectively, denote the exact and the numerical solution obtained on the mesh with N mesh intervals in the spatial direction and M mesh intervals in the $t-$direction such that $\Delta t = T/M$ is the uniform time step. In addition, we determine the corresponding rate of convergence by

$$p_\varepsilon^{N,\Delta t} = \log_2 \left(\frac{e_\varepsilon^{N,\Delta t}}{e_\varepsilon^{2N,\Delta t/2}} \right).$$

The calculated maximum point-wise errors $e_\varepsilon^{N,\Delta t}$ and the corresponding rate of convergence $p_\varepsilon^{N,\Delta t}$ for Example 5.5.1 are given in Table 5.1 and Table 5.2, respectively. From these results one can observe the ε–uniform first-order convergence of the numerical solution. One can also compare our results with the well-known layer adopted meshes, the Shishkin mesh and the Bakhvalov mesh. The maximum point-wise errors and the corresponding rate of convergence for the Shishkin and the Bakhvalov meshes are given in Chapter 3, Table 3.5, 3.6, 3.7 3.8, respectively.

Further, we have calculated the normalized flux

$$F_\varepsilon u(x,t) = \varepsilon \frac{\partial u(x,t)}{\partial x},$$

and its numerical approximation

$$F_\varepsilon^N U^{N,\Delta t}(x_i^n, t_n) = \varepsilon D_x^- U_i^n.$$

The errors in the normalized flux have been calculated as

$$r_\varepsilon^{N,\Delta t} = \max_{1\le n\le M} |F_\varepsilon u(x_N^n, t_n) - F_\varepsilon^N U^{N,\Delta t}(x_N^n, t_n)|,$$

and the rate of convergence is determined from

$$q_\varepsilon^{N,\Delta t} = \log_2 \left(\frac{r_\varepsilon^{N,\Delta t}}{r_\varepsilon^{2N,\Delta t/2}} \right).$$

The calculated maximum point-wise errors in the normalized flux $r_\varepsilon^{N,\Delta t}$ and the corresponding rate of convergence $q_\varepsilon^{N,\Delta t}$ for Example 5.5.1 are given in Table 5.3 and Table 5.4. Again, one can see the ε–uniform convergence in Table 5.3, and the first-order convergence rate from Table 5.4. The mesh movement is shown in Figure 5.1. In Figures 5.2 (a) and (b), the maximum point-wise errors in the solution and the normalized flux are plotted respectively, which reflect the fact of first-order convergence independent of ε.

Example 5.5.2. *Consider the following parabolic initial-boundary-value problem:*

$$\begin{cases} u_t - \varepsilon u_{xx} + (2-x^2)u_x + xu = 10t^2 x(1-x)\exp(-t), \quad (x,t) \in (0,1)\times(0,1] \\ u(x,0) = 0, \quad 0 < x < 1, \\ u(0,t) = 0, \quad u(1,t) = 0, \quad 0 \le t \le 1. \end{cases} \tag{5.5.2}$$

As the exact solution of the problem (5.5.2) is not known, to obtain the accuracy of the numerical solution and also to demonstrate the $\varepsilon-$uniform convergence of the proposed scheme, we use the double mesh principle which is given in the following.

Table 5.1: *Maximum point-wise error of the solution* $e_\varepsilon^{N,\Delta t}$ *for Example* 5.5.1 *using equidistribution mesh.*

	Number of Intervals N/Time Step Size Δt					
ε	$32/\frac{1}{10}$	$64/\frac{1}{20}$	$128/\frac{1}{40}$	$256/\frac{1}{80}$	$512/\frac{1}{160}$	$1024/\frac{1}{320}$
10^0	6.8921e-04	3.7085e-04	1.9290e-04	9.8440e-05	4.9739e-05	2.5002e-05
10^{-2}	3.6888e-02	2.0831e-02	1.1153e-02	5.5786e-03	2.8851e-03	1.4696e-03
10^{-4}	5.9879e-02	3.3920e-02	1.6100e-02	7.6389e-03	3.8781e-03	1.9325e-03
10^{-6}	6.6280e-02	3.2432e-02	1.7095e-02	8.0662e-03	3.9206e-03	1.9598e-03
10^{-8}	7.4889e-02	3.8221e-02	1.6669e-02	8.1228e-03	3.9297e-03	1.9714e-03

Table 5.2: *Rate of convergence of the solution* $p_\varepsilon^{N,\Delta t}$ *for Example* 5.5.1 *using equidistribution mesh.*

	Number of Intervals N/Time Step Size Δt				
ε	$32/\frac{1}{10}$	$64/\frac{1}{20}$	$128/\frac{1}{40}$	$256/\frac{1}{80}$	$512/\frac{1}{160}$
10^0	0.8941	0.9430	0.9705	0.9849	0.9923
10^{-2}	0.8244	0.9013	0.9995	0.9513	0.9732
10^{-4}	0.8199	1.0750	1.0757	0.9780	1.0049
10^{-6}	1.0312	0.9238	1.0836	1.0408	1.0004
10^{-8}	0.9704	1.1972	1.0371	1.0475	0.9952

Table 5.3: *Maximum point-wise error of the normalized flux* $r_\varepsilon^{N,\Delta t}$ *for Example* 5.5.1 *using equidistribution mesh.*

	Number of Intervals N/Time Step Size Δt					
ε	$32/\frac{1}{10}$	$64/\frac{1}{20}$	$128/\frac{1}{40}$	$256/\frac{1}{80}$	$512/\frac{1}{160}$	$1024/\frac{1}{320}$
10^0	1.7039e-02	8.8121e-03	4.4877e-03	2.2670e-03	1.1392e-03	5.7103e-04
10^{-2}	1.4594e-01	7.3749e-02	3.7743e-02	2.1485e-02	1.0287e-02	5.0424e-03
10^{-4}	1.8787e-01	1.0280e-01	4.8782e-02	2.3225e-02	1.1695e-02	5.8250e-03
10^{-6}	2.1967e-01	1.0127e-01	5.2334e-02	2.4313e-02	1.1782e-02	5.8870e-03
10^{-8}	2.4466e-01	1.1836e-01	5.0695e-02	2.4525e-02	1.1807e-02	5.9203e-03

Table 5.4: *Rate of convergence of the normalized flux* $q_\varepsilon^{N,\Delta t}$ *for Example* 5.5.1 *using equidistribution mesh.*

	Number of Intervals N/Time Step Size Δt				
ε	$32/\frac{1}{10}$	$64/\frac{1}{20}$	$128/\frac{1}{40}$	$256/\frac{1}{80}$	$512/\frac{1}{160}$
10^{0}	0.9513	0.9735	0.9852	0.9928	0.9964
10^{-2}	0.9847	0.9664	0.8129	1.0625	1.0287
10^{-4}	0.8699	1.0754	1.0706	0.9898	1.0056
10^{-6}	1.1171	0.9525	1.1060	1.0452	1.0010
10^{-8}	1.0476	1.2233	1.0476	1.0546	0.9959

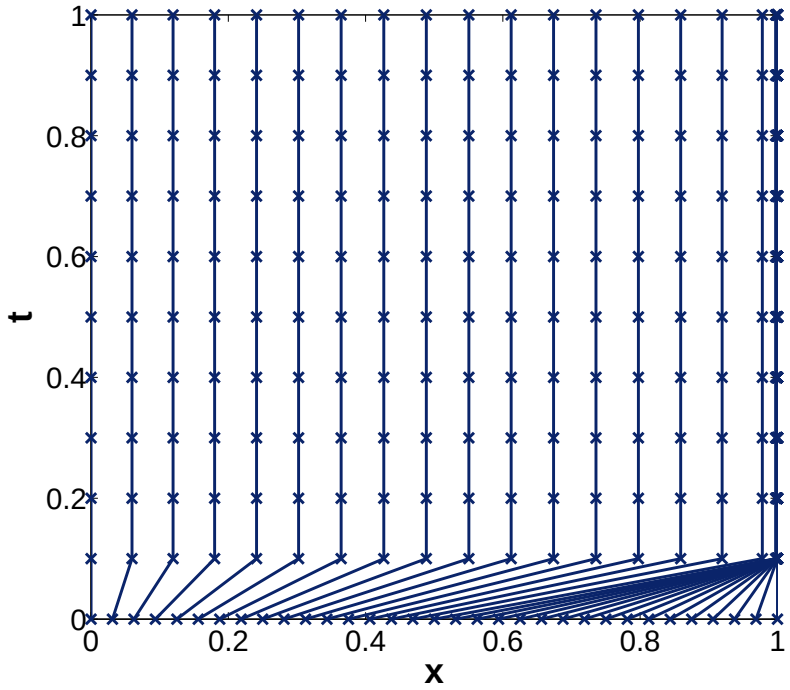

Figure 5.1: *Grid movement of algorithm for Example 5.5.1 with* $N = 32$ *and* $\Delta t = 0.1$.

Table 5.5: *Maximum point-wise error of the solution* $E_\varepsilon^{N,\Delta t}$ *for Example* 5.5.2 *using equidistribution mesh.*

	Number of Intervals N/Time Step Size Δt				
ε	$32/\frac{1}{10}$	$64/\frac{1}{20}$	$128/\frac{1}{40}$	$256/\frac{1}{80}$	$512/\frac{1}{160}$
10^0	8.2372e-04	4.9105e-04	2.5567e-04	1.2828e-04	6.4978e-05
10^{-2}	9.5603e-03	5.3242e-03	2.4656e-03	1.2244e-03	7.0268e-04
10^{-4}	1.2187e-02	6.3136e-03	3.2878e-03	1.7405e-03	9.2980e-04
10^{-6}	1.4171e-02	6.8146e-03	3.3684e-03	1.8254e-03	8.9480e-04
10^{-8}	1.5061e-02	7.1351e-03	3.5691e-03	1.7761e-03	9.0022e-04

Let $\tilde{U}^{2N,\Delta t/2}(x_i^n, t_n)$ be the numerical solution obtained on the fine mesh $\overline{G}^{2N,\Delta t/2} = \overline{\Omega}_x^{2N} \times \overline{\Lambda}_t^{2M}$ with $2N$ mesh intervals in the spatial direction and $2M$ mesh intervals in the $t-$direction. Then for each ε, we calculate the maximum point-wise error by

$$E_\varepsilon^{N,\Delta t} = \max_{(x_i^n,t_n)\in\overline{G}^{N,\Delta t}} \left| U^{N,\Delta t}(x_i^n, t_n) - \tilde{U}^{2N,\Delta t/2}(x_i^n, t_n) \right|,$$

and the corresponding rate of convergence by

$$P_\varepsilon^{N,\Delta t} = \log_2 \left(\frac{E_\varepsilon^{N,\Delta t}}{E_\varepsilon^{2N,\Delta t/2}} \right).$$

The calculated maximum point-wise errors $E_\varepsilon^{N,\Delta t}$ and the corresponding rate of convergence $P_\varepsilon^{N,\Delta t}$ for Example 5.5.2 are given in Table 5.5 and Table 5.6 respectively. The numerical results given in these tables reveal the first-order convergence independent of the diffusion parameter ε.

Further, the errors in the normalized flux have been calculated as

$$R_\varepsilon^{N,\Delta t} = \max_{1\le n\le M} |F_\varepsilon^N U^{N,\Delta t}(x_N, t_n) - F_\varepsilon^N \tilde{U}^{2N,\Delta t/2}(x_N, t_n)|,$$

and the rate of convergence is determined from

$$Q_\varepsilon^{N,\Delta t} = \log_2 \left(\frac{R_\varepsilon^{N,\Delta t}}{R_\varepsilon^{2N,\Delta t/2}} \right).$$

The calculated maximum point-wise errors in the normalized flux $R_\varepsilon^{N,\Delta t}$ and the corresponding rate of convergence $Q_\varepsilon^{N,\Delta t}$ for Example 5.5.2 are given in Table 5.7 and Table 5.8, respectively. The maximum point-wise errors are plotted in log-log scale in Figures 5.3 (a) and (b), for the solution and the normalized flux, respectively. From these figures, one can easily observe the first-order $\varepsilon-$uniform convergence.

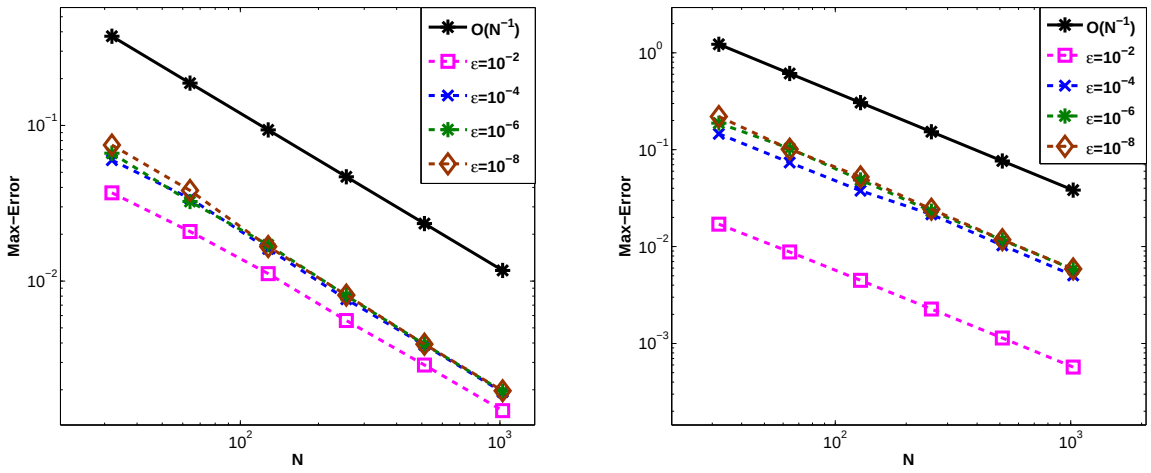

(a) *Maximum point-wise error of the solution* $e_\varepsilon^{N,\Delta t}$.

(b) *Maximum point-wise error of the normalized flux* $r_\varepsilon^{N,\Delta t}$.

Figure 5.2: *Loglog plot for Example 5.5.1.*

Table 5.6: *Rate of convergence of the solution* $P_\varepsilon^{N,\Delta t}$ *for Example* 5.5.2 *using equidistribution mesh.*

	Number of Intervals N/Time Step Size Δt			
ε	$32/\frac{1}{10}$	$64/\frac{1}{20}$	$128/\frac{1}{40}$	$256/\frac{1}{80}$
10^0	0.7463	0.9416	0.9949	0.9813
10^{-2}	0.8445	1.1106	1.0099	0.8011
10^{-4}	0.9488	0.9414	0.9176	0.9045
10^{-6}	1.0562	1.0166	0.8838	1.0286
10^{-8}	1.0779	0.9994	1.0068	0.9804

Table 5.7: *Maximum point-wise error of the normalized flux* $R_\varepsilon^{N,\Delta t}$ *for Example* 5.5.2 *using equidistribution mesh.*

	Number of Intervals N/Time Step Size Δt				
ε	$32/\frac{1}{10}$	$64/\frac{1}{20}$	$128/\frac{1}{40}$	$256/\frac{1}{80}$	$512/\frac{1}{160}$
10^0	3.4752e-03	2.1005e-03	1.0653e-03	5.3293e-04	2.6710e-04
10^{-2}	1.3569e-02	8.2271e-03	4.1127e-03	1.9809e-03	1.1979e-03
10^{-4}	1.6700e-02	9.2864e-03	4.9741e-03	2.6597e-03	1.3788e-03
10^{-6}	1.9614e-02	9.9915e-03	5.0452e-03	2.7734e-03	1.3586e-03
10^{-8}	2.1953e-02	1.0508e-02	5.4041e-03	2.6760e-03	1.3632e-03

Table 5.8: *Rate of convergence of the normalized flux* $Q_\varepsilon^{N,\Delta t}$ *for Example* 5.5.2 *using equidistribution mesh.*

	Number of Intervals N/Time Step Size Δt			
ε	$32/\frac{1}{10}$	$64/\frac{1}{20}$	$128/\frac{1}{40}$	$256/\frac{1}{80}$
10^{0}	0.7264	0.9794	0.9993	0.9965
10^{-2}	0.7219	1.0003	1.0540	0.7256
10^{-4}	0.8467	0.9007	0.9032	0.9478
10^{-6}	0.9731	0.9858	0.8633	1.0295
10^{-8}	1.0630	0.9593	1.0140	0.9731

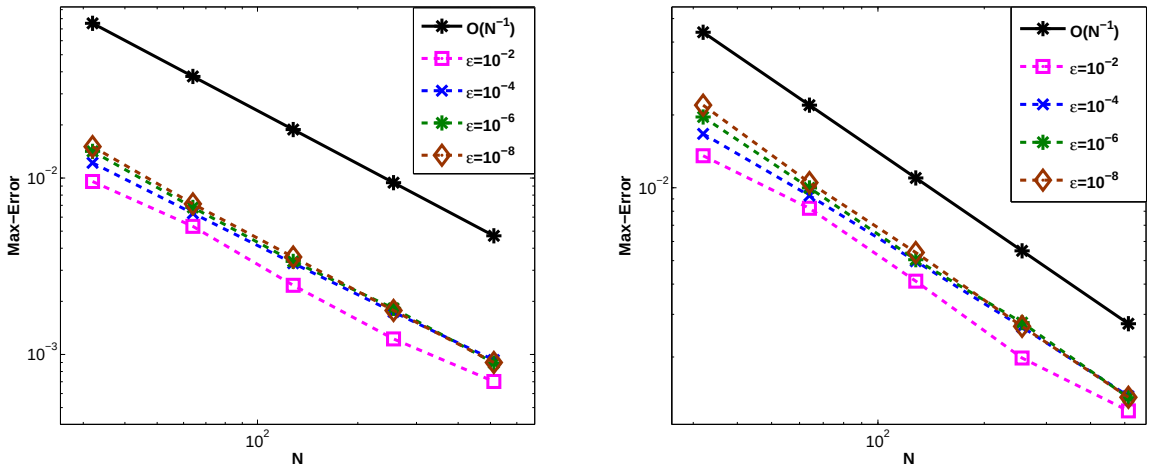

(a) *Maximum point-wise error of the solution* $E_\varepsilon^{N,\Delta t}$.

(b) *Maximum point-wise error of the normalized flux* $R_\varepsilon^{N,\Delta t}$.

Figure 5.3: *Loglog plot for Example 5.5.2.*

Example 5.5.3. *Consider the following semilinear parabolic initial-boundary-value problem:*

$$\begin{cases} u_t - \varepsilon u_{xx} + (1 + x(1-x))u_x + \exp(u) = f(x,t), \quad (x,t) \in (0,1) \times (0,1], \\ u(x,0) = u_0(x), \quad 0 < x < 1, \\ u(0,t) = 0, \quad u(1,t) = 0, \quad 0 \le t \le 1. \end{cases} \tag{5.5.3}$$

We choose the initial data $u_0(x)$ and the source function $f(x,t)$ to fit with the exact solution

$$u(x,t) = \exp(-t)(C_1 + C_2 x - \exp(-(1-x)\varepsilon)),$$

where $C_1 = \exp(-1/\varepsilon)$, and $C_2 = 1 - \exp(-1/\varepsilon)$.

If we use the Newton linearization process given in (5.4.2), we obtain the following system of linear singular perturbation parabolic PDEs:

$$\begin{cases} u_t^{m+1} - \varepsilon u_{xx}^{m+1} + (1 + x(1-x))u_x^{m+1} + \exp(u^m)u^{m+1} = f(x,t) - \exp(u^m)(1-u^m), \\ u^{m+1}(x,0) = u_0(x), \quad 0 < x < 1, \\ u^{m+1}(0,t) = 0, \quad u^{m+1}(1,t) = 0, \quad 0 \le t \le 1. \end{cases} \tag{5.5.4}$$

Hence for a fixed m, we solve (5.5.4) using computational method discussed earlier. Once we get the prescribed tolerance bound we terminate the iteration and take that as the solution to the problem.

As the exact solution of the problem (5.5.3) is known, for each ε, we calculate the maximum point-wise error and the corresponding rate of convergence as given Example 5.5.1. We also calculate the maximum point-wise errors in the normalized flux and the corresponding rate of convergence as given Example 5.5.1.

The calculated maximum point-wise errors $e_\varepsilon^{N,\Delta t}$ and the corresponding rate of convergence $p_\varepsilon^{N,\Delta t}$ for Example 5.5.3 are given in Table 5.9 and Table 5.10, respectively. From these results one can observe the ε–uniform first-order convergence of the numerical solution.

The calculated maximum point-wise errors in the normalized flux $r_\varepsilon^{N,\Delta t}$ and the corresponding rate of convergence $q_\varepsilon^{N,\Delta t}$ for Example 5.5.3 are given in Table 5.11 and Table 5.12. Again, one can see the ε–uniform convergence in Table 5.11, and the first-order convergence rate from Table 5.12.

Example 5.5.4. *Consider the following quasilinear parabolic initial-boundary-value*

Table 5.9: *Maximum point-wise error of the solution* $e_\varepsilon^{N,\Delta t}$ *for Example* 5.5.3 *using equidistribution mesh.*

	Number of Intervals N/Time Step Size Δt					
ε	$32/\frac{1}{10}$	$64/\frac{1}{20}$	$128/\frac{1}{40}$	$256/\frac{1}{80}$	$512/\frac{1}{160}$	$1024/\frac{1}{320}$
10^0	6.2800e-04	3.3697e-04	1.7557e-04	8.9658e-05	4.5313e-05	2.2780e-05
10^{-2}	3.8431e-02	2.0924e-02	1.0798e-02	5.5555e-03	2.8236e-03	1.4162e-03
10^{-4}	6.2851e-02	3.0700e-02	1.5383e-02	7.6399e-03	3.8503e-03	1.9319e-03
10^{-6}	6.4547e-02	3.2368e-02	1.5914e-02	7.8894e-03	3.9221e-03	1.9562e-03
10^{-8}	6.4616e-02	3.4589e-02	1.6305e-02	7.9850e-03	3.9390e-03	1.9629e-03

Table 5.10: *Rate of convergence of the solution* $p_\varepsilon^{N,\Delta t}$ *for Example* 5.5.3 *using equidistribution mesh.*

	Number of Intervals N/Time Step Size Δt				
ε	$32/\frac{1}{10}$	$64/\frac{1}{20}$	$128/\frac{1}{40}$	$256/\frac{1}{80}$	$512/\frac{1}{160}$
10^0	0.8981	0.9406	0.9695	0.9845	0.9921
10^{-2}	0.8771	0.9544	0.9588	0.9764	0.9955
10^{-4}	1.0337	0.9969	1.0097	0.9886	0.9950
10^{-6}	0.9958	1.0243	1.0123	1.0083	1.0036
10^{-8}	0.9016	1.0850	1.0299	1.0194	1.0048

Table 5.11: *Maximum point-wise error of the normalized flux* $r_\varepsilon^{N,\Delta t}$ *for Example* 5.5.3 *using equidistribution mesh.*

	Number of Intervals N/Time Step Size Δt					
ε	$32/\frac{1}{10}$	$64/\frac{1}{20}$	$128/\frac{1}{40}$	$256/\frac{1}{80}$	$512/\frac{1}{160}$	$1024/\frac{1}{320}$
10^0	1.5246e-02	7.8438e-03	3.9846e-03	2.0102e-03	1.0095e-03	5.0590e-04
10^{-2}	1.3977e-01	7.3419e-02	3.7278e-02	1.8975e-02	9.5992e-03	4.9650e-03
10^{-4}	1.9161e-01	9.3615e-02	4.6724e-02	2.3224e-02	1.1618e-02	5.8246e-03
10^{-6}	1.9830e-01	9.8063e-02	4.8000e-02	2.3742e-02	1.1787e-02	5.8761e-03
10^{-8}	1.9958e-01	9.9767e-02	5.0106e-02	2.4025e-02	1.1837e-02	5.8933e-03

Table 5.12: *Rate of convergence of the normalized flux* $q_\varepsilon^{N,\Delta t}$ *for Example* 5.5.3 *using equidistribution mesh.*

	Number of Intervals N/Time Step Size Δt				
ε	$32/\frac{1}{10}$	$64/\frac{1}{20}$	$128/\frac{1}{40}$	$256/\frac{1}{80}$	$512/\frac{1}{160}$
10^{0}	0.9588	0.9771	0.9871	0.9936	0.9968
10^{-2}	0.9288	0.9778	0.9743	0.9831	0.9511
10^{-4}	1.0334	1.0026	1.0085	0.9993	0.9961
10^{-6}	1.0159	1.0307	1.0156	1.0103	1.0042
10^{-8}	1.0003	0.9936	1.0604	1.0213	1.0061

problem (the Burger's equation):

$$\begin{cases} u_t(x,t) - \varepsilon u_{xx}(x,t) + u(x,t)u_x(x,t) = 0, \quad (x,t) \in (0,1)\times(0,1], \\ u(x,0) = \sin(\pi x), \quad 0 < x < 1, \\ u(0,t) = 0, \quad u(1,t) = 0, \quad 0 \le t \le 1. \end{cases} \tag{5.5.5}$$

If we use the Newton linearization process, we obtain the following system of linear singular perturbation parabolic PDEs:

$$\begin{cases} u_t^{m+1} - \varepsilon u_{xx}^{m+1} + u^m u_x^{m+1} + u_x^m u^{m+1} = u_x^m u^m, \quad (x,t) \in (0,1)\times(0,1], \\ u^{m+1}(x,0) = \sin(\pi x), \quad 0 < x < 1, \\ u^{m+1}(0,t) = 0, \quad u^{m+1}(1,t) = 0, \quad 0 \le t \le 1. \end{cases} \tag{5.5.6}$$

Hence for a fixed m, we solve (5.5.6) using computational method discussed earlier. Once we get the prescribed tolerance bound we terminate the iteration and take that as the solution to the problem.

As the exact solution of the problem (5.5.4) is not known, to obtain the accuracy of the numerical solution and also to demonstrate the $\varepsilon-$uniform convergence of the proposed scheme, we use the double mesh principle as given in Example 5.5.2.

The numerical solution is plotted for the various time levels in Figures 5.4 (a) and (b) for $\varepsilon = 1e-1$ and $\varepsilon = 1e-2$, respectively. These figures show the existence of the boundary layer near $x = 1$.

The calculated maximum point-wise errors $E_\varepsilon^{N,\Delta t}$ and the corresponding rate of convergence $P_\varepsilon^{N,\Delta t}$ for Example 5.5.4 are given in Table 5.13 and Table 5.14, respectively. The numerical results given in these tables reveal the first-order convergence independent of the diffusion parameter ε. The calculated maximum point-wise errors in the normalized flux $R_\varepsilon^{N,\Delta t}$ and the corresponding rate of convergence $Q_\varepsilon^{N,\Delta t}$ for Example 5.5.4 are given in Table 5.15 and Table 5.16, respectively.

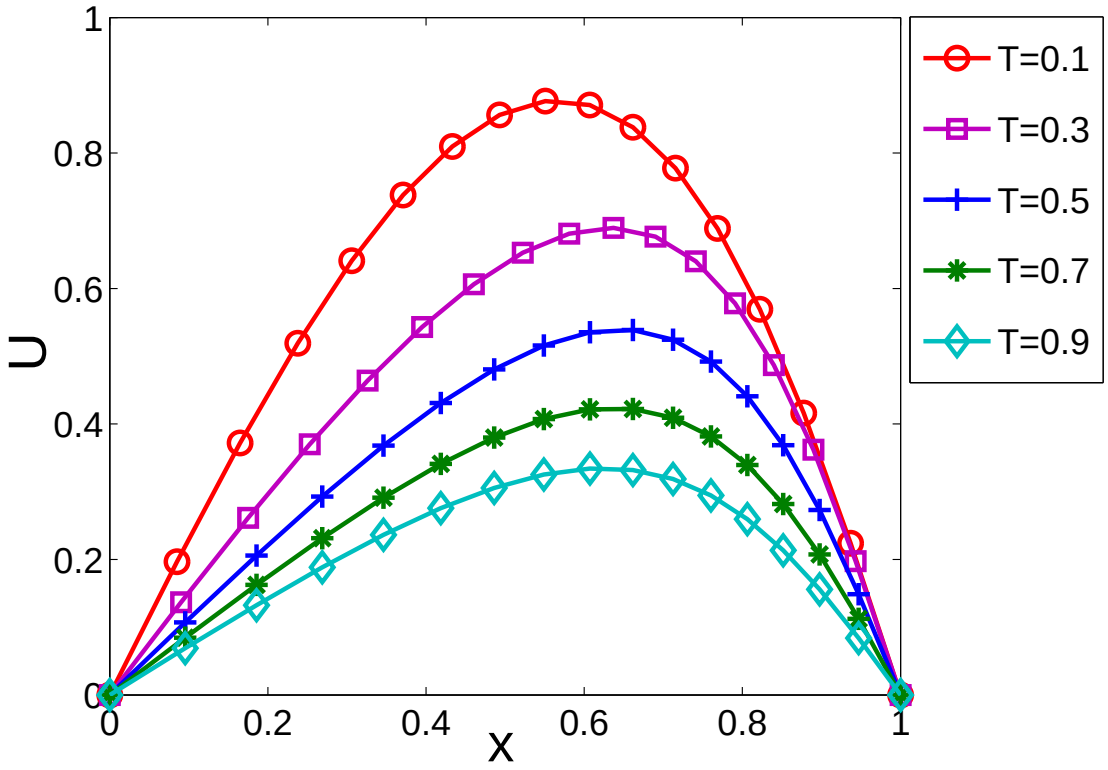

(a) $\varepsilon = 10^{-1}$.

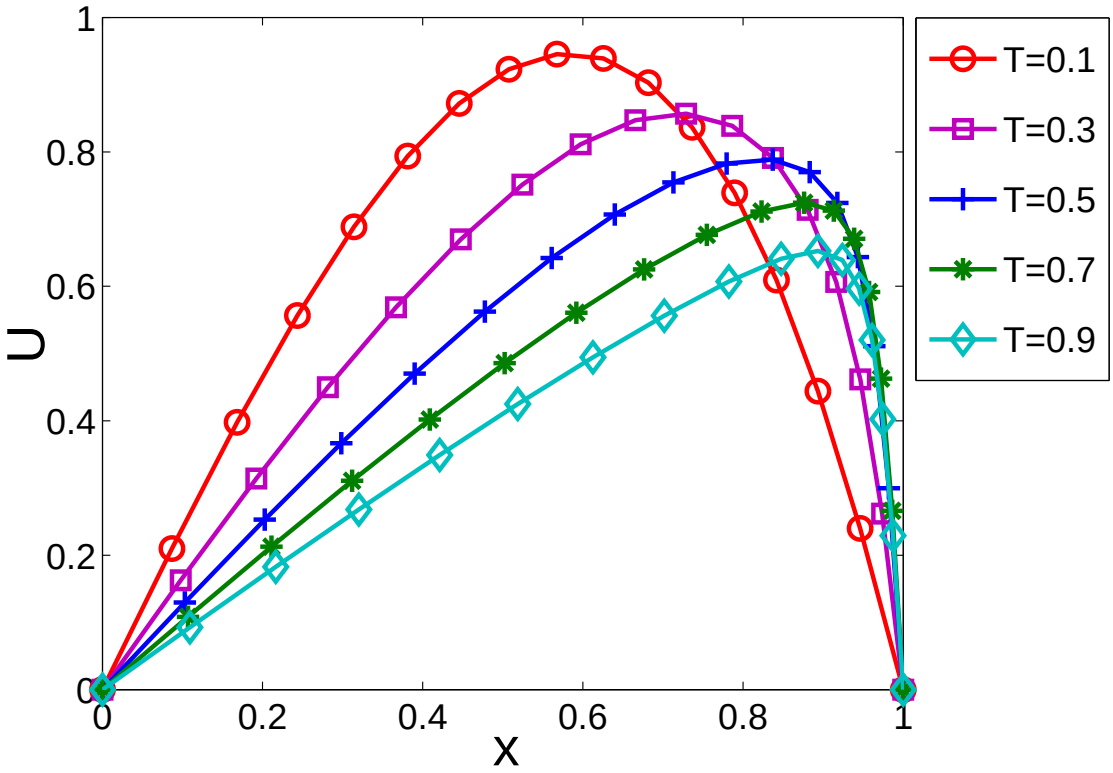

(b) $\varepsilon = 10^{-2}$.

Figure 5.4: *Numerical solution at various time levels of Example 5.5.4 for* $N = 16$ *and* $\Delta t = 1/20$.

Table 5.13: *Maximum point-wise error of the solution* $E_\varepsilon^{N,\Delta t}$ *for Example* 5.5.4 *using equidistribution mesh.*

ε	Number of Intervals N/Time Step Size Δt			
	$128/\frac{1}{20}$	$256/\frac{1}{40}$	$512/\frac{1}{80}$	$1024/\frac{1}{160}$
10^0	4.9105e-04	2.5567e-04	1.2828e-04	6.4978e-05
10^{-2}	5.3242e-03	2.4656e-03	1.2244e-03	7.0268e-04
10^{-4}	6.3136e-03	3.2878e-03	1.7405e-03	9.2980e-04
10^{-6}	6.8146e-03	3.3684e-03	1.8254e-03	8.9480e-04
10^{-8}	7.1351e-03	3.5691e-03	1.7761e-03	9.0022e-04

Table 5.14: *Rate of convergence of the solution* $P_\varepsilon^{N,\Delta t}$ *for Example* 5.5.4 *using equidistribution mesh.*

ε	Number of Intervals N/Time Step Size Δt		
	$128/\frac{1}{20}$	$256/\frac{1}{40}$	$512/\frac{1}{80}$
10^0	0.9416	0.9949	0.9813
10^{-2}	1.1106	1.0099	0.8011
10^{-4}	0.9414	0.9176	0.9045
10^{-6}	1.0166	0.8838	1.0286
10^{-8}	0.9994	1.0068	0.9804

Table 5.15: *Maximum point-wise error of the normalized flux* $R_\varepsilon^{N,\Delta t}$ *for Example* 5.5.4 *using equidistribution mesh.*

ε	Number of Intervals N/Time Step Size Δt			
	$128/\frac{1}{20}$	$256/\frac{1}{40}$	$512/\frac{1}{80}$	$1024/\frac{1}{160}$
10^0	2.1005e-03	1.0653e-03	5.3293e-04	2.6710e-04
10^{-2}	8.2271e-03	4.1127e-03	1.9809e-03	1.1979e-03
10^{-4}	9.2864e-03	4.9741e-03	2.6597e-03	1.3788e-03
10^{-6}	9.9915e-03	5.0452e-03	2.7734e-03	1.3586e-03
10^{-8}	1.0508e-02	5.4041e-03	2.6760e-03	1.3632e-03

Table 5.16: *Rate of convergence of the normalized flux* $Q_\varepsilon^{N,\Delta t}$ *for Example* 5.5.4 *using equidistribution mesh.*

	Number of Intervals N/Time Step Size Δt		
ε	$128/\frac{1}{20}$	$256/\frac{1}{40}$	$512/\frac{1}{80}$
10^{0}	0.9794	0.9993	0.9965
10^{-2}	1.0003	1.0540	0.7256
10^{-4}	0.9007	0.9032	0.9478
10^{-6}	0.9858	0.8633	1.0295
10^{-8}	0.9593	1.0140	0.9731

5.6 Conclusions

In this chapter, we have solved the singularly perturbed time-dependent convection-diffusion problems (5.1.1) numerically by the upwind finite difference scheme on layer-adapted nonuniform grids obtained through the positive monitor function given in (5.2.6) on each time level. The truncation error and stability analysis are obtained. The proposed numerical scheme is of first-order convergence in both the spatial and the temporal variables, *i.e.*, $O(\Delta t + N^{-1})$. Error estimates are derived for the numerical scheme, which are independent of the diffusion parameter ε. Numerical results are carried out to verify the theoretical error estimates.

CHAPTER 6

Robust Numerical Scheme for Singularly Perturbed Delay Parabolic Initial-Boundary-Value Problems on Equidistributed Grids

In this chapter, we propose a parameter-uniform computational technique to solve singularly perturbed delay parabolic initial-boundary-value problems exhibiting parabolic layers. The domain is discretized with a uniform mesh on the time direction and a nonuniform mesh obtained via equidistribution of a monitor function for the spatial variable. The numerical scheme consists of the implicit-Euler scheme for the time derivative and the classical central difference scheme for the spatial derivative. Truncation error, and stability analysis are carried out, it is shown that the method converges uniformly in the discrete supremum norm with an optimal error bound. Error estimates are derived, and numerical examples are presented.

6.1 Introduction

Here, we develop an ε-uniform numerical method for the following class of singularly perturbed delay parabolic initial-boundary-value problems with Dirichlet boundary conditions on the boundaries. Let $\Omega = (0,1)$, $G = \Omega \times (0,T]$, and $\Gamma = \Gamma_l \cup \Gamma_b \cup \Gamma_r$, where Γ_l and Γ_r are the left and the right sides of the rectangular domain G corresponding to $x = 0$ and $x = 1$, respectively, and $\Gamma_b = \overline{\Omega} \times [-\tau, 0]$.

$$\begin{cases} \left(\dfrac{\partial}{\partial t} + \mathcal{L}_\varepsilon\right) u(x,t) = -b(x,t)u(x,t-\tau) + f(x,t), \quad (x,t) \in G \\ u(x,t) = \phi_b(x,t), \quad (x,t) = \Gamma_b, \\ u(0,t) = \phi_l(t), \quad \text{on } \Gamma_l = \{(0,t) : 0 \le t \le T\}, \\ u(1,t) = \phi_r(t), \quad \text{on } \Gamma_r = \{(1,t) : 0 \le t \le T\}, \end{cases} \tag{6.1.1}$$

where

$$\mathcal{L}_\varepsilon u(x,t) = -\varepsilon u_{xx}(x,t) + a(x)u(x,t),$$

$0 < \varepsilon \ll 1$ and $\tau > 0$ are given constants, $a(x)$, $b(x,t)$, $f(x,t)$, $(x,t) \in \overline{G}$, and $\phi_l(t)$, $\phi_r(t)$, $\phi_b(x,t)$, $(x,t) \in \Gamma$, are sufficiently smooth and bounded functions that satisfy

$$a(x) \geq 0, \quad b(x,t) \geq \beta > 0, \quad (x,t) \in \overline{G}.$$

The terminal time T is assumed to satisfy the condition $T = k\tau$ for some positive integer k. The required compatibility condition at the corner points and the delay terms are

$$\phi_b(0,0) = \phi_l(0), \quad \phi_b(1,0) = \phi_r(0), \tag{6.1.2}$$

and

$$\begin{aligned} \frac{d\phi_l(0)}{dt} - \varepsilon\frac{\partial^2\phi_b(0,0)}{\partial x^2} + a(0)\phi_b(0,0) &= -b(0,0)\phi_b(0,-\tau) + f(0,0), \\ \frac{d\phi_r(0)}{dt} - \varepsilon\frac{\partial^2\phi_b(1,0)}{\partial x^2} + a(1)\phi_b(1,0) &= -b(1,0)\phi_b(1,-\tau) + f(1,0). \end{aligned} \tag{6.1.3}$$

Note that $\phi_l(t)$, $\phi_b(x,t)$ and $\phi_r(t)$ are assumed to be smooth for (6.1.3) to make sense.

Under the above assumptions and the compatibility conditions, problem (6.1.1) admits a unique solution [2], and the solution exhibits boundary layers along $x = 0$, $x = 1$.

The main goal of this chapter is to provide an ε-uniform numerical method for the IBVP (6.1.1) on adaptive mesh. We obtain the adaptive mesh through the idea of equidistribution of the singular component of $u(x,t)$ at some fixed time T_0, $0 < T_0 \leq T$, because the problem (6.1.1) exhibits boundary layers along the boundary which do not have any effect on the time variable. In this method, the time derivative is replaced by the backward-Euler scheme, and the spatial derivative is replaced by the central difference scheme. The proposed scheme is parameter-uniform convergent of order $O(\Delta t + N^{-2})$, which is of optimal order compare to other methods in the literature [2], [49]. It is shown that the method converges uniformly in the discrete supremum norm with an optimal error bound. Truncation errors are derived, stability analysis is carried out; and ε-uniform error estimates are obtained. We also shown that the numerical solution converges uniformly of second-order in the space and first-order in the time by appropriate tables and figures.

We organize the rest of the chapter as follows: In Section 6.2, we provide *apriori* bounds on the derivatives of the analytical solution via decomposition. Section 6.3 introduces the implicit-Euler for the time derivative on uniform mesh and central difference scheme for the spatial derivatives on adaptive spatial mesh via equidistribution principle. Afterwards, we carry out the error analysis for the upwind scheme in Section 6.4 and prove the main theoretical result, *i.e.,* the ε-uniform optimal error bounds of

the scheme on the adaptive mesh. In Section 6.5, we present the numerical results for two linear test problems to validate the theoretical error estimates. Finally in Section 6.6, we summarize the main conclusions.

6.2 Analytic Solution

In this section, we present some bounds for the analytical solution $u(x,t)$ of (6.1.1) and its partial derivatives and the maximum principle for the differential operator.

The reduced problem, by setting the parameter value $\varepsilon = 0$ and removing the boundary conditions in (6.1.1) is

$$\begin{cases} (u_0)_t(x,t) - a(x)u_0(x,t) = -b(x,t)u_0(x,t-\tau) + f(x,t), & (x,t) \in G, \\ u_0(x,t) = \phi_b(x,t), & (x,t) \in \Gamma_b. \end{cases} \tag{6.2.1}$$

Then it is clear that the solution of (6.1.1) forms boundary layers on Γ_l and Γ_r in order to satisfy the boundary conditions. The characteristics of (6.2.1) are the vertical lines $x = C$, which implies that any boundary layers arising in the solution are of parabolic type. This type of problem can be solved by fixing the spatial gird on all temporal levels.

The differential operator $\left(\frac{\partial}{\partial t} + \mathcal{L}_\varepsilon\right)$ in (6.1.1) satisfies the following maximum principle.

Lemma 6.2.1. (**Maximum principle**) *Let $\Psi(x,t)$ be a sufficiently smooth function satisfying $\Psi(x,t) \geq 0$ on Γ, then $\left(\frac{\partial}{\partial t} + \mathcal{L}_\varepsilon\right)\Psi(x,t) \geq 0$ in G implies that $\Psi(x,t) \geq 0$ in $\overline{G}$.*

The following theorem gives the stability of the continuous operator $\left(\frac{\partial}{\partial t} + \mathcal{L}_\varepsilon\right)$ and ε-uniform bound for the problem (6.1.1) in the maximum norm.

Theorem 6.2.2. *Let v be any function in the domain of definition of the differential operator $\left(\frac{\partial}{\partial t} + \mathcal{L}_\varepsilon\right)$ in (6.1.1). Then*

$$\|v\|_\infty \leq (1+\alpha T)\max\left\{\left\|\left(\frac{\partial}{\partial t} + \mathcal{L}_\varepsilon\right)v\right\|_\infty, \|v\|_{\infty,\Gamma}\right\},$$

and any solution u of (6.1.1) has the ε-uniform upper bound

$$\|u\|_\infty \leq (1+\alpha T)\max\left\{\|f\|_\infty, \|\phi\|_{\infty,\Gamma}\right\},$$

where the constant $\alpha = \max_{\overline{\Omega}}\{0, 1-a\} \leq 1$.

Here ϕ on Γ means the notation

$$\phi = \begin{cases} \phi_l & \text{on } \Gamma_l, \\ \phi_r & \text{on } \Gamma_r, \\ \phi_b & \text{on } \Gamma_b. \end{cases}$$

Theorem 6.2.3. *Let the data* $a \in \mathcal{C}^{2+\alpha}([0,1])$, $b, f \in \mathcal{C}^{(2+\alpha,1+\alpha/2)}(\overline{G})$, $\phi_l \in \mathcal{C}^{2+\alpha/2}([0,T])$, $\phi_b \in \mathcal{C}^{(4+\alpha,2+\alpha/2)}(\Gamma_b)$, $\phi_r \in \mathcal{C}^{2+\alpha/2}([0,T])$, $\alpha \in (0,1)$, *with sufficient compatibility condition on the corner is fulfilled. Then (6.1.1) has a unique solution* u *and* $u \in \mathcal{C}^{(4+\alpha,2+\alpha/2)}(\overline{G})$. *Furthermore, the derivatives of the solution* u *satisfy, for all non-negative integers* i, j *such that* $0 \le i + 2j \le 4$,

$$\left\| \frac{\partial^{i+j} u}{\partial x^i \partial t^j} \right\|_\infty \le C\varepsilon^{-i/2}.$$

Proof. The proof of this theorem can be found in [2]. ∎

The above bounds do not show the explicit dependence on the boundary layer component. Therefore, to obtain stronger estimates on the solution $u(x,t)$ and its partial derivatives we decompose the solution $u(x,t)$ into the regular and the singular components.

Let u be the solution of (6.1.1) and it can be decomposed as

$$u = v + w, \tag{6.2.2}$$

where v and w are the regular and the singular components of u defined in the following way. The regular component is further decomposed into

$$v = v_0 + \varepsilon v_1,$$

where v_0, v_1 are defined by

$$\begin{cases} (v_0)_t + a v_0 = -b v_0(x, t-\tau) + f, & (x,t) \in G, \\ v_0(x,t) = \phi_b(x,t), & (x,t) \in \Gamma_b, \end{cases}$$

and

$$\begin{cases} \left(\dfrac{\partial}{\partial t} + \mathcal{L}_\varepsilon\right) v_1 = -b v_1(x, t-\tau) + (v_0)_{xx}, & (x,t) \in G, \\ v_1(x,t) = 0, & (x,t) \in \Gamma. \end{cases}$$

By the above definition of v_0 and v_1 the regular component v and the singular component w can be defined as follows,

$$\begin{cases} \left(\dfrac{\partial}{\partial t} + \mathcal{L}_\varepsilon\right) v(x,t) = -b v(x, t-\tau) + f, & (x,t) \in G, \\ v(x,t) = \phi_b(x,t), & (x,t) \in \Gamma_b, \\ v(0,t) = v_0(0,t), & (x,t) \in \Gamma_l, \quad v(1,t) = v_0(1,t), \quad (x,t) \in \Gamma_r. \end{cases}$$

$$\begin{cases} \left(\dfrac{\partial}{\partial t} + \mathcal{L}_\varepsilon\right) w(x,t) = -bw(x,t-\tau), \quad (x,t) \in G, \\ w(x,t) = 0,\ (x,t) \in \Gamma_b, \\ w(0,t) = \phi_l(t) - v_0(0,t), \quad (x,t) \in \Gamma_l, \quad w(1,t) = \phi_r(t) - v_0(1,t), \quad (x,t) \in \Gamma_r. \end{cases}$$

We further decompose the singular component into the left and the right singular components w_l and w_r, respectively, as follows

$$w(x,t) = w_l(x,t) + w_r(x,t), \tag{6.2.3}$$

where w_l and w_r are satisfies the following PDEs,

$$\begin{cases} \left(\dfrac{\partial}{\partial t} + \mathcal{L}_\varepsilon\right) w_l(x,t) = -bw_l(x,t-\tau), \quad (x,t) \in G, \\ w_l(0,t) = \phi_l(t) - v_0(0,t),\ (x,t) \in \Gamma_l, \quad w_l(x,t) = 0,\ (x,t) \in \Gamma_b \cup \Gamma_r, \end{cases}$$

and

$$\begin{cases} \left(\dfrac{\partial}{\partial t} + \mathcal{L}_\varepsilon\right) w_r(x,t) = -bw_r(x,t-\tau), \quad (x,t) \in G, \\ w_r(1,t) = \phi_r(t) - v_0(1,t),\ (x,t) \in \Gamma_r, \quad w_r(x,t) = 0,\ (x,t) \in \Gamma_b \cup \Gamma_l. \end{cases}$$

The following theorem gives the bounds on the regular component v and the singular component w and its partial derivatives which play a crucial role in the error analysis in Section 6.4.

Theorem 6.2.4. *Assume that* $a \in \mathfrak{C}^{4+\alpha}([0,1])$, $b, f \in \mathfrak{C}^{(4+\alpha,2+\alpha/2)}(\overline{G})$, $\phi_l \in \mathfrak{C}^{3+\alpha/2}([0,T])$, $\phi_b \in \mathfrak{C}^{(6+\alpha,3+\alpha/2)}(\Gamma_b)$, $\phi_r \in \mathfrak{C}^{3+\alpha/2}([0,T])$, $\alpha \in (0,1)$, *with sufficient compatibility condition at the corner are fulfilled. Then, for integers* i, j *such that* $0 \le i + 2j \le 4$, *we have the estimates*

$$\left\| \frac{\partial^{i+j} v}{\partial x^i \partial t^j} \right\|_\infty \le C(1 + \varepsilon^{1-i/2}), \tag{6.2.4}$$

$$\left| \frac{\partial^{i+j} w_l}{\partial x^i \partial t^j}(x,t) \right| \le C\varepsilon^{-i/2} \exp\left(-x/\sqrt{\varepsilon}\right), \quad (x,t) \in \overline{G}, \tag{6.2.5}$$

$$\left| \frac{\partial^{i+j} w_r}{\partial x^i \partial t^j}(x,t) \right| \le C\varepsilon^{-i/2} \exp\left(-(1-x)/\sqrt{\varepsilon}\right), \quad (x,t) \in \overline{G}, \tag{6.2.6}$$

where C *is independent of* ε.

Proof. The proof of this theorem can be found in [2]. ∎

Theorem 6.2.5. *The partial derivatives of* $w(x,t)$ *satisfy*

$$\left| \frac{\partial^{i+j} w}{\partial x^i \partial t^j} \right| \le C\varepsilon^{-i/2} \left(\exp\left(-x/\sqrt{\varepsilon}\right) + \exp\left(-(1-x)/\sqrt{\varepsilon}\right)\right), \quad (x,t) \in \overline{G}, \tag{6.2.7}$$

for integers i, j *such that* $0 \le i + 2j \le 4$.

Proof. The theorem can be proved by using the estimates in Theorem 6.2.4 and decomposition (6.2.3). ∎

6.3 The Numerical Solution

In this section, we discretize the parabolic delay IBVP (6.1.1), the time derivative is replaced by the backward-Euler scheme, and the spatial derivative is replaced by the central difference scheme. Later, we introduce the equidistribution grid, and derive the finite difference scheme. Finally, we provide the numerical algorithm to obtain the equidistributed grids.

6.3.1 Finite difference scheme

On the time domain [0,T], we introduce the equidistant meshes with uniform time step Δt such that

$$\overline{\Lambda}_t^M = \{t_n = n\Delta t,\ n = 0, \ldots, M,\ \Delta t = T/M\},$$

where M denotes the number of mesh intervals in the interval $[0, T]$ and the step length Δt satisfies the constraint $p\Delta t = \tau$, where p is a positive integer, $t_n = n\Delta t$, $n \geq -p$.

We consider the finite difference approximation of (6.1.1) on a nonuniform spatial discretization

$$\overline{\Omega}_x^N = \{0 = x_0 < x_1 < \cdots < x_N = 1\},$$

and denote the spatial step sizes by

$$h_i = x_i - x_{i-1}, \quad i = 1, \ldots, N.$$

We use methods of steps to prove the ε-uniform convergence in Section 6.4. Here we define the discretization of the domain into a systematic way. We define the discretized domain $\overline{G}^{N,\Delta t} = \overline{\Omega}_x^N \times \overline{\Lambda}_t^M$, $\Gamma_b^N = \overline{\Omega}_x^N \times \overline{\Lambda}_t^p$ where $\overline{\Lambda}_t^p$ is $p+1$ uniform mesh intervals in $[\tau, 0]$. The boundary points Γ^N of $\overline{G}^{N,\Delta t}$ are $\Gamma^N = \overline{G}^{N,\Delta t} \cap \Gamma$. Similarly we define the left and the right boundary points by $\Gamma_l^N = \overline{G}^{N,\Delta t} \cap \Gamma_l$ and $\Gamma_r^N = \overline{G}^{N,\Delta t} \cap \Gamma_r$, respectively.

We further discretize $\overline{G}_j^{N,\Delta t} = \overline{\Omega}_x^N \times \overline{\Lambda}_{j,t}^p$ where $\overline{\Lambda}_{j,t}^p$ is $p+1$ uniform mesh intervals in $[(j-1)\tau, j\tau]$ for $j = 1, 2, \cdots, k$. From above discretization we can also observe that $\overline{G}^{N,\Delta t} = \bigcup_{j=1}^k \overline{G}_j^{N,\Delta t}$. The above notations are primarily used in Section 6.4, where the error in the numerical solutions are analyzed for the ε-uniform convergence.

We discretize the problem (6.1.1) by means of the backward-Euler scheme for the temporal derivative, and the central difference for the spatial derivative. Hence the discretization of (6.1.1) takes the form, for $n = 0, 1, \ldots, M-1$,

$$\begin{cases} \dfrac{U_i^{n+1} - U_i^n}{\Delta t} + \mathcal{L}_\varepsilon^N U_i^{n+1} = -b(x_i, t_{n+1})U_i^{n-p} + f(x_i, t_{n+1}), & \text{for } i = 1, \ldots, N-1, \\ U_0^{n+1} = \phi_l(t_{n+1}), \quad U_N^{n+1} = \phi_r(t_{n+1}), \\ U_i^{-j} = \phi_b(x_i, -t_j), \quad \text{for } i = 1, \ldots, N-1, \end{cases} \tag{6.3.1}$$

where

$$\mathcal{L}_\varepsilon^N U_i^{n+1} = -\varepsilon\delta_x^2 U_i^{n+1} + a_i U_i^{n+1}. \tag{6.3.2}$$

After rearranging the terms in (6.3.1), we obtain the following form of the difference scheme: for $n = 0, 1, \ldots, M-1$,

$$\begin{cases} r_i^- U_{i-1}^{n+1} + r_i^c U_i^{n+1} + r_i^+ U_{i+1}^{n+1} = g_i^n, \quad \text{for } i = 1, \ldots, N-1, \\ U_0^{n+1} = \phi_l(t_{n+1}), \quad U_N^{n+1} = \phi_r(t_{n+1}), \\ U_i^{-j} = \phi_b(x_i, -t_j), \quad \text{for } i = 1, \ldots, N-1, \end{cases} \tag{6.3.3}$$

where

$$r_i^- = \frac{-2\varepsilon\Delta t}{h_i(h_i + h_{i+1})}, \qquad r_i^+ = \frac{-2\varepsilon\Delta t}{h_{i+1}(h_i + h_{i+1})}, \qquad r_i^c = 1 + \Delta t a_i - r_i^- - r_i^+,$$
$$a_i = a(x_i), \qquad g_i^n = U_i^n + \Delta t\{-b(x_i, t_{n+1})U_i^{n-p} + f(x_i, t_{n+1})\}.$$

To determine the value of the monitor function (6.3.5), we have to know the approximate value of the singular component $w(x,t)$. To calculate the numerical value W_i^n of $w(x_i, t_n)$, we use the numerical approximate value V_i^n of $v(x_i, t_n)$ from the following recurrence relation: for $n = 0, 1, \ldots, M-1$,

$$\begin{cases} (1 + \Delta t a(x_i))V_i^{n+1} = V_i^n + \Delta t\{-b(x_i, t_{n+1})V_i^{n-p} + f(x_i, t_{n+1})\}, \quad \text{for } i = 1, \ldots, N, \\ V_i^{-j} = \phi_b(x_i, -t_j). \end{cases} \tag{6.3.4}$$

Then, the value of W_i^n will be calculated from $W_i^n = U_i^n - V_i^n$.

6.3.2 Adaptive spatial grids via equidistribution

Since the solution $u(x,t)$ of the IBVP (6.1.1) exhibits boundary layers, one has to use layer-adapted nonuniform spatial grids, which are fine inside the boundary layer region, and coarse in the outer region. To obtain such a grid, we use the idea of equidistribution of a positive monitor function given in (6.3.5). Here we consider the equidistribution of $u(x,t)$ at some fixed time T_0, $0 < T_0 \leq T$, because the problem (6.1.1) exhibits a regular layer along the boundaries, which will not have any impact on the temporal component.

Here, we consider the following monitor function

$$M(u(x, T_0), x) = \alpha_c + |w_{xx}(x, T_0)|^{1/m}, \quad m \geq 2, \tag{6.3.5}$$

where $\alpha_c = \int_0^1 |w_{xx}(s, T_0)|^{1/m} ds$ and $w(x,t)$ is the singular component of $u(x,t)$. In all of our numerical experiments, we will take $m = 2$. In order to compute the value of

the monitor function at the ith interior node of the spatial mesh, M_i, we assume that $w(x_i, T_0) = W_i^S$, where $S\Delta t = T_0$,

$$M_i = \alpha_{dis} + |\delta_x^2 W_i^S|^{1/m}, \quad \text{for } i = 1, \ldots, N-1, \tag{6.3.6}$$

where α_{dis} is the discrete form of α_c, which can be written as

$$\alpha_{dis} = h_1 \, |\delta_x^2 W_1^S|^{1/m} + \sum_{i=2}^{N-1} h_i \left\{ \frac{|\delta_x^2 W_{i-1}^S|^{1/m} + |\delta_x^2 W_i^S|^{1/m}}{2} \right\} + h_N \, |\delta_x^2 W_{N-1}^S|^{1/m}.$$

For a truly adaptive algorithm, the monitor function has to be approximated from the numerical solution. For example, a simple discretization of the equidistribution principle results in the set of equations

$$M_{i-1/2}(x_i - x_{i-1}) = M_{i+1/2}(x_{i+1} - x_i), \quad \text{for } i = 1, \ldots, N-1,$$

where $M_{i+1/2}$ is an approximation to $M(u(x_{i+1/2}, T_0), x_{i+1/2})$. This is equivalent to the approximation of the monitor function by the piecewise-constant function.

Lemma 6.3.1. *For $i = 1, 2, \ldots, N$, the step size satisfies*

$$h_i \leq CN^{-1}. \tag{6.3.7}$$

Proof. From the equidistribution principle, we have

$$\int_{x_{i-1}}^{x_i} M(u(s, T_0), s) ds = \frac{1}{N} \int_0^1 M(u(s, T_0), s) ds, \quad i = 1, \ldots, N.$$

Applying the Mean-Value Theorem, we get

$$h_i M(u(\eta_i, T_0), \eta_i) = N^{-1} \int_0^1 M(u(s, T_0), s) ds,$$

for some $\eta_i \in (x_{i-1}, x_i)$. Thus, we have

$$h_i = N^{-1} \frac{\displaystyle\int_0^1 M(u(s, T_0), s) ds}{M(u(\eta_i, T_0), \eta_i)} \leq CN^{-1}.$$

This completes the proof. ∎

In the numerical algorithm given in Section 2.3.3, we use the discrete form of the monitor function given in (6.3.6). Difference schemes for the solution and the regular parts are given in (6.3.3) and (6.3.4), respectively.

6.4 Error Analysis

Here, we carry out the stability analysis of the discrete operator defined in (6.3.1). Finally, we obtain the ε-uniform error estimate in the discrete maximum norm.

The following lemma provides the stability result for a general numerical scheme for the IBVP (6.1.1). A partial proof of this lemma can be found in the book of [78].

Lemma 6.4.1. *Consider the IBVP (6.1.1) and the difference scheme (6.3.2), the difference scheme (excluding the initial and boundary conditions) can be written as*

$$\delta_t U^{n+1} + \mathcal{L}_\varepsilon^N U^{n+1} := AU^{n+1} - DU^n = F^n, \quad \text{for } n = 0, \cdots, M-1, \tag{6.4.1}$$

where $U^n = (U_1^n, \cdots, U_{N-1}^n)^T$, F^n is a vector independent of the computed solution, and A and D are matrices and also that A is an M-matrix, and $D \geq 0$.

Let y and z be two mesh functions, such that $y^n = (y_0^n, \cdots, y_N^n)^T$, and $z^n = (z_0^n, \cdots, z_N^n)^T$ for each n. Assume that $\left|\delta_t y^{n+1} + \mathcal{L}_\varepsilon^N y^{n+1}\right| \leq \delta_t z^{n+1} + \mathcal{L}_\varepsilon^N z^{n+1}$, for $n = 0, \cdots, M-1$, and $|y| \leq z$ on the boundary $\Gamma_b \cup \Gamma_l \cup \Gamma_r$. Then, $|y| \leq z$ on $\overline{\Omega}_x^N \times \overline{\Lambda}_t^M$.

Proof. The difference scheme (6.3.2) can be written in the form of (6.4.1) for $n = 1, 2, \ldots, p$, with $A = (a_{ij})$ and $D = (d_{ij})$ as

$$a_{i,i-1} = \frac{r_i^-}{\Delta t}, \quad a_{i,i} = \frac{r_i^c}{\Delta t}, \quad a_{i,i+1} = \frac{r_i^+}{\Delta t},$$
$$d_{i,i} = \frac{1}{\Delta t}.$$

Simple calculation shows that the matrix A is an M-matrix and the matrix $D \geq 0$. Therefore, the difference scheme satisfies the hypotheses of Lemma 3.2 in[78] and immediately the result follows. The above argument can also be extended to other temporal levels. ∎

The finite difference operator $\left(\delta_t + \mathcal{L}_\varepsilon^N\right)$ in (6.3.2) satisfies the following discrete maximum principle on $\overline{G}^{N,\Delta t}$.

Lemma 6.4.2. (**Discrete maximum principle**) *Assume that $\Psi(x_i, t_n)$ satisfies $\Psi(x_i, t_n) \geq 0$ on $(x_i, t_n) \in \Gamma^N$. Then $\left(\delta_t + \mathcal{L}_\varepsilon^N\right)\Psi(x_i, t_n) \geq 0$ on $(x_i, t_n) \in \overline{G}^{N,\Delta t}$ implies that $\Psi(x_i, t_n) \geq 0$ at each point of $(x_i, t_n) \in \overline{G}^{N,\Delta t}$.*

Here we provide the important theorem for the ε-uniform convergence of the numerical solution in the discrete maximum norm.

Theorem 6.4.3. *Let u and U be respectively the continuous and the numerical solutions of the IBVPs (6.1.1) and (6.3.3) and satisfying sufficient compatibility condition at the corners. Then, we have the following bound*

$$\max_{i,n} |(u-U)(x_i,t_n)| \leq C[\Delta t + N^{-2}] \quad \text{for all } (x_i,t_n) \in \overline{G}^{N,\Delta t}, \tag{6.4.2}$$

where $U(x_i,t_n) = U_i^n$.

Proof. We prove the theorem through the following steps. We first prove the result on the interval $[0,\tau]$, *i.e.,* the time discretization parameter n varies from 0 to p. Let $\eta_i^n = u_i^n - U_i^n$ be the truncation error in the computed solution at each mesh point (x_i,t_n). We write the scheme (6.3.1) as

$$\delta_t U_i^n + \mathcal{L}_\varepsilon^N U_i^n = -b_i^n \phi_b(x_i,t_{n-p}) + f_i^n \quad i = 1,\ldots,N-1, \quad n = 1,\ldots,p.$$

Therefore, the truncation error of the above scheme can be written in the following way as given in [49] and [17],

$$\delta_t \eta_i^n + \mathcal{L}_\varepsilon^N \eta_i^n = \chi_{1,i}^n + \chi_{2,i}^n, \quad \text{for } (x_i,t_n) \in \overline{G}_1^{N,\Delta t},$$

where $\chi_{1,i}^n$ and $\chi_{2,i}^n$ as follows,

$$\chi_{1,i}^n := \mathcal{L}_\varepsilon^N u_i^n - (\mathcal{L}_\varepsilon u)_i^n \quad \text{and} \quad \chi_{2,i}^n := \delta_t u_i^n - (u_t)_i^n.$$

With this splitting of the truncation error we can decompose the error η as $\eta = \phi + \psi$. Here the function ϕ_i^n is, for each fixed $n = 0,\ldots,p$, the solution of the discrete two-point boundary-value problem

$$\begin{cases} \mathcal{L}_\varepsilon^N \phi_i^n = \chi_{1,i}^n \quad \text{for } i = 1,\ldots,N-1, \\ \phi_0^n = \phi_N^n = 0, \end{cases} \tag{6.4.3}$$

and ψ_i^n, the solution of the discrete parabolic problem

$$\begin{cases} \delta_t \psi_i^n + \mathcal{L}_\varepsilon^N \psi_i^n = \chi_{2,i}^n - \delta_t \phi_i^n \quad \text{for } i = 1,\ldots,N-1, \\ \psi_0^n = \psi_N^n = 0 \quad \text{for } n = 1,\ldots,p, \\ \psi_i^0 = -\phi_i^0 \quad \text{for } i = 0,\ldots,N. \end{cases} \tag{6.4.4}$$

Equation (6.4.3) is a sequence of two-point boundary-value problems that has been discretized using $\mathcal{L}_\varepsilon^N$, with $\chi_{1,i}^n$ playing the role of truncation error and can be bounded using the technique from [7]. The problem (6.1.1) exhibits regular boundary layers and the same is true for the equation (6.4.3), therefore, the error bound derived in [7] can be invoked for all temporal levels:

$$|\phi_i^n| \leq CN^{-2}, \quad \text{for all } i, n \leq p, \tag{6.4.5}$$

with the assumption that $N^{-1} \gg \sqrt{\varepsilon}$ and the fact that our problem exhibits regular boundary layers.

All it remains is to bound the other error component ψ. By Lemma 6.4.1 and the discrete maximum principle (Lemma 6.4.2), we get the following bound for the error component ψ,

$$|\psi_i^n| \;=\; C\left(\max_i |\phi_i^0| + \max_{i,n} |\chi_{2,i}^n - \delta_t \phi_i^n|\right) \quad \text{for } i, n \le p.$$

Using the bounds of $\chi_{2,i}^n$ and (6.4.5), we obtain

$$|\psi_i^n| \;=\; C\left[N^{-2} + \Delta t + \max_{i,n} |\delta_t \phi_i^n|\right] \quad \text{for } i, n \le p. \tag{6.4.6}$$

It remains to bound the term $\delta_t \phi$ in (6.4.6). Using the assumption that $a(x)$ is independent of t, the definition (6.4.3) implies that $\delta_t \phi$ satisfies

$$\begin{cases} \mathcal{L}_\varepsilon^N (\delta_t \phi)_i^n = \delta_t \chi_{1,i}^n, \quad \text{for } i = 1, \ldots, N-1, \\ (\delta_t \phi)_0^n = (\delta_t \phi)_N^n = 0. \end{cases} \tag{6.4.7}$$

To analyze the above sequence of two-point boundary-value problems (6.4.7), observe that the right-hand side of the above equation can be written as,

$$\begin{aligned} \delta_t \chi_{1,i}^n &= \frac{1}{\Delta t}\left(\chi_{1,i}^n - \chi_{1,i}^{n-1}\right) \\ &= \frac{1}{\Delta t}\left((\mathcal{L}_\varepsilon^N u_i^n - (\mathcal{L}_\varepsilon u)_i^n) - (\mathcal{L}_\varepsilon^N u_i^{n-1} - (\mathcal{L}_\varepsilon u)_i^{n-1})\right) \\ &= \frac{1}{\Delta t}\left((\mathcal{L}_\varepsilon^N u_i^n - \mathcal{L}_\varepsilon^N u_i^{n-1}) - ((\mathcal{L}_\varepsilon u)_i^n - (\mathcal{L}_\varepsilon u)_i^{n-1})\right). \end{aligned}$$

Let $\hat{\mathcal{L}}_\varepsilon u = -\varepsilon u_{xx}$ and $\hat{\mathcal{L}}_\varepsilon^N u_i^n = -\varepsilon \delta_x^2 u_i^n$. That is, $\hat{\mathcal{L}}_\varepsilon^N u$ is the discretization of the continuous operator $\hat{\mathcal{L}}_\varepsilon u$. Then one can write the above formula as

$$\delta_t \chi_{1,i}^n = \frac{1}{\Delta t}\int_{t_{n-1}}^{t_n} \left[\hat{\mathcal{L}}_\varepsilon^N \frac{\partial}{\partial t} u(x_i, t) - \hat{\mathcal{L}}_\varepsilon \frac{\partial}{\partial t} u(x_i, t)\right].$$

By using the Peano kernel theorem as in [38], and following the argument given in [17] we obtain the same estimate on $\delta_t \chi_{1,i}^n$ as the corresponding truncation error bounds arising in [7] for a standard reaction-diffusion two-point boundary-value problem. Now analyzing the problem the same way as (6.4.3) we obtain the following bound for $\delta_t \phi_i^n$,

$$|\delta_t \phi_i^n| \le CN^{-2} \quad \text{for all } i, n \le p. \tag{6.4.8}$$

Combining (6.4.5), (6.4.6) and (6.4.8), we get

$$\max_{i,n} |(u - U)(x_i, t_n)| \;\le\; C[\Delta t + N^{-2}], \quad \text{for all } (x_i, t_n) \in \overline{G}_1^{N,\Delta t}, \tag{6.4.9}$$

where $U(x_i, t_n) = U_i^n$.

For $t \geq \tau$, it is not possible to follow the above argument because the delay term, $u(x, t-\tau)$, is explicitly unknown for $t \geq \tau$. For this reason, we examine the detailed proof of the estimate for the difference between the numerical solution U and the solution u itself over the interval $[\tau, 2\tau]$. The proof follows the same approach of [2] in which fitted piecewise-uniform mesh is used for the analysis.

Consider the following singularly perturbed delay parabolic equation on the domain $G_2 = (0,1) \times (\tau, 2\tau]$,

$$\begin{cases} \left(\dfrac{\partial}{\partial t} + \mathcal{L}_\varepsilon\right) u(x,t) = -b(x,t)u(x,t-\tau) + f(x,t), \quad (x,t) \in G_2 \\ u(x,\tau) = u(x,t(p)), \quad x \in \Omega, \\ u(0,t) = \phi_0(t), \quad u(1,t) = \phi_1(t), \quad t \in [\tau, 2\tau]. \end{cases} \tag{6.4.10}$$

We discretize (6.4.10) by means of the backward-Euler scheme for the time derivative, and the central difference for the space derivative. Hence the discretization takes the form,

$$\begin{cases} \left(\delta_t + \mathcal{L}_\varepsilon^N\right) U(x_i, t_n) \equiv \delta_t U_i^n - \varepsilon \delta_x^2 U_i^n + aU = -bU_i^{n-p} + f(x_i, t_n), \quad (x_i, t_n) \in \overline{G}_2^{N,\Delta t}, \\ U(x_i, t_n) = U_1(x_i, t_n), \quad (x_i, t_n) \in \overline{G}_1^{N,\Delta t}, \\ U(0, t_n) = \phi_0(t_n), \quad U(1, t_n) = \phi_1(t_n), \quad t_n \in \overline{\Lambda}_{2,t}^p, \end{cases} \tag{6.4.11}$$

where U_1 is the numerical solution calculated on $\overline{G}_1^{N,\Delta t}$. The solution u of (6.4.10) is decomposed into the regular and the singular components $u = y + z$. The regular component y is further decomposed into $y = y_0 + \varepsilon y_1$, where y_0 and y_1 solve the following problems:

$$\begin{cases} \dfrac{\partial y_0}{\partial t}(x,t) + a y_0(x,t) = -b y_0(x, t-\tau) + f(x,t), \quad (x,t) \in G_2 \\ y_0(x,t) = u(x,t), \quad (x,t) \in \Omega \times [0,\tau], \end{cases}$$

and

$$\begin{cases} \left(\dfrac{\partial}{\partial t} + \mathcal{L}_\varepsilon\right) y_1(x,t) = -b y_1(x, t-\tau) + \dfrac{\partial^2 y_0}{\partial x^2}(x,t), \quad (x,t) \in G_2, \\ y_1(x,t) = 0, \quad (x,t) \in \Omega \times [0,\tau], \\ y_1(0,t) = y_1(1,t) = 0, \quad t \in [\tau, 2\tau]. \end{cases}$$

For the above definition of y_0 and y_1, the regular component y satisfies,

$$\begin{cases} \left(\dfrac{\partial}{\partial t} + \mathcal{L}_\varepsilon\right) y(x,t) = -by(x,t-\tau) + f(x,t), \quad (x,t) \in G_2, \\ y(x,t) = u(x,t), \quad (x,t) \in \Omega \times [0,\tau] \\ \\ y(0,t) = y_0(0,t), \quad y(1,t) = y_0(1,t), \quad t \in [\tau, 2\tau]. \end{cases}$$

The singular component z satisfies,

$$\begin{cases} \left(\dfrac{\partial}{\partial t} + \mathcal{L}_\varepsilon\right) z(x,t) = -bz(x,t-\tau), \quad (x,t) \in G_2, \\ z(x,t) = 0, \quad (x,t) \in \Omega \times [0,\tau] \\ \\ z(0,t) = \phi_l(t) - y_0(0,t), \quad z(1,t) = \phi_r(t) - y_0(1,t), \quad t \in [\tau, 2\tau]. \end{cases}$$

The singular component z can be further decomposed into z_l and z_r, where z_l and z_r are the corresponding to the left-hand and the right-hand layers, respectively:

$$z = z_l + z_r,$$

where z_l and z_r satisfies the following PDEs,

$$\begin{cases} \left(\dfrac{\partial}{\partial t} + \mathcal{L}_\varepsilon\right) z_l(x,t) = -bz_l(x,t-\tau), \quad (x,t) \in G_2, \\ z_l(x,t) = 0, \quad (x,t) \in \Omega \times [0,\tau], \\ \\ z_l(0,t) = \phi_l(t) - y_0(0,t), \quad z_l(1,t) = 0, \quad t \in [\tau, 2\tau]. \end{cases}$$

and

$$\begin{cases} \left(\dfrac{\partial}{\partial t} + \mathcal{L}_\varepsilon\right) z_r(x,t) = -bz_r(x,t-\tau), \quad (x,t) \in G_2, \\ z_r(x,t) = 0, \quad (x,t) \in \Omega \times [0,\tau], \\ \\ z_r(0,t) = 0, \quad z_r(1,t) = \phi_r(t) - y_0(1,t), \quad t \in [\tau, 2\tau]. \end{cases}$$

Similarly, the numerical solution U of (6.4.11) is decomposed into the regular and the singular components in an analogous manner to the decomposition of the solution u of (6.4.10). Thus

$$U = Y + Z,$$

where Y is the solution of the following problem

$$\begin{cases} \left(\delta_t + \mathcal{L}_\varepsilon^N\right) Y(x_i,t_n) = -bY(x_i,t_{n-p}) + f, \quad (x_i,t_n) \in \overline{G}_2^{N,\Delta t}, \\ Y(x_i,t_n) = U_\tau(x_i,t_n), \quad (x_i,t_n) \in \overline{G}_1^{N,\Delta t}, \\ \\ Y(0,t_n) = y(0,t_n), \quad Y(1,t_n) = y(1,t_n) \quad t_n \in \overline{\Lambda}_{2,t}^p. \end{cases}$$

From the above equation the singular component approximation Z satisfies,

$$\begin{cases} \left(\delta_t + \mathcal{L}_\varepsilon^N\right) Z(x_i,t_n) = -bZ(x_i,t_{n-p}), \quad (x_i,t_n) \in \overline{G}_2^{N,\Delta t}, \\ Z(x_i,t_n) = 0, \quad (x_i,t_n) \in \overline{G}_1^{N,\Delta t}, \\ Z(0,t_n) = \phi_l(t_n) - y(0,t_n), \quad Z(1,t_n) = \phi_r(t_n) - y(1,t_n) \quad t_n \in \overline{\Lambda}_{2,t}^p. \end{cases}$$

Therefore, the error at the node (x_i,t_n) can be written in the following way,

$$(U-u)(x_i,t_n) = (Y-y)(x_i,t_n) + (Z-z)(x_i,t_n),$$

thus

$$|(U-u)(x_i,t_n)| \le |(Y-y)(x_i,t_n)| + |(Z-z)(x_i,t_n)|,$$

from the above inequality it is enough to bound the regular and the singular component error with an optimal bound. The truncation error of the regular component can be written as

$$\begin{aligned} \left(\delta_t + \mathcal{L}_\varepsilon^N\right)(Y-y) &= -bY(x_i,t_{n-p}) + f - \left(\delta_t + \mathcal{L}_\varepsilon^N\right) y \\ &= b(y(x_i,t_{n-p}) - Y(x_i,t_{n-p})) + \left(\left(\frac{\partial}{\partial t} + \mathcal{L}_\varepsilon\right) - \left(\delta_t + \mathcal{L}_\varepsilon^N\right)\right) y \\ &= b(u(x_i,t_{n-p}) - U_1(x_i,t_{n-p})) + \left(\left(\frac{\partial}{\partial t} + \mathcal{L}_\varepsilon\right) - \left(\delta_t + \mathcal{L}_\varepsilon^N\right)\right) y, \end{aligned}$$

therefore, we have

$$\left(\delta_t + \mathcal{L}_\varepsilon^N\right)(Y-y) = -b\left(u(x_i,t_{n-p}) - U_1(x_i,t_{n-p})\right) - \varepsilon\left(\frac{\partial^2}{\partial x^2} - \delta_x^2\right) y + \left(\frac{\partial}{\partial t} - \delta_t\right) y.$$

Now taking the modulus and using (6.4.9) for the first part it reduces to,

$$\left|\left(\delta_t + \mathcal{L}_\varepsilon^N\right)(Y-y)(x_i,t_n)\right| \le C(N^{-2} + \Delta t) + \varepsilon\left|\left(\frac{\partial^2}{\partial x^2} - \delta_x^2\right) y\right| + \left|\left(\frac{\partial}{\partial t} - \delta_t\right) y\right|.$$

Using Taylor series expansions it is easy to show that,

$$\left|\left(\delta_t + \mathcal{L}_\varepsilon^N\right)(Y-y)(x_i,t_n)\right| \le C\left(N^{-2} + \Delta t + (h_{i+1}+h_i)^2\,\varepsilon\left\|\frac{\partial^4 y}{\partial x^4}\right\|_\infty + \Delta t\left\|\frac{\partial^2 y}{\partial t^2}\right\|_\infty\right).$$

Applying Lemma 6.3.1, and the estimates of the derivatives given in (6.2.4), we obtain

$$\left|\left(\delta_t + \mathcal{L}_\varepsilon^N\right)(Y-y)(x_i,t_n)\right| \le C(N^{-2} + \Delta t), \quad \text{for } (x_i,t_n) \in \overline{G}_2^{N,\Delta t}.$$

Now using the fact that the discrete operator $\left(\delta_t + \mathcal{L}_\varepsilon^N\right)$ satisfies the discrete maximum principle (Lemma 6.4.2) and the inverse operator is uniformly bounded, the above inequality can be reduced to,

$$|(Y-y)(x_i,t_n)| \le C(N^{-2} + \Delta t), \quad \text{for } (x_i,t_n) \in \overline{G}_2^{N,\Delta t}. \tag{6.4.12}$$

To estimate error of the the singular component, we decompose Z as the way its continuous counterpart z is decomposed,

$$Z = Z_l + Z_r,$$

where Z_l and Z_r are the left and the right part layers of the approximate solutions respectively, that are defined as

$$\begin{cases} \left(\delta_t + \mathcal{L}_\varepsilon^N\right) Z_l = -bZ_l(x_i, t_{n-p}), \quad (x_i, t_n) \in \overline{G}_2^{N,\Delta t}, \\ Z_l(x_i, t_n) = 0, \quad (x_i, t_n) \in \overline{G}_1^{N,\Delta t}, \\ Z_l(0, t_n) = \phi_l(t_n) - y(0, t_n), \quad Z_l(1, t_n) = 0 \quad t_n \in \Omega_2^{N_\tau}, \end{cases}$$

and

$$\begin{cases} \left(\delta_t + \mathcal{L}_\varepsilon^N\right) Z_r = -bZ_r(x_i, t_{n-p}), \quad (x_i, t_n) \in \overline{G}_2^{N,\Delta t}, \\ Z_r(x_i, t_n) = 0, \quad (x_i, t_n) \in \overline{G}_1^{N,\Delta t}, \\ Z_r(0, t_n) = 0, \quad Z_r(1, t_n) = \phi_r(t_n) - y(1, t_n), \quad t_n \in \Omega_2^N. \end{cases}$$

The error can then be written in the form

$$(Z - z)(x_i, t_n) = (Z_l - z_l)(x_i, t_n) + (Z_r - z_r)(x_i, t_n), \quad (x_i, t_n) \in \overline{G}_2^{N,\Delta t},$$

and the errors $Z_l - z_l$ and $Z_r - z_r$, associated with boundary layers of Γ_l and Γ_r respectively, can be estimated separately. Consider the error $Z_l - z_l$,

$$\begin{aligned} \left(\delta_t + \mathcal{L}_\varepsilon^N\right)(Z_l - z_l) &= \left(\left(\frac{\partial}{\partial t} + \mathcal{L}_\varepsilon\right) - \left(\delta_t + \mathcal{L}_\varepsilon^N\right)\right) z_l \\ &= -\varepsilon\left(\frac{\partial^2}{\partial x^2} - \delta_x^2\right) z_l + \left(\frac{\partial}{\partial t} - \delta_t\right) z_l. \end{aligned}$$

Taking the modulus and using the Taylor series expansions on time, we obtain

$$\begin{aligned} \left|\left(\delta_t + \mathcal{L}_\varepsilon^N\right)(Z_l - z_l)\right| &\leq C\left(N^{-2} + \Delta t + \varepsilon\left\|\left(\frac{\partial^2}{\partial x^2} - \delta_x^2\right) z_l\right\|_\infty + \Delta t\left\|\frac{\partial^2 z_l}{\partial t^2}\right\|_\infty\right), \\ &\leq C\left(N^{-2} + \Delta t + \varepsilon\left\|\left(\frac{\partial^2}{\partial x^2} - \delta_x^2\right) z_l\right\|_\infty\right). \end{aligned}$$

By fixing t, the lateral part of the above inequality can be seen as the truncation error of the reaction-diffusion two-point boundary-value problem as in [7] corresponding to the left-hand layer part. By this observation the truncation error in space can be analyzed the same way as [7, Lemmas 8, 9], the only difference is that there it is given for both sides layers but here, we need only for the left layer part, hence we obtain

$$\left|\left(\delta_t + \mathcal{L}_\varepsilon^N\right)(Z_l - z_l)(x_i, t_n)\right| \leq C(N^{-2} + \Delta t), \quad (x_i, t_n) \in \overline{G}_2^{N,\Delta t}. \tag{6.4.13}$$

Now using the fact that the discrete operator $\left(\delta_t + \mathcal{L}_\varepsilon^N\right)$ satisfies the discrete maximum principle (Lemma 6.4.2) and the inverse operator is uniformly bounded, the above inequality can be reduced to,

$$|(Z_l - z_l)(x_i, t_n)| \leq C(N^{-2} + \Delta t), \quad \text{for } (x_i, t_n) \in \overline{G}_2^{N,\Delta t}. \tag{6.4.14}$$

Similar analysis shows that the error of the right-hand part can also be bounded as

$$|(Z_r - z_r)(x_i, t_n)| \leq C(N^{-2} + \Delta t), \quad \text{for } (x_i, t_n) \in \overline{G}_2^{N,\Delta t}. \tag{6.4.15}$$

Combining (6.4.12), (6.4.14) and (6.4.15) completes the proof on the second interval $[\tau, 2\tau]$. Similarly, we can prove the estimate of the successive intervals in the temporal direction. This completes the proof. ∎

6.5 Numerical Results

In this section, we shall present the numerical results obtained by the difference scheme (6.3.3) for two test problems on the rectangular mesh $\overline{G}^{N,\Delta t} = \overline{\Omega}_x^N \times \overline{\Lambda}_t^M$, where $\overline{\Omega}_x^N$ is the equidistribution grid obtained from the numerical algorithm. In all the numerical experiments we will fix $m = 2$, which is necessary to define the monitor function (6.3.5). Moreover, in all the tables we begin with $N = 32$ and the time step $\Delta t = 0.1$ and we multiply N by two and divide Δt by four. The reason of dividing Δt by four is to justify the spatial order of convergence properly.

Example 6.5.1. *Consider the following delay parabolic initial-boundary-value problem:*

$$\begin{cases} u_t(x,t) - \varepsilon u_{xx}(x,t) = -2\exp(-1)u(x,t-1), \quad (x,t) \in (0,1)\times(0,2] \\ u(x,t) = \exp\left(-(t + x/\sqrt{\varepsilon})\right), \quad (x,t) \in [0,1]\times[-1,0], \\ u(0,t) = \exp(-t), \quad u(1,t) = \exp\left(-(t+1/\sqrt{\varepsilon})\right), \quad t \in [0,2]. \end{cases} \tag{6.5.1}$$

The exact solution is $u(x,t) = \exp\left(-(t + x/\sqrt{\varepsilon})\right)$. It is clear that there is a parabolic boundary layer in the neighborhood of Γ_l, but because of the boundary values there is no boundary layer on Γ_r

As the exact solution of the problem (6.5.1) is known, for each ε, we calculate the maximum point-wise error by

$$e_\varepsilon^{N,\Delta t} = \max_{(x_i,t_n)\in\overline{G}^{N,\Delta t}} \left|u(x_i,t_n) - U^{N,\Delta t}(x_i,t_n)\right|,$$

where $u(x_i,t_n)$ and $U^{N,\Delta t}(x_i,t_n)$ respectively, denote the exact and the numerical solution obtained on the mesh with N mesh intervals in the spatial direction and M mesh

intervals in the $t-$direction such that $\Delta t = T/M$ is the uniform time step. In addition, we determine the corresponding rate of convergence by

$$p_{\varepsilon}^{N,\Delta t} = \log_2 \left(\frac{e_{\varepsilon}^{N,\Delta t}}{e_{\varepsilon}^{2N,\Delta t/4}} \right).$$

The calculated maximum point-wise errors $e_{\varepsilon}^{N,\Delta t}$ and the corresponding rate of convergence $p_{\varepsilon}^{N,\Delta t}$ for Example 6.5.1 are given in Table 6.1 and Table 6.2, respectively. From these results one can observe the ε–uniform convergence of the numerical solution.

The calculated maximum point-wise errors in the normalized flux $r_{\varepsilon}^{N,\Delta t}$ and the corresponding rate of convergence $q_{\varepsilon}^{N,\Delta t}$ for Example 6.5.1 are given in Table 6.3 and Table 6.4. Again, one can see the ε–uniform convergence in Table 6.3, and the second-order convergence rate from Table 6.4. In Figures 6.1 (a) and (b), the maximum point-wise errors in the solution and the normalized flux are plotted respectively, which reflect the fact of second-order convergence independent of ε.

Further, we have calculated the normalized flux

$$F_{\varepsilon} u(x,t) = \sqrt{\varepsilon} \frac{\partial u(x,t)}{\partial x},$$

and its numerical approximation

$$F_{\varepsilon}^{N} U^{N,\Delta t}(x_i, t_n) = \sqrt{\varepsilon} \delta_x^{+} U_i^n.$$

The errors in the normalized flux have been calculated as

$$r_{\varepsilon}^{N,\Delta t} = \max_{1 \le n \le M} |F_{\varepsilon} u(x_0, t_n) - F_{\varepsilon}^{N} U^{N,\Delta t}(x_0, t_n)|,$$

and the rate of convergence is determined from

$$q_{\varepsilon}^{N,\Delta t} = \log_2 \left(\frac{r_{\varepsilon}^{N,\Delta t}}{r_{\varepsilon}^{2N,\Delta t/4}} \right).$$

Example 6.5.2. *Consider the following delay parabolic initial-boundary-value problem:*

$$\begin{cases} u_t - \varepsilon u_{xx} + \dfrac{(1+x)^2}{2} u = t^3 - u(x, t-1), \quad (x,t) \in (0,1) \times (0,2], \\ u(x,t) = 0, \quad (x,t) \in [0,1] \times [-1,0] \\ u(0,t) = 0 = u(1,t), \quad 0 \le t \le 2. \end{cases} \tag{6.5.2}$$

As the exact solution of the problem (6.5.2) is not known, to obtain the accuracy of the numerical solution and also to demonstrate the $\varepsilon-$uniform convergence of the proposed scheme, we use the double mesh principle which is given in the following.

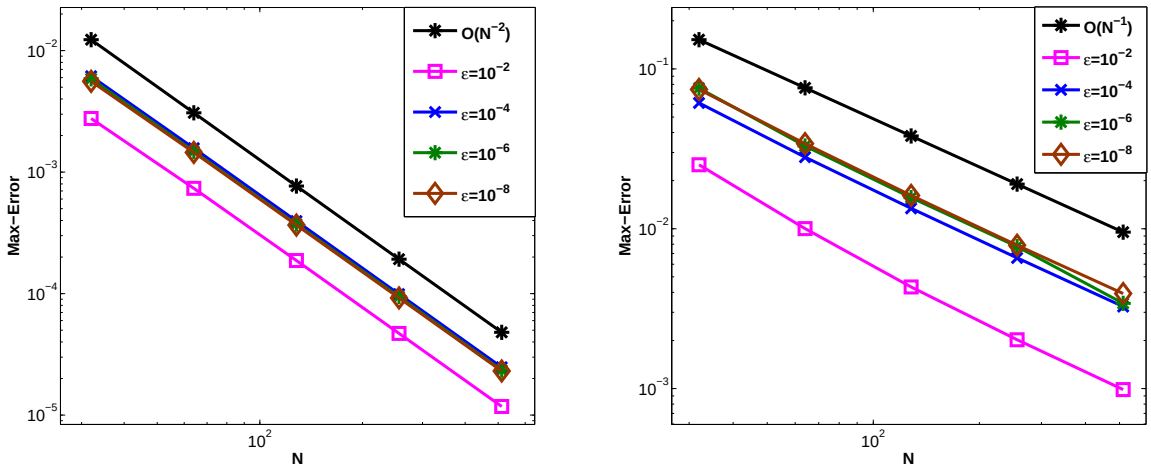

(a) *Maximum point-wise error of the solution* $e_\varepsilon^{N,\Delta t}$.

(b) *Maximum point-wise error of the normalized flux* $r_\varepsilon^{N,\Delta t}$.

Figure 6.1: *Loglog plot for Example 6.5.1.*

Table 6.1: *Maximum point-wise error of the solution* $e_\varepsilon^{N,\Delta t}$ *for Example* 6.5.1 *using equidistribution mesh.*

	Number of Intervals N/Time Step Size Δt				
ε	$32/\frac{1}{10}$	$64/\frac{1}{40}$	$128/\frac{1}{160}$	$256/\frac{1}{640}$	$512/\frac{1}{2560}$
10^0	2.7636e-03	7.3566e-04	1.8725e-04	4.7040e-05	1.1774e-05
10^{-2}	6.1484e-03	1.5722e-03	3.9528e-04	9.8968e-05	2.4751e-05
10^{-4}	5.8657e-03	1.4826e-03	3.7294e-04	9.4594e-05	2.3439e-05
10^{-6}	5.5893e-03	1.4529e-03	3.6683e-04	9.2121e-05	2.3063e-05
10^{-8}	5.5955e-03	1.4285e-03	3.6602e-04	9.1809e-05	2.2997e-05

Table 6.2: *Rate of convergence of the solution* $p_\varepsilon^{N,\Delta t}$ *for Example* 6.5.1 *using equidistribution mesh.*

	Number of Intervals N/Time Step Size Δt			
ε	$32/\frac{1}{10}$	$64/\frac{1}{40}$	$128/\frac{1}{160}$	$256/\frac{1}{640}$
10^0	1.9094	1.9741	1.9930	1.9982
10^{-2}	1.9674	1.9919	1.9979	1.9995
10^{-4}	1.9842	1.9911	1.9791	2.0129
10^{-6}	1.9437	1.9858	1.9935	1.9979
10^{-8}	1.9698	1.9645	1.9952	1.9972

Table 6.3: *Maximum point-wise error of the normalized flux* $r_\varepsilon^{N,\Delta t}$ *for Example* 6.5.1 *using equidistribution mesh.*

	Number of Intervals N/Time Step Size Δt				
ε	$32/\frac{1}{10}$	$64/\frac{1}{40}$	$128/\frac{1}{160}$	$256/\frac{1}{640}$	$512/\frac{1}{2560}$
10^{0}	2.5152e-02	1.0016e-02	4.3257e-03	2.0201e-03	9.8607e-04
10^{-2}	6.1271e-02	2.8039e-02	1.3411e-02	6.5732e-03	3.2593e-03
10^{-4}	7.5813e-02	3.2941e-02	1.5666e-02	7.7375e-03	3.4147e-03
10^{-6}	7.4361e-02	3.4075e-02	1.6160e-02	7.8819e-03	3.9305e-03
10^{-8}	7.6126e-02	3.6189e-02	1.6228e-02	7.9736e-03	3.9454e-03

Table 6.4: *Rate of convergence of the normalized flux* $q_\varepsilon^{N,\Delta t}$ *for Example* 6.5.1 *using equidistribution mesh.*

	Number of Intervals N/Time Step Size Δt			
ε	$32/\frac{1}{10}$	$64/\frac{1}{40}$	$128/\frac{1}{160}$	$256/\frac{1}{640}$
10^{0}	1.3284	1.2113	1.0985	1.0347
10^{-2}	1.1278	1.0640	1.0287	1.0120
10^{-4}	1.2026	1.0722	1.0177	1.1801
10^{-6}	1.1258	1.0763	1.0358	1.0038
10^{-8}	1.0728	1.1571	1.0252	1.0151

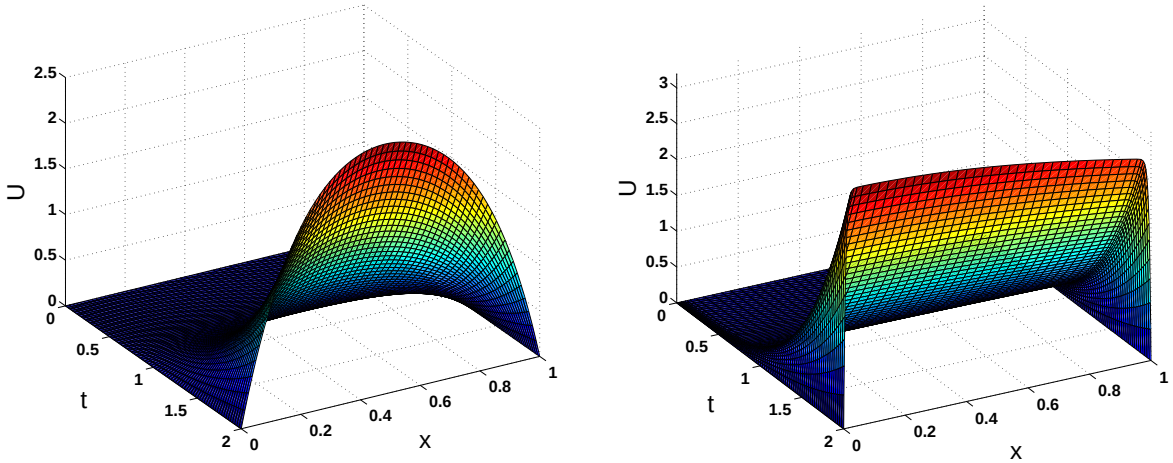

(a) $\varepsilon = 10^{-1}$. (b) $\varepsilon = 10^{-4}$.

Figure 6.2: *Numerical solution of Example 6.5.2 for* $N = 64$ *and* $\Delta t = 0.01$.

Table 6.5: *Maximum point-wise error of the solution* $E_\varepsilon^{N,\Delta t}$ *for Example* 6.5.2 *using equidistribution mesh.*

	Number of Intervals N/Time Step Size Δt			
ε	$32/\frac{1}{10}$	$64/\frac{1}{40}$	$128/\frac{1}{160}$	$256/\frac{1}{640}$
10^0	4.1424e-03	1.0515e-03	2.6387e-04	6.6030e-05
10^{-2}	1.5664e-01	3.9664e-02	9.9476e-03	2.4885e-03
10^{-4}	1.7038e-01	4.2971e-02	1.0809e-02	2.6916e-03
10^{-6}	1.7120e-01	4.4325e-02	1.1403e-02	2.8745e-03
10^{-8}	1.7083e-01	4.3954e-02	1.1329e-02	2.9009e-03

Let $\tilde{U}^{2N,\Delta t/4}(x_i,t_n)$ be the numerical solution obtained on the fine mesh $\overline{G}^{2N,\Delta t/4} = \overline{\Omega}_x^{2N} \times \overline{\Lambda}_t^{4M}$ with $2N$ mesh intervals in the spatial direction and $2M$ mesh intervals in the $t-$direction. Then for each ε, we calculate the maximum point-wise error by

$$E_\varepsilon^{N,\Delta t} = \max_{(x_i,t_n)\in\overline{G}^{N,\Delta t}} \left| U^{N,\Delta t}(x_i,t_n) - \tilde{U}^{2N,\Delta t/4}(x_i,t_n) \right|,$$

and the corresponding rate of convergence by

$$P_\varepsilon^{N,\Delta t} = \log_2 \left(\frac{E_\varepsilon^{N,\Delta t}}{E_\varepsilon^{2N,\Delta t/4}} \right).$$

The calculated maximum point-wise errors $E_\varepsilon^{N,\Delta t}$ and the corresponding rate of convergence $P_\varepsilon^{N,\Delta t}$ for Example 6.5.2 are given in Table 6.5 and Table 6.6, respectively. The numerical results given in these tables reveal the convergence independent of the diffusion parameter ε.

The numerical solution is plotted in Figures 6.2 (a) and (b) for $\varepsilon = 1e-1$ and $\varepsilon = 1e-4$, respectively. These figures show the existence of the boundary layers near $x = 0$ and $x = 1$.

The maximum point-wise errors are plotted in log-log scale in Figures 6.3, for the solution. From the figure, one can easily observe the ε–uniform convergence.

6.6 Conclusions

In this chapter, we solved the singularly perturbed time-dependent delay reaction-diffusion problems (6.1.1) numerically by the scheme, which consists of the backward-Euler scheme for the time derivative and the central difference for the spatial derivative on layer-adapted nonuniform grids obtained by equidistributing the monitor function

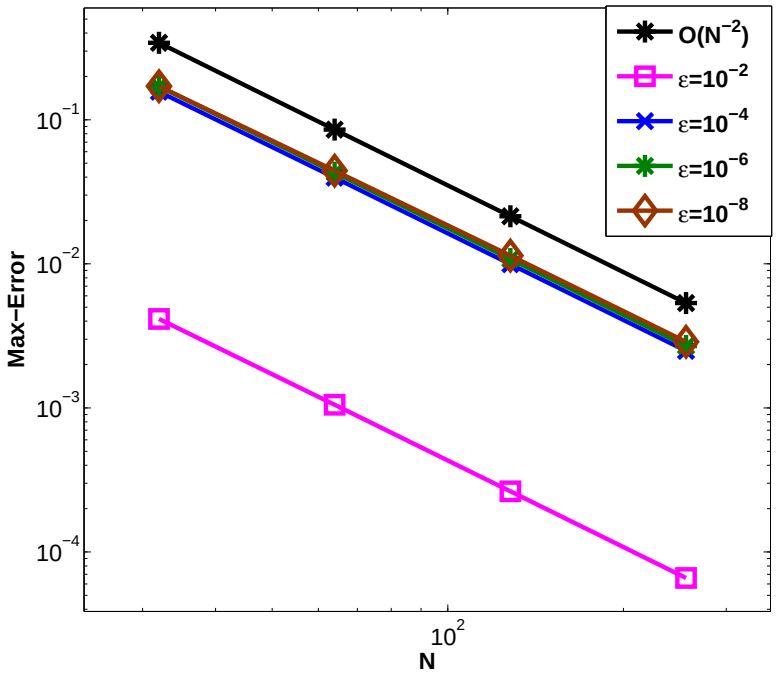

Figure 6.3: *Loglog plot of maximum point-wise error of the solution* $E_{\varepsilon}^{N,\Delta t}$ *of Example 6.5.2.*

Table 6.6: *Rate of convergence of the solution* $P_{\varepsilon}^{N,\Delta t}$ *for Example* 6.5.2 *using equidistribution mesh.*

	Number of Intervals N/Time Step Size Δt		
ε	$32/\frac{1}{10}$	$64/\frac{1}{40}$	$128/\frac{1}{160}$
10^{0}	1.9780	1.9946	1.9986
10^{-2}	1.9816	1.9954	1.9990
10^{-4}	1.9874	1.9911	2.0057
10^{-6}	1.9495	1.9588	1.9880
10^{-8}	1.9585	1.9560	1.9654

given in (6.3.5). The truncation error and stability analysis are obtained. The proposed numerical scheme is of first-order in the temporal variable and second-order in the spatial variable, *i.e.*, $O(\Delta t + N^{-2})$. Error estimates are derived for the numerical scheme, which are independent of the diffusion parameter ε. Numerical results reveal the theoretical error bounds.

CHAPTER 7

Uniform Convergence for Delay Parabolic Convection-Diffusion Problems on Piecewise-Uniform Shishkin Mesh

This chapter studies the numerical solution of singularly perturbed delay parabolic convection-diffusion problems with a delay in time. We divide the domain by using a piecewise-uniform Shishkin mesh in the spatial direction and uniform mesh in the temporal direction. Further, we discretize the problem by the backward-Euler difference scheme for the time derivative and an upwind difference scheme for the spatial derivative. We obtain the maximum principle and carry out the stability analysis. Then we prove numerical scheme is ε-uniform convergence of first-order in time and first-order up to logarithmic factor in space. Numerical results are carried out to verify the theoretical error estimates.

7.1 Introduction

In this chapter, we consider following class of singularly perturbed delay parabolic initial-boundary-value problems (IBVPs) with Dirichlet boundary conditions on the boundary. Let $\Omega = (0,1)$, $G = \Omega \times (0,T]$, and $\Gamma = \Gamma_l \cup \Gamma_b \cup \Gamma_r$, where Γ_l and Γ_r are the left and right sides of the rectangular G corresponding to $x = 0$ and 1, respectively, and $\Gamma_b = [0,1] \times [-\tau, 0]$:

$$\begin{cases} \left(\dfrac{\partial}{\partial t} + \mathbb{L}_\varepsilon\right) u(x,t) = -b(x,t)u(x,t-\tau) + f(x,t), \quad (x,t) \in G, \\ u(x,t) = \phi_b(x,t), \quad (x,t) = \Gamma_b, \\ u(0,t) = \phi_l(t), \quad \text{on } \Gamma_l = \{(0,t) : 0 \le t \le T\}, \\ u(1,t) = \phi_r(t), \quad \text{on } \Gamma_r = \{(1,t) : 0 \le t \le T\}, \end{cases} \tag{7.1.1}$$

where

$$\mathbb{L}_\varepsilon u(x,t) = -\varepsilon u_{xx}(x,t) + c(x)u_x(x,t) + a(x,t)u(x,t),$$

$0 < \varepsilon \ll 1$ and $\tau > 0$ are given constants, $a(x,t)$, $b(x,t)$, $f(x,t)$, $c(x)$, $(x,t) \in \overline{G}$, and $\phi_l(t)$, $\phi_r(t)$, $\phi_b(x,t)$, $(x,t) \in \Gamma$, are sufficiently smooth and bounded functions that satisfies

$$a(x,t) \geq 0, \quad b(x,t) \geq \beta > 0, \quad c(x) \geq \alpha > 0 \quad (x,t) \in \overline{G}.$$

The terminal time T is assumed to satisfy the condition $T = k\tau$ for some positive integer k. The required compatibility condition at the corner points and the delay terms are

$$\phi_b(0,0) = \phi_l(0), \quad \phi_b(1,0) = \phi_r(0), \tag{7.1.2}$$

and

$$\begin{aligned}
&\frac{d\phi_l(0)}{dt} - \varepsilon\frac{\partial^2\phi_b(0,0)}{\partial x^2} + c(0)\frac{\partial\phi_b(0,0)}{\partial x} + a(0,0)\phi_b(0,0) = -b(0,0)\phi_b(0,-\tau) + f(0,0),\\
&\frac{d\phi_r(0)}{dt} - \varepsilon\frac{\partial^2\phi_b(1,0)}{\partial x^2} + c(1)\frac{\partial\phi_b(1,0)}{\partial x} + a(1,0)\phi_b(1,0) = -b(1,0)\phi_b(1,-\tau) + f(1,0).
\end{aligned} \tag{7.1.3}$$

Note that $\phi_l(t)$, $\phi_b(x,t)$ and $\phi_r(t)$ are assumed to be smooth for (7.1.3) to make sense. Under the above assumptions and conditions, problem (7.1.1) has a unique solution [2]. Numerical treatment of the IBVP (7.1.1) is difficult because of the presence of boundary layers in its solution. In particular, classical finite difference methods on uniform meshes fail to yield satisfactory numerical results, and to obtain stability one has to reduce the spatial step-size in relation with ε. The same is true for finite element methods in the case of uniform mesh and polynomial basis functions. When regular layers are present it is possible to obtain an ε-uniform method by constructing an appropriate fitted finite difference operator (*i.e.,* finite difference scheme with fitting factor) on uniform meshes.

The chapter is organized in the following manner: Section 7.2 studies the bound on the analytic solution of the IBVP (7.1.1), and the bounds on the regular and the singular components of the solution. Section 7.3 describes the piecewise-uniform Shishkin mesh and gives the detailed construction of the finite difference scheme. The stability and ε–uniform error estimates are obtained in Section 7.4. Numerical results are presented in Section 7.5, and the chapter ends with a conclusion.

7.2 The Analytic Solution

In the study of the numerical aspects of SPPs, their analytical results play an important role. In this section, we are concerned with the analytical properties of the solution of (7.1.1) that will be required to prove the convergence and the maximum principle for the differential operator.

The reduced problem corresponding to (7.1.1) is

$$\begin{cases} (u_0)_t(x,t) + c(x)(u_0)_x(x,t) + a(x,t)u_0(x,t) = -b(x,t)u_0(x,t-\tau) + f(x,t), & (x,t) \in G, \\ u_0(x,t) = \phi_b(x,t), \quad (x,t) \in \Gamma_b, \quad u_0(x,t) = \phi_l(x), \quad (x,t) \in \Gamma_l. \end{cases} \tag{7.2.1}$$

Then it is clear that the solution of (7.1.1) has boundary layer along the boundary Γ_r. The characteristics of (7.2.1) are the vertical lines $x =$ constant, which implies that any boundary layer arising in the solution is of parabolic type.

Theorem 7.2.1. *Let the data $c \in \mathcal{C}^{2+\alpha}(\overline{\Omega})$, $a, b, f \in \mathcal{C}^{(2+\alpha,1+\alpha/2)}(\overline{G})$, $\phi_l \in \mathcal{C}^{2+\alpha/2}([0,T])$, $\phi_b \in \mathcal{C}^{(4+\alpha,2+\alpha/2)}(\Gamma_b)$, $\phi_r \in \mathcal{C}^{2+\alpha/2}([0,T])$, $\alpha \in (0,1)$, with sufficient compatibility condition on the corner is fulfilled. Then (7.1.1) has a unique solution u and $u \in \mathcal{C}^{(4+\alpha,2+\alpha/2)}(\overline{G})$. Furthermore, the derivatives of the solution u_ε satisfy, for all non-negative integers i, j such that $0 \le i + 2j \le 4$,*

$$\left\| \frac{\partial^{i+j} u}{\partial x^i \partial y^j} \right\|_\infty \le C\varepsilon^{-i/2}.$$

Proof. The proof of this theorem for $t < \tau$ can be found in [45]. The arguments can be extended to $t \in [\tau, T]$ with necessary compatibility conditions. ∎

Lemma 7.2.2. (**Maximum principle**) *Suppose the function $\psi(x,t) \in \mathcal{C}^0(\overline{G}) \cap \mathcal{C}^2(G)$, satisfies $\psi(x,t) \ge 0$ for all $(x,t) \in \Gamma$ and $\psi_t(x,t) + \mathbb{L}_\varepsilon\psi(x,t) \ge 0$ for all $(x,t) \in G$, then $\psi(x,t) \ge 0$ for all $(x,t) \in \overline{G}$.*

Proof. Assume that there exists $(x^*, t^*) \in \overline{G}$ such that

$$\psi(x^*, t^*) = \min_{(x,t)\in\overline{G}} \psi(x,t) < 0,$$

it is clear that the point $(x^*, t^*) \notin \partial G$ which implies $(x^*, t^*) \in G$.

Applying the differential operator to ψ, we obtain that

$$\psi_t + \mathbb{L}_\varepsilon\psi = \psi_t - \varepsilon\psi_{xx} + c(x)\psi_x + a(x,t)\psi$$

and at the point (x^*, t^*) the value becomes

$$(\psi_t + \mathbb{L}_\varepsilon\psi)(x^*, t^*) = \psi_t(x^*, t^*) - \varepsilon\psi_{xx}(x^*, t^*) + c(x)\psi_x(x^*, t^*) + a(x,t)\psi(x^*, t^*),$$

since $\psi_{xx}(x^*, t^*) \ge 0$, $\psi_x(x^*, t^*) = 0$, and $\psi_t(x^*, t^*) = 0$, therefore, we have

$$(\psi_t + \mathbb{L}_\varepsilon\psi)(x^*, t^*) < 0,$$

which is a contradiction as

$$(\psi_t + \mathbb{L}_\varepsilon\psi)(x,t) \ge 0, \quad \forall (x,t) \in G,$$

thus, we can conclude that the minimum of ψ is non-negative. ∎

We decompose the exact solution $u(x,t)$ of the IBVP (7.1.1) into the regular and the singular components as

$$u(x,t) = v(x,t) + w(x,t), \quad (x,t) \in \overline{G}.$$

We take further decomposition of the regular component v for any prescribed order k by assuming necessary compatibility condition as

$$v(x,t) = \sum_{j=0}^{k+1} \varepsilon^j v_j(x,t), \quad (x,t) \in \overline{G},$$

where the functions v_j, $j = 0, 1, \ldots, k$, are the solutions of the following first-order problems

$$\begin{cases} (v_0)_t + c(x)(v_0)_x + a(x,t)v_0 = -b(x,t)v_0(x,t-\tau) + f(x,t), & (x,t) \in G, \\ v_0(x,t) = \phi_b(x,t), & (x,t) \in \Gamma_b, \\ v_0(x,t) = \phi_l(x,t), & (x,t) \in \Gamma_l, \end{cases} \tag{7.2.2}$$

and

$$\begin{cases} (v_j)_t + c(x)(v_j)_x + a(x,t)v_j = -b(x,t)v_j(x,t-\tau) \\ \qquad\qquad\qquad\qquad +(v_{j-1})_{xx}(x,t), \ (x,t) \in G, \ j = 1, 2, \ldots, k, \\ v_j(x,t) = 0, \quad (x,t) \in \Gamma_b, \\ v_j(0,t) = 0, \quad 0 \le t \le T, \end{cases} \tag{7.2.3}$$

and lastly, the function v_{k+1} satisfies

$$\begin{cases} (v_{k+1})_t(x,t) + \mathbb{L}_\varepsilon v_{k+1}(x,t) = -b(x,t)v_{k+1}(x,t-\tau) + (v_k)_{xx}(x,t), & (x,t) \in G, \\ v_{k+1}(x,t) = 0, \quad (x,t) \in \Gamma_b, \\ v_{k+1}(0,t) = 0 = v_{k+1}(1,t), \quad 0 \le t \le T. \end{cases} \tag{7.2.4}$$

Hence, the regular component $v(x,t)$ satisfies the following IBVP:

$$\begin{cases} v_t(x,t) + \mathbb{L}_\varepsilon v(x,t) = -b(x,t)v(x,t-\tau) + f(x,t), & (x,t) \in G, \\ v(x,t) = u(x,t), \quad (x,t) \in \Gamma_b, \\ v(0,t) = u(0,t), \quad 0 \le t \le T, \\ v(1,t) = \displaystyle\sum_{j=0}^{k+1} \varepsilon^j v_j(1,t), \quad 0 \le t \le T, \end{cases} \tag{7.2.5}$$

and therefore, the singular component $w(x,t)$ must satisfies the homogeneous problem

$$\begin{cases} w_t(x,t) + \mathbb{L}_\varepsilon w(x,t) = -b(x,t)w(x,t-\tau), & (x,t) \in G, \\ w(x,t) = 0, \quad (x,t) \in \Gamma_b, \\ w(0,t) = 0, \quad 0 \le t \le T, \\ w(1,t) = u(1,t) - v(1,t), \quad 0 \le t \le T. \end{cases} \tag{7.2.6}$$

Theorem 7.2.3. *Let $u(x,t)$ be the solution of (7.1.1). The derivatives of $u(x,t)$ satisfy the following bound*

$$\left|\frac{\partial^k u(x,t)}{\partial x^k}\right| \leq C\left(1+\varepsilon^{-k}\exp(-\alpha(1-x)/\varepsilon)\right), \quad x\in[0,1],\ k=0,1$$

for any $t\in[0,T]$.

Proof. The proof of this theorem for $t<\tau$ can be found in [45]. The arguments can be extended to $t\in[\tau,T]$ with necessary compatibility conditions. ∎

Theorem 7.2.4. *Let $w(x,t)$ be the solution of (7.2.6). The bound of $w(x,t)$ is given by*

$$|w(x,t)| \leq C\exp(-\alpha(1-x)/\varepsilon), \qquad \forall (x,t)\in\overline{G}.$$

Proof. The proof of this theorem for $t<\tau$ can be found in [45]. The arguments can be extended to $t\in[\tau,T]$ with necessary compatibility conditions. ∎

Theorem 7.2.5. *For all non-negative integers p,q, satisfying $0\leq p+q\leq k+2$, and with sufficient compatibility condition at the corners the regular component $v(x,t)$ and the singular component $w(x,t)$, defined in (7.2.5) and (7.2.6), respectively, satisfy the following bounds,*

$$\left\|\frac{\partial^{p+q}v}{\partial x^p\partial t^q}(x,t)\right\|_\infty \leq C\big(1+\varepsilon^{k+1-p}\big),$$

and

$$\left|\frac{\partial^{p+q}w}{\partial x^p\partial t^q}(x,t)\right| \leq C\varepsilon^{-p}\exp\big(-\alpha(1-x)/\varepsilon\big), \quad (x,t)\in G.$$

Proof. Refer [66] for the detailed proof for $k=3$ and $t<\tau$. The arguments presented in [66] can be extended to any arbitrary k and $t\in[\tau,T]$ with necessary compatibility conditions on the boundary and the initial conditions. ∎

7.3 The Numerical Solution

In this section, we discretize the parabolic delay IBVP (7.1.1), the time derivative is replaced by the backward-Euler difference scheme, and the spatial derivative is replaced by the upwind difference scheme.

7.3.1 Finite difference scheme

On the time domain [0,T], we introduce the equidistant meshes with uniform time step Δt such that

$$\overline{\Lambda}_t^M = \{t_n = n\Delta t,\ n=0,\ldots,M,\ \Delta t = T/M\},$$

where M denotes the total number of mesh intervals in the interval $[0,T]$ and the step length Δt satisfies the constraint $p\Delta t = \tau$, where p is a positive integer, $t_j = j\Delta t$, $j \geq -p$.

Consider the spatial domain $\overline{\Omega} = [0,1]$ and let $N > 4$ be a positive even integer. Since the problem (7.1.1) has only a regular layer at $x = 1$, to define the piecewise-uniform mesh we divide the domain $\overline{\Omega}$ into two sub-domain's $[0, 1-\rho]$ and $[1-\rho, 1]$ and then divide each sub-domain into $N/2$ equal intervals by the points

$$\overline{\Omega}_x^N = \{0 = x_0, x_1, \ldots, x_{N/2} = 1-\rho, \ldots, x_N = 1\},$$

where

$$x_i = \begin{cases} i\dfrac{2(1-\rho)}{N}, & i = 0, \ldots, \dfrac{N}{2}, \\ (1-\rho) + \left(i - \dfrac{N}{2}\right)\dfrac{2\rho}{N}, & i = \dfrac{N}{2}+1, \ldots, N. \end{cases} \tag{7.3.1}$$

Here, the transition point $(1-\rho)$, which separates the coarse and fine portions of the mesh, is obtained by taking

$$\rho = \min\left\{\frac{1}{2}, \rho_0 \varepsilon \ln N\right\},$$

where $\rho_0 \geq 1/\alpha$. In the analysis, we shall assume that $\rho = \rho_0 \varepsilon \ln N$, as otherwise N is exponentially large compared with ε and the analysis can then be carried out using the standard classical techniques.

We now define the spatial step size by

$$h_i = x_i - x_{i-1},\ i = 1, 2, \ldots, N, \quad \widehat{h}_i = (h_i + h_{i+1})/2,\ i = 1, 2, \ldots, N-1,$$

and by the definition of x_i's the spatial step size satisfies the following,

$$H := h_i = \frac{2(1-\rho)}{N}, \quad i = 0, \ldots, \frac{N}{2},$$

$$h := h_i = \frac{2\rho}{N}, \quad i = \frac{N}{2}+1, \ldots, N.$$

Here, H and h are the mesh widths in $[0, 1-\rho]$ and $[1-\rho, 1]$, respectively. Then it is easy to see that

$$N^{-1} \leq H \leq 2N^{-1}, \quad h = 2\rho_0 \varepsilon N^{-1} \ln N.$$

We use various steps to prove the ε-uniform convergence in Section 7.4. Here, we define the discretization of domains in a systematic way to make our presentation clear. We define the discretized domain $\overline{G}^{N,\Delta t} = \overline{\Omega}_x^N \times \overline{\Lambda}_t^M$, $\Gamma_b^N = \overline{\Omega}_x^N \times \overline{\Lambda}_t^p$, where $\overline{\Lambda}_t^p$ is $p+1$ uniform mesh intervals in $[\tau, 0]$. The boundary points Γ^N of $\overline{G}^{N,\Delta t}$ are $\Gamma^N = \overline{G}^{N,\Delta t} \cap \Gamma$.

Similarly we define the right and the left boundary points by $\Gamma_l^N = \overline{G}^{N,\Delta t} \cap \Gamma_l$ and $\Gamma_r^N = \overline{G}^{N,\Delta t} \cap \Gamma_r$, respectively.

We further discretize $\overline{G}_j^{N,\Delta t} = \overline{\Omega}_x^N \times \overline{\Lambda}_{j,t}^p$, where $\overline{\Lambda}_{j,t}^p$ is $p+1$ uniform mesh intervals in $[(j-1)\tau, j\tau]$. From the above discretization we can also observe that $\overline{G}^{N,\Delta t} = \bigcup_{j=1}^k \overline{G}_j^{N,\Delta t}$.

We discretize the equation (7.1.1) by means of the backward-Euler scheme for the time derivative, and the upwind difference scheme for the spatial derivative. Hence the discretization of (7.1.1) takes the form, for $n = 0, 1, \ldots, M-1$,

$$\begin{cases} \dfrac{U_i^{n+1} - U_i^n}{\Delta t} + \mathbb{L}_\varepsilon^N U_i^{n+1} = -b(x_i, t_{n+1}) U_i^{n-p} + f(x_i, t_{n+1}), \quad \text{for } i = 1, \ldots, N-1, \\ U_0^{n+1} = \phi_l(t_{n+1}), \quad U_N^{n+1} = \phi_r(t_{n+1}), \\ U_i^{-j} = \phi_b(x_i, -t_j), \quad \text{for } i = 1, \ldots, N-1 \text{ and } j = 0, \ldots, p, \end{cases} \tag{7.3.2}$$

and for

$$\mathbb{L}_\varepsilon^N U_i^{n+1} = -\varepsilon \delta_x^2 U_i^{n+1} + c_i \delta_x^- U_i^{n+1} + a_{i,n+1} U_i^{n+1}. \tag{7.3.3}$$

After rearranging the terms in (7.3.2), we obtain the following form of the difference scheme: for $n = 0, 1, \ldots, M-1$,

$$\begin{cases} r_{i,n+1}^- U_{i-1}^{n+1} + r_{i,n+1}^c U_i^{n+1} + r_{i,n+1}^+ U_{i+1}^{n+1} = g_i^n, \quad \text{for } i = 1, \ldots, N-1, \\ U_0^{n+1} = \phi_l(t_{n+1}), \quad U_N^{n+1} = \phi_r(t_{n+1}), \\ U_i^{-j} = \phi_b(x_i, -t_j), \quad \text{for } i = 1, \ldots, N-1 \text{ and } j = 0, \ldots, p, \end{cases} \tag{7.3.4}$$

where

$$r_{i,n}^- = -\frac{\varepsilon \Delta t}{h_i \widehat{h}_i} - \frac{c_i \Delta t}{h_i}, \qquad r_{i,n}^+ = -\frac{\varepsilon \Delta t}{h_{i+1} \widehat{h}_i}, \quad r_{i,n}^c = 1 + \Delta t a_{i,n} - r_{i,n}^- - r_{i,n}^+,$$

$$a_{i,n} = a(x_i, t_n), \qquad c_i = c(x_i),$$

$$g_i^n = U_i^n + \Delta t \left\{ -b(x_i, t_{n+1}) U_i^{n-p} + f(x_i, t_{n+1}) \right\}.$$

7.4 Error Analysis

Here, we carry out the stability analysis of the discrete operator defined in (7.3.2). Finally, we obtain the ε-uniform error estimate in the discrete maximum norm.

The following lemma provides the stability result for a general numerical scheme for the IBVP (7.1.1).

Lemma 7.4.1. *Consider the IBVP (7.1.1) and the difference scheme (7.3.2), the difference scheme (excluding the initial and boundary conditions) can be written as*

$$\delta_t U^{n+1} + \mathbb{L}_\varepsilon^N U^{n+1} := AU^{n+1} - BU^n = F^n, \quad \text{for } n = 0, \cdots, M-1, \tag{7.4.1}$$

where $U^n = (U_1^n, \cdots, U_{N-1}^n)^T$, F^n *is a vector independent of the computed solution, and* A *and* B *are matrices and also that* A *is an* M*-matrix, and* $B \geq 0$.

Let y *and* z *be two mesh functions, such that* $y^n = (y_0^n, \cdots, y_N^n)^T$, *and* $z^n = (z_0^n, \cdots, z_N^n)^T$ *for each* n. *Assume that* $\left|\delta_t y^{n+1} + \mathbb{L}_\varepsilon^N y^{n+1}\right| \leq \delta_t z^{n+1} + \mathbb{L}_\varepsilon^N z^{n+1}$, *for* $n = 0, \cdots, M-1$, *and* $|y| \leq z$ *on the boundary* $\Gamma_b \cup \Gamma_l \cup \Gamma_r$. *Then,* $|y| \leq z$ *on* $\overline{\Omega}_x^N \times \overline{\Lambda}_t^M$.

Proof. The difference scheme (7.3.3) can be written in the form of (7.4.1) for $n = 1, 2, \ldots, p$, with $A = (a_{ij})$ and $B = (b_{ij})$ as

$$a_{i,i-1} = \frac{r_{i,n}^-}{\Delta t}, \quad a_{i,i} = \frac{r_{i,n}^c}{\Delta t}, \quad a_{i,i+1} = \frac{r_{i,n}^+}{\Delta t},$$
$$b_{i,i} = \frac{1}{\Delta t}.$$

Simple calculation shows that the matrix A is an M-matrix and the matrix $B \geq 0$. Therefore, the difference scheme satisfies the hypotheses of Lemma 7.4.1 and immediately the required result follows. The above argument can also be extended to other temporal levels. ∎

The finite difference operator $\left(\delta_t + \mathbb{L}_\varepsilon^N\right)$ in (7.3.3) satisfies the following discrete maximum principle on $\overline{G}^{N,\Delta t}$.

Lemma 7.4.2. (**Discrete maximum principle**) *Assume that* $\Psi(x_i, t_n)$ *satisfies* $\Psi(x_i, t_n) \geq 0$ *on* $(x_i, t_n) \in \Gamma^N$. *Then* $\left(\delta_t + \mathbb{L}_\varepsilon^N\right)\Psi(x_i, t_n) \geq 0$ *on* $(x_i, t_n) \in \overline{G}^{N,\Delta t}$ *implies that* $\Psi(x_i, t_n) \geq 0$ *at each point of* $(x_i, t_n) \in \overline{G}^{N,\Delta t}$.

Here we provide the important theorem for the ε-uniform convergence of the numerical solution in the discrete maximum norm.

Theorem 7.4.3. *Let* u *and* U *be respectively the continuous and the numerical solutions of the IBVPs (7.1.1) and (7.3.4) and satisfying sufficient compatibility conditions at the corners. Then, we have the following error bound*

$$\max_{i,n} |(u - U)(x_i, t_n)| \leq C[\Delta t + N^{-1} \ln N] \quad \text{for all } (x_i, t_n) \in \overline{G}^{N,\Delta t}, \tag{7.4.2}$$

where $U(x_i, t_n) = U_i^n$.

Proof. We prove the theorem by various steps. We first prove the result on the interval $[0, \tau]$, *i.e.,* the time discretization parameter n varies from 0 to p. Let $\eta_i^n = u_i^n - U_i^n$ be the truncation error in the computed solution at each mesh point (x_i, t_n). We write the scheme (7.3.2) as

$$\delta_t U_i^n + \mathbb{L}_\varepsilon^N U_i^n = -b_i^n \phi_b(x_i, t_{n-p}) + f_i^n \quad i = 1, \ldots, N-1, \quad n = 1, \ldots, p.$$

Therefore, the truncation error of the above scheme can be written in the following way as given in [49] and [17],

$$\delta_t \eta_i^n + \mathbb{L}_\varepsilon^N \eta_i^n = \chi_{1,i}^n + \chi_{2,i}^n, \quad \text{for } (x_i, t_n) \in \overline{G}_1^{N,\Delta t},$$

where $\chi_{1,i}^n$ and $\chi_{2,i}^n$ as follows,

$$\chi_{1,i}^n := \mathbb{L}_\varepsilon^N u_i^n - (\mathbb{L}_\varepsilon u)_i^n \quad \text{and} \quad \chi_{2,i}^n := \delta_t u_i^n - (u_t)_i^n.$$

With this splitting of the truncation error we can decompose the error η as $\eta = \phi + \psi$. Here the function ϕ_i^n is, for each fixed $n = 0, \ldots, p$, the solution of the discrete two-point boundary-value problem

$$\begin{cases} \mathbb{L}_\varepsilon^N \phi_i^n = \chi_{1,i}^n \quad \text{for } i = 1, \ldots, N-1, \\ \phi_0^n = \phi_N^n = 0, \end{cases} \tag{7.4.3}$$

and ψ_i^n, the solution of the discrete parabolic problem

$$\begin{cases} \delta_t \psi_i^n + \mathbb{L}_\varepsilon^N \psi_i^n = \chi_{2,i}^n - \delta_t \phi_i^n \quad \text{for } i = 1, \ldots, N-1, \\ \psi_0^n = \psi_N^n = 0 \quad \text{for } n = 1, \ldots, p, \\ \psi_i^0 = -\phi_i^0 \quad \text{for } i = 0, \ldots, N. \end{cases} \tag{7.4.4}$$

Equation (7.4.3) is a sequence of two-point boundary-value problems that has been discretized using $\mathbb{L}_\varepsilon^N$, with $\chi_{1,i}^n$ playing the role of truncation error and can be bounded using technique from two-point boundary-value problems. The problem (7.1.1) exhibits regular boundary layers and the same is true for the equation (7.4.3), therefore, the error bound derived for two-point boundary-value problems on the piecewise-uniform mesh can be invoked for all temporal levels:

$$|\phi_i^n| \leq C N^{-1} \ln N, \quad \text{for all } i, n \leq p, \tag{7.4.5}$$

with the fact that our problem exhibits regular boundary layers.

We have to bound the other error component ψ. From Lemma 7.4.1 and the discrete maximum principle (Lemma 7.4.2), we get the following bound for the error component ψ

$$|\psi_i^n| \;=\; C \left(\max_i |\phi_i^0| + \max_{i,n} |\chi_{2,i}^n - \delta_t \phi_i^n| \right), \quad \text{for } i, n \leq p.$$

Using the bounds of $\chi_{2,i}^n$ and (7.4.5) we obtain

$$|\psi_i^n| \;=\; C \left[N^{-1} \ln N + \Delta t + \max_{i,n} |\delta_t \phi_i^n| \right], \quad \text{for } i, n \leq p, \tag{7.4.6}$$

It remains to bound $\delta_t\phi$ in (7.4.6). The two-point boundary-value problem (7.4.3) implies that $\delta_t\phi$ satisfies

$$\begin{cases} \mathbb{L}_\varepsilon^N(\delta_t\phi)_i^n = \delta_t\chi_{1,i}^n - ((\delta_t b)\phi)_i^{j-1} \quad \text{for } i = 1, \ldots, N-1, \\ (\delta_t\phi)_0^n = (\delta_t\phi)_N^n = 0. \end{cases} \tag{7.4.7}$$

We further decompose $\delta_t\phi$ as $\delta_t\phi = \nu + \varrho$, applying it on equation (7.4.7), we get

$$\begin{cases} \mathbb{L}_\varepsilon^N \nu_i^n = \delta_t\chi_{1,i}^n \quad \text{for } i = 1, \ldots, N-1, \\ \nu_0^n = \nu_N^n = 0, \end{cases} \tag{7.4.8}$$

and

$$\begin{cases} \mathbb{L}_\varepsilon^N \varrho_i^n = -((\delta_t b)\phi)_i^{j-1} \quad \text{for } i = 1, \ldots, N-1, \\ \varrho_0^n = \varrho_N^n = 0, \end{cases} \tag{7.4.9}$$

To analyze the above sequence of two-point boundary-value problems (7.4.8), observe that the right-hand side of the equation can be written as

$$\begin{aligned} \delta_t\chi_{1,i}^n &= \frac{1}{\Delta t}\left(\chi_{1,i}^n - \chi_{1,i}^{n-1}\right) \\ &= \frac{1}{\Delta t}\left((\mathbb{L}_\varepsilon^N u_i^n - (\mathbb{L}_\varepsilon u)_i^n) - (\mathbb{L}_\varepsilon^N u_i^{n-1} - (\mathbb{L}_\varepsilon u)_i^{n-1})\right) \\ &= \frac{1}{\Delta t}\left((\mathbb{L}_\varepsilon^N u_i^n - \mathbb{L}_\varepsilon^N u_i^{n-1}) - ((\mathbb{L}_\varepsilon u)_i^n - (\mathbb{L}_\varepsilon u)_i^{n-1})\right). \end{aligned}$$

Let $\widehat{\mathbb{L}}_\varepsilon u = -\varepsilon u_{xx} + cu_x$ and $\widehat{\mathbb{L}}_\varepsilon^N u_i^n = -\varepsilon\delta_x^2 u_i^n + c\delta_x^- u_i^n$. That is, $\widehat{\mathbb{L}}_\varepsilon^N u$ is the discretization of the continuous operator $\widehat{\mathbb{L}}_\varepsilon u$. Then one can write the above formula as

$$\delta_t\chi_{1,i}^n = \frac{1}{\Delta t}\int_{t_{n-1}}^{t_n}\left[\widehat{\mathbb{L}}_\varepsilon^N \frac{\partial}{\partial t}u(x_i,t) - \widehat{\mathbb{L}}_\varepsilon \frac{\partial}{\partial t}u(x_i,t)\right]dt.$$

From the above equation, we obtain

$$\begin{aligned} |\delta_t\chi_{1,i}^n| \leq \quad & C\varepsilon\int_{x_{i-1}}^{x_i}\max_{t\in[t_{n-1},t_n]}|u_{xxxt}(x,t)|dt \\ & + Ch_i\int_{x_{i-1}}^{x_i}\max_{t\in[t_{n-1},t_n]}\left(|u_{xt}| + |u_{xxt}| + |u_{xxxt}|\right)(x,t)dt. \end{aligned}$$

where we have used the Peano kernel theorem, and following the argument given in [17], we obtain the same estimate on $\delta_t\chi_{1,i}^n$ as the corresponding truncation error bounds arising for a standard convection-diffusion two-point boundary-value problem. Now analyzing the problem the same way as for the standard two-point convection-diffusion boundary-value problem, we obtain the following bound for ν_i^n

$$|\nu_i^n| \leq CN^{-1}\ln N, \quad \text{for all } i, n \leq p. \tag{7.4.10}$$

Observe from (7.4.9) that, the operator satisfies the discrete maximum principle as like (7.4.3), therefore,

$$\max_i |\varrho_i^n| \leq C \max_i | - ((\delta_t b)\phi)_i^{n-1} | \leq C \max_i |\phi_i^j| \leq CN^{-1} \ln N, \quad \text{for all } i, n \leq p. \tag{7.4.11}$$

Combining (7.4.10), (7.4.6) and (7.4.11), we get

$$\max_{i,n} |(u - U)(x_i, t_n)| \leq C[\Delta t + N^{-1} \ln N], \quad \text{for all } (x_i, t_n) \in \overline{G}_1^{N,\Delta t}, \tag{7.4.12}$$

where $U(x_i, t_n) = U_i^n$. For $t \geq \tau$ it is not possible to follow the above argument because the delay term, $u(x, t-\tau)$, is explicitly unknown for $t \geq \tau$. For this reason, we examine the detailed proof of the estimate for the difference between the numerical solution U and the solution u itself over the interval $[\tau, 2\tau]$. The proof follows the approach given in [2].

Consider the following singularly perturbed delay parabolic equation on the domain $G_2 = (0,1) \times (\tau, 2\tau]$,

$$\begin{cases} \left(\dfrac{\partial}{\partial t} + \mathbb{L}_\varepsilon\right) u(x,t) = -b(x,t)u(x,t-\tau) + f(x,t), \quad (x,t) \in G_2, \\ u(x,\tau) = u(x,t_p), \quad x \in \Omega, \\ u(0,t) = \phi_0(t), \quad u(1,t) = \phi_1(t), \quad t \in [\tau, 2\tau]. \end{cases} \tag{7.4.13}$$

We discretize (7.4.13) by means of the backward-Euler scheme for the time derivative, and the central difference for the space derivative. Hence the discretization takes the form,

$$\begin{cases} \left(\delta_t + \mathbb{L}_\varepsilon^N\right) U(x_i, t_n) \equiv \delta_t U_i^n - \varepsilon \delta_x^2 U_i^n + c_i \delta_x^- U_i^n + a_{i,n} U \\ \qquad\qquad = -b_{i,n} U_i^{n-p} + f(x_i, t_n), (x_i, t_n) \in \overline{G}_2^{N,\Delta t}, \\ U(x_i, t_n) = U_1(x_i, t_n), \quad (x_i, t_n) \in \overline{G}_1^{N,\Delta t}, \\ U(0, t_n) = \phi_0(t_n), \quad U(1, t_n) = \phi_1(t_n), \quad t_n \in \overline{\Lambda}_{2,t}^p, \end{cases} \tag{7.4.14}$$

where U_1 is the numerical solution calculated on $\overline{G}_1^{N,\Delta t}$. The solution u of (7.4.13) is decomposed into the regular and the singular components $u = y + z$. The regular component y is further decomposed into $y = y_0 + \varepsilon y_1$, where y_0 and y_1 solve the following problems, respectively,

$$\begin{cases} \dfrac{\partial y_0}{\partial t}(x,t) + c\dfrac{\partial y_0}{\partial x}(x,t) + a y_0(x,t) = -b y_0(x, t-\tau) + f(x,t), \quad (x,t) \in G_2 \\ y_0(x,t) = u(x,t), \quad (x,t) \in \Omega \times [0,\tau], \quad y_0(0,t) = u(0,t), \quad t \in [\tau, 2\tau], \end{cases}$$

and

$$\begin{cases} \left(\dfrac{\partial}{\partial t} + \mathbb{L}_\varepsilon\right) y_1(x,t) = -b(x,t) y_1(x, t-\tau) + \dfrac{\partial^2 y_0}{\partial x^2}(x,t), \quad (x,t) \in G_2, \\ y_1(x,t) = 0, \quad (x,t) \in \Omega \times [0,\tau], \quad y_1(0,t) = y_1(1,t) = 0, \quad t \in [\tau, 2\tau]. \end{cases}$$

By the above definition of y_0 and y_1, the regular component y satisfies

$$\begin{cases} \left(\dfrac{\partial}{\partial t} + \mathbb{L}_\varepsilon\right) y(x,t) = -b(x,t)y(x,t-\tau) + f(x,t), \quad (x,t) \in G_2, \\ y(x,t) = u(x,t), \quad (x,t) \in \Omega \times [0,\tau], \\ y(0,t) = y_0(0,t), \quad y(1,t) = y_0(1,t), \quad t \in [\tau, 2\tau]. \end{cases}$$

The singular component z satisfies

$$\begin{cases} \left(\dfrac{\partial}{\partial t} + \mathbb{L}_\varepsilon\right) z(x,t) = -b(x,t)z(x,t-\tau), \quad (x,t) \in G_2, \\ z(x,t) = 0, \quad (x,t) \in \Omega \times [0,\tau], \\ z(0,t) = 0, \quad z(1,t) = \phi_r(t) - y_0(1,t), \quad t \in [\tau, 2\tau]. \end{cases}$$

Similarly the numerical solution U of (7.4.14) is decomposed into the regular and the singular components in an analogous manner to the decomposition of the solution u of (7.4.13). Thus $U = Y + Z$, where Y is the solution of the following problem

$$\begin{cases} \left(\delta_t + \mathbb{L}_\varepsilon^N\right) Y(x_i,t_n) = -b_{i,n}Y(x_i,t_{n-p}) + f, \quad (x_i,t_n) \in \overline{G}_2^{N,\Delta t}, \\ Y(x_i,t_n) = U_1(x_i,t_n), \quad (x_i,t_n) \in \overline{G}_1^{N,\Delta t}, \\ Y(0,t_n) = y(0,t_n), \quad Y(1,t_n) = y(1,t_n) \quad t_n \in \overline{\Lambda}_{2,t}^p. \end{cases}$$

From the above equation the singular component Z satisfies

$$\begin{cases} \left(\delta_t + \mathbb{L}_\varepsilon^N\right) Z(x_i,t_n) = -b_{i,n}Z(x_i,t_{n-p}), \quad (x_i,t_n) \in \overline{G}_2^{N,\Delta t}, \\ Z(x_i,t_n) = 0, \quad (x_i,t_n) \in \overline{G}_1^{N,\Delta t}, \\ Z(0,t_n) = 0, \quad Z(1,t_n) = \phi_r(t_n) - y(1,t_n) \quad t_n \in \overline{\Lambda}_{2,t}^p. \end{cases}$$

Therefore, the error at the node (x_i,t_n) can be written in the following way

$$(U-u)(x_i,t_n) = (Y-y)(x_i,t_n) + (Z-z)(x_i,t_n),$$

thus

$$|(U-u)(x_i,t_n)| \le |(Y-y)(x_i,t_n)| + |(Z-z)(x_i,t_n)|,$$

from the above inequality it is enough to bound the error of the regular and the singular components with an optimal bound. The truncation error of the regular component can be written as

$$\begin{aligned} \left(\delta_t + \mathbb{L}_\varepsilon^N\right)(Y-y) &= -b_{i,n}Y(x_i,t_{n-p}) + f - \left(\delta_t + \mathbb{L}_\varepsilon^N\right) y \\ &= b_{i,n}\left(y(x_i,t_{n-p}) - Y(x_i,t_{n-p})\right) + \left(\left(\frac{\partial}{\partial t} + \mathbb{L}_\varepsilon\right) - \left(\delta_t + \mathbb{L}_\varepsilon^N\right)\right) y \\ &= b_{i,n}(u(x_i,t_{n-p}) - U_1(x_i,t_{n-p})) + \left(\left(\frac{\partial}{\partial t} + \mathbb{L}_\varepsilon\right) - \left(\delta_t + \mathbb{L}_\varepsilon^N\right)\right) y, \end{aligned}$$

therefore, we have

$$\left(\delta_t + \mathbb{L}_\varepsilon^N\right)(Y-y) = b_{i,n}\left(u(x_i,t_{n-p}) - U_1(x_i,t_{n-p})\right) - \varepsilon\left(\frac{\partial^2}{\partial x^2} - \delta_x^2\right)y + c_i\left(\frac{\partial}{\partial x} - \delta^-\right)y + \left(\frac{\partial}{\partial t} - \delta_t\right)y.$$

Now applying the modulus on both sides and using (7.4.12), the above equality reduces to

$$\left|\left(\delta_t + \mathbb{L}_\varepsilon^N\right)(Y-y)(x_i,t_n)\right| \le C\left(N^{-1}\ln N + \Delta t\right) + \varepsilon\left|\left(\frac{\partial^2}{\partial x^2} - \delta_x^2\right)y\right| + \left|\left(\frac{\partial}{\partial x} - \delta^-\right)y\right| + \left|\left(\frac{\partial}{\partial t} - \delta_t\right)y\right|.$$

Using the Taylor series expansions it is easy to show that

$$\left|\left(\delta_t + \mathbb{L}_\varepsilon^N\right)(Y-y)(x_i,t_n)\right| \le C\left(N^{-1}\ln N + \Delta t + (h_{i+1}+h_i)^2\varepsilon\left\|\frac{\partial^4 y}{\partial x^4}\right\|_\infty + h_i\left\|\frac{\partial^2 y}{\partial x^2}\right\|_\infty + \Delta t\left\|\frac{\partial^2 y}{\partial t^2}\right\|_\infty\right).$$

Applying Lemma 7.4.1 and the estimates for the derivatives in (7.2.5), we obtain

$$\left|\left(\delta_t + \mathbb{L}_\varepsilon^N\right)(Y-y)(x_i,t_n)\right| \le C(N^{-1}\ln N + \Delta t), \quad \text{for } (x_i,t_n) \in \overline{G}_2^{N,\Delta t}.$$

Now using the fact that the discrete operator $\left(\delta_t + \mathbb{L}_\varepsilon^N\right)$ satisfies the discrete maximum principle and the inverse operator is uniformly bounded, the above inequality can be reduced to

$$|(Y-y)(x_i,t_n)| \le C(N^{-1}\ln N + \Delta t), \quad \text{for } (x_i,t_n) \in \overline{G}_2^{N,\Delta t}. \tag{7.4.15}$$

Consider the error in the singular component Z,

$$\left(\delta_t + \mathbb{L}_\varepsilon^N\right)(Z-z) = \left(\left(\frac{\partial}{\partial t} + \mathbb{L}_\varepsilon\right) - \left(\delta_t + \mathbb{L}_\varepsilon^N\right)\right)z = -\varepsilon\left(\frac{\partial^2}{\partial x^2} - \delta_x^2\right)z + \left(\frac{\partial}{\partial t} - \delta_t\right)z.$$

Applying the modulus on both sides and using the Taylor series expansions on time, we obtain

$$\begin{aligned}\left|\left(\delta_t + \mathbb{L}_\varepsilon^N\right)(Z-z)\right| &\le C\left(N^{-1}\ln N + \Delta t + \varepsilon\left|\left(\frac{\partial^2}{\partial x^2} - \delta_x^2\right)z\right| + \left|\left(\frac{\partial}{\partial x} - \delta^-\right)z\right| + \Delta t\left\|\frac{\partial^2 z}{\partial t^2}\right\|_\infty\right)\\ &\le C\left(N^{-1}\ln N + \Delta t + \varepsilon\left|\left(\frac{\partial^2}{\partial x^2} - \delta_x^2\right)z\right| + \left|\left(\frac{\partial}{\partial x} - \delta^-\right)z\right|\right).\end{aligned}$$

By fixing t, the lateral part of the above inequality can be seen as the truncation error of the convection-diffusion two-point boundary-value problem. By this observation the truncation error in space can be analyzed the same way as the two-point convection-diffusion boundary-value problems, hence we obtain

$$|\left(\delta_t + \mathbb{L}_\varepsilon^N\right)(Z-z)(x_i,t_n)| \leq C(N^{-1}\ln N + \Delta t), \quad (x_i,t_n) \in \overline{G}_2^{N,\Delta t}. \tag{7.4.16}$$

Now using the fact that the discrete operator $\left(\delta_t + \mathbb{L}_\varepsilon^N\right)$ satisfies discrete maximum principle and the inverse operator is uniformly bounded, the above inequality can be reduced to

$$|(Z-z)(x_i,t_n)| \leq C(N^{-1}\ln N + \Delta t), \quad \text{for } (x_i,t_n) \in \overline{G}_2^{N,\Delta t}. \tag{7.4.17}$$

Combining (7.4.15) and (7.4.17) completes the proof on the second interval $[\tau, 2\tau]$ similarly, we can prove the estimate of the successive intervals in temporal direction. ∎

7.5 Numerical Results

In this section, we shall present the numerical results obtained by the discrete scheme (7.3.4) for two test problems on the rectangular mesh $\overline{G}^{N,\Delta t} = \overline{\Omega}_x^N \times \overline{\Lambda}_t^M$. In all the cases, we perform the numerical experiments by choosing the constant $\rho_0 = 2.2$. Moreover, in all the tables we begin with $N = 16$ and the time step $\Delta t = 0.1$ and we multiply N by two and divide Δt by two.

Example 7.5.1. *Consider the following delay parabolic initial-boundary-value problem:*

$$\begin{cases} u_t - \varepsilon u_{xx} + (1 + x(1-x))u_x = u(x,t-1) + f(x,t), \quad (x,t) \in (0,1)\times(0,2], \\ u(x,t) = u_0(x,t), \quad (x,t) \in [0,1]\times[-1,0], \\ u(0,t) = 0, \quad u(1,t) = 0, \quad 0 \leq t \leq 2. \end{cases} \tag{7.5.1}$$

We choose the initial data $u_0(x,t)$ and the source function $f(x,t)$ to fit with the exact solution

$$u(x,t) = \exp(-t)(C_1 + C_2 x - \exp(-(1-x)\varepsilon)),$$

where $C_1 = \exp(-1/\varepsilon)$, and $C_2 = 1 - \exp(-1/\varepsilon)$. As the exact solution of the problem (7.5.1) is known, for each ε, we calculate the maximum point-wise error by

$$e_\varepsilon^{N,\Delta t} = \max_{(x_i,t_n)\in\overline{G}^{N,\Delta t}} |u(x_i,t_n) - U(x_i,t_n)|,$$

where $u(x_i,t_n)$ and $U(x_i,t_n)$ respectively, denote the exact and the numerical solution obtained on the mesh with N mesh intervals in the spatial direction and M mesh intervals

in the $t-$direction such that $\Delta t = T/M$ is the uniform time step. In addition, we determine the corresponding rate of convergence by

$$p_{\varepsilon}^{N,\Delta t} = \log_2 \left(\frac{e_{\varepsilon}^{N,\Delta t}}{e_{\varepsilon}^{2N,\Delta t/2}} \right).$$

Now, for each N and Δt, we define $e^{N,\Delta t} = \max_{\varepsilon} e_{\varepsilon}^{N,\Delta t}$ as the ε-uniform maximum point-wise error and the corresponding ε-uniform rate of convergence is defined by

$$p^{N,\Delta t} = \log_2 \left(\frac{e^{N,\Delta t}}{e^{2N,\Delta t/2}} \right).$$

The calculated maximum point-wise errors $e_{\varepsilon}^{N,\Delta t}$, $e^{N,\Delta t}$; and the corresponding rate of convergence $p_{\varepsilon}^{N,\Delta t}$, $p^{N,\Delta t}$ for Example 7.5.1 are given in Table 7.1. From these results one can observe that the numerical solution is ε-uniform first-order convergence up to a logarithmic factor. Table 7.2 shows the maximum point-wise errors and corresponding rate of convergence for outside the layer. From the Table 7.2, we observe that convergence of the error corresponding to the regular part is close to first-order. From the results given in the Tables we see the monotonically decreasing behavior of the computed ε-uniform errors. This ensures that the proposed scheme is ε-uniform convergent.

The maximum point-wise error of Example 7.5.1 is plotted in Figures 7.1 (a) and (b) for domain G and out-side the layer, respectively in the log-log scale. From these figures one can observe the error is ε-uniform first-order convergence up to a logarithmic factor also it gives close to first-order outside the layer.

Example 7.5.2. *Consider the following singularly perturbed delay parabolic PDE:*

$$\begin{cases} u_t - \varepsilon u_{xx} + (2-x^2)u_x + (x+1)(t+1)u = u(x,t-1) + 10t^2 \exp(-t)x(1-x), \\ \qquad\qquad\qquad\qquad\qquad\qquad\qquad\qquad\qquad\qquad (x,t) \in (0,1)\times(0,2] \\ u(x,t) = 0, \quad (x,t) \in [0,1]\times[-1,0], \\ u(0,t) = 0, \quad u(1,t) = 0, \quad 0 \le t \le 2. \end{cases} \tag{7.5.2}$$

As the exact solution of the problem (7.5.2) is not known, to obtain the accuracy of the numerical solution and also to demonstrate the $\varepsilon-$uniform convergence of the proposed scheme, we use the double mesh principle which is described as follows:

Let $\widetilde{U}^{2N,\Delta t/2}(x_i,t_n)$ be the numerical solution obtained on the fine mesh $\widetilde{G}^{2N,\Delta t} = \tilde{\Omega}_x^{2N} \times \tilde{\Lambda}_t^{2M}$ with $2N$ mesh intervals in the spatial direction and $2M$ mesh intervals in the $t-$direction, where $\tilde{\Omega}_x^{2N}$ is a piecewise-uniform Shishkin mesh as like $\overline{\Omega}_x^N$ with the transition parameter $\tilde{\rho}$ given by

$$\widetilde{\rho} = \min\left\{ \frac{1}{2}, \rho_0 \varepsilon \ln\left(\frac{N}{2}\right) \right\}$$

Table 7.1: *Maximum point-wise error of the solution* $e_\varepsilon^{N,\Delta t}$ *and its rate of convergence* $p_\varepsilon^{N,\Delta t}$ *for Example* 7.5.1 *using the Shishkin mesh.*

	Number of Intervals N/Time Step Size Δt					
ε	$16/\frac{1}{10}$	$32/\frac{1}{20}$	$64/\frac{1}{40}$	$128/\frac{1}{80}$	$256/\frac{1}{160}$	$512/\frac{1}{320}$
2^{0}	1.9820e-03	1.0306e-03	5.2509e-04	2.6510e-04	1.3319e-04	6.6756e-05
	0.9435	0.9728	0.9860	0.9931	0.9965	
2^{-2}	2.3564e-02	1.2679e-02	6.5647e-03	3.3417e-03	1.6863e-03	8.4703e-04
	0.8942	0.9496	0.9742	0.9867	0.9934	
2^{-4}	7.5770e-02	5.5323e-02	3.1810e-02	1.6766e-02	8.6243e-03	4.3759e-03
	0.4537	0.7984	0.9239	0.9591	0.9788	
2^{-6}	8.8018e-02	6.3710e-02	4.1269e-02	2.5411e-02	1.4965e-02	8.5827e-03
	0.4663	0.6265	0.6996	0.7639	0.8021	
2^{-8}	9.4589e-02	6.8359e-02	4.4419e-02	2.7288e-02	1.6078e-02	9.2150e-03
	0.4685	0.6220	0.7029	0.7632	0.8030	
2^{-10}	9.6841e-02	7.0153e-02	4.5748e-02	2.8085e-02	1.6550e-02	9.4839e-03
	0.4651	0.6168	0.7039	0.7630	0.8032	
2^{-12}	9.7396e-02	7.0964e-02	4.6232e-02	2.8377e-02	1.6719e-02	9.5805e-03
	0.4568	0.6182	0.7042	0.7632	0.8033	
2^{-14}	9.7801e-02	7.1219e-02	4.6422e-02	2.8492e-02	1.6780e-02	9.6136e-03
	0.4576	0.6175	0.7042	0.7638	0.8036	
2^{-16}	9.8083e-02	7.1592e-02	4.6513e-02	2.8522e-02	1.6807e-02	9.6240e-03
	0.4542	0.6222	0.7056	0.7630	0.8043	
2^{-18}	9.8154e-02	7.1686e-02	4.6647e-02	2.8557e-02	1.6811e-02	9.6312e-03
	0.4534	0.6199	0.7079	0.7644	0.8036	
2^{-20}	9.8172e-02	7.1710e-02	4.6680e-02	2.8596e-02	1.6822e-02	9.6319e-03
	0.4531	0.6194	0.7070	0.7655	0.8044	
2^{-22}	9.8177e-02	7.1715e-02	4.6689e-02	2.8606e-02	1.6834e-02	9.6350e-03
	0.4531	0.6192	0.7068	0.7650	0.8050	
2^{-24}	9.8178e-02	7.1717e-02	4.6691e-02	2.8608e-02	1.6836e-02	9.6383e-03
	0.4531	0.6192	0.7067	0.7649	0.8047	
2^{-26}	9.8178e-02	7.1717e-02	4.6691e-02	2.8609e-02	1.6837e-02	9.6392e-03
	0.4531	0.6192	0.7067	0.7648	0.8047	
2^{-28}	9.8178e-02	7.1717e-02	4.6691e-02	2.8609e-02	1.6837e-02	9.6394e-03
	0.4531	0.6192	0.7067	0.7648	0.8047	
$e^{N,\Delta t}$	9.8178e-02	7.1717e-02	4.6691e-02	2.8609e-02	1.6837e-02	9.6394e-03
$p^{N,\Delta t}$	0.4531	0.6192	0.7067	0.7648	0.8047	

Table 7.2: *Maximum point-wise error of the solution* $e_\varepsilon^{N,\Delta t}$ *and its rate of convergence* $p_\varepsilon^{N,\Delta t}$ *for Example* 7.5.1 *for outside the layer using the Shishkin mesh.*

	Number of Intervals N/Time Step Size Δt					
ε	$16/\frac{1}{10}$	$32/\frac{1}{20}$	$64/\frac{1}{40}$	$128/\frac{1}{80}$	$256/\frac{1}{160}$	$512/\frac{1}{320}$
2^{0}	1.8104e-03	9.7161e-04	5.0205e-04	2.5505e-04	1.2852e-04	6.4509e-05
	0.8979	0.9525	0.9771	0.9888	0.9944	
2^{-2}	1.1799e-02	6.7909e-03	3.6401e-03	1.8842e-03	9.5858e-04	4.8345e-04
	0.797	0.8996	0.95	0.975	0.9875	
2^{-4}	7.6665e-04	2.7967e-04	1.5236e-04	7.9541e-05	4.0636e-05	2.0540e-05
	1.4548	0.8762	0.9377	0.9689	0.9843	
2^{-6}	1.6566e-03	1.0185e-03	5.5801e-04	2.9198e-04	1.4433e-04	6.9417e-05
	0.7018	0.8681	0.9344	1.0165	1.0560	
2^{-8}	2.2596e-03	1.3360e-03	7.3218e-04	3.8215e-04	1.9436e-04	9.7402e-05
	0.7582	0.8676	0.9381	0.9754	0.9967	
2^{-10}	2.6170e-03	1.4881e-03	7.9665e-04	4.1219e-04	2.0945e-04	1.0545e-04
	0.8144	0.9015	0.9506	0.9767	0.9900	
2^{-12}	2.7142e-03	1.5307e-03	8.1498e-04	4.2078e-04	2.1376e-04	1.0770e-04
	0.8264	0.9093	0.9537	0.9771	0.9890	
2^{-14}	2.7391e-03	1.5416e-03	8.1974e-04	4.2302e-04	2.1489e-04	1.0829e-04
	0.8292	0.9112	0.9544	0.9771	0.9887	
2^{-16}	2.7453e-03	1.5444e-03	8.2094e-04	4.2359e-04	2.1518e-04	1.0844e-04
	0.8299	0.9117	0.9546	0.9771	0.9886	
2^{-18}	2.7469e-03	1.5451e-03	8.2124e-04	4.2373e-04	2.1525e-04	1.0848e-04
	0.8301	0.9118	0.9546	0.9771	0.9886	
2^{-20}	2.7473e-03	1.5453e-03	8.2132e-04	4.2377e-04	2.1527e-04	1.0849e-04
	0.8301	0.9119	0.9547	0.9771	0.9886	
2^{-22}	2.7474e-03	1.5453e-03	8.2133e-04	4.2378e-04	2.1527e-04	1.0849e-04
	0.8301	0.9119	0.9547	0.9771	0.9886	
2^{-24}	2.7474e-03	1.5453e-03	8.2134e-04	4.2378e-04	2.1528e-04	1.0849e-04
	0.8301	0.9119	0.9547	0.9771	0.9886	
2^{-26}	2.7474e-03	1.5453e-03	8.2134e-04	4.2378e-04	2.1528e-04	1.0849e-04
	0.8301	0.9119	0.9547	0.9771	0.9886	
2^{-28}	2.7474e-03	1.5453e-03	8.2134e-04	4.2378e-04	2.1528e-04	1.0849e-04
	0.8301	0.9119	0.9547	0.9771	0.9886	
$e^{N,\Delta t}$	2.7474e-03	1.5453e-03	8.2134e-04	4.2378e-04	2.1528e-04	1.0849e-04
$p^{N,\Delta t}$	0.8301	0.9119	0.9547	0.9771	0.9886	

such that for $i = 0, 1 \ldots, N$, the ith point of the mesh $\overline{\Omega}_x^N$ coincides with the $2i$th point of the mesh $\tilde{\Omega}_x^{2N}$. Then for each ε, we calculate the maximum point-wise error by

$$E_\varepsilon^{N,\Delta t} = \max_{(x_i,t_n)\in\overline{G}^{N,\Delta t}} \left| U^{N,\Delta t}(x_i,t_n) - \widetilde{U}^{2N,\Delta t/2}(x_i,t_n) \right|,$$

and the corresponding rate of convergence by

$$P_\varepsilon^{N,\Delta t} = \log_2 \left(\frac{E_\varepsilon^{N,\Delta t}}{E_\varepsilon^{2N,\Delta t/2}} \right).$$

For each N and Δt, the quantities $E^{N,\Delta t}$ and $P^{N,\Delta t}$ are defined analogously to $e^{N,\Delta t}$ and $p^{N,\Delta t}$ based on the error $E_\varepsilon^{N,\Delta t}$ as in the previous example.

The calculated maximum point-wise errors $E_\varepsilon^{N,\Delta t}$ and the corresponding rate of convergence $P_\varepsilon^{N,\Delta t}$ for Example 7.5.2 are given in Table 7.3. The numerical results given in these tables reveal the first-order up-to a logarithmic factor convergence independent of the diffusion parameter ε. Table 7.4 shows the maximum point-wise errors and corresponding rate of convergence for outside the layer. Here also we can observe the same behavior as like Example 7.5.1.

The numerical solution of Example 7.5.2 is plotted in Figures 7.2 (a) and (b) for $\varepsilon = 2e-4$ and $\varepsilon = 2e-20$, respectively. These figures show the existence of the boundary layer along $x = 1$. The maximum point-wise error of Example 7.5.2 is plotted in Figures 7.3 (a) and (b) for domain G and out-side the layer, respectively, in the log-log scale. From these figures one can observe that the error is ε-uniform first-order convergence up-to a logarithmic factor also it gives close to first-order outside the layer.

7.6 Conclusions

In this chapter, we have solved the singularly perturbed parabolic delay convection-diffusion problem (7.1.1) numerically by the backward-Euler scheme for the time derivative and upwind finite difference scheme for the spatial derivative on layer-adapted piecewise-uniform mesh. The truncation errors are obtained and the stability analysis is carried out. The proposed numerical scheme is of first-order uniform convergence in time and first-order up-to a logarithmic factor in space, *i.e.*, $O(\Delta t + N^{-1} \ln N)$. Error estimates are derived for the numerical scheme, which are independent of the diffusion parameter ε. Numerical results are carried out to verify the theoretical error estimates.

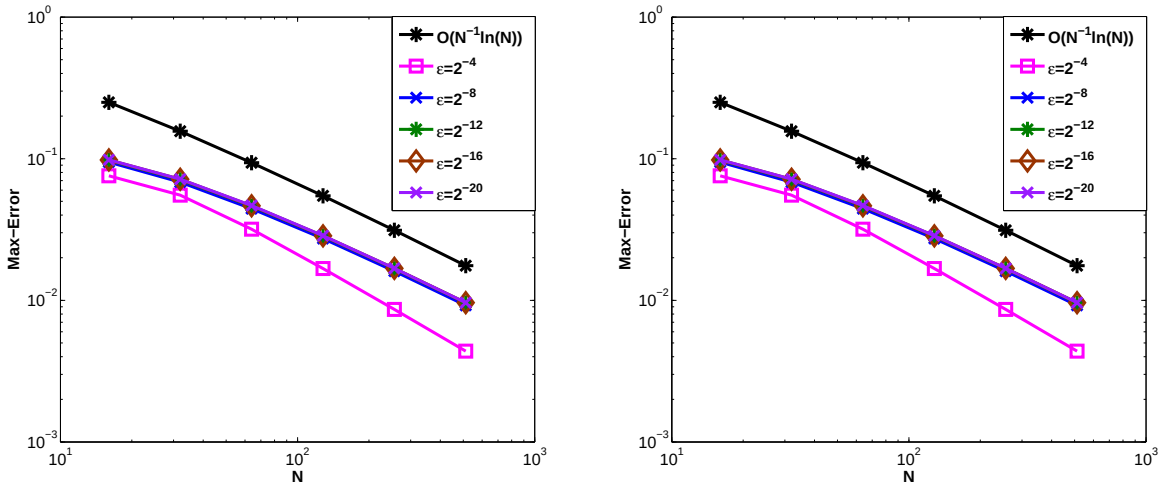

(a) *Maximum point-wise error.* (b) *Maximum point-wise error for outside the layer.*

Figure 7.1: *Loglog plot of maximum point-wise error of the solution* $e_{\varepsilon}^{N,\Delta t}$ *of 7.5.1.*

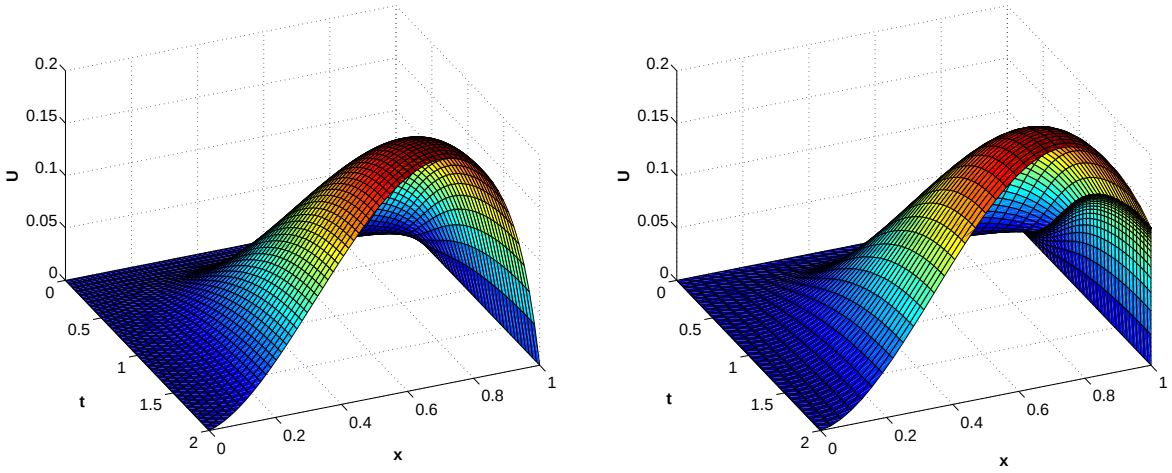

(a) $\varepsilon = 2^{-4}$. (b) $\varepsilon = 2^{-20}$.

Figure 7.2: *Numerical solution of Example 7.5.2 for* $N = 64$ *and* $\Delta t = 0.1$.

Table 7.3: *Maximum point-wise error of the solution* $E_{\varepsilon}^{N,\Delta t}$ *and its rate of convergence* $P_{\varepsilon}^{N,\Delta t}$ *for Example* 7.5.2 *using the Shishkin mesh.*

	Number of Intervals N/Time Step Size Δt					
ε	$16/\frac{1}{10}$	$32/\frac{1}{20}$	$64/\frac{1}{40}$	$128/\frac{1}{80}$	$256/\frac{1}{160}$	$512/\frac{1}{320}$
2^{0}	1.3798e-03	7.6767e-04	4.0315e-04	2.0659e-04	1.0454e-04	5.2587e-05
	0.8459	0.9292	0.9646	0.9827	0.9913	
2^{-2}	4.8025e-03	2.6325e-03	1.3779e-03	7.0520e-04	3.5679e-04	1.7944e-04
	0.8673	0.934	0.9664	0.983	0.9916	
2^{-4}	8.2642e-03	5.5889e-03	3.2765e-03	1.7433e-03	9.0054e-04	4.5791e-04
	0.5643	0.7704	0.9103	0.9530	0.9757	
2^{-6}	1.1582e-02	6.8349e-03	3.9841e-03	2.3059e-03	1.3070e-03	7.2916e-04
	0.7609	0.7786	0.7890	0.8191	0.8419	
2^{-8}	1.4765e-02	8.8375e-03	5.1378e-03	2.9210e-03	1.6270e-03	8.9215e-04
	0.7405	0.7825	0.8147	0.8443	0.8668	
2^{-10}	1.5768e-02	9.6492e-03	5.6471e-03	3.2195e-03	1.7948e-03	9.8368e-04
	0.7085	0.7729	0.8107	0.8430	0.8676	
2^{-12}	1.6031e-02	9.8736e-03	5.8009e-03	3.3117e-03	1.8467e-03	1.0128e-03
	0.6992	0.7673	0.8087	0.8426	0.8666	
2^{-14}	1.6097e-02	9.9311e-03	5.8407e-03	3.3358e-03	1.8603e-03	1.0205e-03
	0.6968	0.7658	0.8081	0.8424	0.8662	
2^{-16}	1.6114e-02	9.9456e-03	5.8507e-03	3.3418e-03	1.8638e-03	1.0226e-03
	0.6962	0.7654	0.8080	0.8424	0.8661	
2^{-18}	1.6118e-02	9.9492e-03	5.8532e-03	3.3434e-03	1.8647e-03	1.0231e-03
	0.6960	0.7654	0.8079	0.8424	0.8660	
2^{-20}	1.6119e-02	9.9501e-03	5.8538e-03	3.3438e-03	1.8649e-03	1.0232e-03
	0.6960	0.7653	0.8079	0.8424	0.8660	
2^{-22}	1.6119e-02	9.9504e-03	5.8540e-03	3.3438e-03	1.8649e-03	1.0232e-03
	0.6960	0.7653	0.8079	0.8424	0.8660	
2^{-24}	1.6119e-02	9.9504e-03	5.8540e-03	3.3439e-03	1.8650e-03	1.0232e-03
	0.6960	0.7653	0.8079	0.8424	0.8660	
2^{-26}	1.6119e-02	9.9504e-03	5.8540e-03	3.3439e-03	1.8650e-03	1.0232e-03
	0.6960	0.7653	0.8079	0.8424	0.8660	
2^{-28}	1.6119e-02	9.9504e-03	5.8541e-03	3.3439e-03	1.8650e-03	1.0232e-03
	0.6960	0.7653	0.8079	0.8424	0.8660	
$E^{N,\Delta t}$	1.6119e-02	9.9504e-03	5.8541e-03	3.3439e-03	1.8650e-03	1.0232e-03
$P^{N,\Delta t}$	0.6960	0.7653	0.8079	0.8424	0.8660	

Table 7.4: *Maximum point-wise error of the solution* $E_\varepsilon^{N,\Delta t}$ *and its rate of convergence* $P_\varepsilon^{N,\Delta t}$ *for Example* 7.5.2 *for outside the layer using the Shishkin mesh.*

	Number of Intervals N/Time Step Size Δt					
ε	$16/\frac{1}{10}$	$32/\frac{1}{20}$	$64/\frac{1}{40}$	$128/\frac{1}{80}$	$256/\frac{1}{160}$	$512/\frac{1}{320}$
2^0	1.3194e-03	7.3489e-04	3.8707e-04	1.9854e-04	1.0054e-04	5.0587e-05
	0.8443	0.925	0.9631	0.9817	0.9909	
2^{-2}	2.4266e-03	1.3160e-03	6.8500e-04	3.4943e-04	1.7646e-04	8.8672e-05
	0.8828	0.9419	0.9711	0.9856	0.9928	
2^{-4}	3.7522e-03	1.7325e-03	8.5664e-04	4.3521e-04	2.1935e-04	1.1012e-04
	1.1149	1.0161	0.9770	0.9885	0.9942	
2^{-6}	1.0737e-02	5.1429e-03	2.4003e-03	1.0997e-03	4.9382e-04	2.3702e-04
	1.0619	1.0994	1.1261	1.1550	1.0590	
2^{-8}	1.3440e-02	7.0683e-03	3.5901e-03	1.7996e-03	9.0150e-04	4.4710e-04
	0.9271	0.9773	0.9963	0.9973	1.0117	
2^{-10}	1.4108e-02	7.5935e-03	3.9240e-03	1.9943e-03	1.0046e-03	5.0471e-04
	0.8937	0.9524	0.9764	0.9892	0.9932	
2^{-12}	1.4271e-02	7.7270e-03	4.0108e-03	2.0458e-03	1.0337e-03	5.1950e-04
	0.8851	0.9460	0.9712	0.9849	0.9926	
2^{-14}	1.4311e-02	7.7605e-03	4.0327e-03	2.0588e-03	1.0411e-03	5.2358e-04
	0.8829	0.9444	0.9699	0.9837	0.9916	
2^{-16}	1.4321e-02	7.7689e-03	4.0382e-03	2.0621e-03	1.0429e-03	5.2461e-04
	0.8824	0.9440	0.9696	0.9835	0.9913	
2^{-18}	1.4324e-02	7.7710e-03	4.0395e-03	2.0629e-03	1.0434e-03	5.2487e-04
	0.8823	0.9439	0.9695	0.9834	0.9912	
2^{-20}	1.4325e-02	7.7715e-03	4.0399e-03	2.0631e-03	1.0435e-03	5.2493e-04
	0.8822	0.9439	0.9695	0.9834	0.9912	
2^{-22}	1.4325e-02	7.7716e-03	4.0400e-03	2.0631e-03	1.0435e-03	5.2495e-04
	0.8822	0.9439	0.9695	0.9834	0.9912	
2^{-24}	1.4325e-02	7.7717e-03	4.0400e-03	2.0631e-03	1.0435e-03	5.2495e-04
	0.8822	0.9439	0.9695	0.9834	0.9912	
2^{-26}	1.4325e-02	7.7717e-03	4.0400e-03	2.0631e-03	1.0435e-03	5.2495e-04
	0.8822	0.9439	0.9695	0.9834	0.9912	
2^{-28}	1.4325e-02	7.7717e-03	4.0400e-03	2.0631e-03	1.0435e-03	5.2495e-04
	0.8822	0.9439	0.9695	0.9834	0.9912	
$E^{N,\Delta t}$	1.4325e-02	7.7717e-03	4.0400e-03	2.0631e-03	1.0435e-03	5.2495e-04
$P^{N,\Delta t}$	0.8822	0.9439	0.9695	0.9834	0.9912	

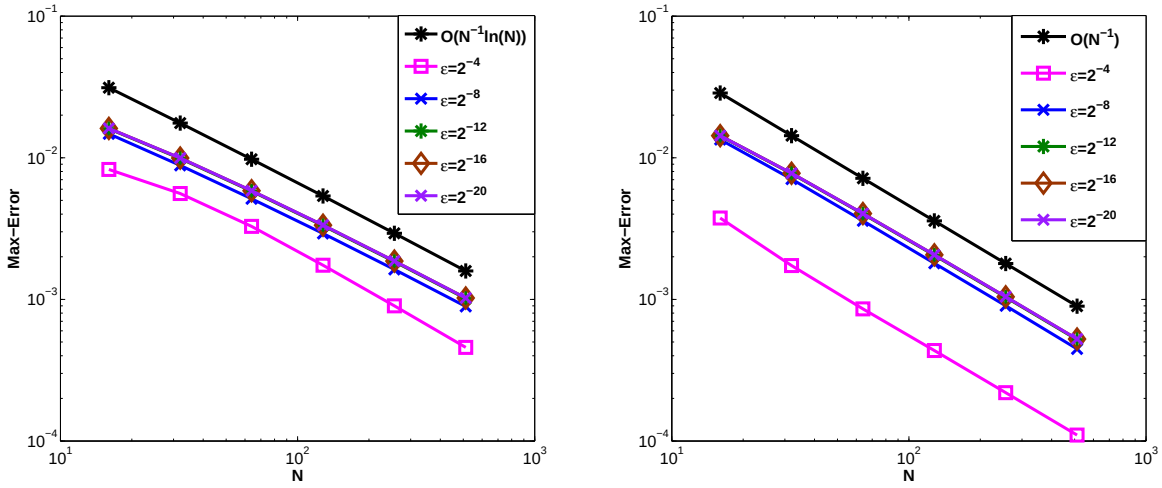

(a) *Maximum point-wise error.* (b) *Maximum point-wise error for outside the layer.*

Figure 7.3: *Loglog plot of maximum point-wise error of the solution* $E_\varepsilon^{N,\Delta t}$ *of Example 7.5.2.*

CHAPTER 8

Summary and Future Scopes

This chapter presents the summary of the results made in this thesis and also presents the techniques used in deriving the results, followed by the future scopes for possible extensions of the present works.

8.1 Summary of the Results

The results of this thesis with some important observations are precisely highlighted below:

- Parameter uniform numerical methods are proposed and analyzed for singularly perturbed parabolic reaction-diffusion problems by the backward-Euler scheme for the time derivative on uniform mesh and the central difference for the spatial derivative on layer-adapted nonuniform meshes obtained equidistributing the monitor function. The monitor function is a positive L^1 integrable function and is a linear combination of the second-order partial derivative with respect to space of the singular component of the solution and its total measure. Numerical algorithm is given to generated adaptive grid iteratively. Numerical experiments are conducted to validate the theoretical error estimates. Numerical results are produced for several linear and semilinear parabolic reaction-diffusion problems. Moreover, the errors in the normalized flux of the exact and the computational solutions are presented in the numerical results section.

- Subsequently, singularly perturbed parabolic convection-diffusion problems are studied using the backward-Euler scheme for the time variable and the upwind finite difference scheme for the spatial variable, because of the fact that the second-order central difference scheme gives non-physical oscillations in the computed solution. The problems are analyzed as like the earlier problem on nonuniform

layer-adapted spatial meshes obtained by equidistributing the monitor function. First, the corresponding semidiscrete problems are studied and subsequently, the fully discrete schemes are studied. The error in the maximum norm is obtained by analyzing the problem in a detailed way. Numerical results of the errors are plotted in the log-log scale to show the convergence rate.

- Then, singularly perturbed PDEs of reaction-diffusion natures are analyzed using modified backward-Euler for the time derivative and central difference for the spatial derivative on adaptive spatial mesh and uniform time mesh. The adaptive spatial meshes are not uniform in the time as like the case of previously discussed nonuniform grids. The equidistributed grids are generated on every time level to allow us to use this technique to a general parabolic problems. The numerical algorithm proposed earlier is modified to tackle the above assumption. Truncation error and the stability analysis are obtained. The parameter-uniform error estimates are derived for the numerical solution. To support the theoretical results, numerical experiments are carried out. Moreover, numerical results of the errors are plotted in the log-log scale to show the convergence rate.

- Next, convection-diffusion parabolic problems are studied using modified backward-Euler finite difference scheme for the time direction on uniform mesh and upwind difference scheme for the spatial direction on layer-adapted nonuniform mesh. The layer-adapted nonuniform meshes are obtained equidistributing the monitor function on every time level. As like the earlier problem the numerical algorithm is modified to adapt to the current assumption. Numerical experiments are conducted to validate the theoretical error estimates. Numerical results are produced for several linear, semilinear and quasilinear parabolic problems. The semilinear (nonlinear) problems are linearized using Newton's linearization process. Moreover, the errors in normalized flux of exact and computational solutions are presented in the numerical results section. Numerical experiments for quasilinear singularly perturbed parabolic problem (the Burger's equation) are produced, which indicates the application to larger class of convection-diffusion problems.

- We proposed a parameter-uniform computational technique to solve singularly perturbed delay parabolic initial-boundary-value problems exhibiting parabolic layers. The domain is discretized with a uniform mesh on the time direction and a nonuniform mesh obtained via equidistribution of a monitor function for the spatial direction. Numerical algorithm is given to generated adaptive grid iteratively. The numerical scheme consists of the implicit-Euler scheme for the time derivative and the classical central difference scheme for the spatial derivative. The proposed

numerical scheme converges in the maximum norm with first-order in temporal variable and second-order in the spatial variable, *i.e.*, $O(\Delta t + N^{-2})$. Error estimates are derived for the numerical scheme, which are independent of the diffusion parameter ε. Numerical results reveal the theoretical error estimate.

- Uniform point-wise convergence for parabolic convection-diffusion problems on the piecewise-uniform Shishkin meshes is studied using the implicit-Euler scheme for the time derivative and upwind difference scheme for the spatial derivative. First, width and location of the boundary layer is calculated using *apriori* information about the problem and the solution. Then, a transition points is fixed using the location and the width of the boundary layer. Afterwards the piecewise-uniform adaptive meshes are computed. We obtain the maximum principle and carry out the stability analysis. The error estimates are derived for the numerical scheme, which are independent of the diffusion parameter, ε. Then we proved the scheme is ε-uniform convergence of first-order in the time and first-order up-to a logarithmic in the space. Numerical experiments are carried out to verify the theoretical error estimates. Appropriately, numerical results of the errors are plotted in the log-log scale to show the convergence rate.

Extensive numerical experiments are conducted to support the theoretical results and also to demonstrate the accuracy of the numerical methods. The corresponding numerical results are presented at the end of each chapter of the thesis. For clarity of the presentation, we have repeatedly described the model problems with suitable information on the given data at the beginning of the subsequent chapters.

8.2 Future Scopes

A brief outline, describing the possible extensions of the present works to be carried out in the future with suitable model problems, are presented below:

In chapter 2 we presented the analysis for a linear reaction-diffusion singularly perturbed IBVP exhibiting boundary layers. The problem is analyzed using backward-Euler difference scheme for the time derivative and central difference for the spatial derivative on a layer-adapted mesh. The numerical schemes is proved to be second-order in the space and first-order in the time. The order of convergence in the time can be increased to two by considering second-order schemes instead of backward-Euler and appropriate analyze can also be done.

Extend the above adaptive method to general (quasilinear and nonlinear) singularly perturbed parabolic reaction-diffusion and convection-diffusion problems where one can't

apply the Shishkin and the Bakhvalov type meshes, by using the equidistribution technique, where we equidistribute the monitor function on each temporal level as discussed in 5. In this approach the grids moves according to the solution for every temporal level. The following are some of the problems we consider,

- **The Burgers' equation:** Burgers' equation is a fundamental partial differential equation from fluid mechanics. It occurs in various areas of applied mathematics, such as modeling of gas dynamics and traffic flow. The Burgers' equation is a nonlinear and one expects to find phenomenon similar to turbulence.

$$\begin{cases} (u_t + uu_x)(x,t) = \varepsilon u_{xx}(x,t), \quad (x,t) \in (0,1) \times (0,T], \\ u(x,0) = f(x), \quad \text{on } S_x = \{(x,0) : 0 \le x \le 1\}, \\ u(0,t) = 0, \quad \text{on } S_0 = \{(0,t) : 0 \le t \le T\}, \\ u(1,t) = 0, \quad \text{on } S_1 = \{(1,t) : 0 \le t \le T\}. \end{cases} \tag{8.2.1}$$

- **The Burger-Huxley equation** The equation describes the interaction between convection, diffusion and reaction and being a nonlinear partial differential equation is of high importance for describing the interaction between reaction mechanisms, convection effects, and diffusion transports. Since there exists no general technique for finding analytical solutions of nonlinear diffusion equations so far, numerical solutions of nonlinear differential equations are of great importance in physical problems. More information about the problem and numerical methods can be found in [31, 58, 79, 22].

$$\begin{cases} u_t + \alpha u u_x = \varepsilon u_{xx} + \beta(1-u)(u-\gamma)u, \quad (x,t) \in (0,1) \times (0,T], \\ u(x,0) = \phi(x), \quad \text{on } S_x = \{(x,0) : 0 \le x \le 1\}, \\ u(0,t) = 0, \quad \text{on } S_0 = \{(0,t) : 0 \le t \le T\}, \\ u(1,t) = 0, \quad \text{on } S_1 = \{(1,t) : 0 \le t \le T\}, \end{cases} \tag{8.2.2}$$

  where $\alpha, \beta \ge 0$, $\gamma \in (0,1)$.

- **General nonlinear problem** It is well-known that the nonlinear equation with a small parameter plays an important role in nonlinear physics. Approximate solutions of nonlinear differential equations are of importance in physical problems. Also it is of great practical interest to study the nonlinear phenomena. So far there exists no general method for finding solutions of nonlinear diffusion equations. In order to solve nonlinear problems various numerical approaches are proposed by

researchers. The method discussed in this thesis can be extended to these types of problems.

$$\begin{cases} u_t - \varepsilon u_{xx} + a(x,t,u)u_x + b(x,t,u) = 0, \quad (x,t) \in (0,1) \times (0,T], \\ u(x,0) = u_0(x), \quad x \in \Omega, \\ u(0,t) = u(1,t) = 0, \quad t \in (0,T]. \end{cases} \tag{8.2.3}$$

Although, the equidistribution technique to interior layer problems are challenging task but it can be done by appropriately altering the numerical algorithm presented in this thesis. Still, proving the optimal uniform convergence in maximum norm is a challenging task.

Analyzing and finding ε-uniform numerical methods to higher-dimensional singularly perturbed parabolic problems and system of singularly perturbed parabolic problems based on adaptive grid. One can possibly extend the method discussed in this thesis to the following 2D singularly perturbed parabolic convection-diffusion IBVP with Dirichlet (or first-type) boundary condition or Robin type boundary conditions on the domain $\mathcal{G} = \mathcal{D} \times (0,T]$, $\mathcal{D} = (0,1)^2$, $\mathbf{x} = (x,y) \in \mathbb{R}^2$:

$$\begin{cases} \dfrac{\partial u}{\partial t}(\mathbf{x},t) + \mathcal{L}_\varepsilon u(\mathbf{x},t) \;=\; f(\mathbf{x},t), \quad (\mathbf{x},t) \in \mathcal{G}, \\ u(\mathbf{x},0) = u_0(\mathbf{x}), \quad \mathbf{x} \in \overline{\mathcal{D}}, \\ u(\mathbf{x},t) = 0, \quad (\mathbf{x},t) \in \partial\mathcal{D} \times (0,T], \end{cases} \tag{8.2.4}$$

where

$$\mathcal{L}_\varepsilon u \;\equiv\; -\varepsilon \triangle u + \mathbf{a}(\mathbf{x}) \cdot \nabla u + b(\mathbf{x})u,$$

$0 < \varepsilon \ll 1$ is a small parameter and the coefficients $\mathbf{a} = (a_1, a_2)$, b are sufficiently smooth functions such that

$$a_i(\mathbf{x}) \geq \alpha_i > 0, \; i = 1,2, \quad b(\mathbf{x}) \geq 0, \quad \text{on } \overline{\mathcal{D}}. \tag{8.2.5}$$

Under sufficient smoothness and necessary compatibility conditions [[45], §4.5] imposed on the functions u_0 and f, the parabolic IBVP (8.2.4)-(8.2.5), admits a unique solution $u(\mathbf{x},t)$ which exhibits a regular boundary layer of width $O(\varepsilon)$ at the sides $x = 1$ and $y = 1$ (see, e.g., [54]). One can see the asymptotic results about this kind of problem in [37].

[1] S. Adjerid and J. E. Flaherty. A moving finite element method with error estimation and refinement for one-dimensional time dependent partial differential equations. *SIAM J. Numer. Anal.*, 23(4):778–796, 1986.

[2] A. R. Ansari, S. A. Bakr, and G. I. Shishkin. A parameter-robust finite difference method for singularly perturbed delay parabolic partial differential equations. *J. Comput. Appl. Math.*, 205(1):552–566, 2007.

[3] A. R. Ansari and A. F. Hegarty. Numerical solution of a convection diffusion problem with Robin boundary conditions. *J. Comput. Appl. Math.*, 156(1):221–238, 2003.

[4] A. S. Bakhvalov. On the optimization of methods for solving boundary value problems with boundary layers. *J. Vychisl. Mat. i Mat. Fiz.*, 9:841–859, 1969.

[5] G. Beckett. *The robust and efficient numerical solution of singularly perturbed boundary value problem using grid adaptivity.* PhD thesis. Department of Mathematics, University of Strathclyde, UK, 1998.

[6] G. Beckett and J. A. Mackenzie. Convergence analysis of finite difference approximations on equidistributed grids to a singularly perturbed boundary value problem. *Appl. Numer. Math.*, 35(2):87–109, 2000.

[7] G. Beckett and J. A. Mackenzie. On a uniformly accurate finite difference approximation of a singularly perturbed reaction-diffusion problem using grid equidistribution. *J. Comput. Appl. Math.*, 131(1-2):381–405, 2001.

[8] G. Beckett, J. A. Mackenzie, A. Ramage, and D. M. Sloan. On the numerical soltuion of one-dimensional pdes using adaptive methods based on equidistribution. *J. Comp. Phys.*, 167(2):372–392, 2001.

[9] S. C. Brenner and L. R. Scott. *The Mathematical Theory of Finite Element Methods.* Texts in Applied Mathematics. Springer, New York, 2008.

[10] C. J. Budd, W. Huang, and R. D. Russell. Adaptivity with moving grids. *Acta Numer.*, 18:111–241, 2009.

[11] A. W. Bush. *Perturbation Methods for Engineers and Scientists.* CRC Press, London, 1992.

[12] Y. Chen. Uniform pointwise convergence for a singularly perturbed problem using arc-length equidistribution. *J. Comput. Appl. Math.*, 159(1):25–34, 2003.

[13] P. Ciarlet and J. Lions, editors. *Handbook of Numerical Analysis.* North-Holland, Amsterdam, 1990.

[14] C. Clavero and J. L. Gracia. A high order HODIE finite difference scheme for 1D parabolic singularly perturbed reaction-diffusion problems. *Appl. Math. Comput.*, 218(9):5067–5080, 2012.

[15] C. Clavero, J. L. Gracia, and J. C. Jorge. High-order numerical methods for one-dimensional parabolic singularly perturbed problems with regular layers. *Numer. Methods Partial Differential Equations*, 21(1):148–169, 2005.

[16] C. Clavero, J. L. Gracia, and J. C. Jorge. A uniformly convergence alternating direction HODIE finite difference scheme for 2D time-dependent convection-diffusion problems. *IMA J. Numer. Anal.*, 26(1):155–172, 2006.

[17] C. Clavero, J. L. Gracia, and M. Stynes. A simpler analysis of a hybrid numerical method for time-dependent convection-diffusion problems. *J. Comput. Appl. Math.*, 235(17):5240–5248, 2011.

[18] C. Clavero, J. C. Jorge, and F. Lisbona. A uniformly convergent scheme on a nonuniform mesh for convection-diffusion parabolic problems. *J. Comput. Appl. Math.*, 154(2):415–429, 2003.

[19] E. P. Doolan, J. J. H. Miller, and W. H. A. Schilders. *Uniform Numerical Methods for Problems with Initial and Boundary Layers*. Boole Press, Dún Laoghaire, 1980.

[20] W. Eckhaus. *Asymptotic Analysis of Singular Perturbations*. Studies in Mathematics and its Applications. North-Holland Publishing Co., Amsterdam, 1979.

[21] P. A. Farrell, A. F. Hegarty, J. J. H. Miller, E. O'Riordan, and G. I. Shishkin. *Robust Computational Techniques for Boundary Layers*. Applied Mathematics.

[22] Z. Feng, J. Tian, S. Zheng, and H. Lu. Travelling wave solutions of the Burgers-Huxley equation. *IMA J. Appl. Math.*, 77(3):316–325, 2012.

[23] S. Franz and T. Linß. Superconvergence analysis of the Galerkin FEM for a singularly perturbed convection-diffusion problem with characteristic layers. *Numer. Methods Partial Differential Equations*, 24(1):144–164, 2008.

[24] S. Franz, F. Liu, H.-G. Roos, M. Stynes, and A. Zhou. The combination technique for a two-dimensional convection-diffusion problem with exponential layers. *Appl. Math.*, 54(3):203–223, 2009.

[25] K. Friedrichs and W. Wasow. Singular perturbations of nonlinear oscillations. *Duke Math. J.*, **13**:367–381, 1946.

[26] M. J. Gander and R. D. Haynes. Domain decomposition approaches for mesh generation via the equidistribution principle. *SIAM J. Numer. Anal.*, 50(4):2111–2135, 2012.

[27] S. Gowrisankar and S. Natesan. Uniformly convergent numerical method for singularly perturbed parabolic initial-boundary-value problems with equidistributed grids. *Int. J. Comput. Math.*, 2013.

[28] J. L. Gracia and C. Clavero. A compact finite difference scheme for 2D reaction-diffusion singularly perturbed problems. *J. Comput. Appl. Math.*, 192(1):152–167, 2006.

[29] J. L. Gracia and E. O'Riordan. A singularly perturbed convection-diffusion problem with a moving interior layer. *Int. J. Numer. Anal. Model.*, 9(4):823–843, 2012.

[30] J. L. Gracia and E. O'Riordan. A singularly perturbed parabolic problem with a layer in the initial condition. *Appl. Math. Comput.*, 219(2):498–510, 2012.

[31] V. Gupta and M. K. Kadalbajoo. A singular perturbation approach to solve Burgers-Huxley equation via monotone finite difference scheme on layer-adaptive mesh. *Commun. Nonlinear Sci. Numer. Simul.*, 16(4):1825–1844, 2011.

[32] W. Huang, Y. Ren, and R. Russell. Moving mesh partial differential equations (MMPDES) based on the equidistribution principle. *SIAM J. Numer. Anal.*, 31(3), 1994.

[33] W. Huang, Y. Ren, and R. D. Russell. Moving mesh partial differential equations (MMPDES) based on the equidistribution principle. *SIAM J. Numer. Anal.*, 31(3):709–730, 1994.

[34] W. Huang and R. D. Russell. Analysis of moving mesh partial differential equations with spatial smoothing. *SIAM J. Numer. Anal.*, 34(3):1106–1126, 1997.

[35] W. Huang and R. D. Russell. *Adaptive Moving Mesh Methods*. Applied Mathematical Sciences. Springer, New York, 2011.

[36] C. Johnson. *Numerical Solution of Partial Differential Equations by The Finite Element Method*. Dover Publications Inc., Mineola, NY, 2009.

[37] R. Kellogg and S. Shih. Asymptotic analysis of a singular perturbation problem. *SIAM J. Math. Anal.*, **18**(5):1467–1511, 1987.

[38] R. Kellogg and A. Tsan. Analysis of some differences approximations for a singular perturbation problem without turning point. *Math. Comp.*, **32**(144):1025–1039, 1978.

[39] J. Kevorkian and J. D. Cole. *Multiple Scale and Singular Perturbation Methods*. Applied Mathematical Sciences. Springer-Verlag, New York, 1996.

[40] A. Q. M. Khaliq, B. Wade, M. Yousuf, and J. Vigo-Aguiar. High order smoothing schemes for inhomogeneous parabolic problems with applications in option pricing. *Numer. Methods Partial Differential Equations*, **23**(5):1249–1276, 2007.

[41] N. Kopteva. Maximum norm a posteriori error estimates for a 1D singularly perturbed semilinear reaction-diffusion problem. *IMA J. Numer. Anal.*, 27(3):576–592, 2007.

[42] N. Kopteva, N. Madden, and M. Stynes. Grid equidistribution for reaction-diffusion problems in one dimension. *Numer. Algorithms*, 40(3):305–322, 2005.

[43] N. Kopteva and M. Stynes. A robust adaptive method for a quasi-linear one-dimensional convection-diffusion problem. *SIAM J. Numer. Anal.*, 39(4):1446–1467 (electronic), 2001.

[44] N. Kopteva and M. Stynes. Stabilised approximation of interior-layer solutions of a singularly perturbed semilinear reaction-diffusion problem. *Numer. Math.*, 119(4):787–810, 2011.

[45] O. A. Ladyženskaja, V. A. Solonnikov, and N. N. Ural′ceva. *Linear and Quasilinear Equations of Parabolic Type*. American Mathematical Society, Providence, R.I., 1968.

[46] P. A. Lagerstrom. *Matched Asymptotic Expansions*, volume 76 of *Applied Mathematical Sciences*. Springer-Verlag, New York, 1988. Ideas and techniques.

[47] T. Linß. Uniform pointwise convergence of finite difference schemes using grid equidistribution. *Computing*, 66(1):27–39, 2001.

[48] T. Linß. Sufficient conditions for uniform convergence on layer-adapted meshes for one-dimensional reaction-diffusion problems. *Numer. Algorithms*, 40(1):23–32, 2005.

[49] T. Linß. Layer-adapted meshes and FEM for time-dependent singularly perturbed reaction-diffusion problems. *Int. J. Comput. Sci. Math.*, 1(2-4):259–270, 2007.

[50] T. Linß and N. Madden. Parameter uniform approximations for time-dependent reaction-diffusion problems. *Numer. Methods Partial Differential Equations*, 23(6):1290–1300, 2007.

[51] T. Linß, G. Radojev, and H. Zarin. Approximation of singularly perturbed reaction-diffusion problems by quadratic C^1-splines. *Numer. Algorithms*, 61(1):35–55, 2012.

[52] J. Mackenzie. Uniform convergence analysis of an upwind finite-difference approximation of a convection-diffusion boundary value problem on an adaptive grid. *IMA J. Numer. Anal.*, 19(2):233–249, 1999.

[53] J. J. H. Miller, E. O'Riordan, and G. I. Shishkin. On piecewise-uniform meshes for upwind- and central-difference operators for solving singularly perturbed problems. *IMA J. Numer. Anal.*, 15(1):89–99, 1995.

[54] J. J. H. Miller, E. O'Riordan, and G. I. Shishkin. *Fitted Numerical Methods for Singular Perturbation Problems*. World Scientific Publishing Co. Pte. Ltd., Hackensack, NJ, 2012.

[55] J. J. H. Miller, E. O'Riordan, G. I. Shishkin, and L. P. Shishkina. Fitted mesh methods for problems with parabolic boundary layers. *Math. Proc. R. Ir. Acad.*, 98A(2):173–190, 1998.

[56] K. Miller and R. N. Miller. Moving finite elements. I. *SIAM J. Numer. Anal.*, 18(6):1019–1032, 1981.

[57] P. D. Miller. *Applied Asymptotic Analysis*. Graduate Studies in Mathematics. American Mathematical Society, Providence, RI, 2006.

[58] R. Mohammadi. B-spline collocation algorithm for numerical solution of the generalized Burger's-Huxley equation. *Numer. Methods Partial Differential Equations*, 29(4):1173–1191, 2013.

[59] J. Mohapatra and S. Natesan. Parameter-uniform numerical methods for singularly perturbed mixed boundary value problems using grid equidistribution. *J. Appl. Math. Comput.*, 37(1-2):247–265, 2011.

[60] J. Mohapatra and S. Natesan. Uniformly convergent numerical method for singularly perturbed differential-difference equation using grid equidistribution. *Int. J. Numer. Methods Biomed. Eng.*, 27(9):1427–1445, 2011.

[61] K. Morton and D. Mayers. *Numerical Solution of Partial differential Equations: An Introduction*. Cambridge University Press, Cambridge, 1994.

[62] K. W. Morton. *Numerical Solution of Convection-Diffusion Problems*. Chapman & Hall, London, 1996.

[63] K. Mukherjee and S. Natesan. Parameter-uniform hybrid numerical scheme for time-dependent convection-dominated initial-boundary-value problems. *Computing*, 84(3-4):209–230, 2009.

[64] K. Mukherjee and S. Natesan. ϵ-uniform error estimate of hybrid numerical scheme for singularly perturbed parabolic problems with interior layers. *Numer. Algorithms*, 58(1):103–141, 2011.

[65] K. Mukherjee and S. Natesan. Optimal error estimate of upwind scheme on Shishkin-type meshes for singularly perturbed parabolic problems with discontinuous convection coefficients. *BIT*, 51(2):289–315, 2011.

[66] K. Mukherjee and S. Natesan. Richardson extrapolation technique for singularly perturbed parabolic convection-diffusion problems. *Computing*, 92(1):1–32, 2011.

[67] L. S. Mulholland, Y. Qiu, and D. M. Sloan. Solution of evolutionary partial differential equations using adaptive finite differences with pseudospectral post-processing. *J. Comput. Phys.*, 131(2):280–298, 1997.

[68] S. Natesan and S. Gowrisankar. Robust numerical scheme for singularly perturbed parabolic initial-boundary-value problems on equidistributed mesh. *CMES: Comput. Model. Eng. Sci.*, 88(4):245–268, 2012.

[69] A. H. Nayfeh. *Perturbation Methods*. Wiley Classics Library.

[70] R. E. O'Malley, Jr. *Introduction to Singular Perturbations*. Academic Press, New York-London, 1974.

[71] R. E. O'Malley, Jr. *Singular Perturbation Methods for Ordinary Differential Equations*. Applied Mathematical Sciences. Springer-Verlag, New York, 1991.

[72] L. Prandtl. Uber flussigkeits-bewegung bei kleiner reibung. In *Verhandlungen, III Inter. Math. Kongresses, Tuebner, Leipzig*, pages 484–491, 1905.

[73] Y. Qiu and D. M. Sloan. Analysis of difference approximations to a singularly perturbed two-point boundary value problem on an adaptively generated grid. *J. Comput. Appl. Math.*, 101(1-2):1–25, 1999.

[74] Y. Qiu, D. M. Sloan, and T. Tang. Numerical solution of a singularly perturbed two-point boundary value problem using equidistribution: analysis of convergence. *J. Comput. Appl. Math.*, 116(1):121–143, 2000.

[75] A. Quarteroni, R. Sacco, and F. Saleri. *Numerical Mathematics*. Texts in Applied Mathematics. Springer-Verlag, Berlin, 2007.

[76] H.-G. Roos and C. Reibiger. Numerical analysis of a system of singularly perturbed convection-diffusion equations related to optimal control. *Numer. Math. Theory Methods Appl.*, 4(4):562–575, 2011.

[77] H.-G. Roos and M. Schopf. Analysis of finite element methods on Bakhvalov-type meshes for linear convection-diffusion problems in 2D. *Appl. Math.*, 57(2):97–108, 2012.

[78] H.-G. Roos, M. Stynes, and L. Tobiska. *Robust Numerical Methods for Singularly Perturbed Differential Equations*. Springer-Verlag, Berlin, 2008.

[79] M. Sari, G. Gürarslan, and A. Zeytinoğlu. High-order finite difference schemes for numerical solutions of the generalized Burgers-Huxley equation. *Numer. Methods Partial Differential Equations*, 27(5):1313–1326, 2011.

[80] G. I. Shishkin. Approximation of solutions of singularly perturbed boundary value problems with a parabolic boundary layer. *Zh. Vychisl. Mat. i Mat. Fiz.*, 29(7):963–977, 1102, 1989.

[81] G. Smith. *Numerical Solution of Partial Differential Equations: Finite Difference Methods*. Clarendon Press, Oxford, 1994.

[82] P. Šolín. *Partial Differential Equations and the Finite Element Method*. Pure and Applied Mathematics. Wiley-Interscience, Hoboken, NJ, 2006.

[83] M. Stynes and E. O'Riordan. Uniformly convergent difference schemes for singularly perturbed parabolic diffusion-convection problems without turning points. *Numer. Math.*, 55(5):521–544, 1989.

[84] M. Stynes and H.-G. Roos. The midpoint upwind scheme. *Appl. Numer. Math.*, 23(3):361–374, 1997.

[85] V. Thomée. *Galerkin Finite Element Methods for Parabolic Problems*. Springer Series in Computational Mathematics. Springer-Verlag, Berlin, 2006.

[86] B. Wade and K. Jayasuriya. Convergence of semidiscrete Galerkin finite element schemes for nonhomogeneous parabolic evolution problems. *J. Math. Anal. Appl.*, **195**(3):645–657, 1995.

[87] B. Wade and A. Khaliq. On smoothing of the Crank-Nicolson scheme for nonhomogeneous parabolic problems. *J. Comput. Meth. Sci. Eng.*, **1**(1):107–124, 2001.

[88] B. Wade, A. Q. M. Khaliq, M. Siddique, and M. Yousuf. Smoothing with positivity-preserving pade schemes for parabolic problems with nonsmooth data. *Numer. Methods Partial Differential Equations*, **21**(3):553–573, 2005.

[89] A. B. White, Jr. On selection of equidistributing meshes for two-point boundary-value problems. *SIAM J. Numer. Anal.*, 16(3):472–502, 1979.

[90] Z. Xie and Z. Zhang. Superconvergence of DG method for one-dimensional singularly perturbed problems. *J. Comput. Math.*, 25(2):185–200, 2007.

[91] Z. Xie and Z. Zhang. Uniform superconvergence analysis of the discontinuous Galerkin method for a singularly perturbed problem in 1-D. *Math. Comp.*, 79(269):35–45, 2010.

[92] X. Xu, W. Huang, R. D. Russell, and J. F. Williams. Convergence of de Boor's algorithm for the generation of equidistributing meshes. *IMA J. Numer. Anal.*, 31(2):580–596, 2011.

[93] Z. Zhang. Finite element superconvergence approximation for one-dimensional singularly perturbed problems. *Numer. Methods Partial Differential Equations*, 18(3):374–395, 2002.

[94] Z. Zhang. On the *hp* finite element method for the one dimensional singularly perturbed convection-diffusion problems. *J. Comput. Math.*, 20(6):599–610, 2002.

[95] Z. Zhang. Finite element superconvergence on Shishkin mesh for 2-D convection-diffusion problems. *Math. Comp.*, 72(243):1147–1177, 2003.

[96] H. Zhu, H. Tian, and Z. Zhang. Convergence analysis of the LDG method for singularly perturbed two-point boundary value problems. *Commun. Math. Sci.*, 9(4):1013–1032, 2011.

List of published and communicated papers

Based on the work in this thesis, the following research articles are published or communicated.

1. S. Natesan and S. Gowrisankar. Robust numerical scheme for singularly perturbed parabolic initial-boundary-value problems on equidistributed mesh, *CMES: Comput. Model. Eng. Sci.*, 88(4):245–268, 2012.
2. S. Gowrisankar and S. Natesan. The parameter uniform numerical method for parabolic reaction-diffusion problems on equidistributed grids, *Appl. Math. Lett.*, 26(11):1053–1060, 2013.
3. S. Gowrisankar and S. Natesan. Uniformly convergent numerical method for singularly perturbed parabolic initial-boundary-value problems with equidistributed grids, *Int. J. Comput. Math.*, 2013, http://dx.doi.org/10.1080/00207160.2013.792925.
4. S. Gowrisankar and S. Natesan. Robust numerical scheme for singularly perturbed convection-diffusion parabolic initial-boundary-value problems on equidistributed grids (Communicated).
5. S. Gowrisankar and S. Natesan. Robust numerical scheme for singularly perturbed delay parabolic initial-boundary-value problems on equidistributed grids (Communicated).
6. S. Gowrisankar and S. Natesan. Uniform point-wise convergence for parabolic convection-diffusion problems on piecewise uniform Shishkin mesh (Communicated).